University of Southampton

Faculty of Engineering and Applied Science
Department of Civil and Environmental Engineering

A Study of Secondary Moments and Moment Redistribution in Continuous Prestressed Concrete Beams

by

Laurence Weekes, B.Eng

Supervisor: Dr. S.S.J.Moy

A thesis submitted for the degree of Doctor of Philosophy

August 1994

For My Mum, Dad, and Sister

University of Southampton

Faculty of Engineering and Applied Science
Department of Civil and Environmental Engineering

Doctor of Philosophy

A Study of Secondary Moments and Moment Redistribution in Continuous Prestressed Concrete Beams

by Laurence Weekes

ABSTRACT

Secondary or Parasitic internal bending moments in statically indeterminate continuous prestressed concrete beams are produced by the presence of the redundant reactions at the internal supports, assuming that the tendon profile does not coincide with the line of pressure produced in the concrete, i.e. that the tendon is not concordant.

Whilst behaving in an elastic manner, these Secondary moments may be separated from the total internal bending moment (Secondary moment plus moment produced by applied loads) using various methods such as equivalent loads, together with a stiffness analysis. Beyond the Serviceability Limit State, the beam will begin to crack, altering the flexural stiffness as well as causing local increases in the tendon force, in turn altering the Secondary Moment. Therefore if the designer wishes to incorporate Moment Redistribution at the Ultimate Limit State, assuming that the critical sections have sufficient ductility, how to include Secondary Moments, if at all, is of much debate.

Many different approaches have been adopted to shed light on the problem, the majority using nonlinear analyses of various forms. The advent of Finite Elements has seen an increase in their popularity for application to such nonlinear problems.

This study begins with a Finite Element analysis of simply supported prestressed concrete beams, followed by an analysis of a two span example with a single curved tendon profile, fully bonded to the concrete, up to Ultimate Limit State. Although these analyses allowed an investigation of the overall nonlinear behaviour, the Secondary moment could not be separated from the Internal moment in the post cracking stage.

As a result of the Finite Element Analyses, a method of applying equivalent loads past the Serviceability Limit State in an attempt to estimate the magnitude Secondary Moments up to the point where the beam is rendered statically determinate, was developed and utilised in a computer program. Two two-span beam examples and a three span beam, both with curved fully bonded parabolic tendon profiles were analysed to highlight the possible effects the secondary moment could have on the behaviour at Ultimate Limit State.

Acknowledgements

I would like to thank Dr. Stuart Moy for his expert help, opinions, and guidance throughout the duration of this project, not to mention his extreme patience.

I am grateful to Robin Whittle of Ove Arup Partnership for organising a short period of work with the Research and Development group at Ove Arup.

Thanks are due to Dr. Tony Lock, Paul Bickmore, and Mark Foster for their advice on computers in general, and to Christine Telford and Richard Downes of the Computer Services Department for their help with mastering the Silicon Graphics and Sun computer systems.

I also would like to express my gratitude to SERC for the financial support during the project, as well as Ove Arup Partnership for providing the CASE award.

Finally I am indebted to my parents for their support (thanks Mum and Dad!)

CONTENTS

Appendices

Glossary of Terms

Concordant Tendon Profile. A tendon profile which is concordant is coincident with the compressive force trajectory in the concrete. This means that there is no internal moment present, i.e. the secondary moment in a continuous beam is zero.

Equivalent Load. The effects of prestress on any beam system can be represented by a set of equivalent transverse loads, and moments at the ends of the member. These equivalent loads are useful in the determination of prestress effects, such as secondary moments.

Internal Equilibrium and Internal Moment. Regardless of the external forces acting on a static structure, internal equilibrium of forces must be maintained if it is to remain so. It is well known that the basic idea in reinforced and prestressed concrete beams is that the concrete, being strong in compression and weak in tension, relies on the steel to take the tensile forces, whilst the concrete will take the compressive forces.

A short end section of a simply supported prestressed concrete beam, with a straight tendon profile displaced downwards at an eccentricity e from the section centroid, is shown in figure 1 as two separate free body diagrams, of the concrete (a), and the steel tendon (b) . We will assume no applied transverse load, and ignore self weight of the beam, hence the only force acting on the structure is that due to the prestress. The concrete will be subject to the compressive force P and the steel will take the tensile force T. The tensile force in the steel can only act along the profile of the tendon. At this stage, the trajectory of the compressive force in the concrete must also act along the line of the tendon, so that equilibrium is maintained. This becomes obvious when we imagine the two free body diagrams in the composite section, where P is equal and coincident to T at both the left and right ends of the free body.

Figure 2 shows the same portion of beam with an applied transverse U.D.L. Again, the beam is divided into free bodies for the concrete (a) and the steel (b) . Looking at the free body for the concrete (a), and taking moments about the simple support, the force P acting on the right side of the section must move vertically up the beam to maintain equilibrium. The force acting on the left end of the section has not

moved however. Looking at the steel, the tensile force T remains the same and is fixed in position by the tendon profile. In the composite section, comparing with figure 1, the compressive force P has moved in relation to T on the right hand side of the section to create an internal moment. This internal moment can be thought of as an internal resisting moment which balances the bending moment produced by the transverse load.

In general it is the line of the compressive force in the concrete which alters its trajectory (often referred to as the compressive force path CFP, or the line of pressure) to produce this internal moment to balance any bending moment induced in the beam, caused by external forces or effects. This has implications when considering statically indeterminate prestressed concrete beams.

In a statically indeterminate prestressed concrete beam, secondary (sometimes called parasitic) moments can be produced by the effects of the internal supports restraining the natural deflection of the beam assuming the internal supports were not present. Equivalent loads (section 2.2) can be used to determine secondary moments prior to cracking. This is achieved by subtracting the primary moment (the product of prestress force and tendon eccentricity) from the resultant moments (calculated from the equivalent loads). The secondary moment therefore sets up an internal couple, where the compressive force path in the concrete is no longer coincident with the tensile force in the tendon. Hence as load is applied to the beam, the internal moment is the addition of the bending moment caused by the applied load and any secondary moment present. This addition is valid up to collapse, although the secondary moment may alter after cracking has commenced.

Linear Transformation. Linear transformation is the process of raising or lowering the tendon profile of a multispan prestressed concrete beam, at the internal supports only, so that the basic shape of the tendon profile between the ends of the member is not altered. A linear change in the tendon eccentricity (with distance) from the internal supports of the member has been applied to the tendon, hence the name *linear transformation* This process has the effect of 'adding' a linear eccentricity function to the original eccentricity function, so that the primary moment (the product of tendon force and eccentricity) is altered in a linear fashion along the beam.

However, when the equivalent load is calculated from the new primary moment, there is no change, as the equivalent load is the second differential of the primary moment, and any linear function change in the primary moment will disappear during the differentiation. This means that the resultant moments calculated from the equivalent loads will also not be altered by the process. The consequences of this are that the elastic secondary moment (the subtraction of the primary moments from the resultant moments) can be altered, and if necessary, eliminated totally, producing a concordant profile. It should be noted that the eccentricity of the tendon at the ends of the member must not be altered. If they are, the equivalent load (in the form of end moments) will be altered, and the process is no longer valid.

Primary Moment (M1). The product of tendon force and eccentricity from the section centroid at all locations along the beam length.

Resultant Moment (M3). The reactant moments in the beam caused by equivalent loads (and also by the prestress itself). These are effectively the primary bending moment plus any secondary moment prestress effect caused by the statical indeterminacy of a beam. They can be calculated from the equivalent load using a stiffness (e.g. moment distribution) procedure.

Secondary or Parasitic Moment (M2). The internal moment caused by prestress only (i.e. a prestress effect), caused by the statical indeterminacy of a beam. This is the subtraction of the primary moment from the resultant moment.

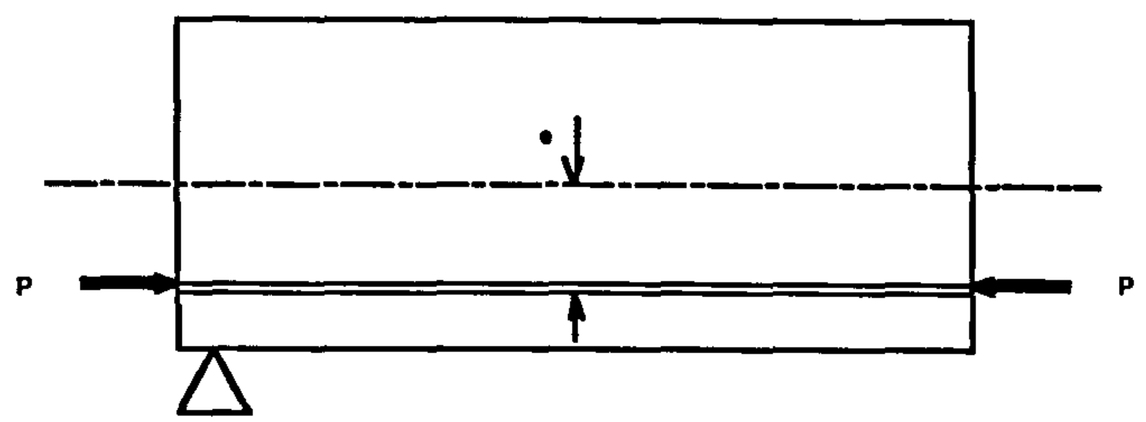

(a) Free Body Diagram of Concrete

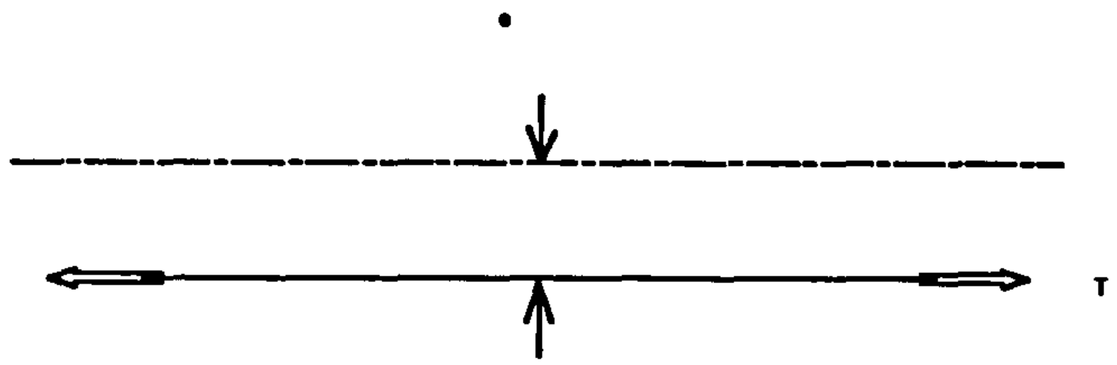

(b) Free Body Diagram of Steel

Figure 1

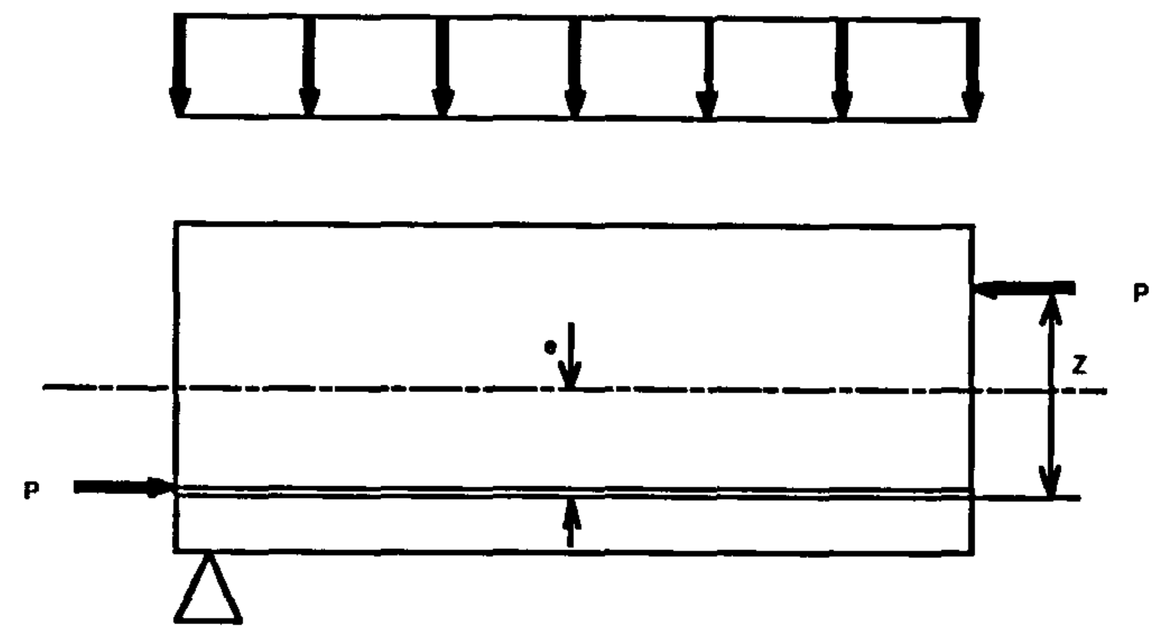

(a) Free Body Diagram of Concrete

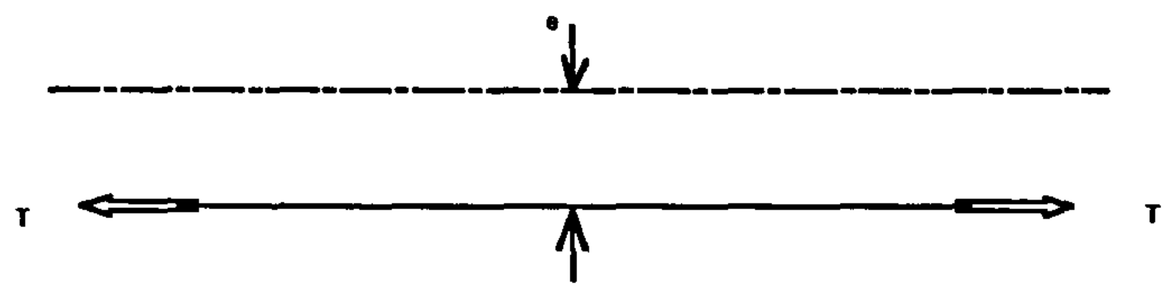

(b) Free Body Diagram of Steel

Figure 2

Notation

The most frequently used abbreviations and symbols are given here. Some less frequently used symbols do not appear here and are locally explained in the text. The details for the notation for Appendix F can be found in BS8110 [50]

Abbreviations

C.F.P.	Compressive Force Path
C.S.A.	Cross Sectional Area
F.E.	Finite Element(s)
R.C.	Reinforced Concrete
P.C.	Prestressed Concrete
U.D.L.	Uniformly Distributed Load

Latin Symbols

A_c	Area of Concrete
A_s or A_{ps}	Area of Prestressing Steel
c	Carry-Over Factor
d	Effective Depth
E	Elastic or Youngs Modulus
e_i	Tendon Eccentricity (where 'I' is a reference number)
f_{cu}	Characteristic Concrete Cube Strength
f_{pu}	Characteristic Strength of Prestressing Steel
f_{tu}	Modulus of Rupture (tensile Strength of Concrete)
I	Second Moment of Area
L	Length
l_b	Bond Length
M_i	Bending Moment (where 'i' is a reference number)

M_p	Plastic Moment
M1	Primary Moment
M2	Secondary Moment
M3	Resultant Moment
P	Prestress Force, or Load
p	Prestress
Q	Load
s	Stiffness Factor
T	Total Force in Steel
u	Bond Stress
x	Neutral Axis Depth, or Horizontal Cartesian Coordinate of Length
y	Vertical Cartesian Coordinate of Length

Greek Symbols

β_b	$\frac{\text{Moment at Section after Redistribution}}{\text{Moment at Section before Redistribution}}$
δ	Distribution Factor
ε	Strain
ε_c	Concrete Fibre Strain
ε_s	Steel Strain
γ_m	Material Factor
ϕ	Curvature
θ	Angular Rotation
σ	Stress

1/ Introduction

Statically indeterminate prestressed concrete beams and frames have a number of advantages and disadvantages over statically determinate prestressed concrete structures, as outlined by Nilson, [2]. Firstly, one significant difference is the formation of an internal moment, referred to as the secondary or parasitic moment, by the presence of redundant reactions in the statically indeterminate prestressed structure. The centre or line of compression within the section is no longer coincident with the line of the tendon profile, and the secondary moment will vary linearly between support sections. In the case of continuous beams, by treating the prestress as an equivalent load on the beam, the bending moments within the member may be split into primary, secondary, and total moments, so that the elastic secondary moments may be calculated. Linear transformation of the tendon profile at the internal supports will alter the primary and secondary moment so that the total moments remain the same, and the stresses in the section are unaffected. Therefore if desired, the secondary moment may be eliminated, and the tendon profile in this case is termed concordant. However, in the design process, this is not always possible or desirable.

Secondly, in certain circumstances, statically indeterminate structures at ultimate limit state possess the ability to carry loads passed the values predicted by elastic theory. This overload behaviour is caused directly by the statical indeterminacy of the beam, coupled with plastic behaviour of the critical sections in the member. Once a critical section has reached its ultimate moment capacity in a statically indeterminate member, a number of possibilities exist for the subsequent behaviour. If the section is not ductile and has no rotation capacity, then the structure will fail immediately, and the failure load is that predicted by elastic theory. If the structure has ductility and rotation capacity in all of its critical sections, then this will allow redistribution of bending moment to the stiffer parts of the structure until the ultimate moment capacities at enough critical sections have been reached so as to form a collapse mechanism. The failure load is that predicted by plastic methods, and will be greater than that predicted by an elastic approach. A structure which is moderately ductile may exhibit partial redistribution of the ultimate bending moments, until the rotation capacity of a critical section reaches its ultimate rotation.

In the case of reinforced and prestressed concrete statically indeterminate structures, if ultimate elastic moments are to be redistributed at the ultimate limit state, then the designer will try to ensure that enough rotation capacity is available at the critical sections for the desired amount of redistribution to occur. For prestressed concrete continuous beams, how to treat secondary moments in the design at the ultimate limit state has been of much debate. Whilst the beam is behaving elastically, these secondary moments may be readily calculated

using elastic methods such as equivalent loads. In the post cracking stage up to ultimate load, elastic methods cannot be used, and the secondary moment cannot be monitored by normal nonlinear analysis techniques or by experimental tests. The tendon force and stiffness changes at cracks would suggest an alteration of the secondary moment in the post cracking stage, which casts doubts on current design procedures, and how they incorporate elastic secondary moments at the ultimate limit state. The following section reviews work related to the subject of secondary moments and their effect on moment redistribution.

1.1/ Research on Secondary Moments and Moment Redistribution in Continuous Prestressed Structures

A World Conference on prestressed concrete in 1957, [30], saw a gathering of the current knowledge about the subject, ranging from materials, techniques, buildings, manufacturing processes, and research. Morice, [25], presented a direct design method for statically indeterminate prestressed concrete structures, using the 'influence coefficient' method to calculate the moment envelopes due to both dead and imposed loading, and the subsequent determination of concordant profiles by an analysis of the line of pressure within the concrete. This method therefore tried to eliminate any secondary moments caused by the statical indeterminacy of the structure, by the calculation of a permissible zone in which the 'concordant tendon' could lie.

Morice and Lewis, [24], carried out a number of analyses on prestressed concrete continuous beams and plane frames, and concluded that if the tendon profile undergoes a linear transformation, the stresses in the structure remain the same in the elastic range, and that at ultimate load, this was also theoretically true. Work carried out by Macchi at the same time contradicted this. Full redistribution was designed for, and obtained in the tests carried out by Morice, where the failure at the critical sections was due to failure of the prestressing steel, giving these sections ductility and rotation capacity. In Macchi's case, there were a number of failures due to crushing of the concrete, causing only partial redistribution of the ultimate moments. Hence, this required further research.

Moment-Curvature relationships for both reinforced and prestressed concrete sections were investigated by a number of researchers, and Burns, [16], describes their calculation and design implications for partially prestressed (class 3) members. For sections with differing properties, such as the quantity and location of the steel, the moment curvature relationships behave differently, with those curves displaying a long plateau being the more ductile. By knowing either the moment-curvature, or the load-deflection relationship of

various critical sections along the member the ultimate load could be theoretically estimated, and controlled for design purposes.

Priestley et al., [19], began their programme of research into the moment redistribution of prestressed concrete continuous beams with an investigation of moment-curvature relationships. Simply supported beams with a constant moment zone, created by the application of two transverse equidistant point loads in the span, were modelled both experimentally and theoretically. The theory accounted for the concrete tension between cracks and attempted to predict average curvatures along the length of the member, as well as the curvatures at cracks. The results revealed that the differences between the average curvature in the constant moment zone, and the maximum curvature at a particular crack at a critical section were significant, and the average curvature gave better results for the subsequent calculation of deflections. The theory was implemented in a computer program, and the theoretical and experimental results were in good agreement. To analyse zones where the bending moment was not constant, the member would have to be broken down into small segments and the moment treated as constant over the segment length.

These relationships between moment and average curvature were then used to predict the overload behaviour of continuous beams, Priestley et al.,[20]. A number of two span beams were constructed and tested to failure with a single point load in each span. The tendon profile was linear between supports and points of load application (i.e. harped at the points of load application). Load-deflection and moment-load curves for both theory and experiment were in good agreement. A number of the beams tested in the experiment were designed to reach ultimate before full moment redistribution could take place, with an estimated 10% tolerance on the calculated ultimate load, without the confining effects of the supports on the crushed concrete at critical sections. No mention was made of the significance of secondary moments, as their analysis accounted for prestress effects within the calculation.

Bennet et al., [31], carried out twenty tests on both two and three span prestressed concrete beams to assess how the curvature distribution along their lengths varied with the distribution of both moment and ultimate load. An Institution of Civil Engineers report dealing with the ultimate load design of prestressed concrete structures put forward three methods of design, which were tested using the integrated curvature measurements from the tests. The results showed that the hyperelastic curvature was concentrated over a short length at critical sections. Hence the calculation of the ultimate load was found to be fairly accurate by treating the deformations as rotating hinges. Also, they concluded that the linear

transformation of the tendon profile did not affect the ultimate load (i.e. the secondary moment had no effect), although no mention was made of the secondary moment.

Mallick, [17], carried out tests on 21 continuous two-span beams with similar load arrangements to those of Priestley. His aim was to apply an analytical method for the computation of redistribution proposed by Guyon*, although he found that most of his test results were not as predicted by the method. An alteration (extension) to the method whereby the curvatures in the vicinity of the plastic hinges were assumed to be concentrated at the hinge gave a better comparison.

The problem of the treatment in design of secondary moments with regard to moment redistribution in continuous prestressed concrete beams was addressed by Lin and Thornton, [18]. Discrepancies in the 1971 ACI Building Code with respect to the inclusion of secondary moments in the design procedure, suggested that in theory, when enough plastic hinges are formed to render the member statically determinate, the secondary moments would disappear. Lin points out that the only case in which this would be true is if full redistribution of moment can be realised, and that the ultimate load will be the same if the secondary moment is present or not. Also, because it had been shown that a linear transformation of the tendon profile had no effect on the ultimate load, this was the basis behind the statement in the code that only the dead and live load design moments need be considered at the ultimate limit state. Yet if the redistribution was not allowed (or incomplete), and the beam was assumed to be behaving in an elastic manner, the secondary moments were present at their full capacity and should not be neglected, contradicting the Code's statement about their treatment. Two numerical examples confirmed the difference in ultimate load carrying capacities in the beam with respect to the influence of secondary moments. The intermediate case where partial redistribution takes place could be analysed as before, by considering the moment curvature relationships in the beam up to ultimate. A load balancing approach was suggested to account for the inclusion of secondary moments in the ultimate load condition, although the results were somewhat conservative.

In the light of the 1971 ACI code anomaly, there was increasing concern about how to correctly deal with secondary moments in the design process. Huber, [32], reiterates that linear transformation of the tendon profile does not affect the total moments or concrete stresses in the elastic range, and that the ultimate load is unaffected whilst full redistribution is assured. Consequently, rather than use a method of analysis which requires proportional loading up to ultimate limit state, he suggests a 'shakedown' approach such that the applied

---

* The strength of statically indeterminate prestressed concrete structures. *Symposium on the strength of concrete structures, London May 1956.* London C&CA, 1958. Session C, Paper No.2.

loads are variable, causing residual moments in the beam due to the inelastic deformations, after which the beam may be treated as elastic once the deformations have stabilised. However an incremental shakedown collapse is less likely than a proportional short term loading failure.

A treatise on the Australian Concrete Codes was presented by Wyche et al, [33]. Comparisons were made of the British, American, and Australian codes with respect to moment redistribution and the inclusion of secondary effects, i.e. secondary moments. This is discussed in more detail in section 2.1. A simplified moment-curvature approach was used to theoretically analyse the effects of the inclusion of secondary moments. By incrementing the load on two, two-span beam examples, one with a concordant tendon profile, the other with a positive secondary moment, the moment-curvature relationships at the critical sections in the span and over the centre support were followed. The results showed that the prestress secondary moments affect the ductility and the ultimate load of the beam, with positive secondary moments having ductility benefits over negative secondary moments). The analysis assumed that the secondary moment did not change from its elastically calculated value during the stage from cracking up to first plastic hinge formation.

Scholtz, [34], presents an analysis of the ductility demand and capacities of partially prestressed concrete continuous beams, and suggests improved values for the amount of moment redistribution allowed in the design codes of practice. A unique expression is developed to allow the secondary moment to be included in the redistribution process. This yields more economical designs, although shear and bond failures have not been addressed.

Mattock, [35], describes how the shape of the tendon profile which causes secondary moments to occur in a prestressed concrete continuous beam, causes relative rotations at ultimate moment at the ends of the beam segments, changing the distribution of moments at ultimate load by an amount equal to the elastic secondary moments. He argues that if a tendon profile is transformed downward at an internal support (shifting the secondary moment to a more positive value), then the inelastic rotation required for a given amount of redistribution of moment is reduced by the amount of relative end rotation caused by the tendon transformation. If the tendon profile is raised, then the rotational capacity is increased, increasing the amount of moment distribution, with the amount of increase/decrease being equal to the elastic secondary moment. In the cases where no moment redistribution was allowed, these arguments would also hold true, as the secondary moment would be included at ultimate. From some beam tests, he concludes that the secondary moment does not change from the cracking stage up to ultimate moment, due to the rate of increase in the support moment as the load was applied being nearly that predicted

by elastic theory. As to why local increases in the tendon force would not change the secondary moment, this is attributed to the fact that secondary moments are caused by the suppression of deformations due to the prestress. The applied loads cause the beam to deform and increase the tendon force, locally at cracks, although this increase of force does not cause any extra deformations, hence the secondary moment will remain at its elastically calculated value.

A non-linear analysis using the imposed deformation method was carried out by Aguado et al, [36], and applied to the Glatt Bridge at Opfikon (Switzerland), which was tested to destruction, [37]. Excellent agreement of internal forces and deformations between the two was observed, and the non-linear analysis showed that secondary moments should be included in the design of such structures.

Warner and Faulkes, [38], looked at the treatment of secondary moments and shears in the limit state design of continuous prestressed concrete beams. Whether to treat the tendon force as a load or a resistance component was also investigated. It was concluded that the prestress force could be treated as a load at transfer and under service conditions, whereas at ultimate, it should be treated as a resistance component. Secondary moments and shears were to be considered at the serviceability limit state, and at ultimate where the critical sections failed by crushing of the concrete, so that no moment redistribution occurs. For ductile sections showing high levels of redistribution, secondary moments and shears were insignificant. The design for ductility requirements of critical sections was left open.

These references reveal a number of conflicting opinions, backed up by empirical work and theoretical analyses, as to the treatment of prestressing effects in statically indeterminate structures, especially with regard to their design. A vast amount of current research involves non-linear analyses which are implemented in various ways, mainly through finite elements. Research involving non-linear and finite element analyses are discussed in detail in section 3.1.

2/ Procedures in Limit State Design

2.1/ Moment Redistribution in Statically Indeterminate Structures

One advantage of statically indeterminate structures is that in most cases their ultimate load capacity will be greater than that calculated using elastic theory. This is due to the presence of redundant reactions which require the structure to reach its ultimate moment capacity at more than one critical section, so that a collapse mechanism can form, causing ultimate failure (assuming rotation capacities at plastic hinges have sufficient rotation for full moment redistribution).

Using a linear-elastic approach, the bending moment envelope can be obtained at various levels of applied load, and will increase proportionally with the load. When the bending moment at a particular critical section reaches the ultimate moment capacity, it can become no larger. A collapse mechanism does not form at this stage due to the statical indeterminacy of the structure, so as the load is increased, the bending moment envelope 'redistributes' from its elastically calculated shape. When enough critical sections have reached their ultimate moment capacity to form a mechanism, the structure will collapse, and the applied load is deemed the ultimate load.

Full redistribution of bending moments requires the formation of near perfectly plastic hinges at critical sections, with a large amount of plastic rotation available at each hinge. Ductile materials such as steel have a large plateau in their stress-strain relationships, and exhibit excellent plastic behaviour. Statically indeterminate steel structures therefore have a large amount of rotation available at critical sections, and plastic methods for full redistribution of moments can be applied. Less ductile materials, those with small ranges of plastic behaviour on the stress-strain curves, will have only limited rotation capacity when the formation of plastic hinges occurs at critical sections. When the ultimate moment capacity at a critical section is reached, a plastic hinge will form and attempt to rotate to redistribute the bending moment to the stiffer parts of the structure. If the section has limited ductility, at some stage it is possible that the rotation capacity of the hinge will be reached, so that it will fail in a brittle manner, causing immediate collapse of the structure. In this case only partial redistribution of moment occurs before the ultimate load capacity has been reached, having a value between that predicted by an elastic analysis, and that predicted using plastic methods. In some cases, a structure may have negligible rotation capacity at its critical sections, and will fail at a load calculated directly from elastic theory.

Reinforced and prestressed concrete are essentially composite structures, consisting of the brittle concrete, and the much more ductile steel reinforcement. Depending on the amount of reinforcement present in a concrete structure, and the particular design, this will have a bearing on the ductility of a particular section, and hence the amount of rotation available. An under-reinforced section, where the reinforcement reaches its yield stress before the concrete fails, (i.e. when the extreme compressive fibre of the concrete reaches a strain of approximately 0.0035) will exhibit an ability to rotate at its ultimate moment capacity. The amount of rotation possible depends on how under-reinforced the section is. Sections where the concrete reaches its ultimate strain simultaneously with the yielding of the reinforcement will have negligible rotation, and those which are over-reinforced will fail immediately the ultimate moment capacity is reached.

The neutral axis depth at the ultimate moment gives a good indication as to how the section will 'fail', governed either by the concrete, or the steel. Figure 2.1.1 shows two accounts of the same section, figure 2.1.1.(a) with a small neutral-axis depth, and figure 2.1.1.(b) with a large neutral axis depth. It can be seen that the linear strain distribution across the depth of the section with the small neutral-axis depth will tend to give a large strain in the steel compared with the compression strain in the top fibre of the concrete, and hence will tend to produce an under-reinforced section having some plastic rotation capacity. The large neutral-axis depth will cause the strain in the steel to be small compared with that at the top concrete compression fibre, and the concrete will reach its compressive strain capacity before the steel yields, allowing no rotation capacity. Therefore the neutral-axis depth reflects a vital property in the design of reinforced and prestressed concrete as far as moment redistribution is concerned.

The major concern in the redistribution of bending moment in reinforced and prestressed concrete is the provision of enough rotation capacity at critical sections to allow the amount of redistribution required for the design. Also, as the redistribution is carried out at the ultimate limit state, the design has been effectively modified, so the desired behaviour at the serviceability limit states must be ensured. In B.S.8110 this is achieved by a requirement that the redistributed envelope must not violate a service load envelope, the latter being calculated either directly from the service loads, or as a percentage (70% for R.C, 80% for P.C.) of the elastic ultimate moments before redistribution. This percentage line method will ensure that the points of contraflexure (positions of zero moment) of both the service and ultimate envelopes remain unaltered in their location along the beam.

2.1.1/ Design procedure for the redistribution of moments for R.C. to B.S.8110

Firstly a definition for the term 'redistribution of moment' must be established, with regard to the design procedure. A two-span continuous beam subject to two point loads of magnitude Q in each span is shown in figure 2.1.2.(a). As the load is increased, an elastic analysis will give the bending moment in the spans and at the central support as $M_1 = 5QL/32$ and $M_2 = 3QL/16$ respectively, figure 2.1.2.(b). The bending moment envelope will, at a particular load, reach its moment of resistance, $M_2 = M_p$ at the central support, figure 2.1.2.(c), assuming the beam has identical moment of resistance values in the spans and at the support. Assuming unlimited rotation capacity at this hinge, the moment at the central support will remain unchanged, whilst the span moments will increase. When the applied loads are increased, two further hinges will form in each span, producing the collapse mechanism shown in figure 2.1.2.(d). This ultimate moment diagram is caused by the collapse load and is based solely on plastic behaviour. The original elastic bending moments redistribute as the plastic hinges form. However, in B.S.8110, redistribution is considered in a different manner. Using the same example as in figure 2.1.2., a bending moment envelope for the collapse load, say Q, is calculated using elastic methods, giving the bending moment envelope shown in figure 2.1.2.(b). The support moments are then reduced to the plastic moment value, $M_p = QL/6$ in the example (derived from figure 2.1.2.(d).). To satisfy equilibrium requirements however, the span moments must be increased, so that the free bending moment remains the same. This is the same as superimposing the free bending moment on the changed reactant support moments, Moy[11]. The procedures required for the design to B.S.8110 are illustrated in more detail in the following section.

An elastic bending moment envelope for a continuous beam under ultimate load is calculated from the following combinations of loading :-

a/ All spans loaded with 1.4× Dead Load+ 1.6× Imposed Load

b/ Alternate spans loaded with 1.4× Dead Load+ 1.6× Imposed Load and all others with 1.0× Dead Load

B.S.8110 clause 3.2.2.1 requires that the maximum amount by which any moment may be reduced is 30%, therefore the resistance moment provided by any section must be at least 70% of this elastically calculated envelope. In this respect it is useful to have an envelope of 70% of the elastic moments for comparison purposes after redistribution has been carried out.

To illustrate the procedure, consider a new model of a span in the middle of a multispan continuous beam system, subject to a point load at its centre. Figure 2.1.3.(c). shows the ultimate moment envelope obtained from two moment envelopes shown in figures 2.1.3.(a). and 2.1.3.(b), obtained from two separate load cases. The support moments in figure 2.1.3.(a). can be reduced by 30% to -105 kNm and -175 kNm at the left and right hand ends respectively, causing an increase in the span moment to 210 kNm, as shown in figure 2.1.4.(a). Alternatively if the span moment in figure 2.1.3.(b). is reduced by 30% to 175 kNm , the support moments would increase to -175 kNm and -225 kNm respectively, figure 2.1.4.(b)., an increase on the original values in figure 2.1.3.(a). Alternatively by increasing the support moments in figure 2.1.3.(b). to -105 kNm and -175 kNm, the span moment may be reduced by 15 kNm to 235 kNm. This redistribution will be adopted, figure 2.1.5.(a). Comparing this with the envelope of ultimate moments in figure. 2.1.3.(c). and figure 2.1.5.(b), it can be seen that the positions of zero moment (contraflexure), have moved towards the supports in the negative hogging moment region, and away from the supports in the positive sagging moment region. An envelope of 70% of the ultimate moments will cross the axis at the same position as the full ultimate moments, figure. 2.1.5.(b). Thus the redistributed envelope violates the 70% envelope in the regions of contra flexure. The redistributed envelope must be revised to comply with the 70% ultimate envelope, to ensure that sufficient lengths in the hogging and sagging regions are reinforced to satisfy service conditions as shown in figure 2.1.5.(c).

Clause 3.2.2.1, condition 2, ensures the provision of adequate rotation capacity, and states that at positions where moments have been reduced by the redistribution, the neutral axis limit should not be greater than 0.6 of the effective depth, obtained from the expression $x \leq (\beta_b - 0.4)d$, where :

$$\beta_b = \frac{\text{Moment at section after redistribution}}{\text{Moment at section before redistribution}} \leq 1$$

Where : x = Neutral axis depth

d = Effective depth

This maximum value for x assumes that no redistribution has taken place, and that $\beta_b = 1$. At the other extreme, if the full 30% reduction has taken place, the neutral axis depth x will be 0.3 of the effective depth. For design purposes, assuming that some redistribution of moments has taken place, the limiting value on the neutral axis depth is obtained from β_b

and the required reinforcement calculated from design equations such that this limit is not violated.

2.1.2/ Design Procedure for the redistribution of moments for P.C. to B.S.8110

The provisions for the redistribution of moments in prestressed concrete continuous members are covered by clause 4.2.3. In this case the reduction of the design ultimate moments is limited to 20%, and hence the neutral axis depth should not exceed $(\beta_b - 0.5)d$. Therefore the allowed level of adjustment in the ultimate envelope is less than for reinforced concrete because of the reduced ability to predict rotation capacities in prestressed concrete. The question of how to treat secondary moments in the analysis is of major concern, as plastic theory would dictate that the addition of any residual moment such as the secondary moment would not affect the ultimate load. The only case in which this can be guaranteed would be when complete redistribution (in the plastic theory sense) has taken place, i.e. when the rotation capacity at critical sections is known to be sufficient for full redistribution. Due to this uncertainty involved with the design of critical sections, how to include the effects of secondary moments is of extreme importance. Plastic theory would suggest that whether to include the secondary moments at the ultimate limit state or not, will yield the same result, yet if full redistribution cannot be assured, (i.e. sections cannot be designed with the required ductility), this is definitely not the case. B.S.8110 comes to a compromise by including the secondary moments with a load factor of 1.0 with the ultimate bending moments before redistribution, so that they are present in the calculation of the limit to the neutral axis depth (for ductility of critical sections), obtained from Clause 3.2.2.1, condition 2.

2.1.3/ Design Procedure for the redistribution of moments for P.C. to A.C.I. Code

ACI 318-89 permits a reduction of moments based on 'reinforcement indices' which are in turn related to the rotation capacity of the sections which are of concern. Specifically the reinforcement indices are,

$$\omega = \frac{A_s f_y}{b d f_c'} \qquad \omega' = \frac{A_s' f_y}{b d f_c'} \qquad \omega_p = \frac{A_p f_{ps}}{b d_p f_c'}$$

for non-prestressed tension steel, non-prestressed compression steel, and prestressed steel respectively. The elastic ultimate moment envelope is then calculated from all possible loading conditions, and the maximum percentages by which negative moments may be decreased or increased are,

For rectangular sections with prestressed steel only :

$$20\left(1-\frac{\omega_p}{0.36\beta_1}\right)\%$$

For rectangular sections with prestressed and non-prestressed reinforcement :

$$20\left(1-\frac{\omega_p+\frac{d}{d_p}\left(\omega-\omega'\right)}{0.36\beta_1}\right)\%$$

For flanged sections with prestressed and non-prestressed reinforcement :

$$20\left(1-\frac{\omega_{pw}+\frac{d}{d_p}\left(\omega_w-\omega'_w\right)}{0.36\beta_1}\right)\%$$

where the term β_1 is the factor by which the neutral axis depth is multiplied to obtain the depth of the equivalent rectangular stress block, and the subscript w refers to the reinforcement indices calculated from the breadth of the flange. It can be seen that the maximum possible percentage redistribution, like the British code, is twenty percent. However, the moment in the spans must be calculated from the same loading arrangement as that which produced the negative support moment values which have been altered. Also, there is a requirement to the effect that the reinforcement index (given by any of the three numerators in the above fractions) must not exceed $0.24\beta_1$, and a minimum amount of bonded reinforcement is required at the support sections. Both of these requirements ensure ductility.

Secondary moments are included in situations where the required ductility and rotation capacity cannot be guaranteed to create the desired full redistribution of bending moments, and in these cases they are included with a load factor of 1.0. The difference here is that they are included after redistribution of moments has taken place for calculation of the design ultimate moment.

The implications of this procedure for the inclusion of secondary moments, are described by Wyche et. al.,[33]. In the same reference the procedures in the Australian 'AS' codes and NAASRA, the Australian bridge design code, are compared with the American ACI, Canadian, and British Standard 5400 codes, and the advantages and disadvantages are examined in detail.

The conclusions that can be drawn from this is that there are a number of conflicting design methods which attempt to include the effects of secondary moments in the design. The correct way in which they should be treated has been, and is, a subject of much debate. Research has shown that they may have both beneficial and detrimental effects depending on their magnitude and sign, and also upon their inclusion or exclusion in the design. When they are included, they are assumed to act at their full elastic value, but as tendon forces and flexural stiffnesses change after cracking has occurred, this can no longer be valid. Only when a statically determinate system has been created due to the formation of a plastic hinge(s), will it be true that the secondary moment has become zero and has no further effect. However, the secondary moment is present up to statical determinacy, and therefore affects both the load at which this occurs, and the available rotation capacity at the critical sections thereafter, hence affecting the amount of redistribution which can take place. The secondary moment affects when the plastic moment is reached, and thus the amount of rotation required before the mechanism forms.

2.2/ Equivalent Load Analysis

The theory of equivalent loads provides a useful tool for the analysis of both simply supported and continuous beams, and is sometimes referred to as the tendon reaction method of analysis, and is described by Hurst, [1] and Nilson, [2]. By deflecting a stressed tendon from a perfectly horizontal profile, the concrete must exert a transverse force on the tendon to hold it in position, and hence, the tendon will exert an equal and opposite force on the concrete. Tendon profiles which are continuously curved will produce distributed transverse loads on the member, whereas those with sharp changes of profile will produce concentrated loads at the change points. These transverse loads produce the same bending moments as the prestressing force, and are called equivalent loads. Although these equivalent loads are treated as transverse loads, theoretically they are directed towards the centre of curvature of the tendon profile, in the case of continuously curved tendons, but in most cases, as the tendon is of shallow inclination, the equivalent load can be assumed vertical. At the ends of the member where the anchorages bear on the concrete, moments are produced by the eccentricity of the anchorage from the centroidal axis of the member. As a result of this equivalence between these transverse loads and the prestress, prestressed concrete beams may be analysed by considering the tendon force as a set of externally applied equivalent loads.

2.2.1/ Elastic analysis of simply supported beams

Figure 2.2.1. shows a simply supported beam with a continuously curved parabolic profile. The equation of the profile is calculated as:

$$y = e_1 - \frac{x}{L}(e_2 - e_1) + 4d_r x\frac{(L-x)}{L^2} \qquad (2.1)$$

where d_r is the drape of the tendon. It has be shown in many texts, Hurst [1], that the equivalent load is equal to P/r_{ps}, where r_{ps} is the radius of curvature of the tendon profile. If, as is normally assumed, the profile is reasonably flat, $/r_{ps}$ can be approximated by d^2y/dx^2. Differentiating equation (2.1) twice, and multiplying by the tendon force gives the equivalent load, in this case a uniformly distributed load of magnitude :

$$w = -\frac{8Pd_r}{L^2} \qquad (2.2)$$

It can be seen that rearrangement of this equation gives the well known formula for the maximum bending moment in a simply supported beam subject to a uniformly distributed load w, i.e.

$$P.d_r = -\frac{wL^2}{8} \qquad (2.3)$$

This is analogous to the relations between load, shear force, and bending moment. The equivalent load is thus the second derivative of the bending moment, i.e.

$$q = -\frac{dV}{dx} = -\frac{d^2M}{dx^2} \qquad (2.4)$$

Also, the moments at the ends of the beam are :

$$M_1 = Pe_1\cos\theta_1 \qquad M_2 = Pe_2\cos\theta_2 \qquad (2.5)$$

Thus, the primary moment $-Py$, can be used to calculate the equivalent load using the aforementioned method(i.e. $W = P(d^2y/dx^2)$). It should be noted that if the tendon force P varies along the profile as a function of x, this must also be included in equation (2.1) before the differentiation process.

For sharp changes in profile where the tendon has been held down or 'harped', as shown in figure 2.2.2., the concentrated load is obtained using $W = P(\sin\alpha + \sin\beta)$.

2.2.2/ Elastic Analysis of Continuous Beams

A beam continuous over three supports is shown in figure 2.2.3., and the primary moments, the product of the effective prestress force (4000kN) multiplied by the eccentricity of the tendon profile from the section centroid, are displayed in figure 2.2.4.(a)., denoted by M_1. For the left hand span, the parabolic tendon profile creates a uniformly distributed load as dictated by equation (2.2) :

$$w = -\frac{8Pd_r}{L^2} = -\frac{8\times 4000\times 0.5}{20^2} = -40\ \text{kN/m} \qquad (2.6)$$

The same result will be obtained if the change in slope between points A and B is calculated, i.e. d^2M/dx^2. This method is employed to calculate the concentrated load in the right hand span. At point C the change in slope is equal to :

$$= -100\text{kNm/m} - 300\text{kNm/m} = -400\text{ kN} \qquad (2.7)$$

Also, as the tendon at end D is non-coincident with the section centroid, an end moment of 400 kNm exists here. To obtain the resultant moment in the beam, a number of methods can be employed, such as flexibility and stiffness (many software programs are available for this). Moment distribution which is based on the stiffness method lends itself to hand calculations, and is carried out on the system of equivalent loads, shown in figure. 2.2.4.(b).

2.2.3/ Moment Distribution

The fixed end moments for the spans are :

First Span:

$$\text{Left Hand End} = -\frac{wL^2}{12} = -\frac{40\times 20^2}{12} = -1333.3\text{ kNm}$$

$$\text{Right Hand End} = +\frac{wL^2}{12} = +\frac{40\times 20^2}{12} = +1333.3\text{ kNm}$$

Right Hand Span:

$$\text{Left Hand End} = -\frac{Wab^2}{L^2} = -\frac{400\times 8\times 12^2}{20^2} = -1152\text{ kNm}$$

$$\text{Right Hand End} = +\frac{Wa^2b}{L^2} = +\frac{400\times 8^2\times 12}{20^2} = +768\text{ kNm}$$

Joint No.	A1	A2	B2	B3	Ext.
Distn. Factors	0	0.5	0.5	1	0
F.E.M.s	-1333.3	+1333.3	-1152	+768	+400
Relax	+1333.3	-90.7	-90.7	-1168	0
Carry Over	0	+666.7	-584	0	0
Relax	0	-41.4	-41.4	0	0
Total kNm	0	-1867.9	-1868.1	-400	+400

The resultant moments are shown in figure 2.2.4.(c), and these represent the total moments within the beam, denoted by M_3. The difference between these resultant moments and the primary moments, M_1, figure 2.2.4.(a)., is the secondary or parasitic moment, M_2,(i.e. $M_3 = M_1 + M_2$), shown in figure 2.2.4.(d), representing the net internal moment within the beam, caused by the statical indeterminacy of the beam. This may also be visualised as the central support applying a restraining external reaction, causing the centre of compression within the beam to be no longer coincident with the line of the tendon, setting up the internal secondary moment.

2.2.4/ Linear Transformation

If we imagine a linear transformation of the tendon profile by raising or lowering the tendon at internal support sections, the equivalent loads will not alter as the change of slope of the primary moment function remains the same. Thus the resultant moments in the beam will remain the same if the profile is transformed in this manner, however the primary prestress moments will differ due to the change in eccentricity of the profile. As a result, the secondary moments are changed, and if so desired, they can be totally eliminated by the production of a concordant tendon profile, whereby the tendon is coincident with the trajectory of the centre of compression in the beam. There can be a number of different concordant profiles for particular continuous beam systems, although in a great deal of cases these profiles are impractical, and the secondary moment cannot be completely eliminated.

2.2.5/ Overload Behaviour

The equivalent load method provides a means by which total resultant moments in the beam can be found. These are a combination of both primary and secondary moments, the latter of which reveals itself as the net internal moment. As vertical load is applied to the continuous beam, the internal moment becomes the addition of the secondary moment and those moments caused directly by the applied load. Whilst operating in the pre-cracked stage, in an elastic, serviceable manner, the equivalent load analysis can be applied with sufficient accuracy to find total and secondary moments, as the tendon force change due to the application of external loads is negligible, and an assumed effective prestress force is adequate. As the beam is overloaded, cracking will commence at some stage, and the nature of the beam will change. Local increases in tendon force occur at cracks, the magnitude of the change depending on bond characteristics, the location of the cracks, and the amount of cracking which has taken place. The onset of cracking is also accompanied by a change in the beam stiffness. Therefore at the serviceability limit state, the secondary moment due to

the prestress and internal moment due to applied loads can be separated readily, with easily calculable secondary moments, but beyond these loads up to the ultimate limit state, separation of the changing secondary moment from the internal moment becomes a difficult task, due to the aforementioned complications. The magnitude of the secondary moment may be a significant value at the onset of the formation of plastic hinges when possible redistribution of bending moments occurs, affecting the eventual ultimate load . Hence there are a number of factors to consider which complicate any attempted analysis of a cracked continuous beam using equivalent loads.

The monitoring of resultant moments has been carried out by a number of researchers such as Campbell and Moucessian, [23], and Campbell and Kodur, [29], employing finite element (stiffness) techniques and implementing them in computer programmes, with various degrees of success. Of concern here is the treatment of secondary moments in codes of practice for design purposes, and as this is the root of the problem, it is desirable to have a means of estimating them in the post-cracking stage of loading and their effect on the ultimate load. The following is an outline of the necessary procedures for an equivalent load analysis to determine the magnitude of secondary moments after the initiation of cracking.

2.2.6/ <u>The application of Equivalent Loads to determine the magnitude of Secondary Moments in the Post-Cracking stage</u>

As described in the previous section, the equivalent load can be found directly from the primary moment function by evaluating the second derivative with respect to x, assuming a continuously curved tendon profile. With no applied load, a stiffness analysis in the form of moment distribution (for hand calculation) is carried out with the necessary fixed-end moments, carry over factors, and relative stiffnesses of members, due to the equivalent loads, to calculate total moments, and secondary moments by subtraction of the primary moment. When an external load is applied the procedure remains the same as long as the beam is behaving elastically. The primary moment and equivalent loads remain the same, yielding the same resultant and secondary moments. The secondary moment may thus still be separated from the internal moment.

With a continuous beam system, let us assume that the first crack occurs at an internal support in a region of high negative (hogging) bending moment, at a particular magnitude of applied load. At the location of the crack, the tendon force is increased. This increase may be calculated by performing a cracked section analysis on the section in question, subject to the internal moment at that location. Immediately to the left and right of

the crack, the tendon force will decrease in some manner to its effective prestress force value, at a distance away from the crack governed by the bond characteristics between the steel and the concrete. This change in tendon force will cause an alteration in the primary prestress moment, affecting the equivalent load. At the crack, the stiffness (EI value) of the section has been reduced, so that the fixed-end moments, carry-over factors, and stiffness factors will be different in the moment distribution from the elastically calculated values. If these factors can be calculated successfully, the resultant moment due solely to the equivalent load may be obtained, and a value for the secondary moment established. The main components of the calculation are :-

1/ To find the second derivative of the primary moment, i.e. the equivalent load.

2/ To calculate the stiffness and carry-over factors of the beam, and carry out moment distribution (or stiffness calculation).

3/ To perform a cracked section analysis of the prestressed concrete member.

A calculation involving procedures 1 to 3 would be far too complex to carry out by hand, but is suited for solution by computer. A computer programme SMAREL (Secondary Moment And Redistribution by Equivalent Load) has been written to estimate the magnitude of secondary moments in two and three span prestressed concrete continuous beams, up to the point of first plastic hinge formation. The programme procedure is described in Appendix A, and its features detailed in section 5.

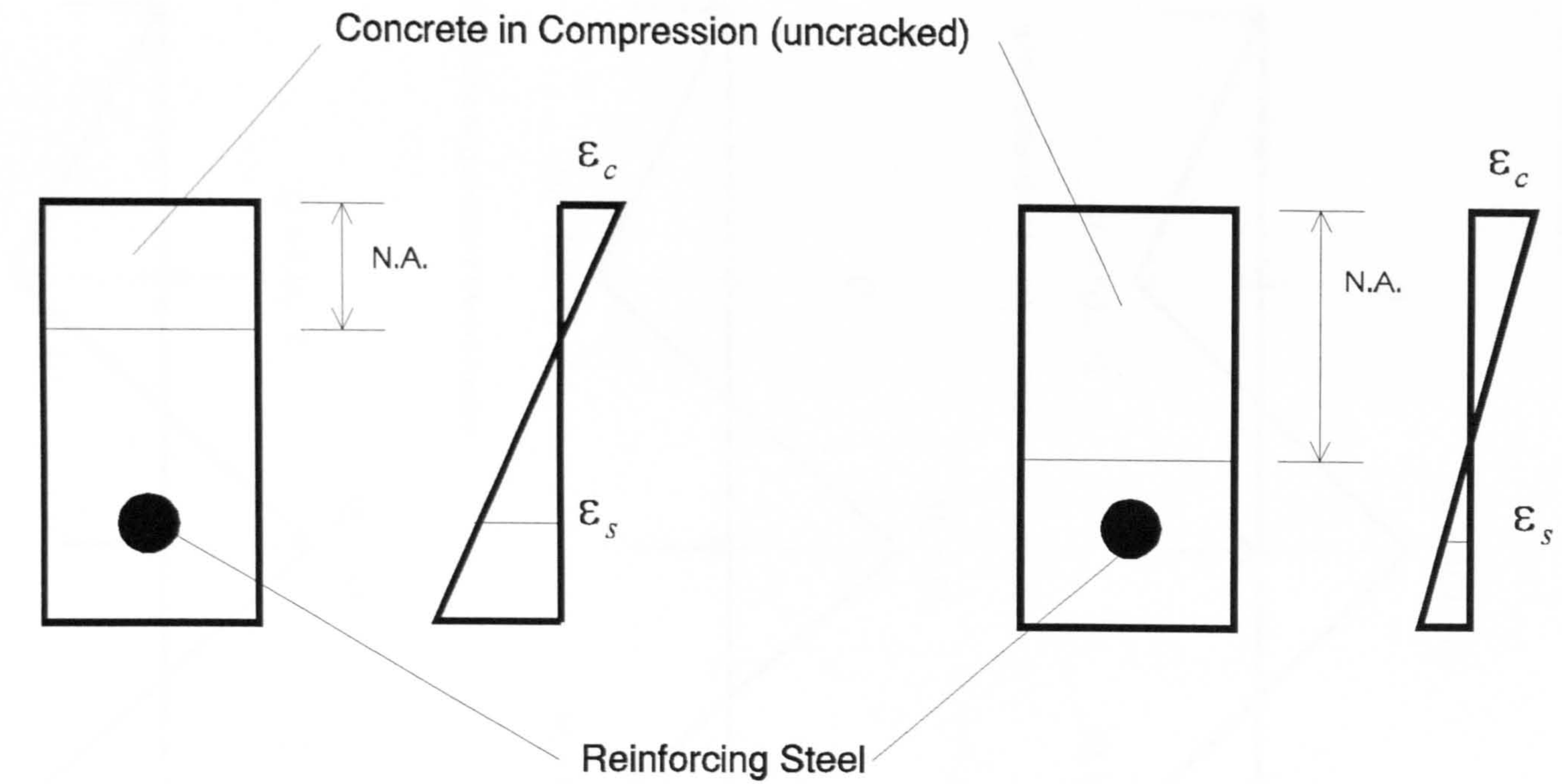

Effect of Neutral Axis Depth on Steel Strain

Figure 2.1.1.

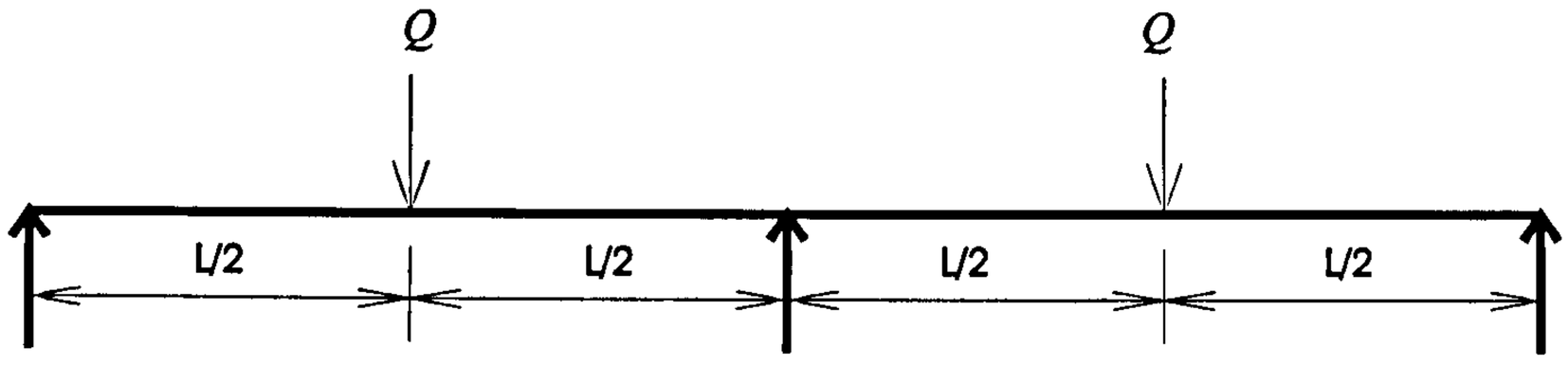

(a) Two Span Beam

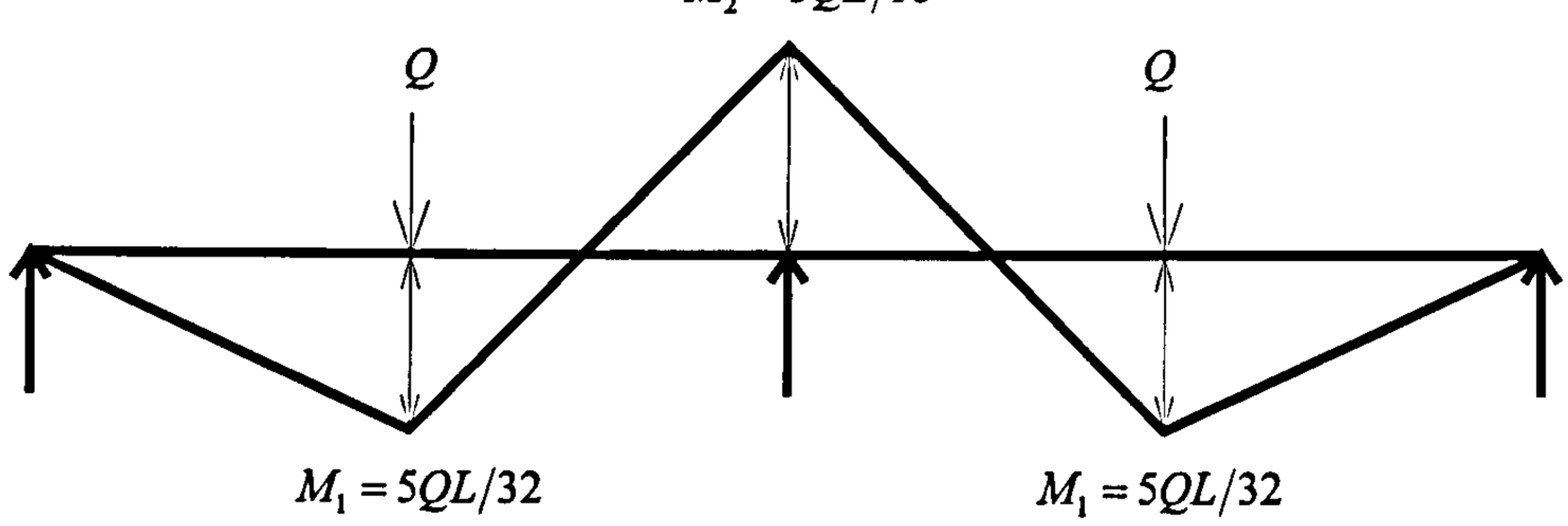

(b) Elastic Bending Moments Envelope

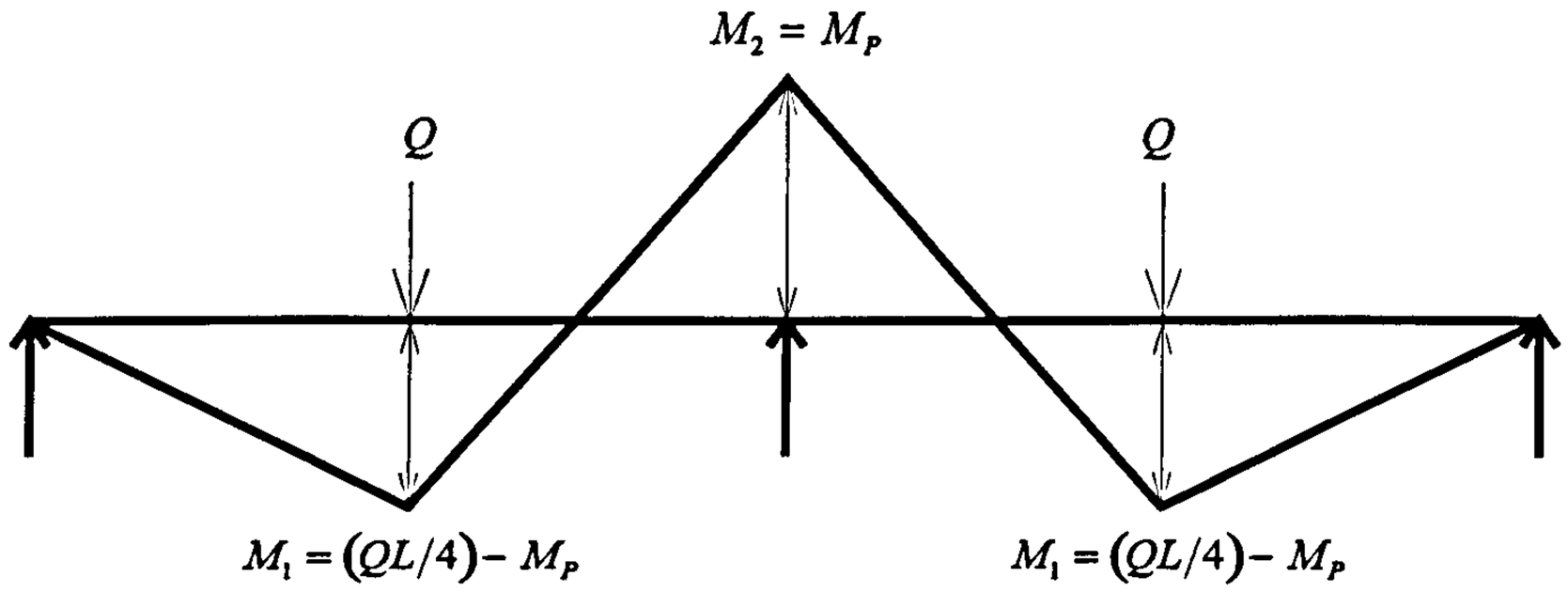

(c) Plastic Hinge Forms at Central Support

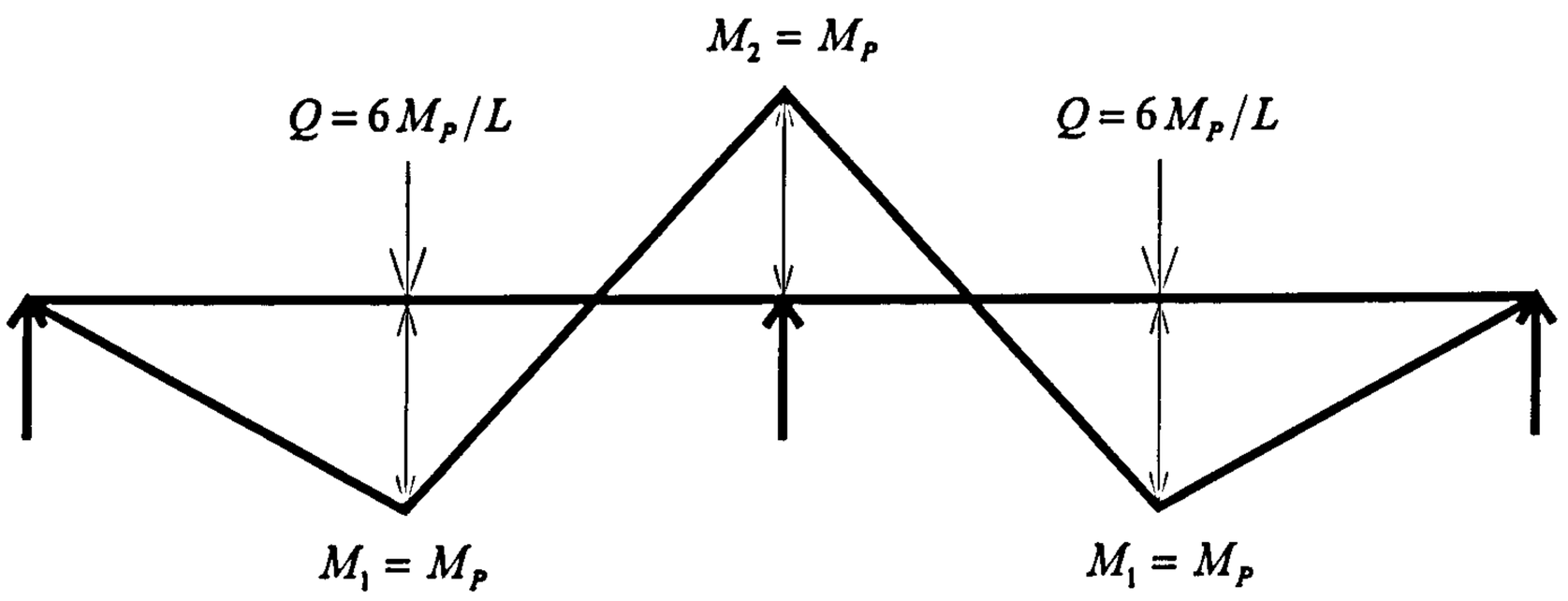

(d) Ultimate Bending Moment Envelope

Figure 2.1.2

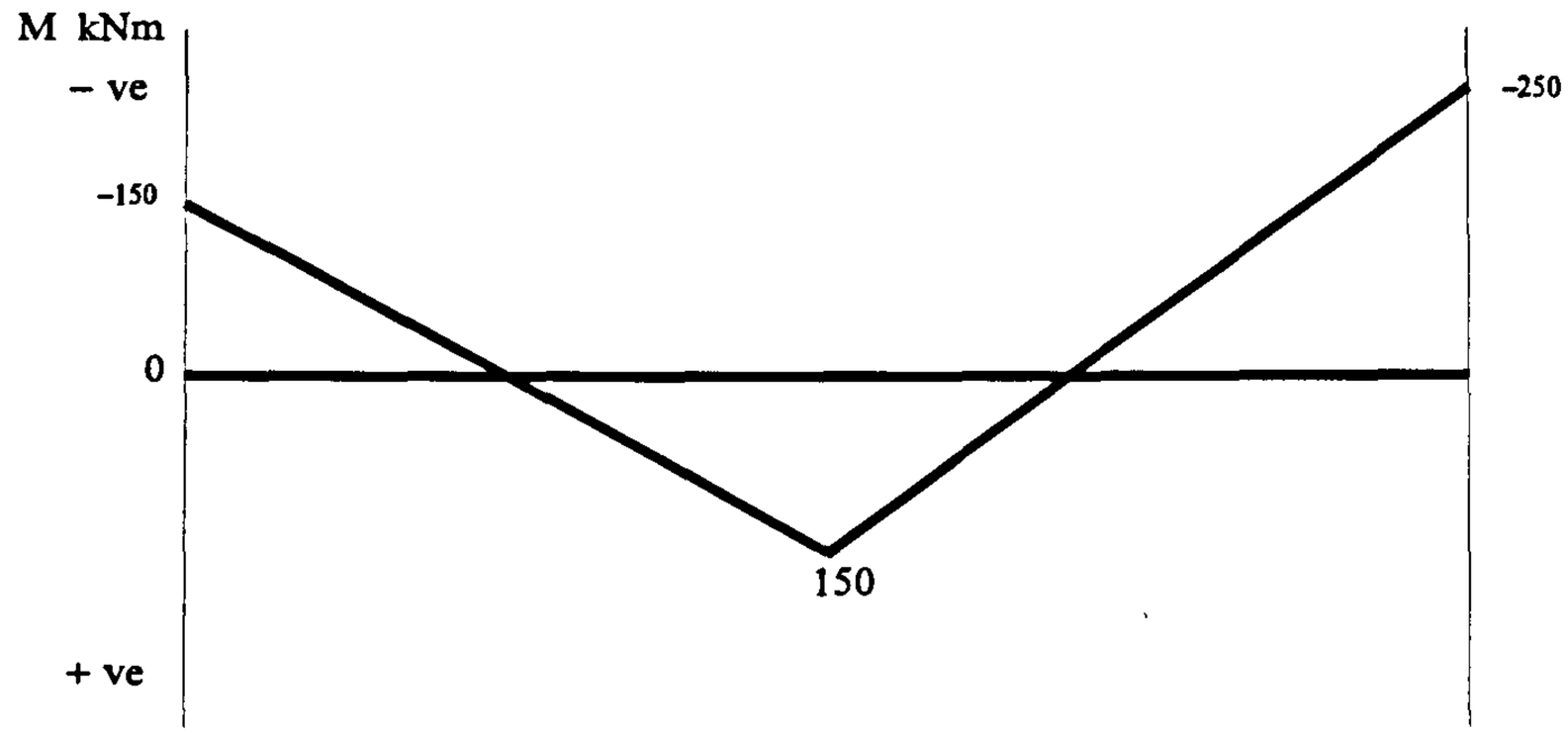

(a) First Bending Moment Envelope

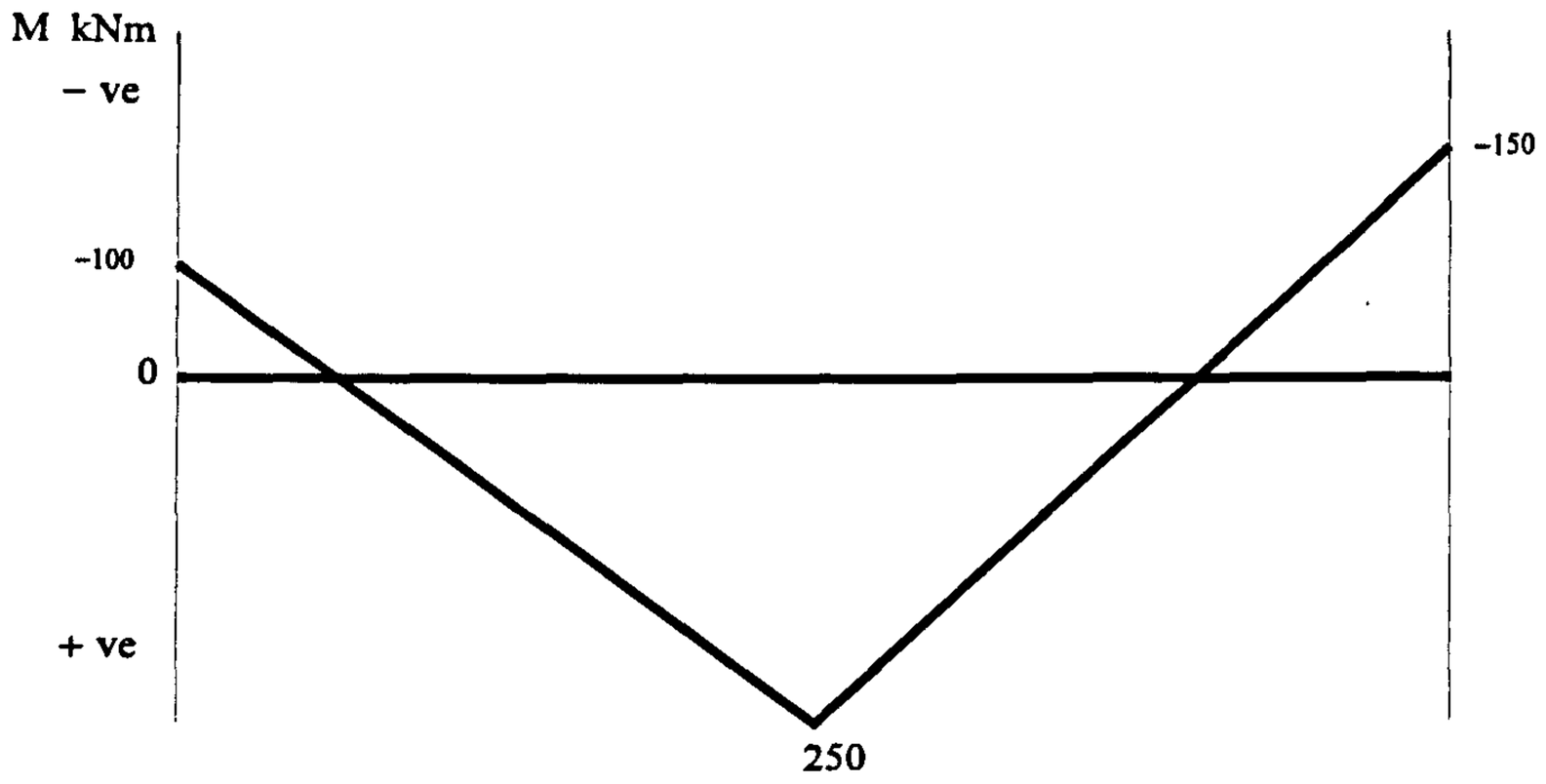

(b) Second Bending Moment Envelope

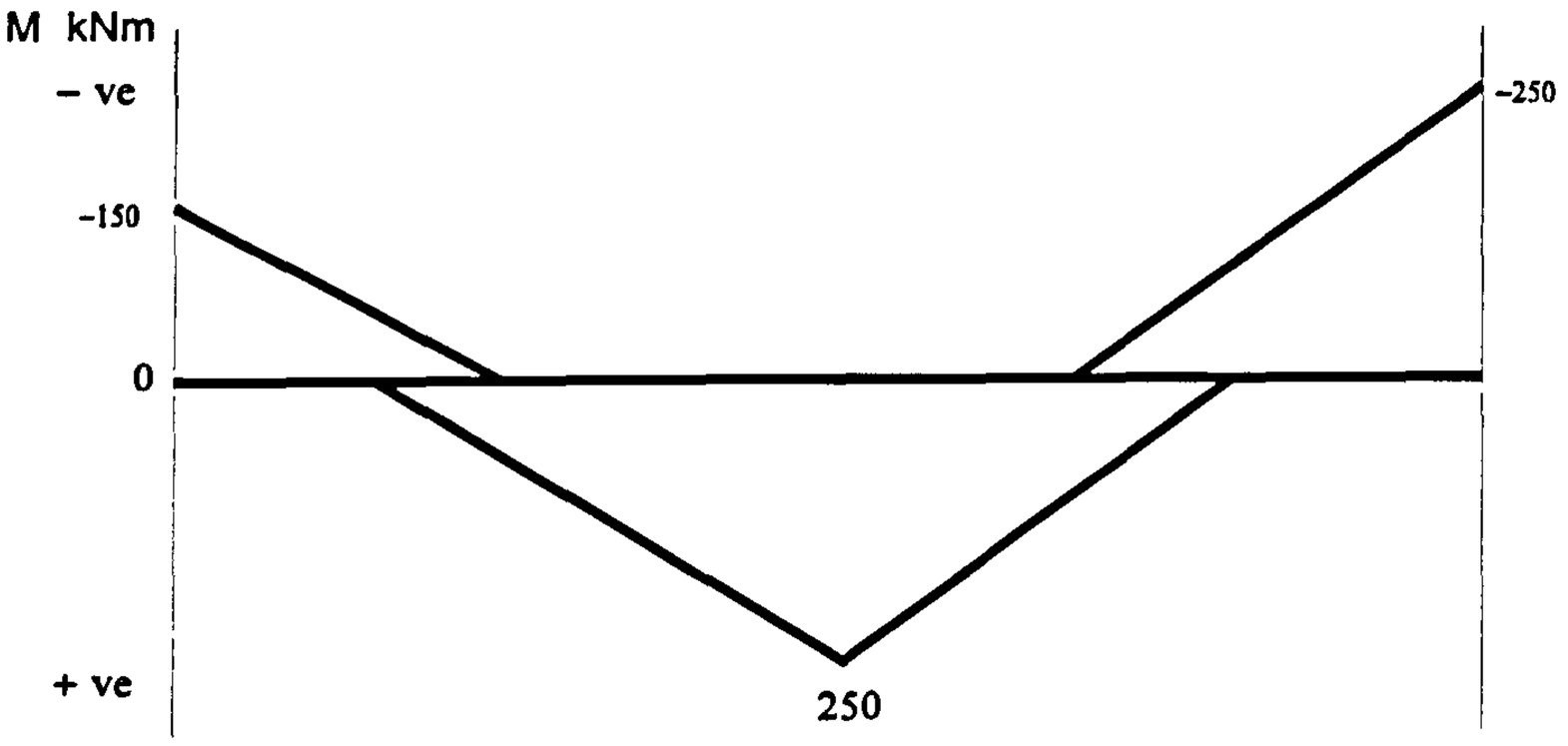

(c) Ultimate Bending Moment Envelope

Figure 2.1.3

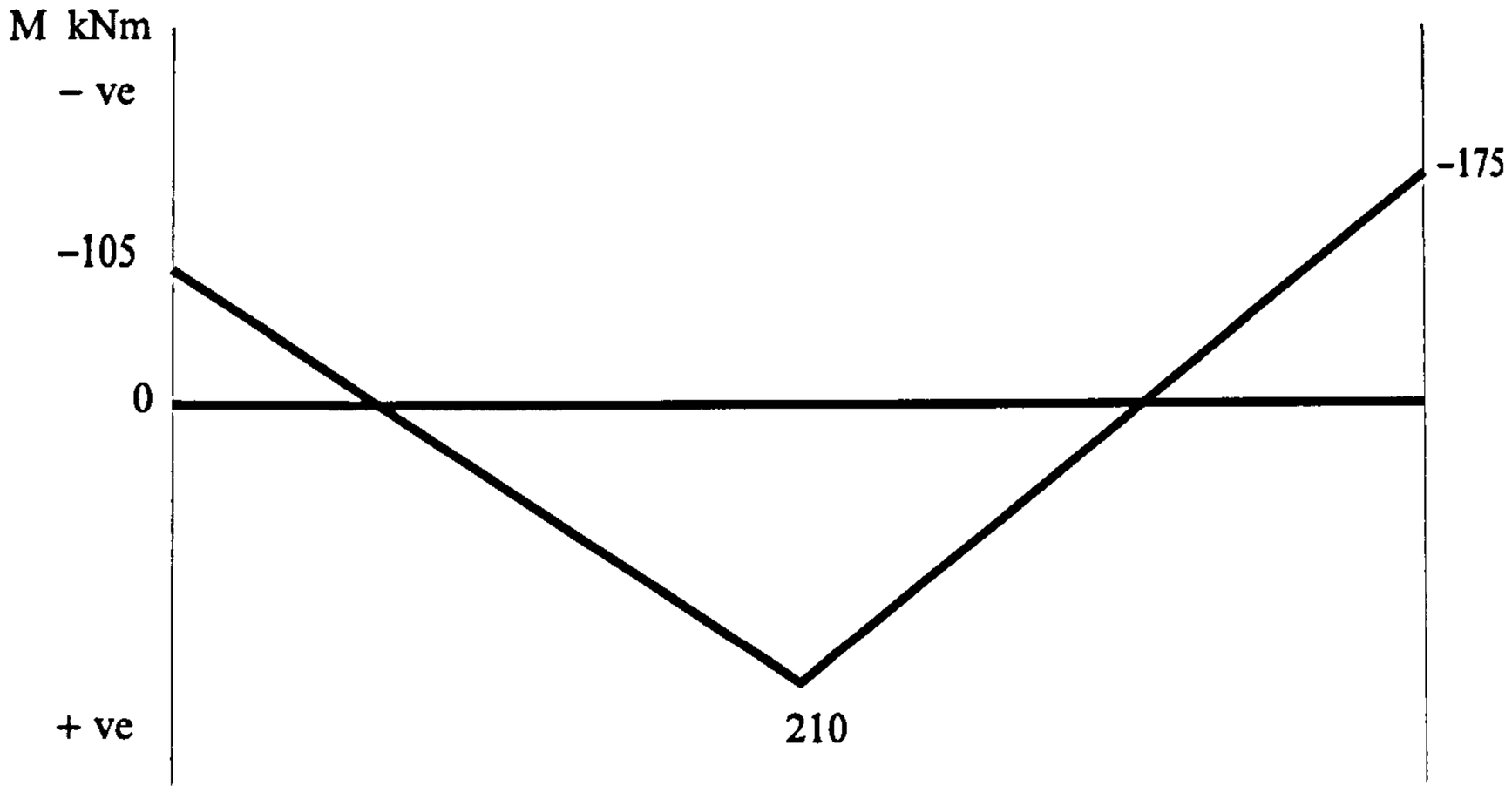

(a) Reduced Support Moments

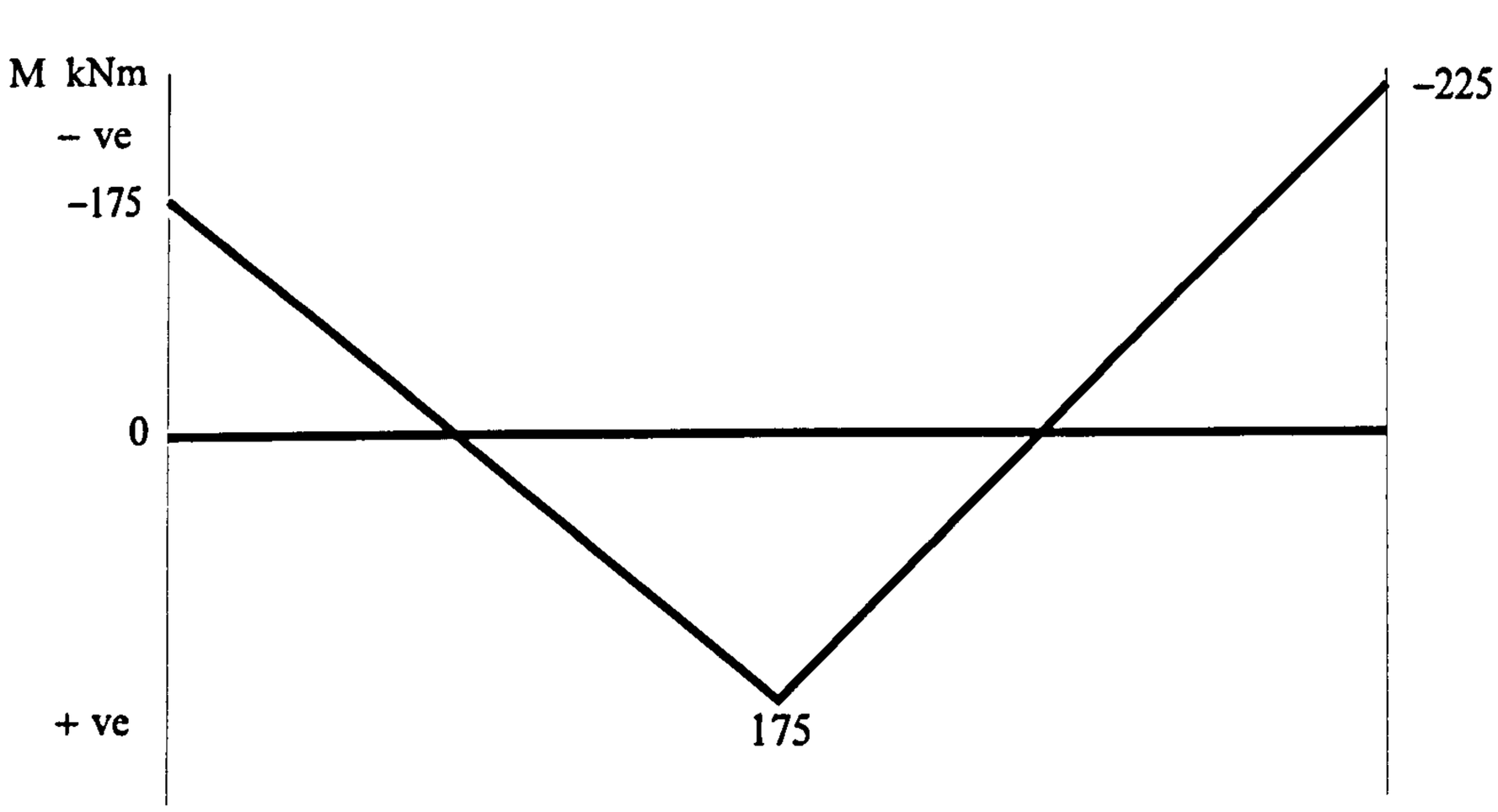

(b) Reduced Span Moment

Figure 2.1.4.

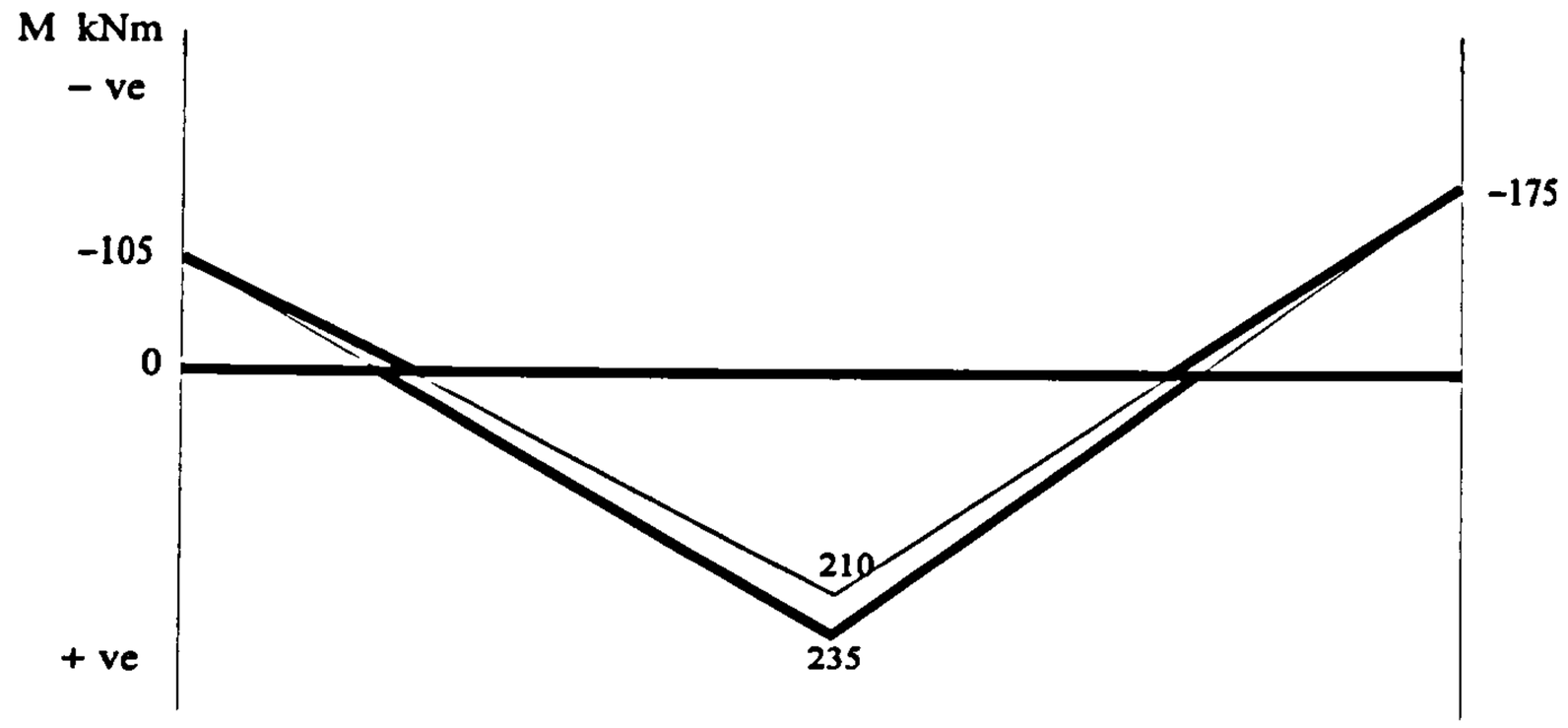

(a) Redistributed Bending Moment Envelope

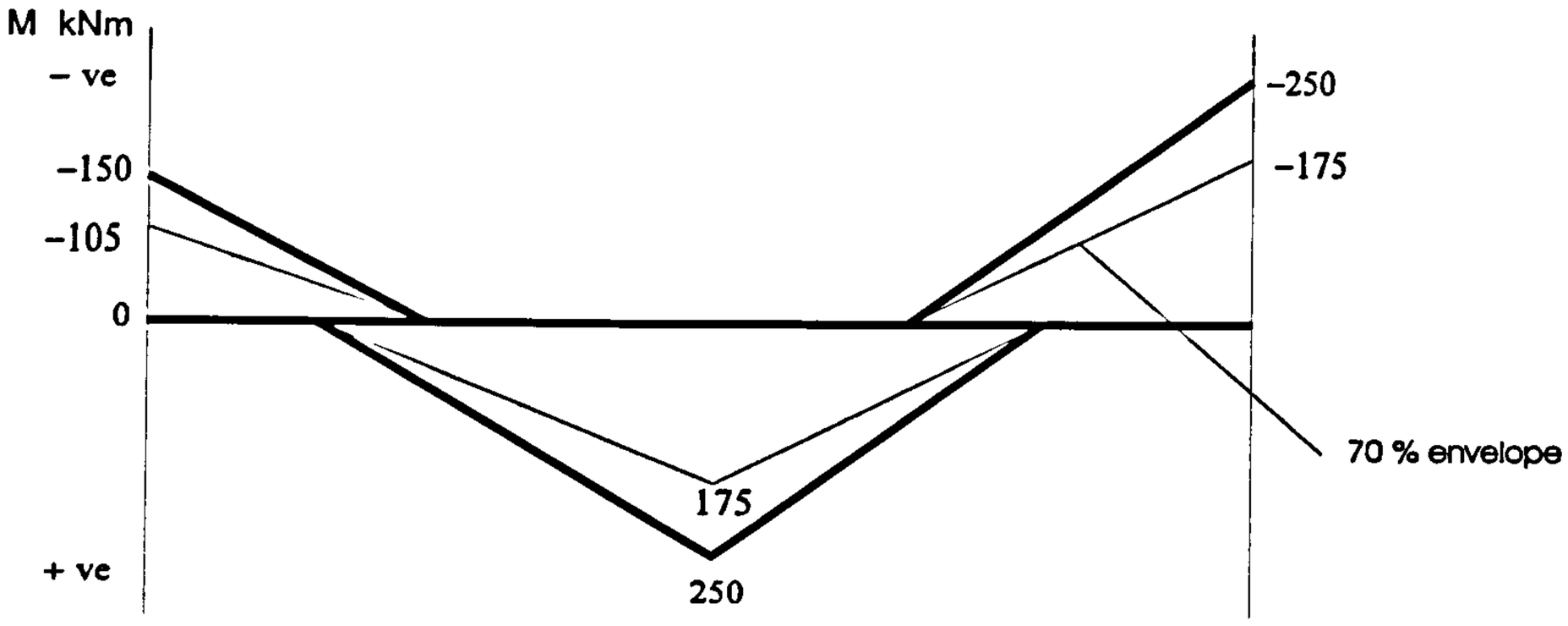

(b) Ultimate and 70 % Bending Moment Envelopes

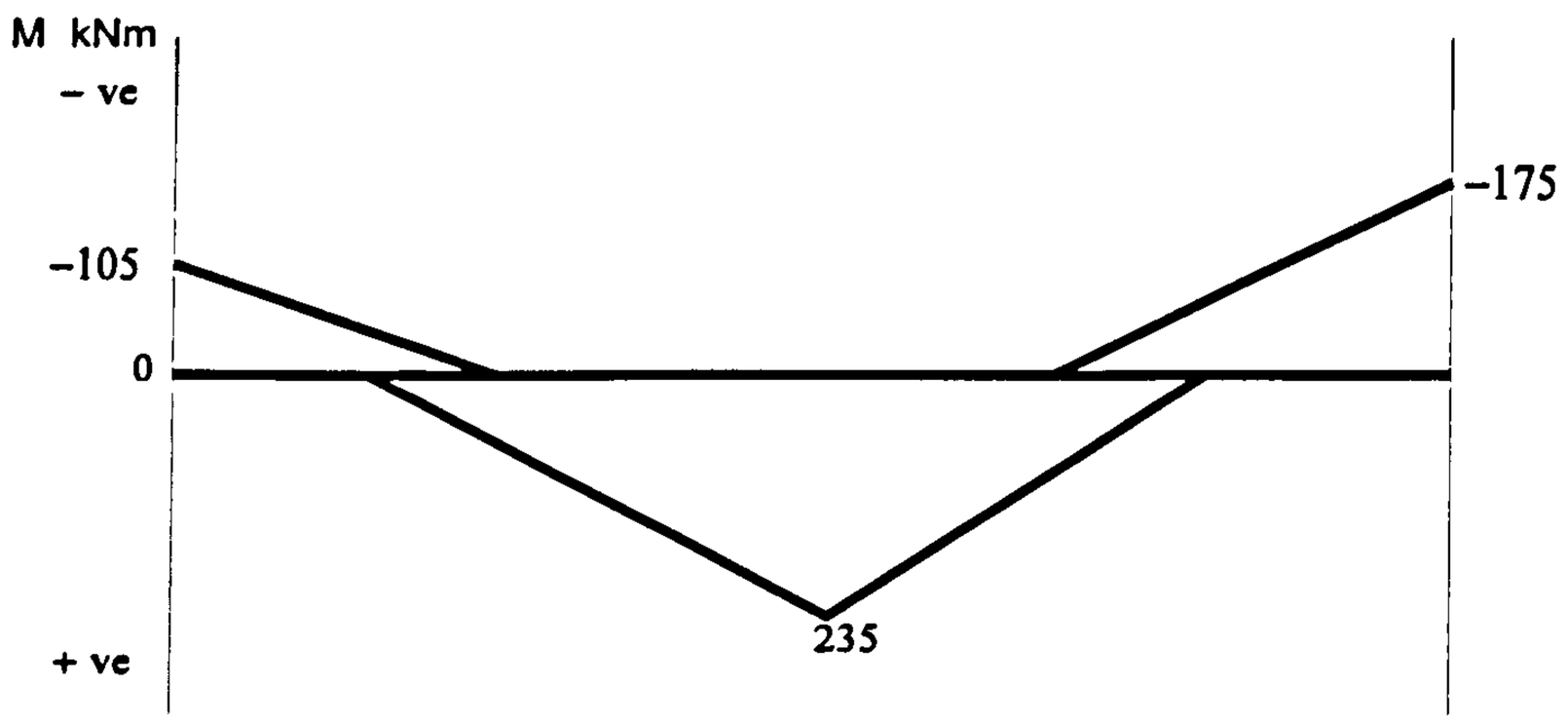

(c) Actual Redistributed Bending Moment Envelope to comply with 70 % line

Figure 2.1.5.

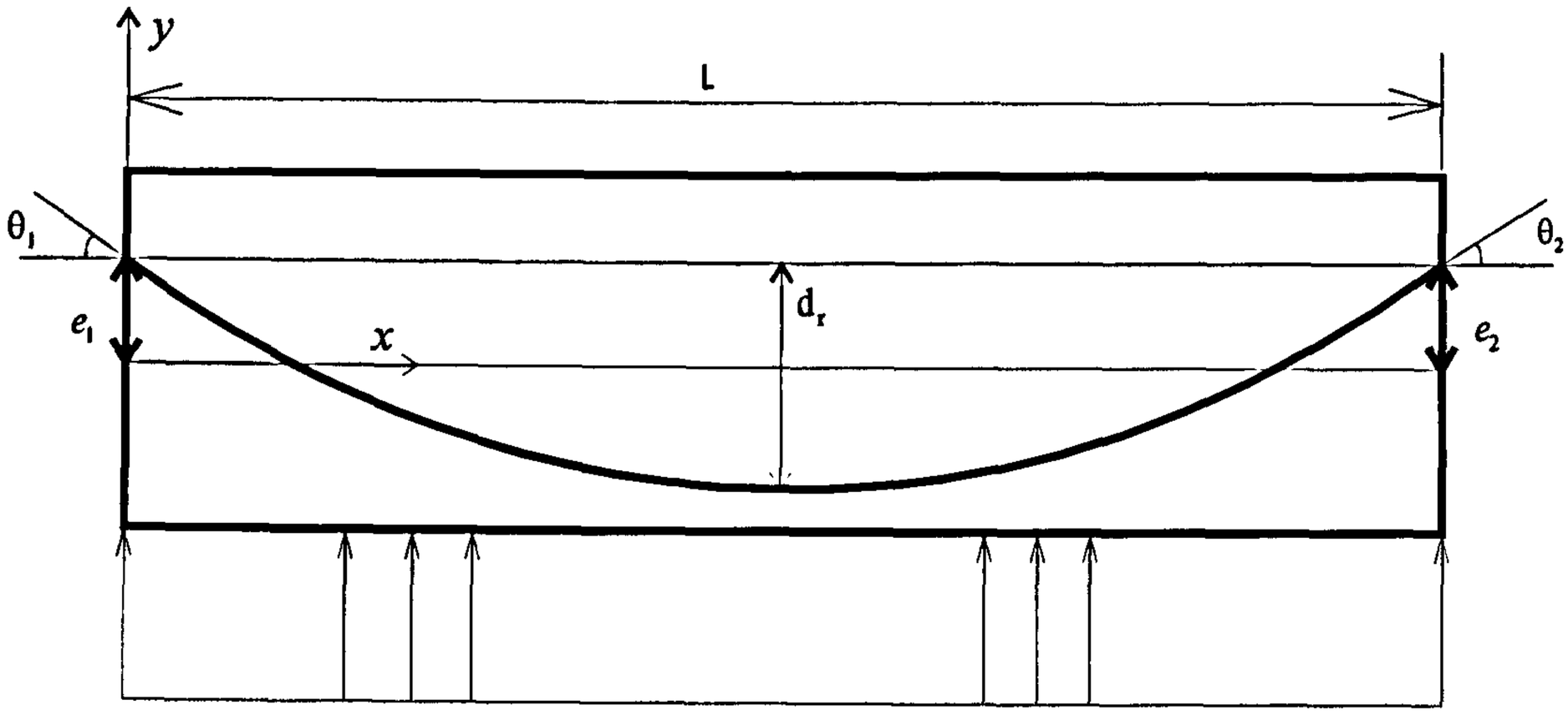

$$w = -\frac{8P\,d_r}{L^2}$$

Figure 2.2.1. Simply Supported Member withContinuously Curved Parabolic Tendon Profile

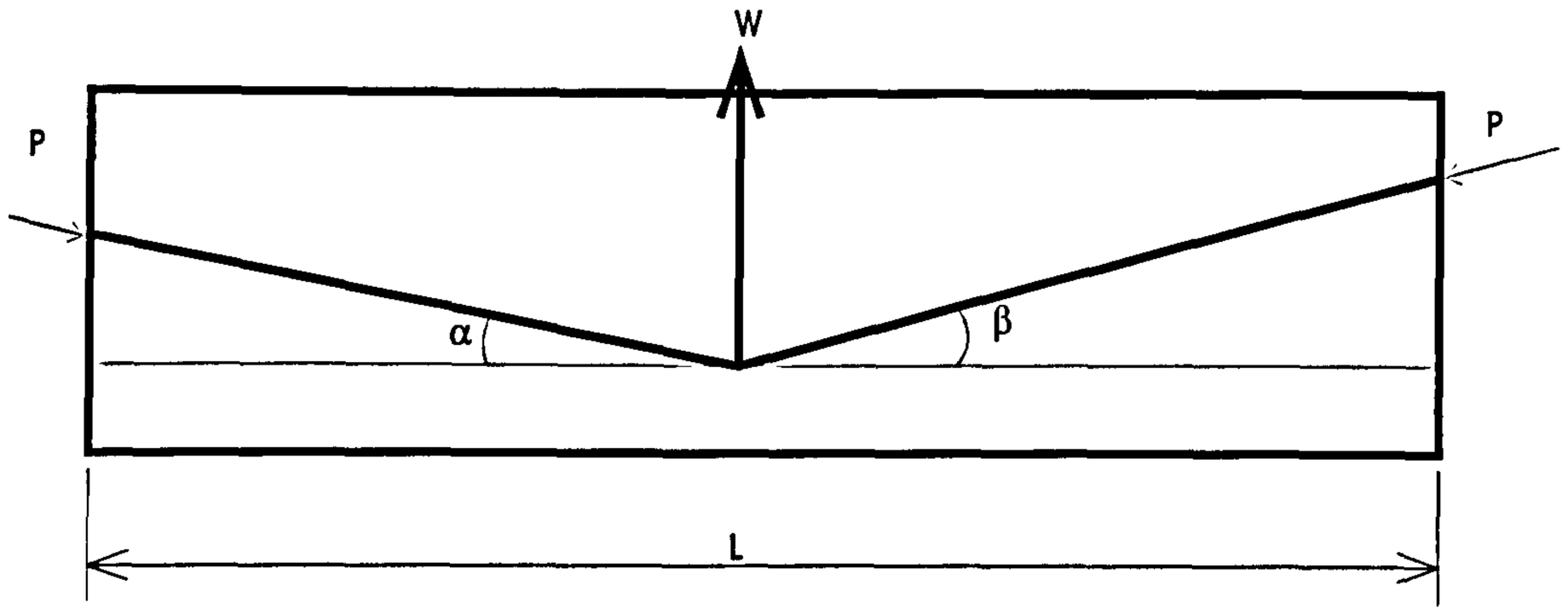

Figure 2.2.2. Sharp Changes in Tendon Profile

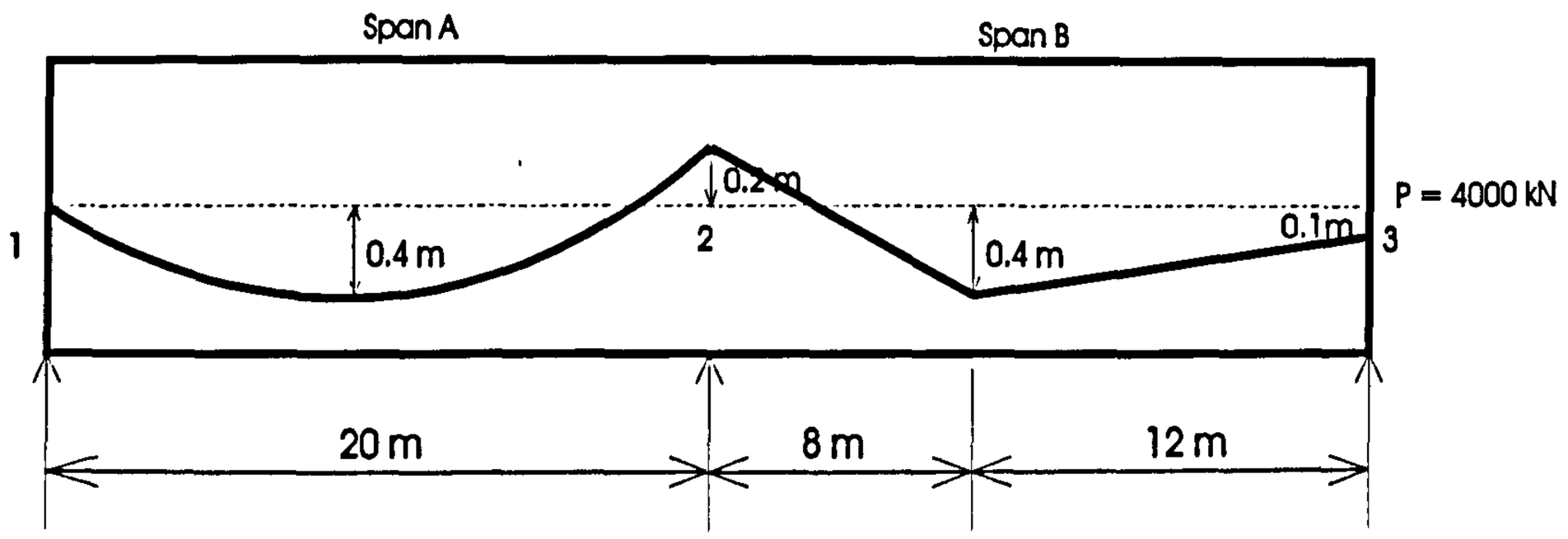

Figure 2.2.3. Two Span Continuous Beam

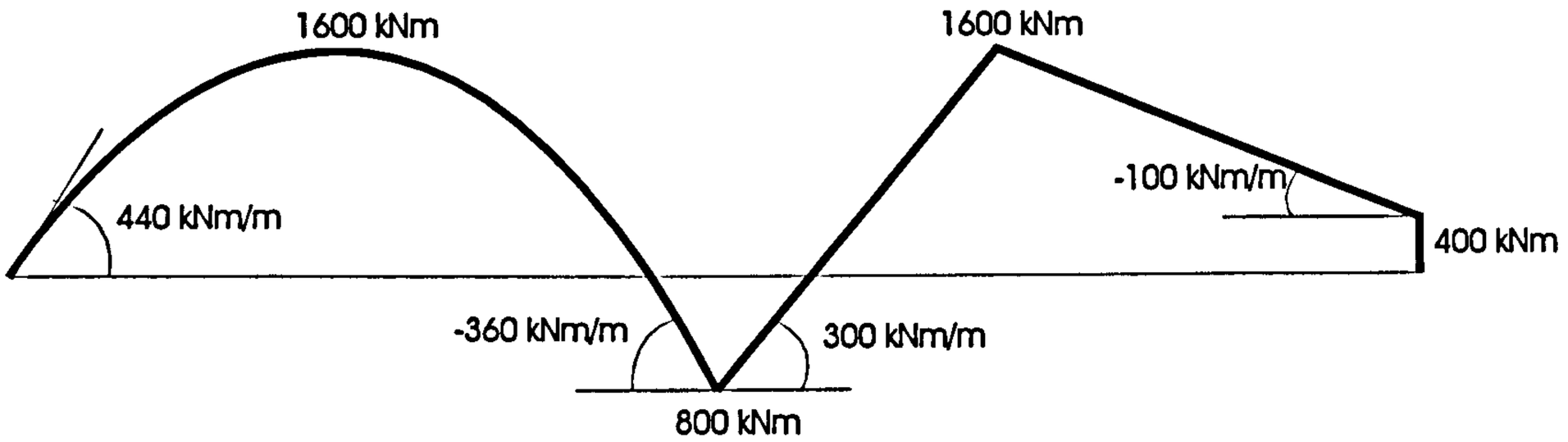

(a). Primary Moment Envelope, M1 (Prestress Force x Tendon Eccentricity)

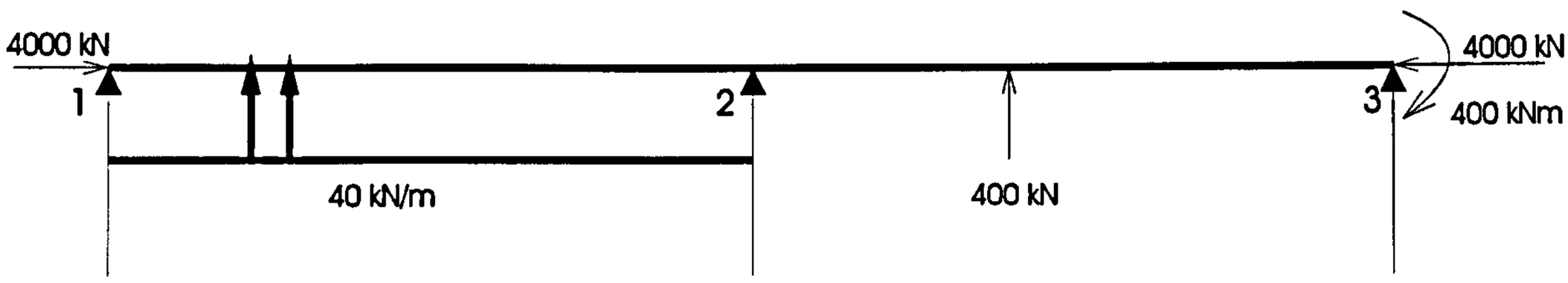

(b). Equivalent Transverse Loads caused by Prestressing

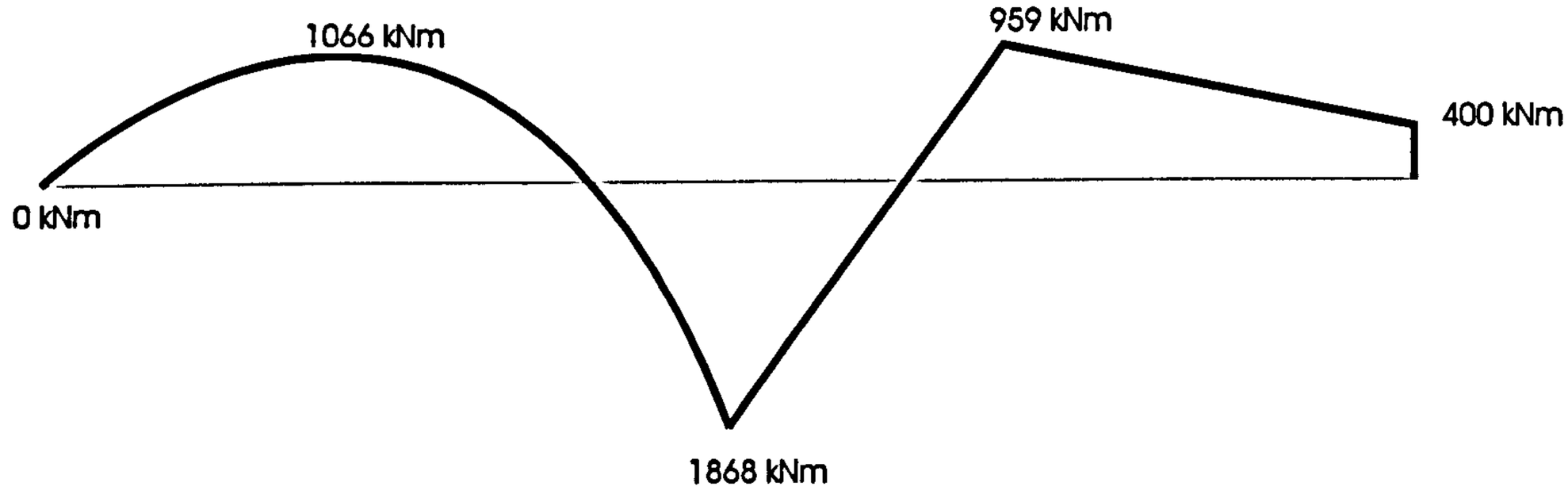

(c). Resultant Moment Envelope, M3 (from Moment Distribution)

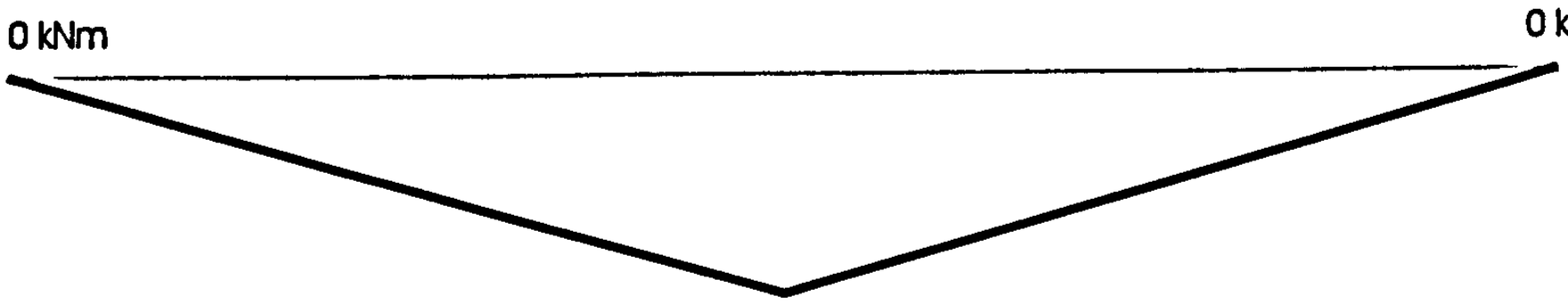

(d). Secondary Moment Envelope, M2 (= M3-M1)

Figure 2.2.4.

3/ Finite Element Analysis of P.C and R.C. Structures

The finite element method provides a powerful tool for analysing a vast range of engineering problems, especially in the field of Structural Engineering. Many texts have been produced regarding the various finite element techniques and their applications, Scordelis [39], accompanied by the production of computer software which is produced commercially for both specific purposes and general applications. There has been an increased interest in the analysis of reinforced and prestressed concrete using finite element techniques over the last twenty five years, and work in this area has yielded many valuable results in comparison with laboratory tests, although codes of practice for design are still largely based on empirical data. Compared with the application of well established theoretical methods which may include approximations for various properties, the actual behaviour of a structure can be analysed more accurately using well constructed finite element models, justifying their use in a large amount of modern structural research. There is no perfect substitute for experimentation, but the finite element method is probably the best alternative, and in most cases when it takes far less time, effort and expenditure for modelling a structure using this method, it has distinct advantages.

There are a number of factors associated with the analysis of R.C. or P.C structures using finite elements which complicate the process and these require correct modelling . Nonlinear stress-strain relationships for both the steel and the concrete must be considered, together with the anisotropy of concrete, i.e. it is strong in compression, weak in tension, and will crack and crush at particular load levels causing a change in the stiffness matrix. The composite action of the steel and the concrete is created by direct bond in ordinary reinforced, pretensioned, and post-tensioned grouted members, whereas with unbonded tendons, this is done by the anchorage and friction transfer stress, so a means of modelling these bond characteristics must be determined. Correct application of the prestress, representation of the load, boundary conditions, and discretization of the elements in the model are also of importance.

3.1/ Review of Previous studies involving Nonlinear analyses of R.C. and P.C.

In the late 1960's a number of researchers were beginning to explore the possibilities of using finite elements to aid in the design and analysis of reinforced concrete.

Mufti et.al. [21], investigated the use of finite elements for the analysis of reinforced concrete, creating a computer programme using two-dimensional triangular elements for both the concrete and the steel, with an incremental loading procedure for the non-linear

analysis. A similar process was used to account for the non-linear bond stress-slip properties. Cracking was included by stopping the analysis and effectively deleting the cracked element concerned from the global stiffness matrix by making its thickness zero. In this particular study this was done automatically, eliminating the need to stop the program, alter the boundary conditions, and restart the analysis from zero load, as for earlier work. Bond linkage elements were used to connect the steel to the concrete, using bond-slip relationships suggested by Nilson in an A.S.C.E. State of the Art Report on Finite Element Analysis of R.C. Structures, [40]. Time dependant properties such as creep, shrinkage and steel relaxation were also included. The results were good, indicating the usefulness of finite elements in the analysis of reinforced and perhaps prestressed concrete.

This State of the Art Report on the Finite Element Analysis of Reinforced Concrete, [40], describes various techniques in the modelling of reinforced concrete using finite elements. Nonlinear analyses, both material and geometric, are discussed in detail, as are the failure criteria of the concrete, bond representation and shear transfer. Three different methods of modelling the reinforcement are dealt with; a distributed representation combined the concrete and steel in a constitutive relation, effectively distributing the steel within the concrete matrix, specifying an orientation for the reinforcement and assuming full bond; isoparametric elements were produced which effectively embedded the steel as an axial component in the concrete element (forming a composite element), with compatible deflections of each material within the element thereby assuming full bond; discrete modelling of the steel by one-dimensional spar or beam elements attached to the concrete, allowing any prestress to be modelled by an initial strain, and bond stress-slip relationships applied through linkage elements. The latter method of modelling reinforcement was the most widely used, as this provided more options such as the inclusion of separate axial, bending, and shear for the steel. Bond could be modelled with linkage elements adopting non-linear relationships in orthogonal directions, lumping properties at nodes, or alternatively with interface elements which distributed the properties along the steel concrete interface. Models of common reinforced structures are included, using the techniques discussed in the report.

In 1983, an International Symposium on the Nonlinearity and Continuity in Prestressed concrete addressed the problems of hyperstatic moments with regard to moment redistribution at the ultimate limit state. Papers on similar themes are gathered in the publication with the aim of throwing light onto the current problems by use of modern nonlinear techniques, including finite elements. Volume 2 of the 3 volume series deals directly with the problems of nonlinear analyses of continuous structures, and includes the following three relevant papers :

Levi et.al., [41], attempt to study the behaviour of prestressed continuous beams by the 'deformation method', analysing a T-section beam of fine mesh subject to an increasing externally applied load up to ultimate limit state, including prestress effects. The deformations (curvature etc.) were calculated at each load step, using an iterative procedure to ensure compatibility and equilibrium. Results suggested that the secondary moment is not affected substantially up to the ultimate limit state.

Cauvin, [42], outlines a similar nonlinear analysis, including cracking, tension stiffening, and plasticity, treating the hyperstatic effects of prestressing as action effects or equivalent loads. Time dependant effects such as creep and shrinkage were also included. His results suggested that hyperstatic effects decrease as the beam stiffness decreases due to cracking , although he does point out the lack of comparisons with experimental work at the time.

Scordelis [39] and [43], outlines computer models which can be used for the nonlinear analysis of reinforced and prestressed concrete structures. Material and geometric nonlinearities are incorporated, with pretensioned or post-tensioned bonded or unbonded tendons. A number of time dependant effects such as creep, shrinkage, and relaxation of the prestressing steel are also included, along with a full description of the numerical formulations involved in the solution. This spawned a number of computer programmes using these proposed computer models, with specific elements developed for the modelling of particular prestressed structures, as part of a major research programme at the University of California.

One of these programmes PCFRAME which analyses reinforced and prestressed concrete planar frames, beams, and columns was used by Campbell, [23], to investigate the failure loads of two-span continuous beams with various load patterns, nonprestressed reinforcement and prestressed tendon profiles. From the results of the analyses, two parameters, one for the quantitative measurement of moment redistribution available, and another which gave consideration to the secondary moment in the analysis, were put forward for use in calculation of the load carrying capacity of prestressed two-span beams. A subsequent comment by Mattock, [44] suggested that a number of the beams in the study did not conform with the American design codes, ACI 318-83, and that a similar parameter for measuring available redistribution had already been defined by Bennet, [31]

Campbell, [29], describes the continuation of the research at Queens University in Canada, where a curvature incrementing technique was used for the nonlinear analysis of

prestressed concrete continuous beams. A macroscopic model was used in this instance, and the nonlinear analysis carried out by incrementing the curvature of a predetermined critical section, having already calculated the moment curvature relationships for each segment of the structure. An assessment of the acceptable aspect ratios of the macroscopic segments at critical sections revealed that a ratio of width to depth of zero would yield exact failure loads, but as this was not possible, a range of 0.2 to 0.4 was acceptable for the prediction of the beams behaviour, compared with empirical data.

Seraj et.al., [22], carried out nonlinear finite element analyses of prestressed concrete members, using a three dimensional finite element package, designed specifically for reinforced concrete. The prestress in this case was applied as an equivalent load, and the corresponding portion of the steel stress-strain curve removed to take account of this. Results from these tests were favourable with a design procedure based on an analysis of the trajectory of the compressive force path (CFP) in the concrete, suggested by Seraj.

A great deal of more recent work involving the application of finite elements, specifically to reinforced or prestressed concrete structures, attempts to refine the ideas mentioned in the previous references, presenting solutions to various individual problems. One such problem, when dealing with prestressed concrete is the curved profile of the tendon. Straight steel profiles either prestressed or non-prestressed can be easily attached to the regular concrete mesh, whether horizontal or inclined at an angle. When the profile is curved, this requires either the concrete mesh to be irregular so that the steel profile can be 'picked up' by the concrete nodes, a situation which is not desirable, or the creation of a very fine regular concrete mesh, causing increased computer solution time and expense. El-Mezaini and Citipitoglu, [45], have presented an isoparametric element of which the edge nodes may be shifted to coincide with the line of the tendon profile. Hence, the concrete mesh may be created first, regardless of the profile, and then the edge nodes are moved to the desired profile, followed by the attachment of the steel. Application to a few examples with continuously curved tendon profiles yielded good results.

A number of general purpose finite element computer software packages have evolved such as ANSYS, [46], and have been constantly upgraded since their production, as the technology of finite elements grows. Many incorporate specific elements in their libraries for the analyses of particular problems such as the modelling of concrete type materials, either singly, or in composite action with other materials, i.e. steel. ANSYS has incorporated a three-dimensional isoparametric concrete element into its library, formulated by Schnobrich, [47]. Each of the eight integration points has the capability of cracking in any of the three principal stress directions which may exceed the maximum tensile stress,

whereupon corresponding alterations are made to the material property matrix. If the concrete reaches its maximum strain, crushing will take place at any integration point where this has occurred, and the material property at this location is set to zero. The element also includes a variety of other features, including distributed modelling of reinforcement if necessary in any direction within the concrete matrix.

In this research, the ANSYS finite element package has been used to model prestressed concrete simply supported and continuous beams of various profiles, in an attempt to shed light on moment redistribution and secondary moments up to the ultimate limit state.

3.2/ ANSYS Overview

The software package ANSYS, [46], produced by Swanson Analysis Systems Inc., is one of the leading general purpose finite element programmes available to both educational and commercial establishments. The programme has a comprehensive menu driven system with general and time-history preprocessors for model creation, solution phase, and general or time-history postprocessors for viewing, analysis and manipulation of the model solution data. An overview of version 4.4a is described here.

After execution of the main program, the user enters the routine begin level of ANSYS, and the menu overlay may then be either turned 'on' or 'off' depending on the users preference and familiarity with the program commands.

3.2.1/ Preprocessor

On entry to the general preprocessor (PREP7) from the routine begin level, the type of analysis is first selected, i.e. structural, thermal, static or dynamic etc. A large element library becomes available with general 1, 2, and 3 dimensional elements, and elements designed for specific purposes, each with their own individual accession or 'STIF' number. The next step is to select all the element types to be used in the model. During their selection, a number of key options are specified for each element type to define certain properties specific to the element in question, such as control of solution printout, or control of element physical properties. Real constant sets are then created, each with their own reference number, for use with these elements to define additional information about their geometric characteristics. Linear material properties are defined with reference numbers for each material, specifying each property, (such as elastic modulus) for a particular material. When a nonlinear stress-strain relationship is required, the form and hysteresis characteristics of the stress-strain graph are defined in a nonlinear table for the material, entering co-ordinates of points on the curve in the appropriate location in the table.

Having already planned out the desired finite element mesh, the nodes are generated first. Cartesian, cylindrical polar and spherical polar co-ordinates systems are available for input of these nodes, with facilities for defining local and global systems. The first 'set' of nodes are normally created such that subsequent node creation can be carried out by a generation procedure of the primary set, assuming the mesh has been well constructed in such a manner as to allow for this. Automatic meshing for more complicated models is also available. With all the nodes created, an element type, an associated real constants set, and a set of material properties are selected for the subsequent assembly. The elements are formed

by assigning them to the correct nodes in a predetermined order. Again, as with the nodes, elements may be generated from an initial pattern. To change an element type or any of its properties, the selection of the appropriate reference number of a real constant set, material property set, or element type will facilitate this. Once the model has been created, boundary conditions and applied loads must be defined. Boundary conditions may be entered at set displacements in the active co-ordinate system, or as constraint equations, thereby allowing an analysis by the specification of a prescribed displacement rather than by direct loading. A variety of external load application is available. Pressures over element faces, point loads at nodal locations, and accelerations coupled with specific material densities provide several means of direct loading.

The data required for the solution phase is written to a file (either file 27 for a linear analysis or file 23 for a nonlinear analysis), and the preprocessing database is written to file 16. This file may be saved for future resumption of model preparation in the preprocessor. Alternatively, each time the preprocessor is used, an ASCII text file, file18 is written with a record of all of the commands for that particular session. This file may be run through the preprocessor so as to create the file16, and as file18 is generally smaller than file16, it is normally more convenient to save or create this text file.

3.2.2/ Solution Phase

After exiting from the preprocessor, the solution phase is initiated at the routine begin level. For a static linear analysis the correct file (either 23 or 27) is input directly by issuing the command 'INPUT 27', and the solution begins. If the menu is in operation, only a limited amount of solution information is displayed, so if the menu is turned off before the solution phase is entered, the progress of the solution can be monitored, which is especially useful if the analysis is nonlinear. Once the solution procedure has finished (converged), and completed the last stress pass, the user is prompted for input of a file (file23) containing the next load step information. This is necessary only for nonlinear analyses, so the FINISH command can be issued to return to the routine begin level. During the solution phase some large files are created on the default directory. File12 contains all relevant solution information for analysis using the postprocessor, and file02 and file03 contain model restart information before and after the last stress pass respectively. If more load steps are required, file03 is necessary for continuation of the analysis using the restart procedure. Other large files contain geometry and triangularized matrices used for the solution process only, and may be discarded.

For a linear static analysis the model will require only one pass in the solution phase for the correct answer, and before exiting from the preprocessor, the solution file27 is written for input for the solution phase. For a non-linear static analysis, a number of iterations will be required to ensure equilibrium, and to account for the effects of plasticity, geometric nonlinearity, and element specific nonlinearities. Also, it may be required that loading occurs in a number of steps of limited size to progress toward a converged solution for a particular load level. Therefore all of this subsequent load step data must be recorded before exiting from the preprocessor. Preprocessing data for the very first load step is saved to file27. Preprocessing data for subsequent load steps must be written to file 23. Assuming that an analysis has already been started, and a file03 exists on the directory ANSYS is currently using, then from the routine begin level the '/LOAD' command can be issued to continue the analysis, and then by typing 'INPUT 23', this will initiate the solution phase again.

3.2.3/ Postprocessor

In the general postprocessor, the required load step number and iteration are set, and file12 is read into the programme. There are a number of advanced techniques for visualising the data graphically, i.e. stresses may be plotted as raster or vector contours superimposed upon element plots, which can be viewed from any desired angle. Comprehensive lists of data may be compiled for viewing graphically or in its raw form, and a certain amount of data manipulation can be performed within the postprocessor, such as summation of forces or moments about specified positions in the model. All data associated with each element has a specific postdata number allocated to each data item, which may be specified and labelled for analysis. Certain 'levels' of data are default for each element and common data may be viewed without any prior preparation. Other data which is rarely needed, is stored on higher data reference levels, and can be stored on file12 by issuing a data level storage number for the element type in question, in the preprocessor. This data can then be accessed by allocating a label to the specific postdata item number in the postprocessor.

3.2.4/ Batch Processing

As mentioned earlier, file18 provides a means of recalling and inputting the programme commands of a preprocessing session for recreation of the file16 containing model data. This is the basis of batch processing in its simplest form, where a set of commands are entered into a text file and executed in sequence. Hence, with enough familiarity with the necessary commands, the preprocessing, solution phase, and postprocessing can be accomplished in one run, by the creation of a text file containing these

commands. Solution data may also be rerouted to a text file from within ANSYS, or externally using the batch process.

3.2.5/ Suggestions on Running a Nonlinear Analysis with ANSYS Version 4.4a

It is important to understand the fundamentals of the use and operation of the ANSYS 4.4a program, as insufficient knowledge can lead to problems, especially with a nonlinear analysis. The size of the model, i.e. the number of elements and nodes created within the preprocessor, will directly affect the size of the model solution file 12, and restart files 2 and 3. These are the largest files to be created, together with temporary scratch and virtual memory swap files which ANSYS uses whilst it is running, therefore a hard disk (or local filestore of some description) must have the capacity to cope with these files, otherwise the analysis will break down during the solution phase. This can prove both time consuming, as the analysis has to be repeated for the load step in question, and disastrous if the model information file 3 (or file 2) for the previous load step has not been saved, thereby requiring the total restart of the analysis from the first load step. If only limited information is needed at the solution of each load step, this can be extracted from file 12 using the postprocessor, and then file 12 can be discarded. Otherwise it is sensible to create a backup library of file 12's, and in any case, have a running backup of the file 3 corresponding to the last load step. This can be done using removable disks or tape streamers. Experimentation with load step sizes is required at various load levels, so careful batching of load steps is required if more than one load step is to be performed in one solution phase, as any breakdown will require restart from the first load step of the batch.

To monitor the progression of the solution of a nonlinear analysis, it is best to turn the menu off, as this will allow the user to view the solution information such as convergence data for all nonlinear elements and properties, as the solution progresses. Therefore if at an early stage the solution appears to be non-converging, the analysis can be stopped and restarted with a smaller load step. With the menu on, the user has no idea as to the progression of the solution, and no estimate of when the solution will finish, so that it will be difficult to enter the next load step promptly. These problems have been addressed with ANSYS version 5.0.

3.3/ Nonlinear Finite Element Analysis

With many physical problems, linear relationships provide an adequate means of solution, especially with regard to structural mechanics. However, there are some situations in which nonlinear effects must be considered, such as when significant stiffness or geometry changes occur, or perhaps buckling and time dependent effects may be present. Two of the main nonlinearities to be considered in the finite element analysis of prestressed concrete beams using ANSYS, material and geometric, have specific solution methods, and are described in more detail here.

3.3.1/ Material Nonlinearity

A material which has been loaded in a certain way whilst behaving in an elastic manner, has the ability to return to its initial state once the load is removed. Plasticity however exhibits itself as a permanent straining after the yield stress has been exceeded, so that when the load is removed or perhaps reversed, this permanent straining affects how the stress-strain curve behaves from that point onwards. This is important when plasticity causes redistribution of the load to the stiffer sections of the structure, as load reversal may occur in those parts which have become plastic. In other words, the application of the load is path dependent, the manner, magnitude and increase to the desired final load must be the same as that for the real structure. Load must be applied slowly in small increments to ensure that spurious permanent plastic straining does not occur, as this will affect the relative behaviour of the structure at higher loads. The standard procedure for the nonlinear analysis is to first apply a load so that the section of the model which is most highly stressed is near the yield stress, but still in the elastic range. Small increments of load, ΔP are then applied, and a solution is obtained for each load step. The solution is recalculated each time with an initial state of stress and strain dictated by the previous load step. Recommended sizes for the increment of load can be estimated as the greater of either $\Delta P = \left(E_{pl}/E\right)P_y$ or $\Delta P = 0.05P_y$, where E and E_{pl} , is the tangent modulus of the stress-strain curve before and after the yield stress has been reached (see figure 3.2), and P_y is the load at first yield. Trial and error is sometimes required in particular cases. For structures where the redistribution of internal loads does not take place, the load need not be incremented in this manner.

The relationship between the applied loads and associated displacement field is represented by the stiffness of the structure in question, usually represented in matrix form. With linear material properties, this stiffness matrix is usually independent of both displacement and applied load, and the structure will behave elastically. If the stiffness and elastic modulus remain constant throughout the loading, then the force-displacement and

stress-strain relationships will be linear, with the gradients of each represented by the stiffness and elastic modulus respectively. When plasticity is to be included in the analysis, this causes nonlinearity in the stress-strain relationship, and hence, the stiffness matrix becomes a function of the displacements. Therefore to solve a problem of this nature, an iterative process must be incorporated in the solution phase.

3.3.1.1/ Example with One Stress Component

A one dimensional example of a bar encastred at its left hand end, figure 3.1, has the stress-strain relationship shown in figure 3.2, and is axially loaded such that the stress in the bar is σ_1, a value exceeding the yield stress of the material σ_y. Using the elastic modulus E to solve the problem, the result will be above the actual stress-strain curve at position B. The strain associated with this result, ε_1, may be split into an elastic component ε_1^{el}, line D-E, and a plastic component ε_1^{pl}, line O-D, separated by line C-D, parallel to O-A, in figure 3.2. To obtain the correct strain corresponding to the stress level σ_1 on the stress-strain curve, a full Newton-Raphson iterative procedure is best suited for this purpose. The basic Newton-Raphson formula for finding the roots of equations, whatever their order, proceeds by formulating better approximations to an initial estimate of the root x, given by equation (3.1).

$$x - \frac{f(x)}{f'(x)} \qquad (3.1)$$

Where $f(x)$ is the function of x, and $f'(x)$ is the first derivative. The process is easily applied to the current problem. In this case, the position where a particular stress level σ_1 cuts the stress-strain axis is to be found. The stress level is known, so the strain ε_1 is the approximation to the root. Referring to figure 3.2, the first iteration gives an approximation to the state of stress and strain at position C, on the curve at a position above the yield stress. For the next iteration, the derivative of the function (i.e. the gradient of the curve, often called the tangent modulus E_T) is equal to E_{PL}, and this produces an approximation which is equal to the actual state of stress and strain at F, hence the solution has converged after two iterations. The tangent modulus E_T of the curve is updated at each cycle depending on the position on the curve of the solution in the previous iteration. Therefore if the stress-strain function consists of piece wise linear portions as in our example, the exact solution can be derived with only a few iterations at a particular load level. The relationship between stress and strain need not comprise discontinuous linear functions but can be of a continuous smooth form of a higher order, although the solution will no longer be exact and as the curve becomes shallower at the higher strains, the number of iterations required for convergence will increase. If the portion of the curve in the plastic range ever becomes horizontal such

that the tangent modulus is zero, this would indicate that the solution would never converge as there is theoretically no solution for the iteration, and full perfect plasticity has been reached. In practice the stiffer elastic parts of the structure attract the load causing a redistribution from the plastic sections, increasing the rate of convergence.

A well used variant of the Newton Raphson method of solution, often referred to as the initial-stiffness method, reuses the tangent modulus of the first iteration for successive iterations, and the approximations to the root are given by equation (3.2),

$$x - \frac{f(x)}{f'(x_1)} \qquad (3.2)$$

where x_1 is the first approximation to the root. Obviously this would mean that the number of iterations required to obtain the final solution is much greater than for the Full Newton-Raphson procedure, although the tangent modulus need only be calculated once in the calculation.

3.3.1.2/ Convergence

To test for the convergence of the solution to within adequate accuracy of the real value, the ratio of the increment in the plastic strain to the elastic strain, $\left(\Delta \varepsilon_i^{pl} / \varepsilon_i^{el}\right)$, is compared to a value which is pre-set at the beginning of the analysis by the user. The default value for this ratio is 0.01, and gives a measure of the distance away from the actual stress-strain curve the converged solution is allowed to be. Thus, for most models, once the solution has converged, all of the integration points will be within this criterion.

3.3.1.3/ Multidimensional Stress Problems

The problem of the single dimensional bar is relatively easy to idealise, with one stress and one strain component in the axial direction, and the stress-strain relationship can be plotted immediately on a set of axes. With solid problems where other stress components cannot be ignored, an equivalent stress and equivalent strain are used to reduce the problem to a single dimension. The stress-strain relationship is then that which exists between the equivalent stress and equivalent strain, and the iterative solution can proceed as before. As there is now more than one stress component present, this allows redistribution of strain between the components, causing an increase in the number of iterations for convergence. It is also evident that at an intermediate step towards a converged solution, although the equivalent stress and equivalent strain would be on the curve, the uniaxial stress and strain

would be above the curve. This has implications for finite element models which use special elements such as the concrete STIF 65 element which allows cracking and crushing at integration points. At an unconverged iteration, the solution may have a stress state causing cracking or crushing (governed by the three principal stresses) which would not otherwise have occurred at the converged solution, hence this requires that the load be applied in small load steps to avoid this happening.

3.3.1.4/ Yield Criterion, Flow Rule, and Hardening Rule

Yielding is initiated at a particular stress level, governed by the Yield Criterion. For a one dimensional problem, this normally states that yielding begins once the stress σ reaches the yield strength σ_y. Any plastic deformation which occurs will alter the stress level at which continued or renewed yielding can take place. With problems of more than one stress component, the equivalent stress is represented as a function of the stress components, $f(\{\sigma\})$. Once the equivalent stress is equal to the material yield parameter σ_y, plastic strains form, which reduce the stress to the material yield surface. The yield surface has effectively grown with the equivalent stress, so that the equivalent stress can never exceed the material yield surface. These yield surfaces can be plotted in stress space (with the principal stresses as the axes), and any stress state which falls inside the surface does not cause plastic strains, and is therefore elastic. Details of these yield surfaces can be found in the ANSYS Manual, [46]

A flow rule relates the increments of stress to the increments of strain. With a single stress component, the stress is related to strain directly by the tangent modulus, i.e. $d\sigma = E_t d\varepsilon$. For multidimensional stress components, the flow rule describes the direction of plastic straining, where $\{d\varepsilon^{pl}\} = \lambda\{\partial Q/\partial\sigma\}$. Q is the plastic potential (usually the yield function, in which case plastic straining occurs in a direction normal to the yield surface) and λ is a plastic multiplier.

To determine how the history of plastic flow changes the yield surface, a hardening rule is introduced. The two main types of hardening are isotropic (often called work) hardening and kinematic hardening, and are shown for a single tensile stress component in figure 3.3. Referring to figure 3.3.(a)., for the isotropic rule, if loading has occurred up to point C only, and has then been reversed, for renewed tensile yielding to occur, $\sigma > \sigma_b$. If unloading occurs into the compressive range, then the stress would still have to exceed σ_b for compressive yielding to occur. Hence the following condition would hold for isotropic hardening : $|\sigma| = \sigma_b$. Kinematic hardening, figure 3.3.(b)., differs in that if loading is reversed into the compressive range, yielding would occur at a stress of $\sigma_b - 2\sigma_y$, thereby preserving

an elastic range of stress of $2\sigma_y$ between the tensile and compressive yield criterion. For problems with more than one stress component, the type of hardening rule adopted will effect how the yield surfaces change with plastic flow. If the yield surfaces are drawn in stress space, the isotropic hardening rule will effectively increase the size of the surface about its axes of symmetry (centreline) as plastic strains develop. The kinematic hardening rule will tend to translate the surface in the stress space rather than alter its size. Details of this and related topics in material nonlinearity are given in Cook et. al.,[15], and the ANSYS Manual, [46].

3.3.2/ Geometric Nonlinearity

As a structure is progressively loaded, it will deform and deflect accordingly. For many structures, the stiffness is such that these deflections are small, and the response of the structure, whilst behaving elastically, is predicted accurately enough by linear elastic theory. With structures of limited stiffness, the deflections can be large enough to affect the equilibrium of the structure. For example, an axially loaded column might undergo sidesway. As the transverse deflections increase, the axial load will increase the bending moments (the $P-\Delta$ effect) and thus the transverse deflections. The change in the geometry of the slender column has altered the behaviour to the extent that the equilibrium equations have become a function of the new geometry. This new geometry is not known at the start of the loading, so an iterative process such as the Newton-Raphson method is adopted to obtain the converged state at which the deformed geometry is in equilibrium with the applied loads.

The details of the algorithms for the solution of both material and geometric nonlinearities by finite elements are not pursued here, but can be found in Cook et. al.,[15], and the ANSYS Manual, [46].

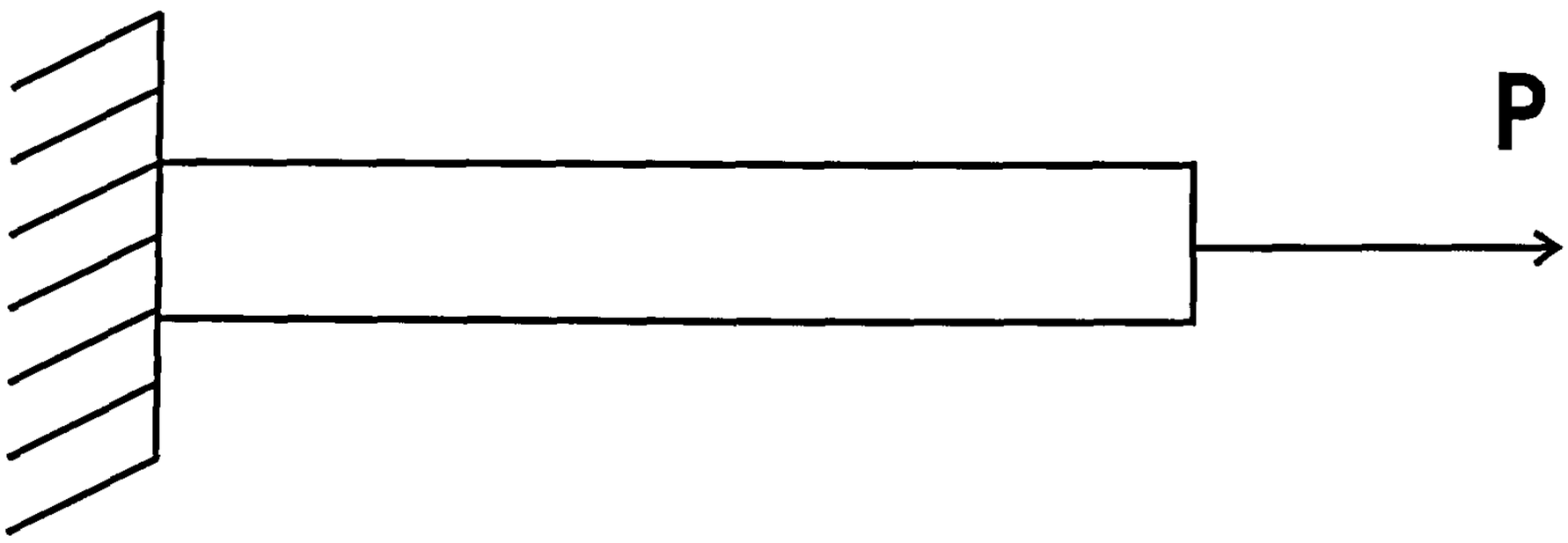

Figure 3.1. Axially Loaded Bar Fixed at Left Hand End

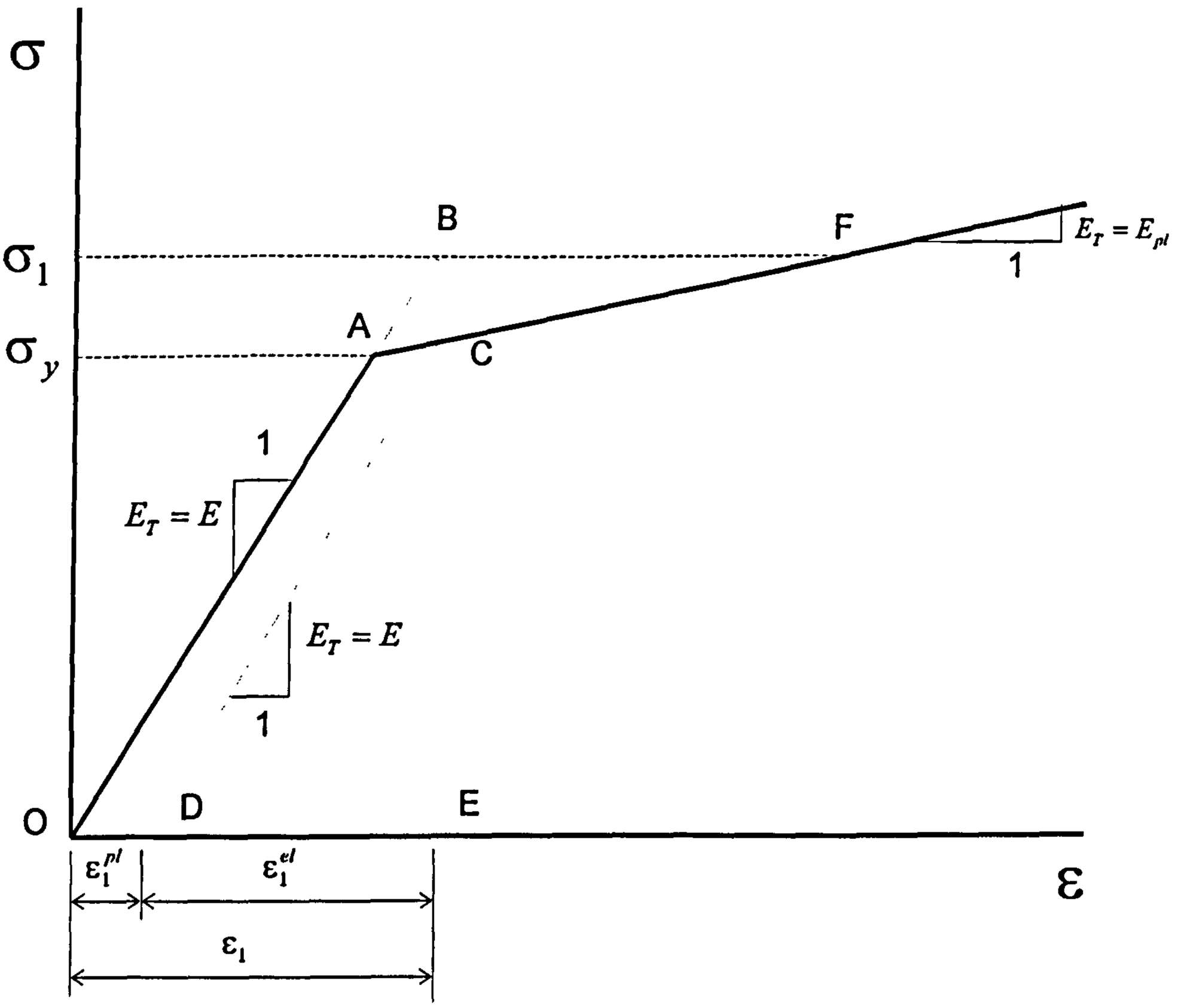

Figure 3.2. Material Stress-Strain Relationship

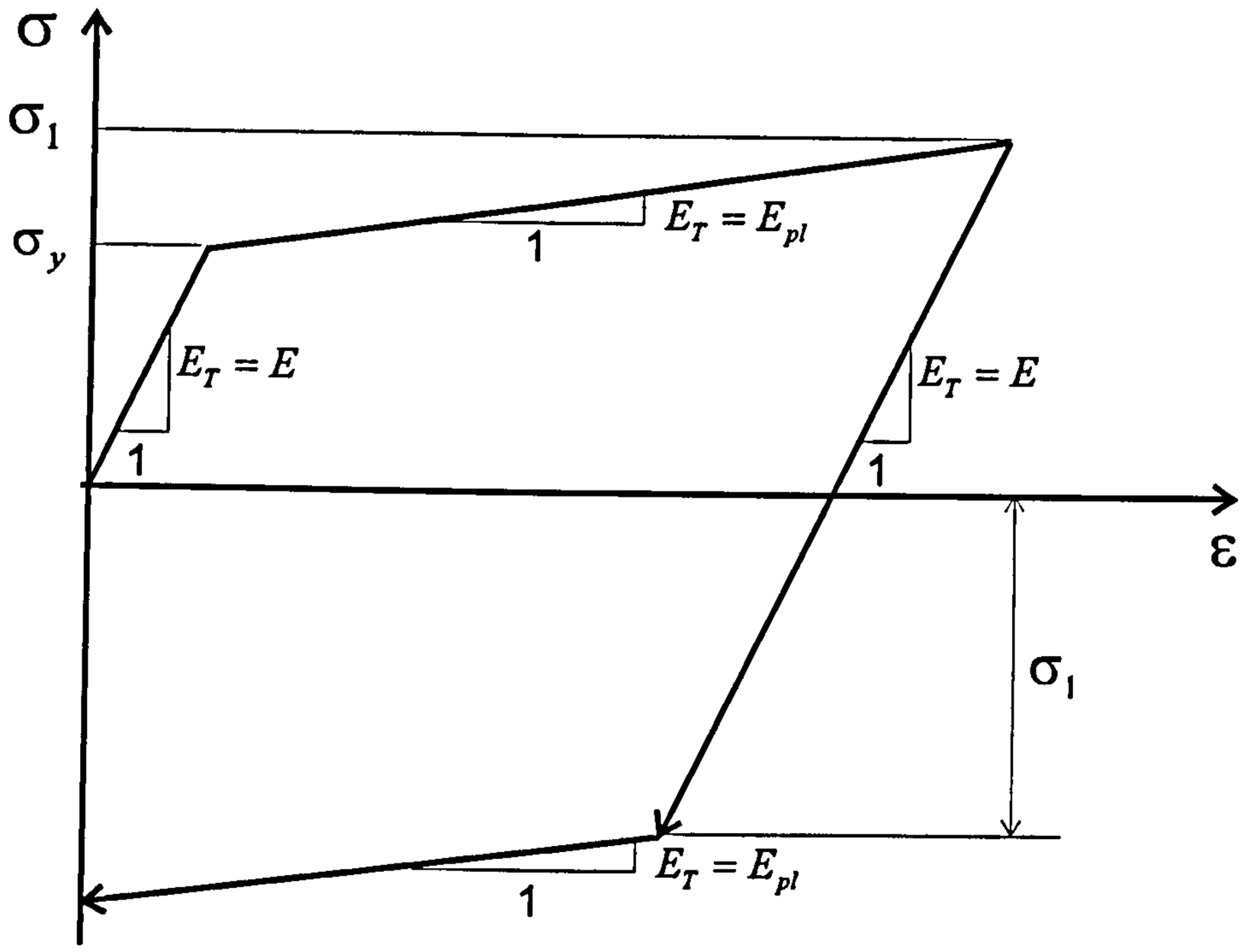

(a). Isotropic Hardening Rule

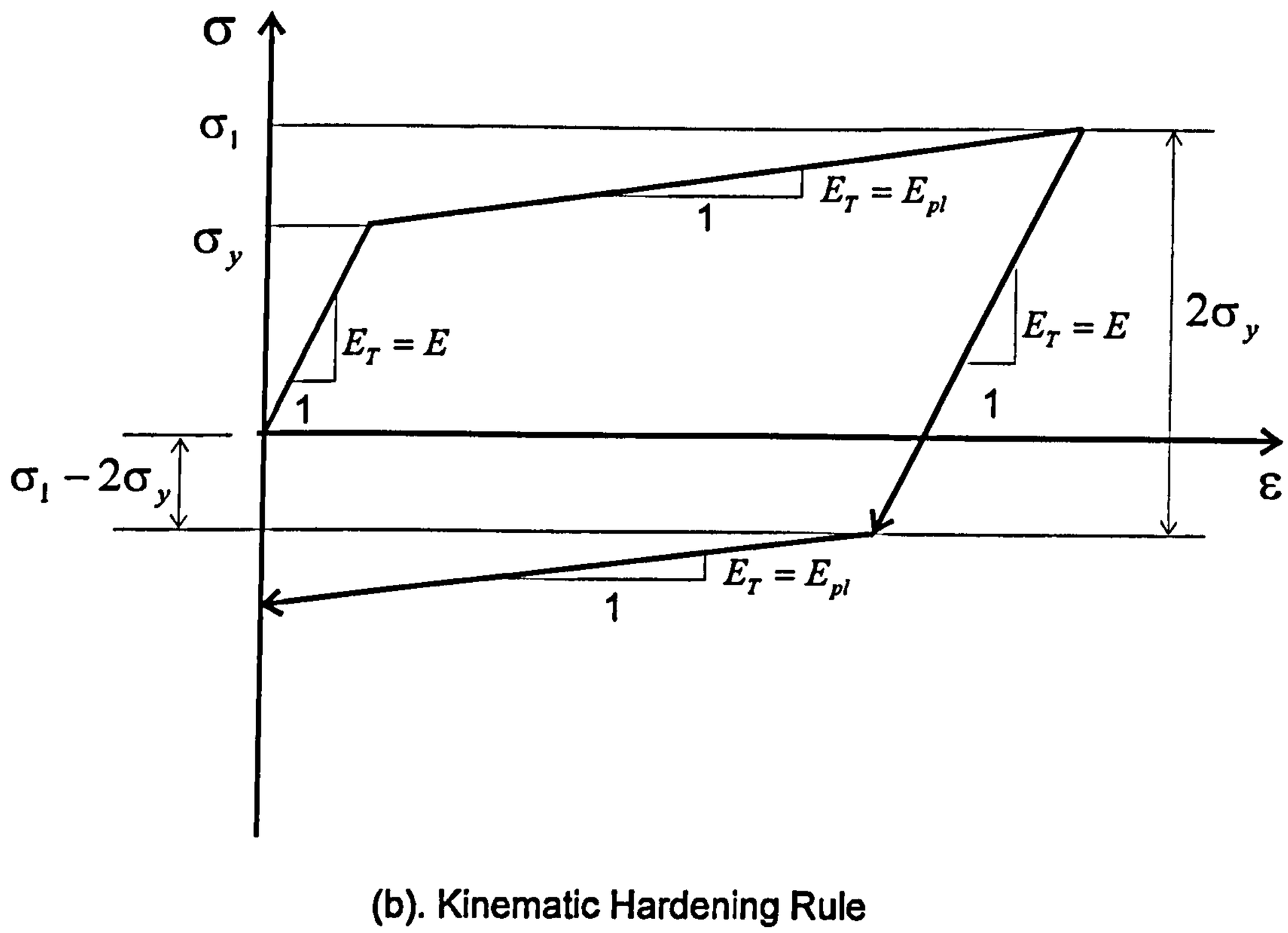

(b). Kinematic Hardening Rule

Figure 3.3. Hardening Rules

4/ Finite Element Beam Models using ANSYS

4.1/ Simply Supported Beam Models

As a forerunner to the analysis of continuous prestressed concrete beams using 'ANSYS', a number of models of simply supported beams, both normally reinforced and prestressed were constructed. These are described in greater detail in Weekes [48].

Rectangular section beams with straight normal reinforcement, or prestressing tendons which were straight or parabolic were used in these models. The main body of the concrete was modelled with STIF 65 three-dimensional isoparametric concrete elements, capable of cracking and crushing at each of its eight integration points, arranged in a rectangular grid fashion as viewed in the beam elevation, and a single column as viewed in the section, with refinement of the mesh in appropriate areas. The representation of the reinforcement and application of the prestress force was experimented with. With a straight prestressed/non-prestressed steel profile, this was first modelled using STIF 45 three-dimensional isoparametric solid elements arranged as a layer in the concrete mesh at the reinforcement level, so that full nodal connectivity was present, i.e. full bond. Figure 4.1.1. shows clearly the type of element arrangement used. Various methods of applying the prestress force through the steel were considered. At first it was applied using direct end forces on the STIF 45 layer. The problem with this was that the forces would not follow the line of the steel as the beam deformed, thereby causing a buckling effect.

The eventual arrangement for the steel consisted of two-dimensional spar elements, connected externally to the concrete mesh at the level of the reinforcement, allowing the prestress to be applied as an initial strain along the whole length of the beam. This also meant that there was no discontinuity in the concrete mesh, as was caused by the STIF 45 layer. The spar elements could be connected directly to the concrete nodes either side of the beam for full bond, or through two-dimensional interface elements so that bond stress-slip relations could be used. Because the steel had to be connected at the same co-ordinate location as the concrete nodes, the shape of the tendon profile dictated the arrangement of the concrete mesh.

At anchorage zones where the stress concentrations were high, the material properties were altered to reinforce these sections. Point loads and point support boundary conditions also caused stress concentrations, so these had to be monitored carefully. Wherever possible, loads were applied as body forces or element surface pressures to alleviate this problem.

Premature failure of some of the beams was traced to the cracking and crushing facilities in the STIF 65 concrete element which had been set to 'on' in the analyses. As discussed in section 3.3.1.3, if these facilities are used in a nonlinear analysis with multidimensional stress components, the solution at an unconverged iteration will lie above the concrete stress-strain curve, which may cause spurious cracking or crushing. Therefore to reduce this affect, the load was applied in small increments. Experimentation with the value at which crushing of the concrete was to take place appeared to produce little variation in the results. The concrete stress-strain curve used in the analyses was based on the design stress-strain curve for normal weight concrete taken from B.S.8110 [50]. The stress-strain curve proposed by Hognestad* probably gives a better representation of the compressive behaviour of the concrete, as the stress actually falls before failure occurs. As the nonlinear procedure of the finite element analysis cannot handle negative gradients in the stress strain curve, it appeared sensible to use the representation given by the code. To help with convergence, the horizontal portion of the curve past the yield point represented by a strain of $2.4\times10^{-4}\sqrt{f_{cu}/\gamma_m}$ was given a slight positive gradient. Again this had little effect on the results as the multidimensional stress state allows the convergence of the result on to a portion of the curve with zero gradient, as the strains can redistribute from one component to the others. Another consideration to note was that the state of stress on the curve used in the analysis was an equivalent stress based on a combination of principal stresses, rather than just a representation of stress in the concrete in the horizontal x-direction along the axis of the beam, as is assumed in design when using the curve from B.S.8110. However, when the stress distributions within the beam were analysed, this did not appear to cause any problems. Eventually, the crushing facility with the concrete elements was turned off, and any beam failures resulting from crushing of the concrete were monitored by looking at the strain within the elements, with crushing occurring at a strain of 0.0035.

All of the beam models were numbered and named sequentially as they were produced, regardless of their intention as models for proper analyses or test models. The numbers and names of the following full test models have been retained, and therefore have non-sequential model numbers.

---

* E.Hognestad, N.R.Hanson and D.McHenry, Concrete stress distribution in ultimate strength design, *j.Am.Concr.Inst.*,**27**(1955) 455-79

4.1.1/ Model 10

General Model Specifications

Simply supported rectangular section prestressed concrete beam with a straight tendon profile at a constant eccentricity from the section centroid, and fully bonded steel tendon. The dimensions and finite element mesh for model 10 are shown in figure 4.1.1., the load arrangements are shown in figure 4.1.4., and general information listed in Table 4.1.

Concrete Specifications

The STIF 65 reinforced isoparametric concrete element was used with the cracking facility enabled and the crushing facility disabled. Other relevant properties concerned with material behaviour were entered into the nonlinear material table. Refinements of the mesh were carried out in the more highly stressed areas, namely at the support and midspan sections. The nonlinear stress-strain curve was of the form given in B.S.8110 (part 1, figure 2.1), for the short term design for normal weight concrete. The load factors were removed from the curve to obtain actual values rather than conservative design values. To model the stress-strain relationship for concrete as accurately as possible, a multilinear approximation to the curved portion was employed, as there was no facility for modelling continuous smooth curvature. Figure 4.1.8. shows this multilinear approximation to the stress-strain curve. As compared to the actual parabolic curve, the multilinear approximation will lie slightly beneath this, touching the actual curve only at the line connections. Key points on the parabolic curved portion were obtained by calculating stresses on the parabola corresponding to strains at equal intervals, hence forming the end points of the lines for the multilinear approximation. Care was taken to ensure that the initial elastic modulus specified as a linear material property corresponded to the slope of the first line of multilinear approximation. These points on the stress-strain curve were then entered into the nonlinear material table at the appropriate locations. For the concrete strength in tension, the value was calculated using the formula given in Appendix B, equation (b1), in this case set to 3 N / mm^2 in the nonlinear material table, and the behaviour is assumed linear up to this value. The kinematic hardening option, as described in section 3.3.1.4., was chosen for the appropriate hardening behaviour with load reversal. For elements which have undergone cracking, a shear transfer coefficient, ranging from 0 to 1 across the crack must be specified. Tests have shown that the value employed does not have a significant effect as long as the value is non-zero, A.S.C.E Report, [40]. Hence values of 0.5 for open cracks and 1.0 for closed cracks were specified in the nonlinear material table. For the linear material

properties, a Poissons ratio of 0.2 was specified together with an initial elastic modulus, and the shear modulus calculated from these two values.

Steel and Bond

STIF 1 spar elements were used for modelling the prestressing steel. The nonlinear stress-strain curve was of the form given in B.S.8110 (part 1, figure 2.3), for the short term design of prestressing tendons, with load factors removed. A multilinear option with kinematic hardening was also used to model the stress-strain curve of the prestressing steel, and this was of the form shown in figure 4.1.9. This stress-strain relationship was assumed the same in tension and compression. To apply the prestress, an initial strain corresponding to the desired prestress was entered into the real constant set for the spar element.

As the steel spar elements were to lie either side of the concrete, the tendon cross sectional area was divided into two equal areas, and the spar elements located either side of the beam at the appropriate location corresponding to the placement of the tendon. At the tendon level, two sets of nodes at coincident co-ordinate locations were produced. The steel spar elements were connected to one set of nodes, and the concrete elements connected to the other set, hence producing two separate element systems. These two coincident nodes sets were then connected by two dimensional interface elements forming bond between the steel and concrete, as shown in figure 4.1.1. The stiffness of the interface elements was given an arbitrarily high value to produce full bond, and a negative gap specification (interference) to prevent premature separation and sliding.

In an actual prestressed concrete beam, the cross sectional area of the concrete per unit depth is smaller at the tendon level due to the presence of the steel. This change of area can be modelled as a reduced relative stiffness in the concrete elements at the level of the tendon, Mufti et. al. [21], although in this analysis, the area reduction has been neglected. The effects of this are directly related to the amount of steel present in the section, but for the amount of steel used here, these effects are minimal.

Boundary Conditions

To reduce the number of elements in the model, only the left hand side of the beam was modelled (the beam being symmetrical about the midspan vertical axis). At midspan the nodes in the vertical plane were restrained from moving in the longitudinal (horizontal) x-direction, so that these nodes would remain in the vertical plane as the beam deflected transversely, effectively holding the rotation about the horizontal z-axis to zero. At the end

of the beam, two concrete elements with cracking and crushing removed were arranged at the base of the beam, effectively between support and beam. The nodes of this layer of elements which were to be in contact with the support were thus restrained in the y- and z-directions.

Load Application

The loading arrangement for the beam is shown in figure 4.1.4. The point loads were applied as a patch pressure on the top surface of the concrete element immediately under the load (see figure 4.1.1.). This alleviated to an extent the stress concentrations which would have occurred if a point load was applied at the appropriate node. The bending moment produced by this load arrangement is such that there is a constant moment zone between the points of load application, with a linear decrease to zero from load point to support. To reduce the effects of shear as compared to the bending moment, the ratio of the distance between the support and the load position, and the effective depth was made as large as possible (in this case a ratio of about 4.5:1). The closer the load point to the midspan position, the greater the bending moment at midspan for a fixed maximum magnitude of shear in the beam, therefore the more likely is a beam failure in bending at midspan.

Analysis Options

The ANSYS program automatically set the nonlinear solution procedure to full Newton-Raphson option. Fifteen iterations per load step were specified, and default convergence criteria for the plasticity ratio and large deflection increment were used. The amount of output results for various elements can be controlled by specifying a results storage level. The default results storage level for most elements is 3, which covers most of the useful data which would normally be required by the user. In this case, the results storage level for the concrete elements was set to 6, so that information about cracking etc. could be accessed if necessary.

4.1.2/ Model 11

The specifications for model 11 were the same as for model 10, only this time the whole length of beam was modelled. The purpose of this was to check the validity of using the half beam representation for further analyses. A mirror image of nodes, elements, boundary conditions, and applied loads from model 10 was created about the beam centreline to produce the whole model 11. All of the nodes at the beam centre were released, and horizontal x-direction movement was prevented at the left hand support only.

4.1.3/ Beams 1 and 2

General Model Specifications

These were simply supported prestressed concrete beams with straight tendon profiles, based on experimental beams. In the experiment, both beams were pretensioned with two steel strands, beam 1 with both strands at the same eccentricity from the section centroid, and beam 2 with the strands at different eccentricities. The cross sectional details of the two beams are shown in figure 4.1.7. The dimensions and finite element meshes for beams 1 and 2 are shown in figures 4.1.2 and 4.1.3. respectively. Load arrangements for both beams are shown in figure 4.1.5, and general information listed in table 4.1.

Concrete Specifications

STIF 65 concrete elements were used as for models 10 and 11. The stress-strain curves were also similar to those used previously, figure 4.1.8., with the necessary adjustments made for the different material properties shown in table 4.2. In the experiment the concrete characteristic strength for short term (i.e. prestress transfer) and long term were different, therefore two separate stress-strain curves were prepared, one for the first load step in which the prestress was transferred to the concrete, and the other for subsequent load steps. Other nonlinear and linear material properties were changed where appropriate. The area (stiffness) reduction of the concrete at the tendon level was again ignored.

Steel and Bond

The prestressing steel and bond were modelled in a similar fashion to that for models 10 and 11. The stress-strain curve was of the form shown in figure 4.1.9., and the material properties, both linear and nonlinear altered accordingly. With beam 2, the steel was present at two separate levels, so the spar and interface elements were positioned at the appropriate locations. The prestress was entered as an initial strain in the corresponding real constant set. STIF 45 elements were provided at the ends of the beams at the anchorage zones to prevent spalling of the concrete, as shown in figure 4.1.3.

Boundary Conditions

Half beam models were used for both beams 1 and 2, with all of the midspan (centreline) nodes prevented from displacing in the longitudinal (horizontal) x-direction.

Layers of concrete were provided under the support sections, with the nodes at the location of the support restrained in the vertical y- and horizontal z- directions.

Load Application

In the experiments, the loads were applied as two point loads positioned along the beam at third points (i.e. equidistant from each other). Therefore the loads were applied as patch loads to the top sides of the appropriate elements. Self-weight of the beam was present in the analysis, and could be modelled by specifying a density for the concrete, and then applying a downward body force, i.e. in the negative y direction. The effects of the self-weight as compared to the applied load were investigated and the difference in the ultimate moment at midspan with or without the self-weight was found to be minimal. Therefore to simplify the analysis only the applied loads were considered.

Analysis Options

Fifteen iterations were specified for each load step, and the default convergence criteria used. The results storage level for the concrete elements was set to 6.

4.1.4./ Model13

General Model Specifications

Rectangular section simply supported beam with a downward parabolic tendon profile of zero eccentricity at the beam ends, and with a fully bonded tendon. The load arrangements are shown in figure 4.1.6., and general information listed in table 4.3. The form of the finite element model is similar to that used for model 10, although the parabolic profile dictates that the finite element mesh as viewed in the elevation will be highly irregular. To show the element mesh sensibly within one diagram would be impossible due to the variation in the scale of the elements. The beam and tendon profile layout have therefore not been shown here, although an ANSYS plot of the beam can be found in Weekes, [48]. Relevant dimensions of the tendon are listed in table 4.1.

To construct the tendon layout, the equation of the parabolic profile was calculated, and a set of co-ordinates which were equally, or conveniently spaced in the vertical plane were noted. These co-ordinates then provided the end nodes for a series of straight steel spar elements forming the tendon. Towards and at the midspan of the beam, the tendon profile

becomes shallower where the gradient of the profile becomes smaller and passes through zero. Therefore for a given vertical spacing, the corresponding horizontal spacing becomes increasingly larger, causing the spar elements to become longer. Hence smaller vertical spacings were used towards the midspan sections to produce steel spar elements of approximately equal length throughout the beam. As a result, the concrete elements at the level of the base of the parabola were thinner in the vertical dimension, causing abnormal aspect ratios. This was a problem which could not be avoided when producing a parabolic tendon profile with finite elements, although in the analysis there appeared to be no adverse effect caused by this.

Concrete Specifications

The concrete was represented as with previous models, with a carefully constructed mesh as viewed in the elevation. The mesh was highly irregular due to the parabolic tendon profile. Refinements of the mesh were introduced at the support and centre sections, requiring the calculation of extra co-ordinate locations along the tendon profile to coincide with the concrete nodes. Linear and nonlinear material properties were represented as before, with appropriate adjustments to the linear properties and the stress-strain curve, figure 4.1.8. Effects of the reduction of the concrete area at the tendon level were ignored.

Steel and Bond

The steel and bond were represented as for previous models, with spar and interface elements. Linear material properties were altered accordingly, together with adjustments to the stress-strain curve, figure 4.1.9. The interface elements were set to model full bond, with a slightly negative gap specification. The prestress was entered as an initial strain in the corresponding real constant set.

Boundary Conditions

A half beam model was used with restraint in the longitudinal x-direction at the centreline. Support layers were present with the centre nodes restrained in the y- and z-directions as before.

Load Application

The parabolic tendon profile was designed to balance a uniformly distributed load of approximately 20 kN/m, as shown in figure 4.1.6.. The self weight of the beam accounted

for about a quarter of this load, so this was implemented separately by applying a downward body force on the concrete equivalent to the downward acceleration due to gravity, and specifying the appropriate density for the concrete. The applied load was then specified as surface pressures to the top faces of the elements at the top of the beam. For the first load step, the transfer condition consisted of the application of the prestress plus the balanced load to produce a uniform stress distribution across the section, and prevent cracking which would have occurred with upward camber. At subsequent load steps the downwards surface pressure was increased uniformly on the top surface of the elements at the top of the beam.

Analysis Options

Fifteen iterations per load step were specified, default convergence criteria were used, and the results storage level of the concrete set to 6.

4.2/ Continuous Beam Models

4.2.1/ Model12

Following the analysis of the simply supported beam models, a preliminary analysis utilising the data for model 11 was used to construct a continuous beam by the introduction of a support at the midspan position, restraining the base of the section from moving in the vertical y direction. The load was applied at the same location as for model 11, and incremented uniformly at each load point, creating a symmetrical bending moment envelope about the central support. The whole beam was modelled to highlight any unsymmetrical behaviour which might occur, although this was not to be expected.

As the tendon profile was straight (horizontal) at a constant eccentricity below the section centroid, the equivalent loads are in the form of end moments upon each span. The primary moment is a constant negative value along the length of the member which would in the absence of the central support cause the section at the central support to hog greatly. Therefore the action of the central support is to create a large positive 'internal' secondary moment here. This is desirable as there is effectively no reinforcement either prestressed or non-prestressed in the tensile region at the central support, where a negative internal moment will cause cracking at the top of the beam. The positive secondary moment will serve to effectively increase the applied load at which the negative cracking moment occurs at the central support.

Having outlined the effective advantages of using such a tendon profile for a continuous beam, it should be noted that it is highly unrealistic and impractical . It is more of an advantage to have a negative eccentricity of the profile over the central support, so that there is prestressed reinforcement present in the tensile region. The equivalent loads will tend to cause a resultant moment diagram which is negative in the spans and positive over the central support, but in this case the primary moment diagram will be of a similar form, rather than a constant negative value as described in the previous example. This means that the secondary moment is now probably of a lower value, either negative, positive, or zero if the profile is concordant. Past serviceability, the straight profile is of no structural use over the central support, as there is no resistance in the tensile region.

The beam dimensions, prestress details, and material properties are given in Table 4.1. The materials, application of load, and analysis options were the same as for model 11. Boundary conditions were modified with the addition of extra restraints in the y-direction at the base of the midspan section. Fifteen iterations per load step were used, with the default

convergence criterion for plasticity and large deflection increment. The results storage level for the concrete was set to 6.

4.2.2/ Model 18

Continuous beam model 18 was constructed as a rectangular section two span beam , with draped parabolic tendon profiles, symmetrical about the centre support, and fully bonded to the concrete. The overall dimensions of the beam and tendon layout are shown in figure 4.2.1. As this beam was exactly the same as for model Twospan 1 used in the SMAREL30 program, the reader is referred to section 5/ for details. Table 5.1. gives the relevant details, together with particulars of prestress and material properties. Due to the shape of the tendon profile, the finite element mesh for the main body of the concrete is highly irregular in both the longitudinal and transverse directions, and to display the mesh diagramatically would produce an untidy representation. For this reason, the reader is referred to the ANSYS input data file shown in Appendix D for a breakdown of the finite element mesh construction, in terms of Cartesian co-ordinates. The mesh is subsequently plotted in the results section 4.3, on the background to the contour plots.

Equivalent Load and Secondary Moment

At the end support, the eccentricity of the tendon profile is zero (coincident with the section centroid, and at the centre support, the parabolic profile has been transformed upwards from the section centroid a distance of 300 mm. The tendon drape at the midspan position was 337.5 mm. Hence, with a prestress force of 2000kN, the primary moment at the centre support was :

$$M_1 = 0.3 \times 2000 = 600\text{kNm}$$

The equivalent U.D.L. is :

$$-\frac{0.3375 \times 2000 \times 8}{15^2} = -24\text{kN/m}$$

This equivalent load produces fixed end moments of :

$$\mp\frac{24 \times 15^2}{12} = \mp 450\text{kNm}$$

From moment distribution (a stiffness analysis), the resultant moment over the centre support is the fixed end moment plus a carry over of half the value of the fixed end moment at the end support with a reversed sign, i.e.

$$M_3 = 450 + (0.5 \times 450) = 675\text{kNm}$$

Hence the magnitude of the secondary moment over the centre support is :

$$M_2 = M_3 - M_1 = 675 - 600 = 75\text{kNm}$$

Where the positive value indicates sagging

Tendon Profile

Having ascertained the required drapes for the parabolic tendon profiles for each span, and the eccentricities at midspan and over the central support, the equation for the profile may be calculated using equation 2.1 in section 2.2.1. The required widths of the columns of elements at the various sections of importance are calculated, and the steel profile will then govern the depth of the elements to be used in each column. Where a steel spar element runs across a concrete element, the two opposite corner nodes of the corresponding concrete element must have co-ordinates which lie on the tendon profile, in order to give the correct tendon shape, as for model 13. At the centre support it can be seen that the tendon has a sharp kink with no reversed curvature to 'smooth' the tendon over the support section. A model incorporating this feature was attempted, but the elastic secondary moment obtained from the finite element analysis was vastly different to that obtained from theory. This was caused by the equivalent load actually being applied by the tendon to the concrete as a series of point loads rather than a continuous U.D.L. as was used in the theory. Hence at the location of the inflexion point of the tendon, the reversal of the equivalent load appears as a gradual change in the point loads applied by the tendon, rather than an immediate step change from one U.D.L. to another opposite one. Refinements of the element mesh at the point of inflexion of the tendon proved to have little effect.

Discretization of Concrete Elements

As a consequence of the tendon profile, the locations and widths of the concrete elements are of irregular proportions, and this must be carried through the entire mesh to avoid mis-shaped elements. As a result, abnormal aspect ratios are produced in certain rows and columns of concrete elements due solely to the fact that the nodes of both steel and

concrete elements must coincide. The disadvantages of this are highlighted by El-Mezaini [45], but as there appeared to be no alternative approach available in the ANSYS software, this was a risk which could not be avoided. Such elements with abnormal aspect ratios were used in model 13 with no adverse effect, so it appeared valid to use them in the continuous beam model. The effects of these elements are discussed in the results.

Concrete Specifications

The main body of the concrete was represented as for previous models, i.e. with STIF 65 elements, with cracking capability only. Linear material properties were altered accordingly, together with adjustments to the stress-strain curve, figure 4.1.8. The concrete stiffness reduction due to the presence of the steel at the tendon level was neglected. The transfer properties of the concrete were assumed to be the same as the long term properties.

Steel and Bond

The steel and bond were represented as for previous models, with spar and interface elements. Linear material properties were altered accordingly, together with adjustments to the stress-strain curve, figure 4.1.9. The interface elements were set to model full bond, with a slightly negative gap specification. The prestress was entered as an initial strain in the corresponding real constant set. From a calculation of the shear resistance of the beam, Appendix E, shear reinforcement was supplied in the form of steel spar elements connected vertically from top to bottom nodes of the concrete in the required areas (i.e. near the support sections). A column of anchorage steel was provided to prevent cracking at the ends of the beam at the lower loads.

Boundary Conditions

A half beam model was used with restraint in the longitudinal x direction at the centreline. Support layers were present at the end and centre support sections, with the appropriate nodes restrained in the y and z directions as before.

Load Application

The parabolic tendon profile was designed to produce an equivalent uniformly distributed load of -24 kN/m, so that when this load is applied to the top surface of the beam, the stress distribution across the section (in the vertical y direction) would be

uniform. The self weight of the beam was neglected in this case, and the load applied as a pressure to the top surface of the elements, in steady increments. On the first load step, there was no load applied to beam (apart from the equivalent load). The analysis was then restarted from the first load step with the balanced equivalent load applied. Subsequent load steps were incremented from this load condition.

Analysis Options

Ten iterations per load step were specified, default convergence criteria were used, and the results storage level of the concrete set to 6.

Table 4.1

	Models 10,11,12	Beam 1	Beam 2	Model 13
Length (mm)	2900	2100	2100	12000
Breadth (mm)	50	75	75	300
Overall Depth (mm)	300	125	125	700
Effective Depth (mm)	250	100	87.5&112.5	650 @ midspan
Prestress (N / mm^2)	300	1082	1082	1228.5
Area of Tendon Steel (mm^2)	100	39.27	39.27	1000
Prestress Force (kN)	30	42.7	42.7	1228.5
Tendon Prestrain	0.00154	0.0055	0.0055	0.0063
Concrete Characteristic strength at Transfer (N / mm^2)	N/A	48	48	N/A
Concrete Characteristic Strength (N / mm^2)	40	55	55	55
Steel Characteristic Strength (N / mm^2)	1750	1670	1670	1750
Elastic Modulus of Concrete (N / mm^2)	30855	36229	36229	36229
Elastic Modulus of Steel (N / mm^2)	195000	195000	195000	195000

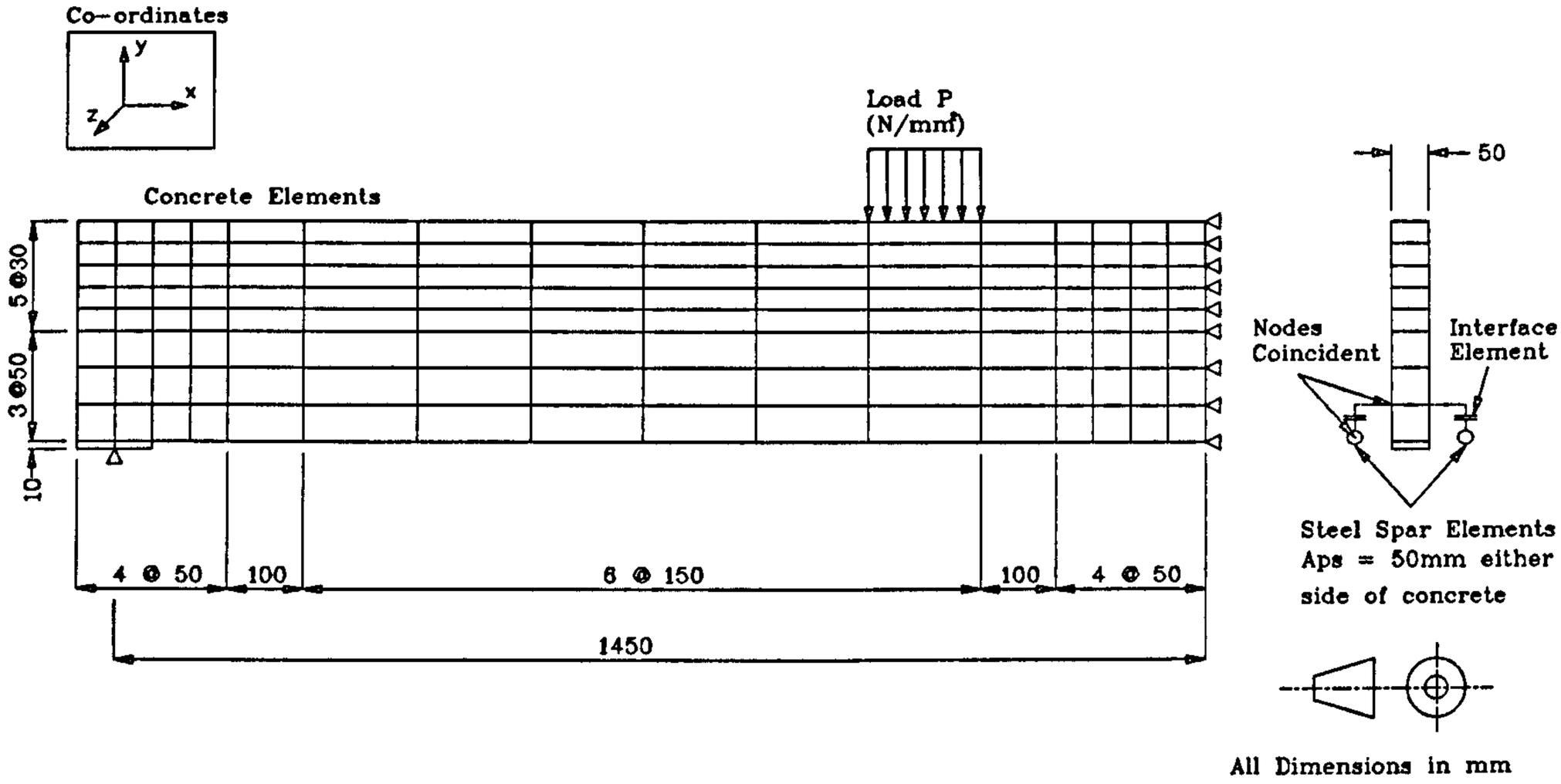

Figure 4.1.1. Finite Element Mesh for Simply Supported Beam Models 10 and 11

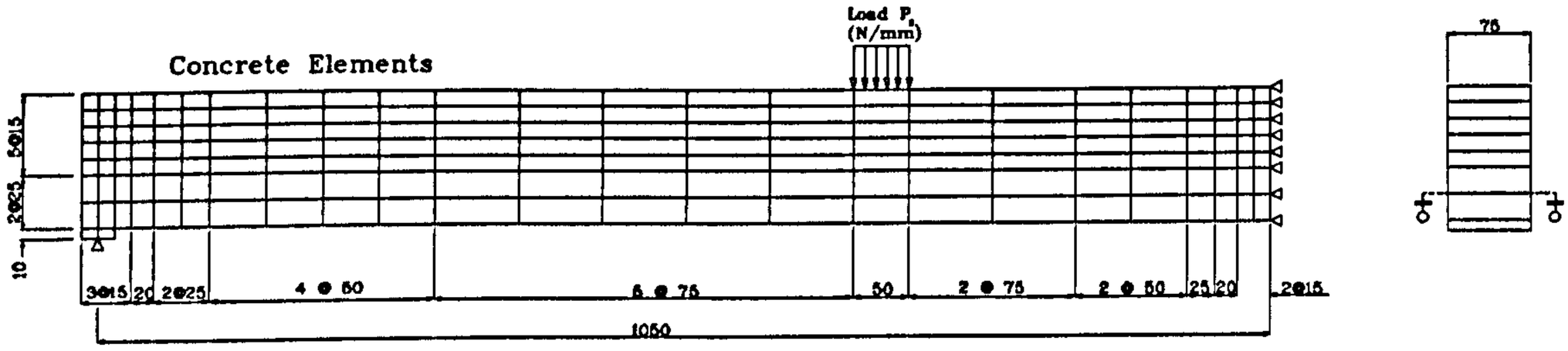

Figure 4.1.2. Finite Element Mesh for Simply Supported Beam, Beam 1

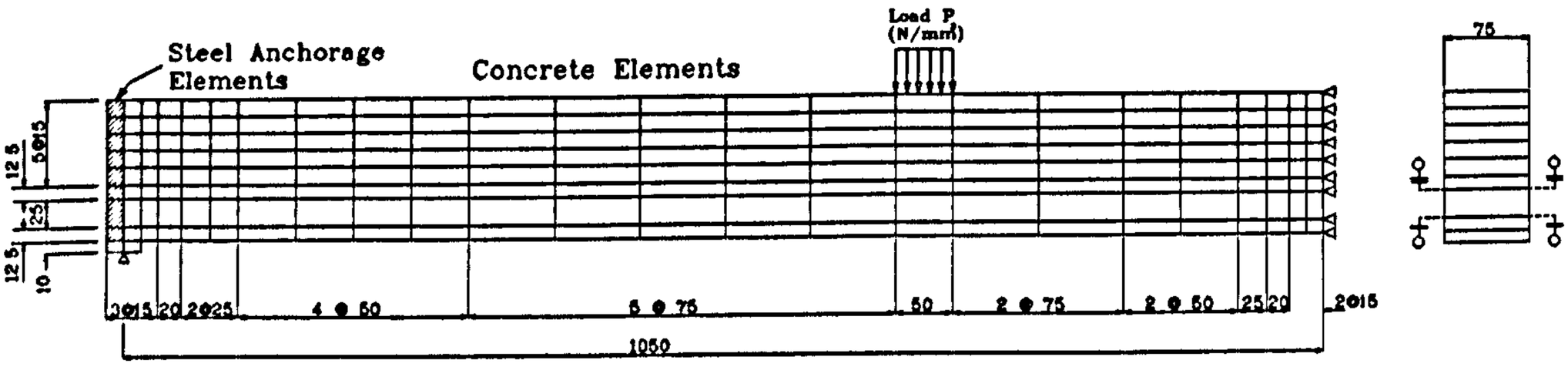

Figure 4.1.3. Finite Element Mesh for Simply Supported Beam, Beam 2

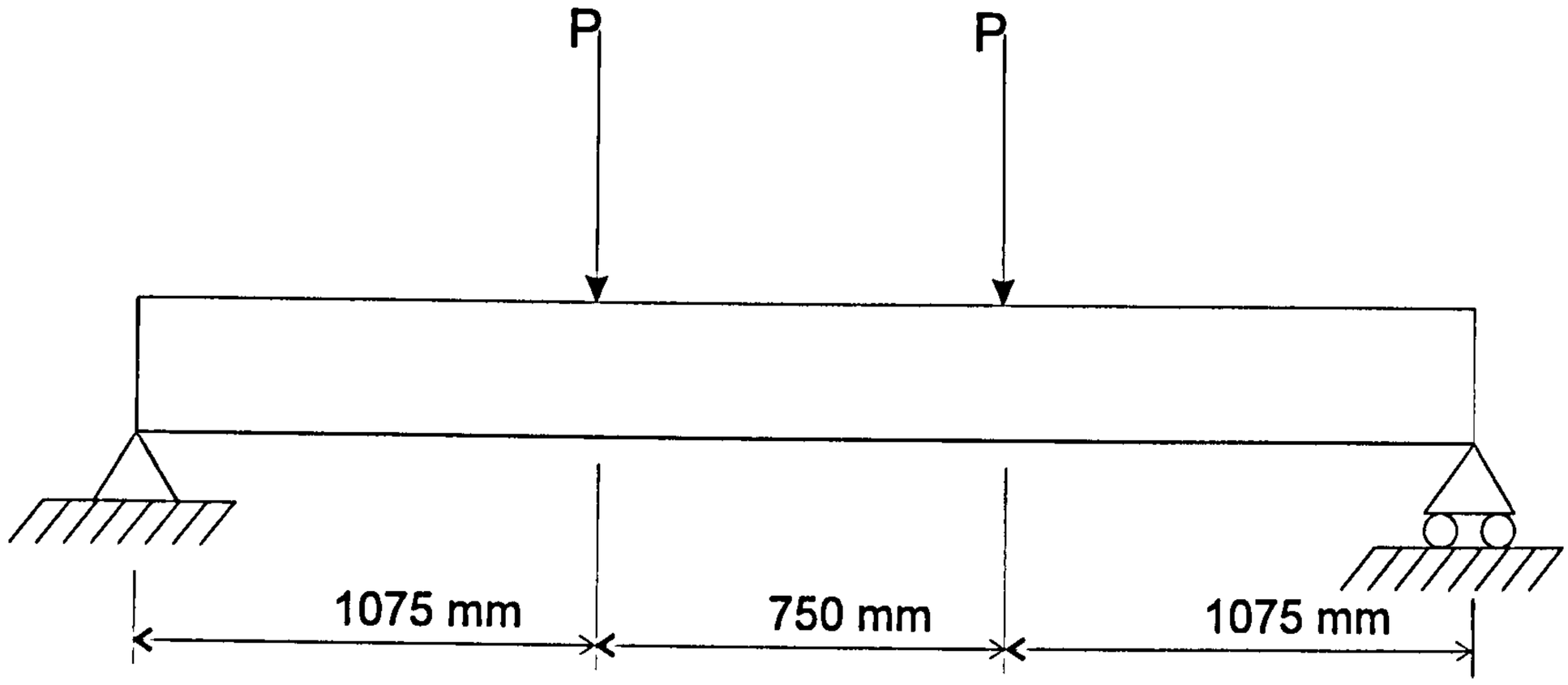

Figure 4.1.4. Load Arrangements for Models 10 and 11

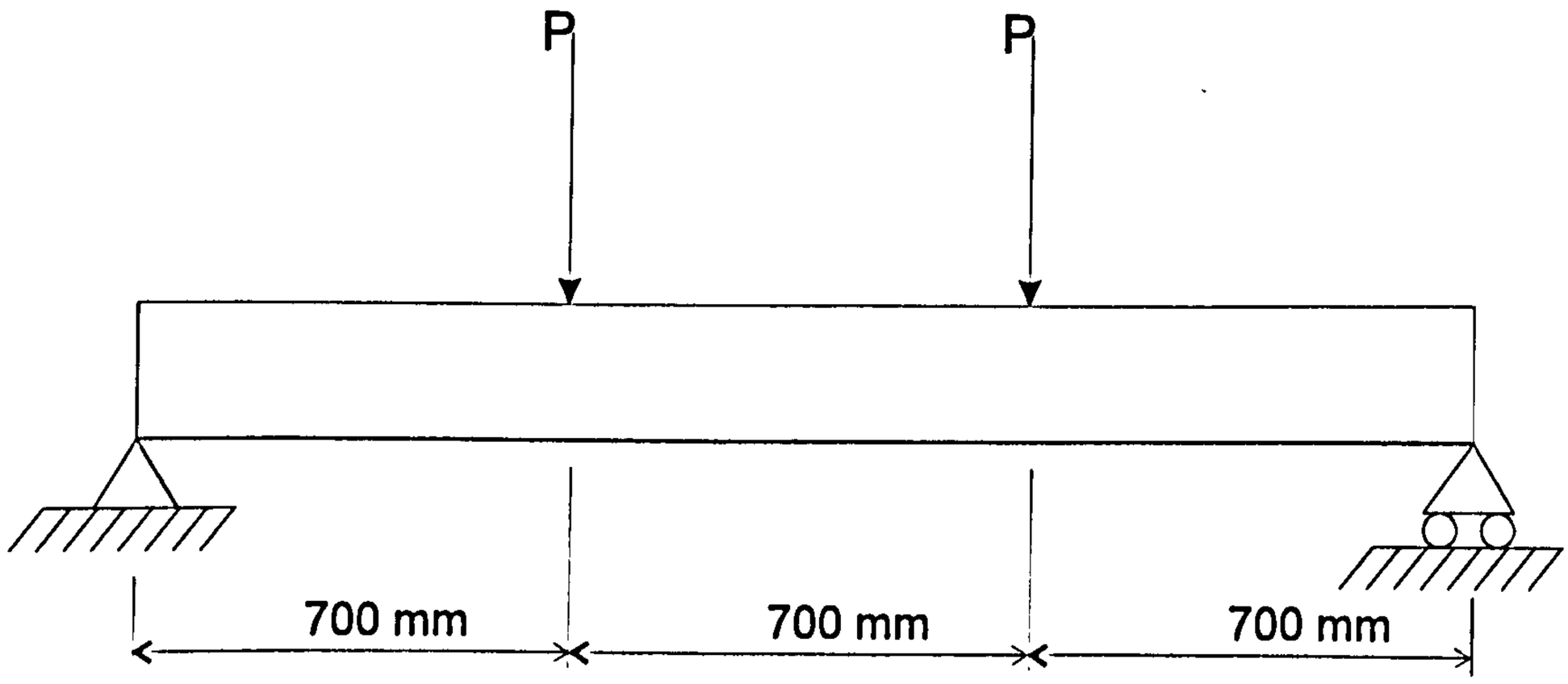

Figure 4.1.5. Load Arrangements for Beams 1 and 2

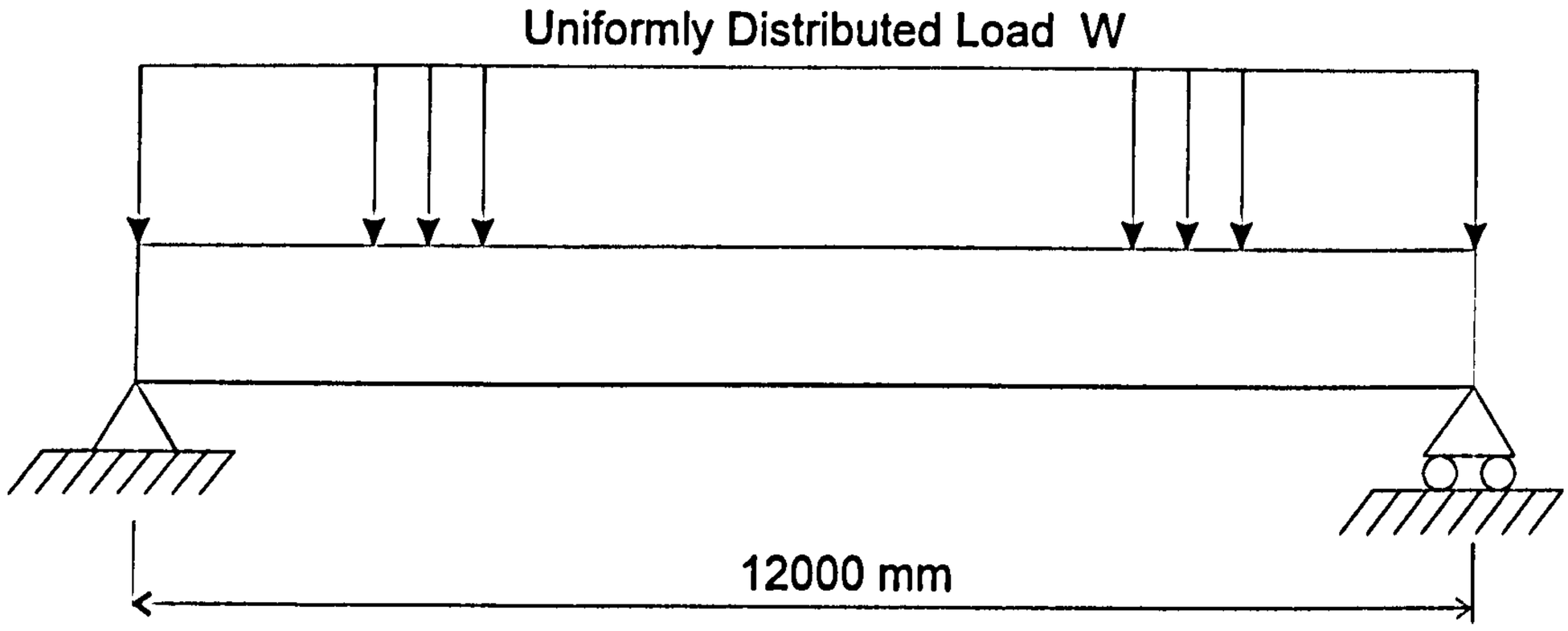

Figure 4.1.6. Load Arrangements for Model 13

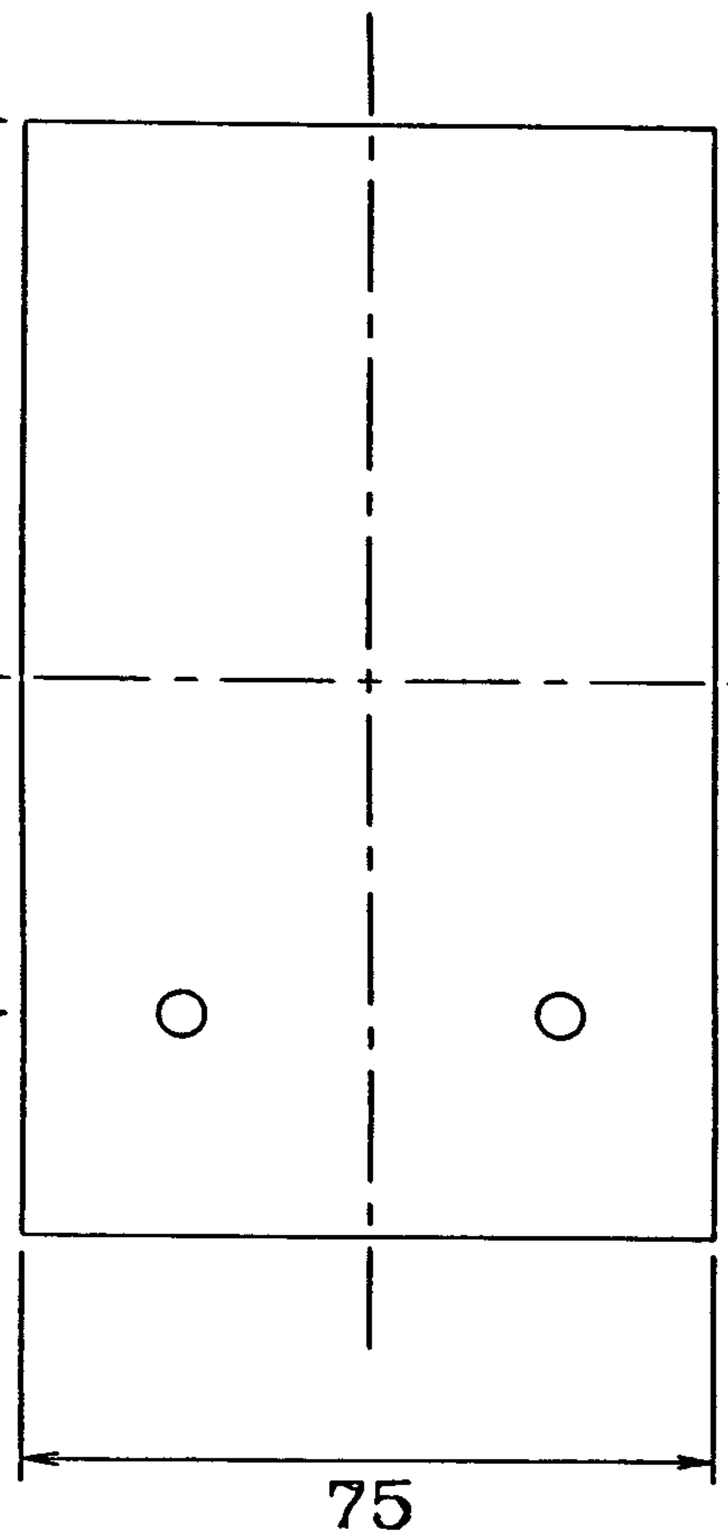

(a) Beam 1

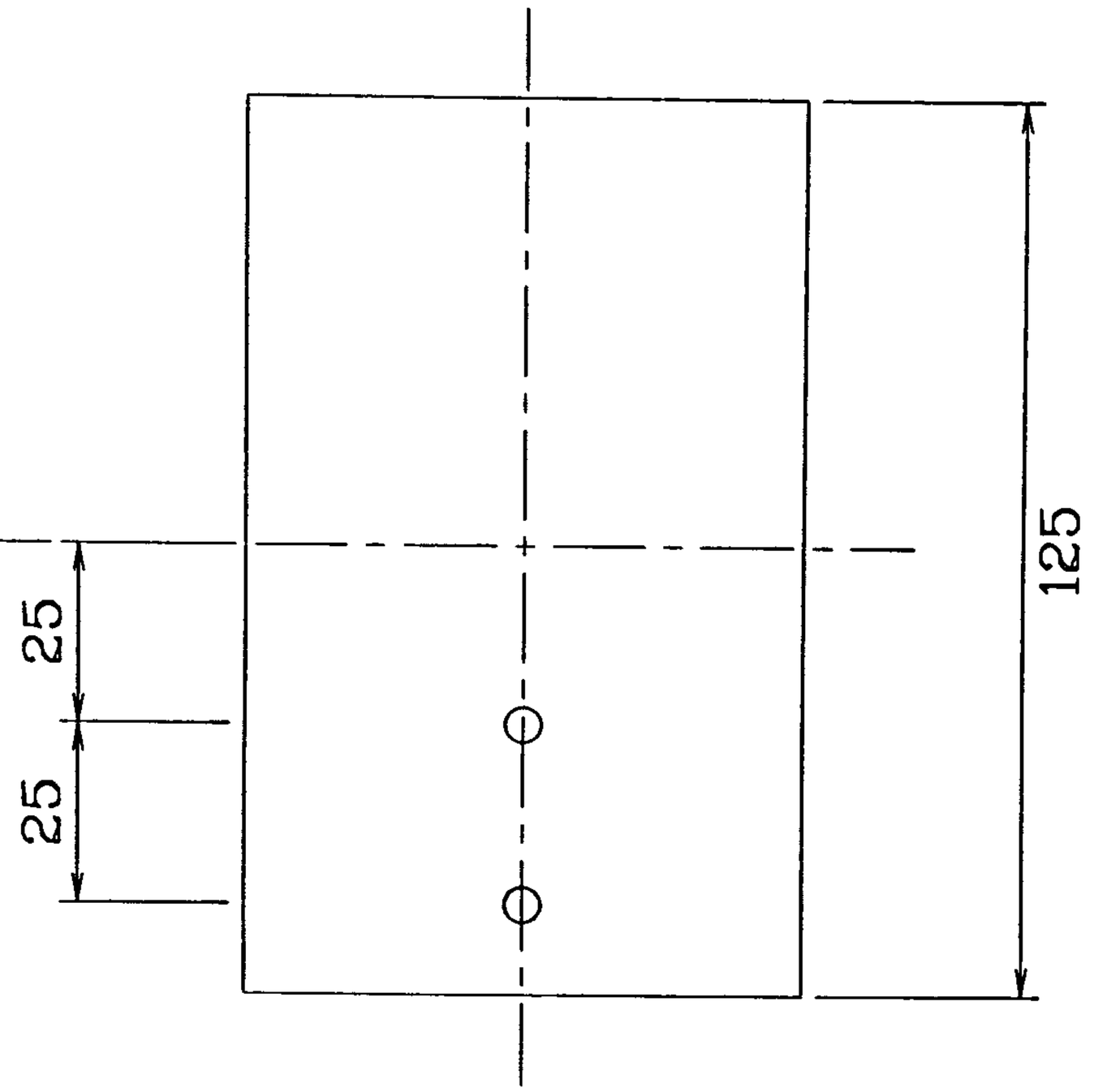

(b) Beam 2

Figure 4.1.7. Cross-Sectional Details of Beams 1 and 2 (all Dimensions in mm)

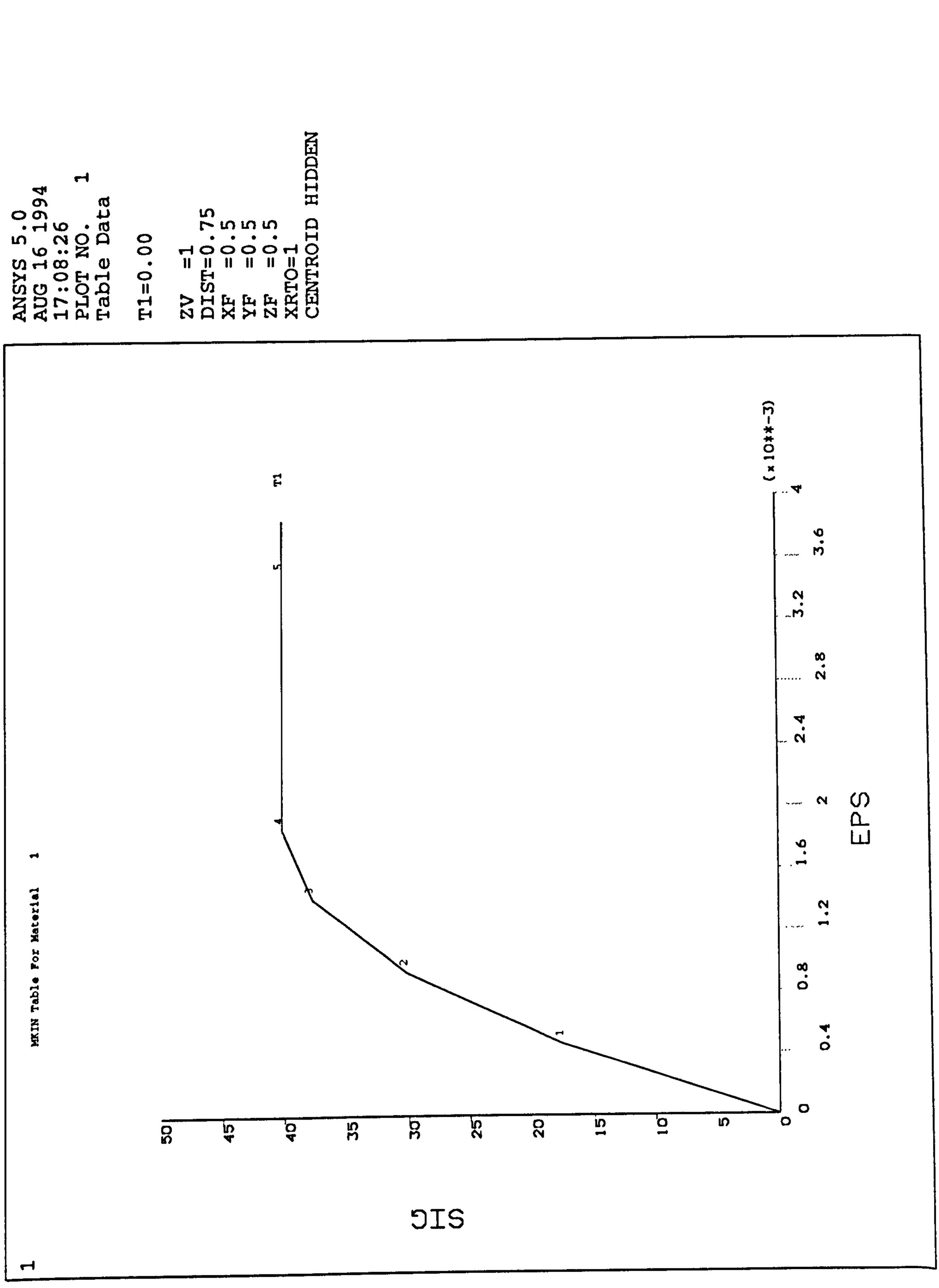

Figure 4.1.8. Stress-Strain Relationship for Concrete in Compression

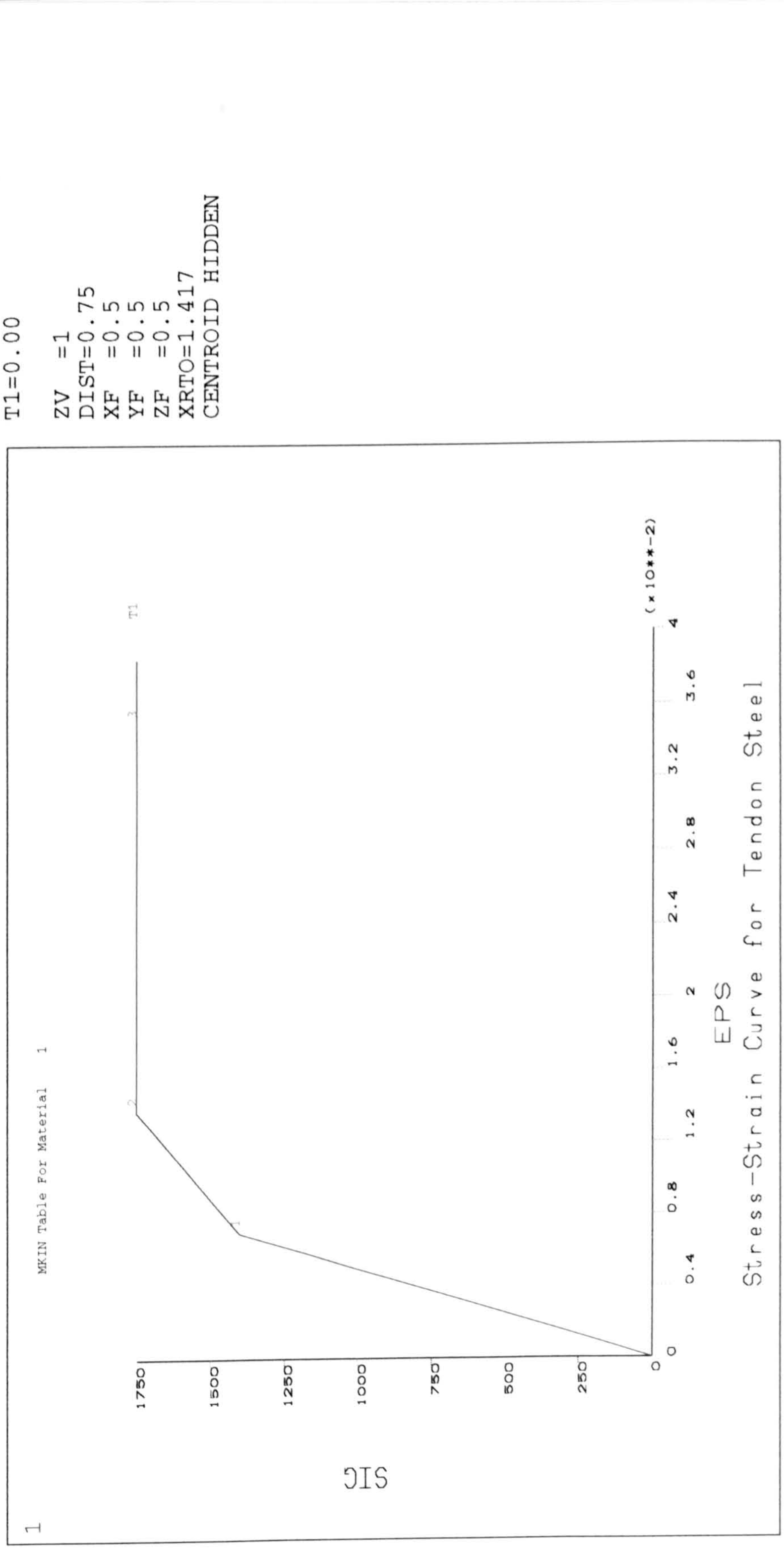

Figure 4.1.9. Stress-Strain Relationship for Tendon Steel

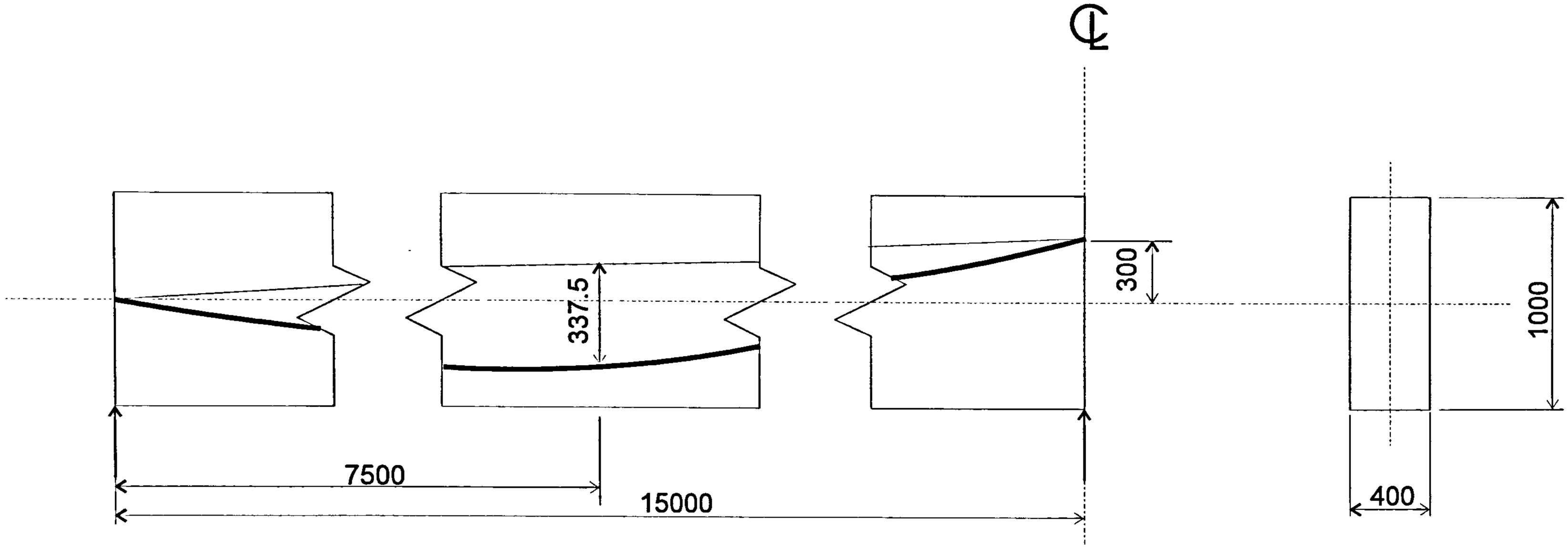

Figure 4.2.1. Tendon Layout and Overall Dimensions of Finite Element Beam Model 18 (all dimensions in mm)

4.3/ Results for Simply Supported Beam Analyses

A summary of the results of the simply supported beam models is presented here. A more detailed description of the results can be found in Weekes, [48].

4.3.1/ Models 10 and 11

The very low prestress value which both beams had, accounted for the failure mode being governed by the concrete. Comparing the ultimate load from the finite element analysis with a value corresponding to the ultimate moment at the centre section, calculated from a cracked section analysis, i.e. 25.07 kNm, then the finite element model reached an ultimate load of approximately 90% of the theoretical value. It should be remembered that when the load steps towards the end of the finite element analysis became unfeasibly small to continue, the analysis was stopped, and the final load step taken as the ultimate load.

At the first load step, only the prestress was present, and elastic shortening of the concrete caused a loss of prestress. The theoretical calculations to obtain the force loss are given in Weekes, [48]. At the midspan section, the prestress value of 300 N/mm^2 is reduced to 273.15 N/mm^2, giving extreme fibre stresses in the beam of 1.82 N/mm^2 tension at the top, and 5.46 N/mm^2 compression at the bottom. These values compare well with the finite element values of 275.2 N/mm^2 for the prestress, with extreme fibre stresses of 1.86 N/mm^2 tension at the top, and 5.5 N/mm^2 compression at the bottom. Along the length of the member, the prestress force is of an approximately constant value from the centre of the beam to the quarter position, with a slight decrease towards the end of the beam.

As the load was increased on finite element models 10 and 11, so the maximum bending moment at the midspan section increased. On the first load step, the net internal moment was zero as expected. This was ascertained by taking moments about any axis in the z-direction along a column of nodes at the centre section (ANSYS does this for you). For subsequent load steps the internal bending moments agreed exactly with those obtained from elastic theory, up to the ultimate load.

Cracking was initiated at the desired load at the midspan section, with an internal moment of 7.3 kNm. An investigation of the concrete stresses at the Midspan section revealed that the correct parabolic, and parabolic-linear shape to the compressive stresses formed at the higher loads up to ultimate. The orientation and pattern of the cracks at concrete integration points revealed that shear was having an effect, although the theoretical

ultimate flexural load was nearly reached in the models. The cracks at the quarter span position showed a flexure-shear type pattern.

A typical midspan deflection vs applied load graph was obtained for an over reinforced concrete section. The actual plot is not shown here, as the details can be found in Weekes, [48]. Graphs comparing the neutral axis depths calculated from a cracked section analysis with the finite element values are also given in Weekes, [48], and are not shown here. Good agreement between the values was obtained up to ultimate load.

4.3.2/ Beams 1 and 2

In both cases the failure was governed by the steel, i.e. under reinforced, as the prestress was a lot higher than for models 10 and 11. For beam 1, the theoretical ultimate load was found from the ultimate moment at midspan, which was calculated from a cracked section analysis, and found to be 5.75 kNm. The failure load from the finite element analyses corresponded to 100% of the theoretical load. Beam 2 had a similar ultimate moment at midspan and similar results for the finite element model. More details are given in Weekes, [48].

For beam 1 the theoretical prestress force after losses after the first load step, matched with the finite element results exactly, i.e. 40.5 kN, as did the top and bottom concrete fibre stresses of 3.46 N / mm^2 tension and 12.1 N / mm^2 compression respectively. Again, for beam 2, the results were similar.

As the load was increased on beams 1 and 2, so the maximum bending moment at the midspan section increased. On the first load step, the net internal moment is zero as expected. For subsequent load steps the internal bending moments agreed exactly with those obtained from elastic beam theory, up to the ultimate load.

Cracking started in beam 1 at the midspan position at an internal bending moment value of 3.33 kNm, corresponding with the theoretical value. For beam 2 the results were similar. In both cases the crack pattern near ultimate load showed the cracks to be mainly vertical, indicating less interference from shear.

Midspan deflection was plotted against applied load for beams 1 and 2, and these can be found in Weekes, [48]. In both cases, after cracking has begun, the curve which forms is of a smaller gradient than for models 10 and 11, indicating that the sections are more ductile. Graphs comparing the neutral axis depths calculated from a cracked section analysis with the

finite element values are also given in Weekes, [48], and are not shown here. Good agreement between the values was obtained up to ultimate load.

4.3.3/ Model 13

Model 13 was designed to have a failure mode governed by the steel. The ultimate moment at midspan was calculated as 992 kNm from a cracked section analysis. Taking into account the self weight of the beam, the total uniformly distributed load on the finite element model at ultimate was 55.5 kN/m, corresponding to a bending moment of 992 kNm at midspan.

At the first load step, the prestress plus the balanced load was present, so the effective stress in the steel, taking this into account, was calculated as 1197 N/mm^2. This gave a uniform concrete compression across the depth of the section of 5.7 N/mm^2. The results from ANSYS agreed closely with these values, with only a slight moment acting to cause a non uniform stress distribution at the first load step. This was probably causes by the slight stress loss in the steel due to elastic shortening.

As the load was increased on model 13, so the maximum bending moment at the midspan section increased. On the first load step, the net internal moment is zero as expected. For subsequent load steps the internal bending moments agreed with those obtained from beam theory, up to the ultimate load.

The theoretical and finite element model cracking moments corresponded well, and the subsequent crack pattern was generally vertical indicating pure flexural cracking behaviour.

The plot of midspan deflection versus applied load showed a shallow curve after cracking similar to beams 1 and 2, indicating ductile behaviour. This is given in Weekes, [48]. Graphs comparing the neutral axis depths calculated from a cracked section analysis with the finite element values are also given in Weekes, [48], and are not shown here. Good agreement between the values near ultimate load was obtained.

4.4/ Results for Continuous Beams

4.4.1/ Model 12

The nature of the straight tendon profile, although impractical, produced a large positive secondary moment at the centre support which increases the load at which cracking occurs at this location. With no reinforcement in the tensile region, a certain amount of moment redistribution occurred from the centre support to the spans. Details are given in Weekes, [48].

The stress and strain distributions in the beam before cracking has begun reveals linear distributions across the depth of the beam sections. At the centre support, a stress concentration manifests, with a larger stress and strain at the bottom of the support section in the compression zone. This is probably due to the local effect of the centre support. A plot of applied load versus vertical deflection at the point of load application reveals a similar trend as for the simply supported beam models with the onset of cracking causing the gradient of the graph to become smaller. This plot can be found in Weekes, [48].

The results of an equivalent load analysis showed that the theoretical secondary moment at the centre support was 4.5 kNm. The results from ANSYS implied that a residual internal moment after losses of 4.21 kNm was present at the centre support, mainly due to elastic shortening causing a loss of prestress force. In both cases the secondary moment falls linearly to zero towards the end of the beam. As the load was applied to the beam the secondary moment at the centre support was monitored up to the point where cracking was initiated, after which it was impossible to ascertain. A slight linear increase in the secondary moment was experienced, reaching a value of 4.7 kNm. This was probably due to slight increases in the tendon force as the load was applied to the beam.

The tendon force along the length of the beam was monitored as the load was applied. This appeared to be fairly linear with only slight variations up to the point at which cracking was initiated. Cracking at the center support produced little variation in tendon force in the vicinity, as the tendon was present in the compressive zone only. Once the spans had cracked, the tension was taken by the tendon alone, causing a local increase in the tendon force, as expected. These results are shown in more detail in Weekes, [48].

Moment Redistribution

The internal bending moment increases linearly up to the stage when cracking occurs at the centre support. The nature of the cracking and the tendon profile dictates that the moment is immediately redistributed from the support to the spans, and the moment becomes a constant negative value at the support. The beam was effectively split into two separate spans. After the split, the span moments increase with applied load whilst the centre support moment remains a its constant negative value. The tendon force at the centre support remains at a low value as the steel is present in the compression zone, whereas the tendon force increases vastly after the onset of cracking in the spans. Eventual failure appears to be caused by a complete split through at the centre support, once the cracks pass the depth of the tendon level

4.4.2/ Model18

The nonlinear analysis of continuous two span beam Model18 was terminated when the applied pressure on the top surface of the beam reached a value equivalent to a load of 87.6 kN/m after 73 loadsteps. The load step increment required to continue the analysis any further was deemed to be unfeasibly small. Cracking occured at the centre support at a load of 52 kN/m, and started in the span at a load value of 62.4kN/m.

Figure 4.4.1 shows internal bending moment versus applied load at the centre support and midspan sections, obtained by selecting lines of nodes and elements at the section in question, and summing forces and moments about any chosen node. It can be seen that a slight deviation from linearity occurs when cracking first begins at the centre support at an applied load of 52 kN/m, evident in both lines on the graph. The rate of change of the internal bending moment function, shown in the figures 4.4.3 to 4.4.6. series of graphs, can be seen to be at a maximum at the centre support, therefore the extent of cracking local to this negative moment zone will be confined to an area close to the support. So, once the cracks have formed local to the centre support, they are more likely to increase in width and depth, rather than spread and increase in number, causing a more gradual change in the bending stiffness of the beam. This effect would account for the apparent smoothness of the internal moment lines between the applied load values of 52 kN/m and 62.4 kN/m, before cracking in the span occurs. During this load stage, the internal bending moment redistributes from the support section into the span, evident from the apparent decrease in gradient of the centre support line, coincident with an increase in the gradient of the span line. After cracking in the span is initiated, the internal moment lines behave more erratically due to the spread of smaller cracks in the span, where the internal bending moment envelope is at its shallowest in the positive zone, and exceeds the cracking moment envelope over a wider area than in the negative zone. The creation of these smaller cracks over a larger section causes more irregular bending stiffness changes in the beam, and hence the distribution of the bending moment along the beam will have a greater fluctuation. The general pattern shows a reversal in the gradient change in both lines, back to values near those before any cracking began.

The tendon force variation with respect to applied load is shown in figure 4.4.2., at various locations along the left hand span (indicated by the legend). At a distance of 350mm away from the centre support, the tendon force can be seen to be at its maximum value throughout the loading. There could be a number of explanations for the causes of this. At the first load steps, with no applied load, and then with the balanced load applied, slight cracking of the concrete element adjacent to the central support position, occupying the

space over which the short (50mm) length of tendon in question acts, would account for a small local decrease in stiffness and increased 'elastic' shortening of the concrete, causing a marked decrease in tendon force loss. The abnormal aspect ratio of this element could not be avoided if the steel was to be discretized correctly. This effect is more evident when the balanced and subsequent loads are applied, as seen in the figures 4.4.7. to 4.4.10. series of graphs of tendon force envelopes along the left hand span. Also, the concentration of stress caused by the point centre support reaction has a significant effect on the distribution of stress across the section.

At zero applied load, the effect of the precompression, primary moment, and internal secondary moment causes a tendon force loss along the beam as shown in figure 4.4.7. As the applied load is increased to the balanced load, the primary moment is counteracted by the internal bending moment caused by the applied load, leaving just the precompression causing elastic shortening and tendon force loss, and internal secondary moment. The tendon force distribution can be seen to be of a more linear form along the span at the balanced load, with a small draw-in at the anchorage zone. As the beam switches from negative bending caused by the primary moment to positive bending from the applied load, so the apparent 'curvature' of the tendon force distribution in the span alters sign accordingly. Figure 4.4.8 shows the marked increase in tendon force local to the centre support as this section cracks, whereas the tendon force distribution remains shallow and smooth in the span. Once cracking in the span is initiated, figure 4.4.9, local increases in the tendon force reveal themselves as a series of spikes spread over a wider area, indicating a greater spread and number of cracks than at the centre support. The cracks continue to spread and increase in number as the load increases, until the final load is reached, as shown in figure 4.4.10. Between cracks, the tendon force is fairly constant in its elastic condition. Obviously the discretization of the steel elements has an influence on this tendon force distribution, as the force is distributed evenly along the length of a particular spar element which models part of the tendon. Those which 'span' across concrete elements which have more cracked integration points experience higher forces than those with a lesser degree of cracking. The presence of the spikes in the tendon force distribution not only indicate that the discretization of the steel in the span was adequate, but also suggest that cracked integration points are grouped together (in a near vertical orientation), with spaces in between each group, simulating the actual situation of cracks forming at a certain spacing.

Stress Contour Plots

A series of contour plots of stresses in the concrete elements in the longitudinal x-direction, taken from ANSYS model 18, are shown in figures 4.4.11 to 4.4.16. These contours are smoothed by the effect of averaging the stresses across the elements. Unaveraged plots were examined and showed a similar form in colour and stress range, indicating that the element mesh was satisfactory. All of the contours are colour coded with the key on the right hand side. The first plot in figure 4.4.11. shows the behaviour of the left hand span with the prestress transferred to the concrete and zero applied load. The tension taken as a positive stress is shown as the brighter red colours with the negative compression shown as the darker blue colours. The deflections are exaggerated with respect to the beam dimensions, and this clearly shows the desired upward camber at the transfer stage. When the balanced load of 24 kN/m is applied, figure 4.4.12., the beam appears to have little deflection, and the dark blue colour indicates that the stress across the depth of the section is uniform as expected. A slight stress concentration exists at the centre support near the location of the tendon (as well as near the simply supported end). Figure 4.4.13. shows the stresses at a load of 48 kN/m just before first cracking at the centre support. The downwards deflection profile has the correct shape and stress distributions in the section are linear as expected. After cracking at the centre support at a load of 52 kN/m, figure 4.4.14. shows how the tensile stress in the concrete at this location falls, and the stresses increase in the span as the moment redistributes. The stress contours just before cracking begins in the span are shown in figure 4.4.15., at a load of 62 kN/m. Comparing this figure with the stress contours of figure 4.4.16., just after the initiation of cracking in the span, it can be seen that there is a decrease in the concrete tensile stresses in the span where the steel begins to take significantly more stress than the concrete. Moment then redistributes back to the centre support.

Secondary Moment

As far as monitoring the secondary moment is concerned, there is no means of separating this from the total internal bending moment once the beam stiffness begins to change. After cracking has begun, the flexural stiffness of the beam alters, affecting the total internal bending moment, which is made up of the secondary moment plus the bending moment which is produced by the applied load. At zero applied load, the secondary moment was close to that predicted by the classical elastic equivalent load method. As load is applied, the internal moment can still be readily seperated into secondary and applied moments, as long as the beam is operating in the elastic range. The magnitude of the

secondary moment was fairly constant in this phase, with only small changes due to elastic shortening effects.

The section of the beam at the centre support was designed so that the steel would yield before the concrete reaches its ultimate strain at its extreme compressed fibre, giving potential for rotation, and hence the formation of a plastic hinge for redistribution of the bending moment. The load at which the analysis was stopped showed a tendon force below the value expected. From figure 4.4.10. it can be seen that this is a local effect close to the centre support, as the tendon force peaks a short distance away from the support. At the position where the tendon force is at a maximum, the section experiences a bending moment which is markedly less than that at the centre support, as the rate of change of the internal bending moment envelope is at a maximum here, in the negative moment zone. Comparison of the applied internal bending moment envelope with the ultimate bending moment envelope shows that the gradient in the negative zone is much greater for the applied moment, therefore sections away from the support experience much smaller moments than their ultimate values, suggesting that the tendon force should decrease in some manner away from the centre support. Also, the effective depth of the tendon also decreases away from the centre support, which means that if a section a short distance away from the support were subject to a moment of the same magnitude as that at the support, the lever arm between the compressive force in the concrete and the tensile force in the steel would be smaller, resulting in a higher tendon force. This effect, however, will have no significance as the moment across the support cannot be assumed to be constant enough to validate this.

Elastic shortening of the concrete at all sections along the beam is evident in the tendon force profile, with variations at the support sections. At the anchorage zone the tendon force profile is similar to that predicted by anchorage draw-in in post-tensioned members, as the tendon force at the end of the beam is non-zero. The block of steel elements at the end of the beam served to prevent cracking of the concrete at the anchorage zone, although the prescence of bursting forces, as for post-tensioned members, has not arisen, suggesting that the beam is behaving in a pre-tensioned manner, whereby a transmission length at the anchorage causes a steady build up of the tendon force as the steel bonds to the concrete further into the span. The actual modelling of the tendon force as a uniform prestrain along the tendon would suggest that once the prestress is transferred to the concrete, the behaviour is comparable with that of a pre-tensioned concrete beam.

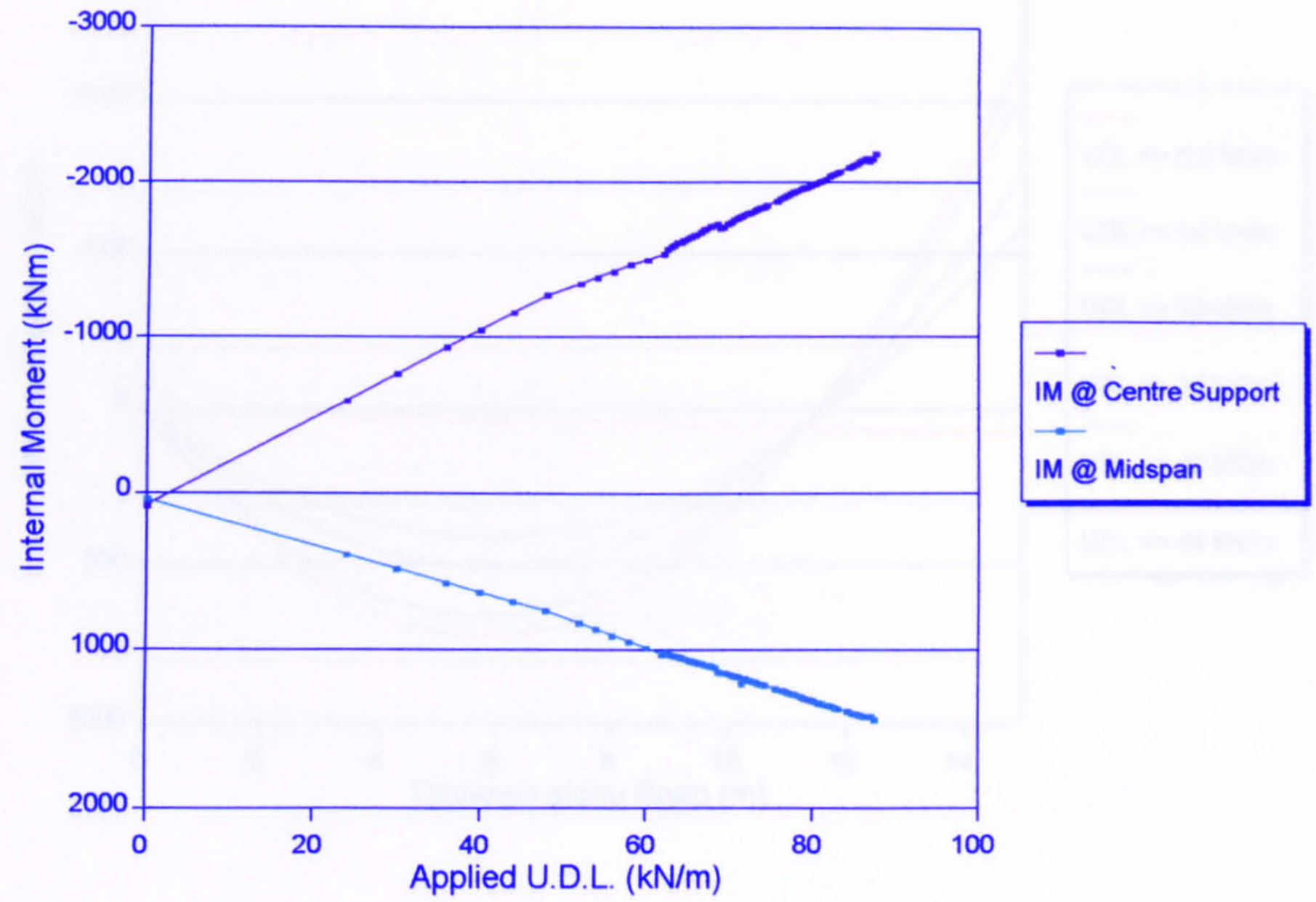

Figure 4.4.1. Internal Moment vs Applied Load, F.E. Model 18

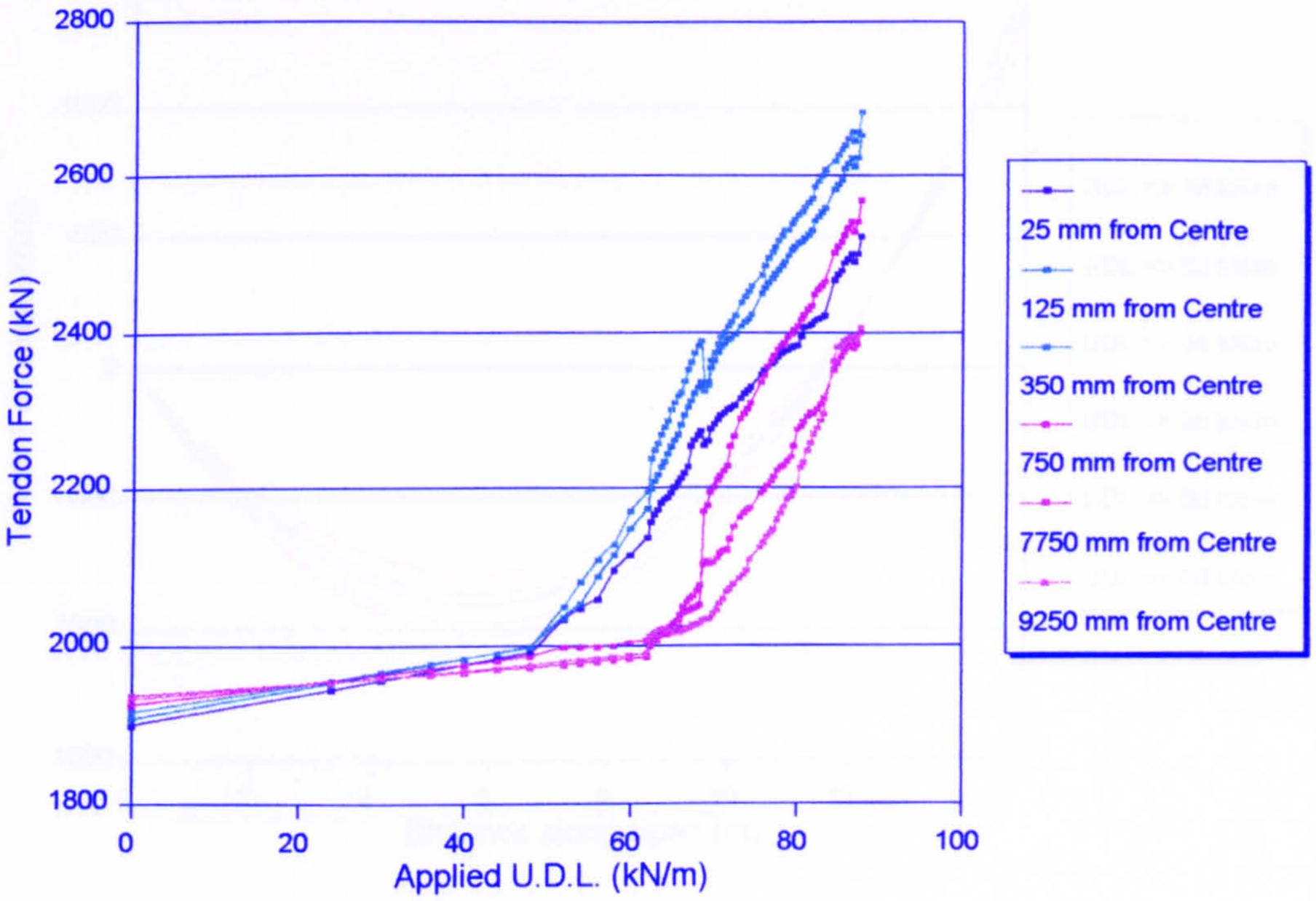

Figure 4.4.2. Tendon Force vs Applied Load, F.E. Model 18

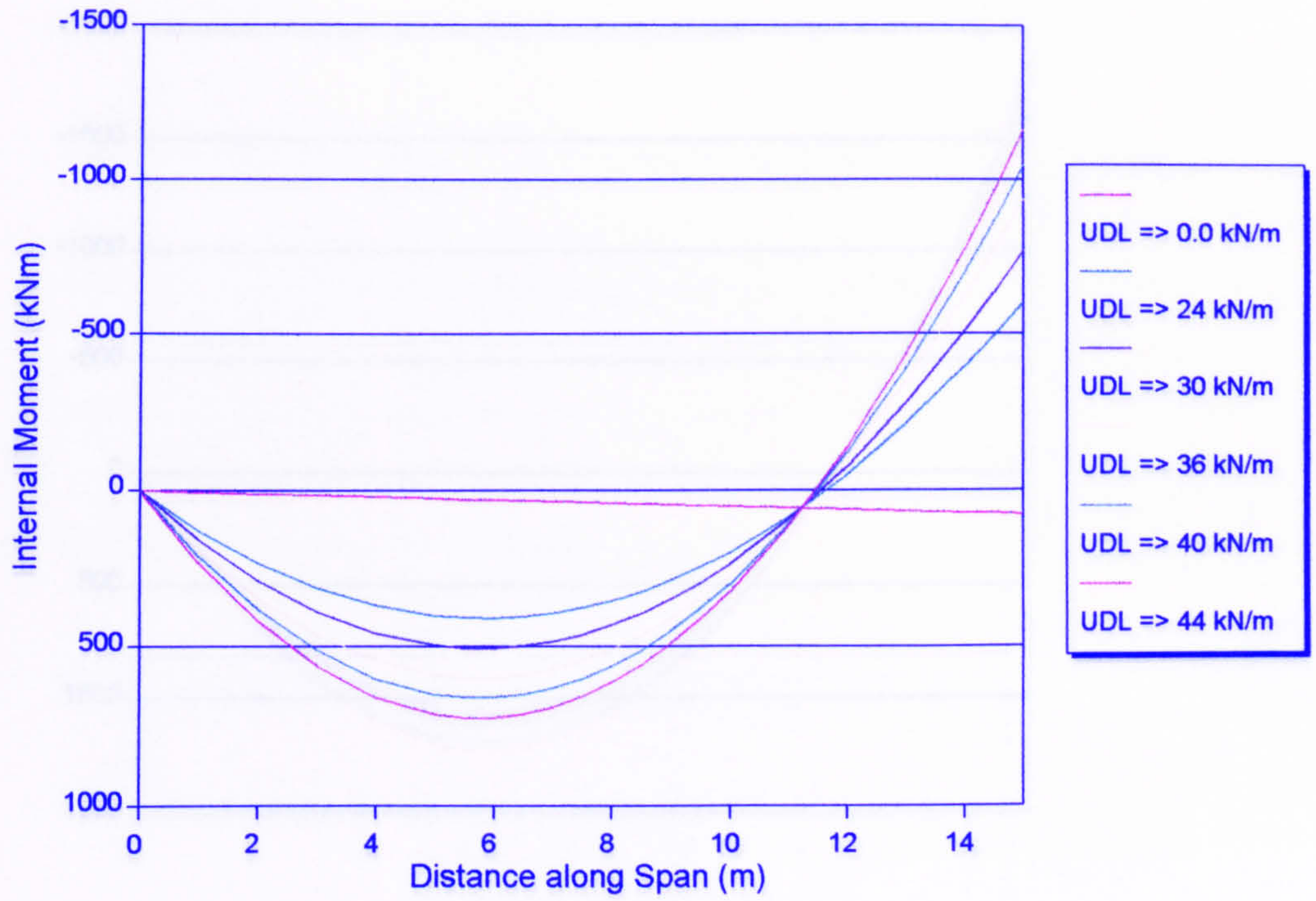

Figure 4.4.3. Internal Moment Envelope, F.E. Model 18

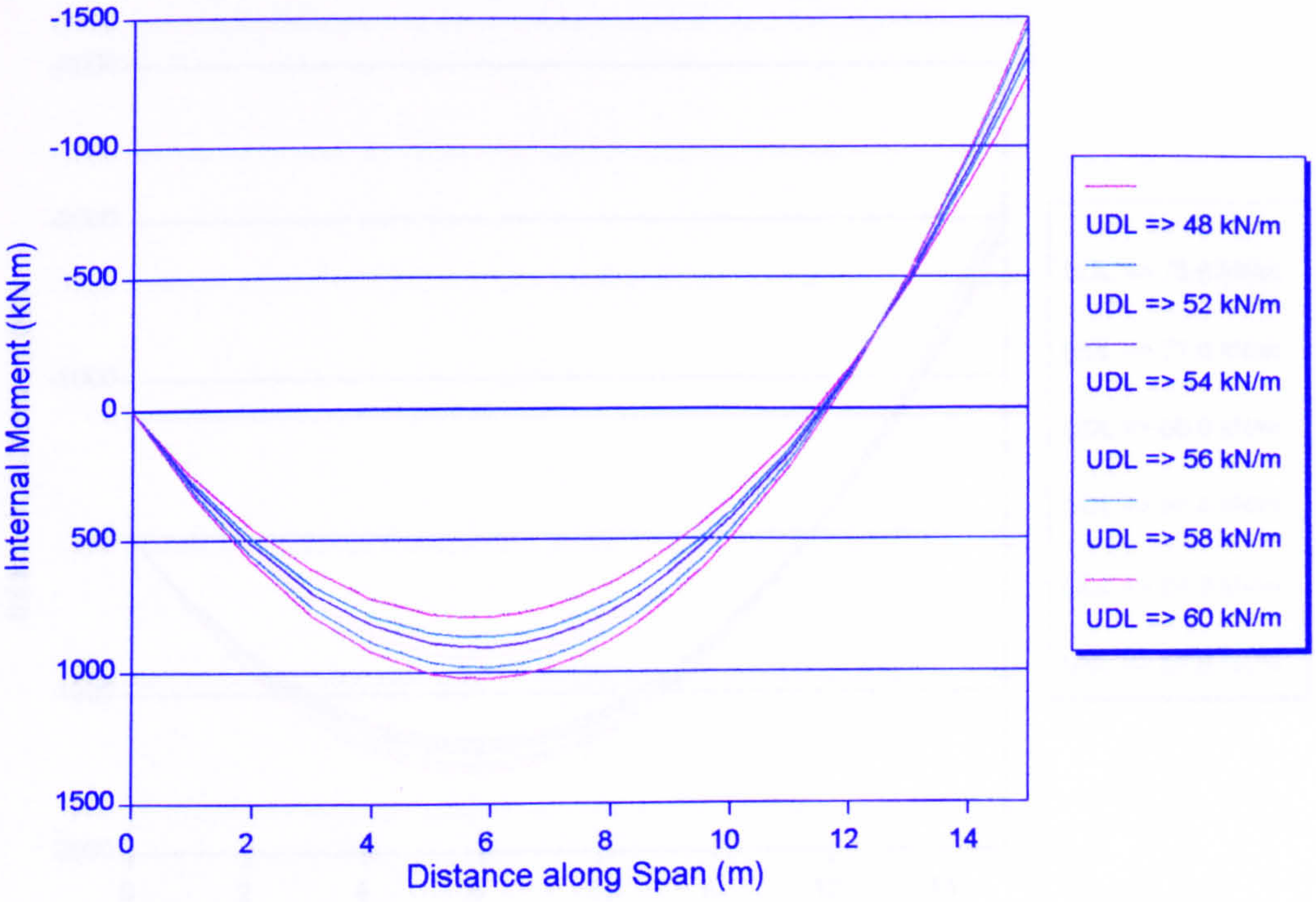

Figure 4.4.4. Internal Moment Envelope, F.E. Model 18

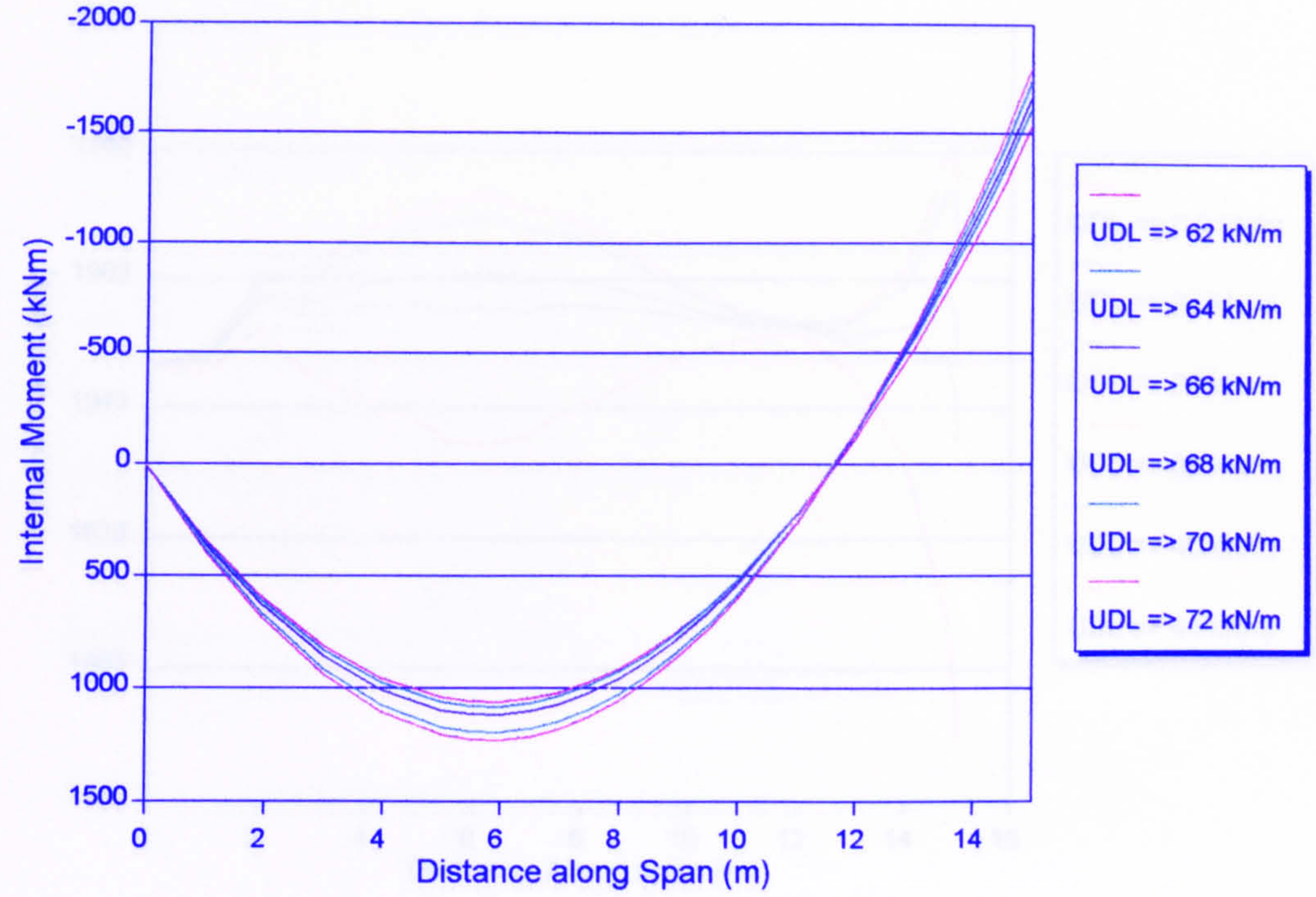

Figure 4.4.5. Internal Moment Envelope, F.E. Model 18

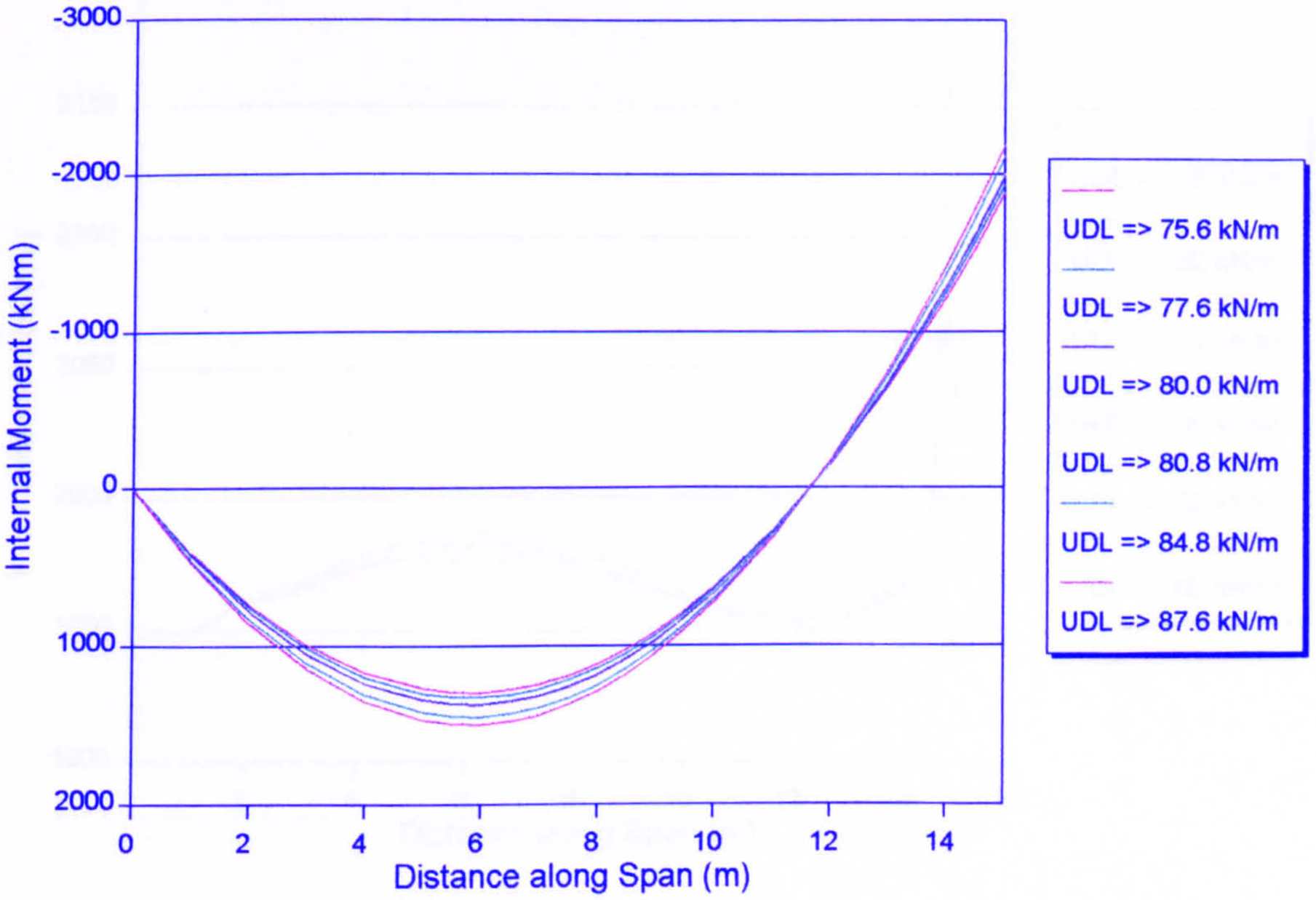

Figure 4.4.6. Internal Moment Envelope, F.E. Model 18

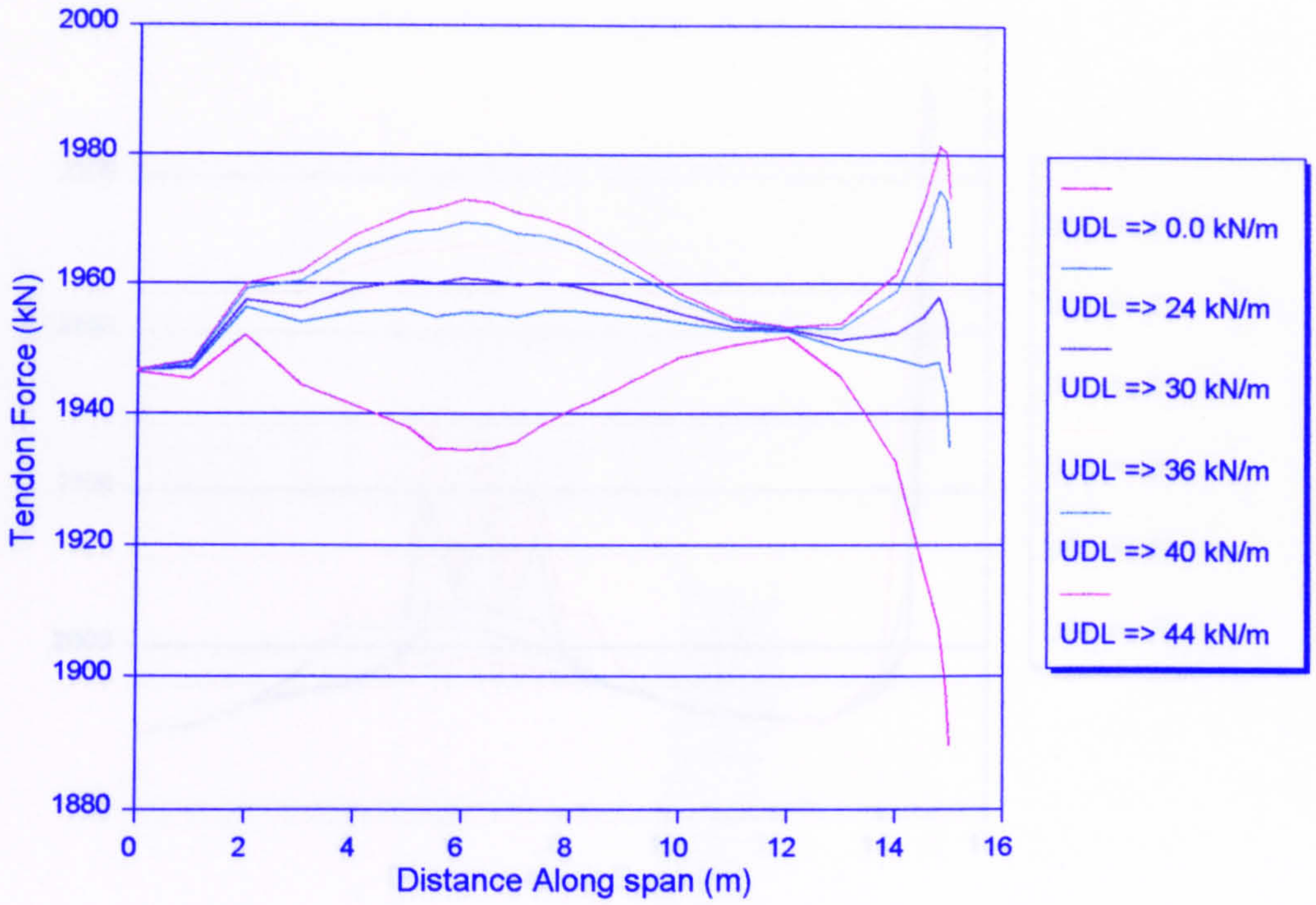

Figure 4.3.7. Tendon Force Envelope, F.E. Model 18

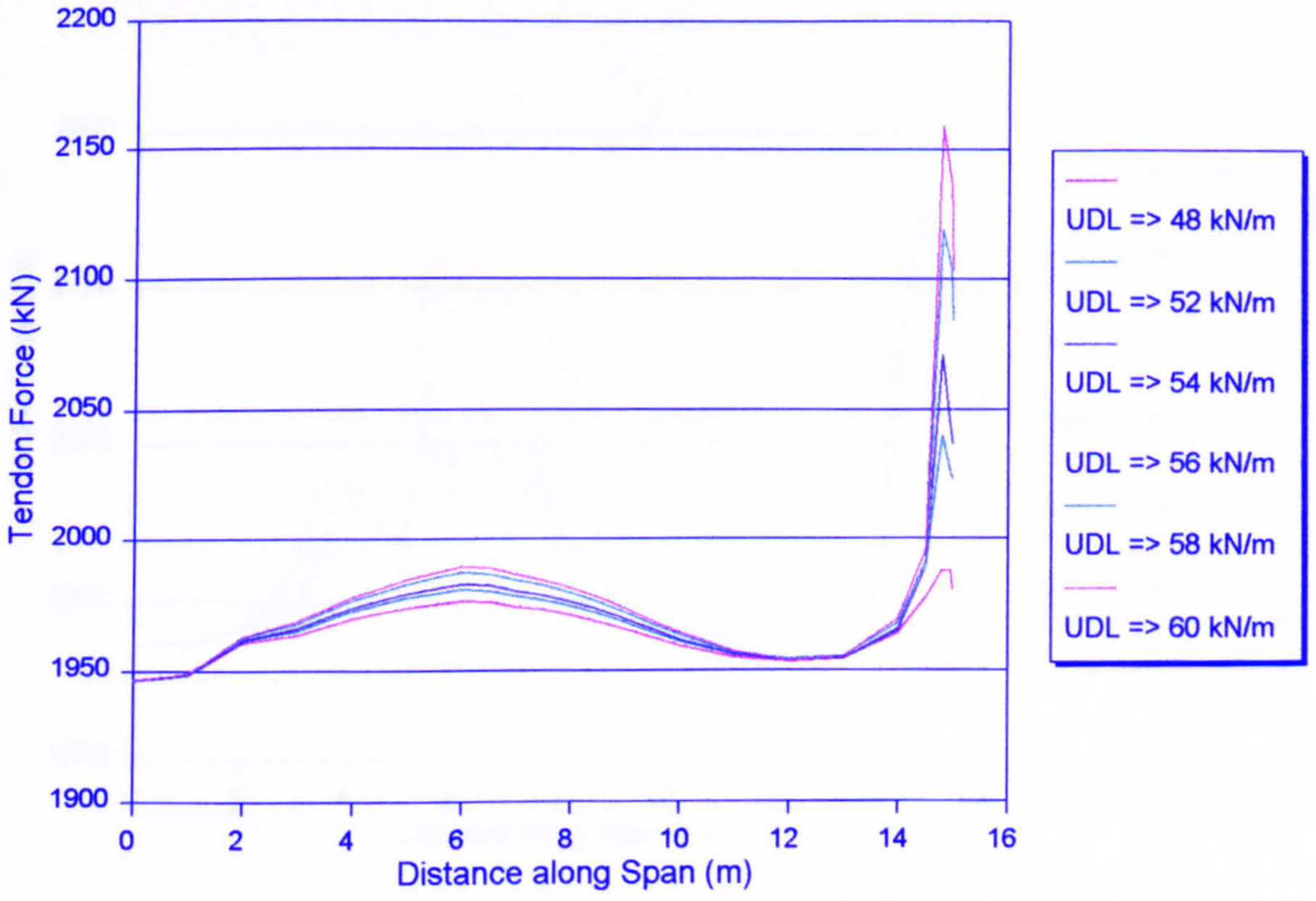

Figure 4.3.8. Tendon Force Envelope, F.E. Model 18

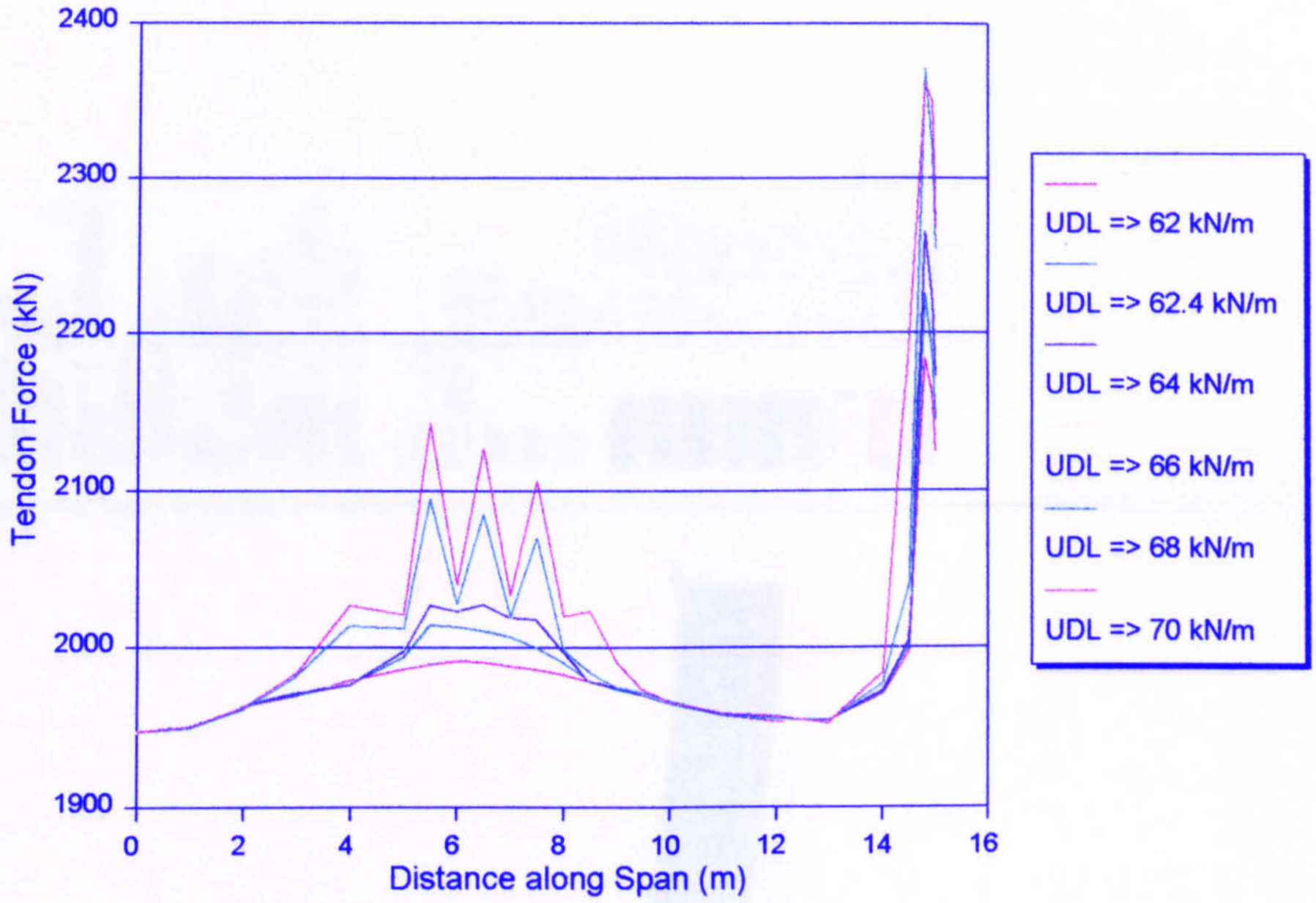

Figure 4.4.9. Tendon Force Envelope, F.E. Model 18

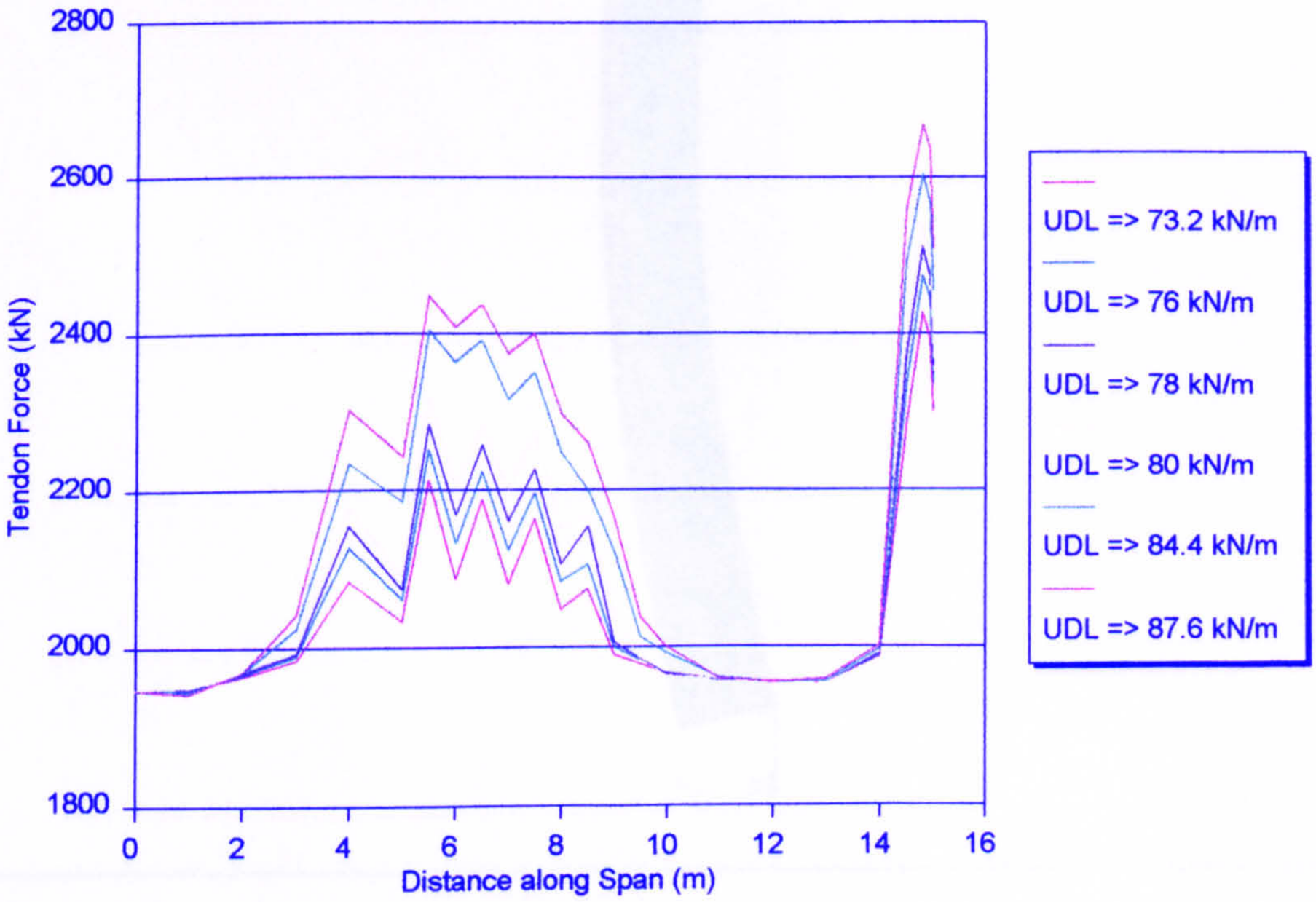

Figure 4.4.10. Tendon Force Envelope, F.E. Model 18

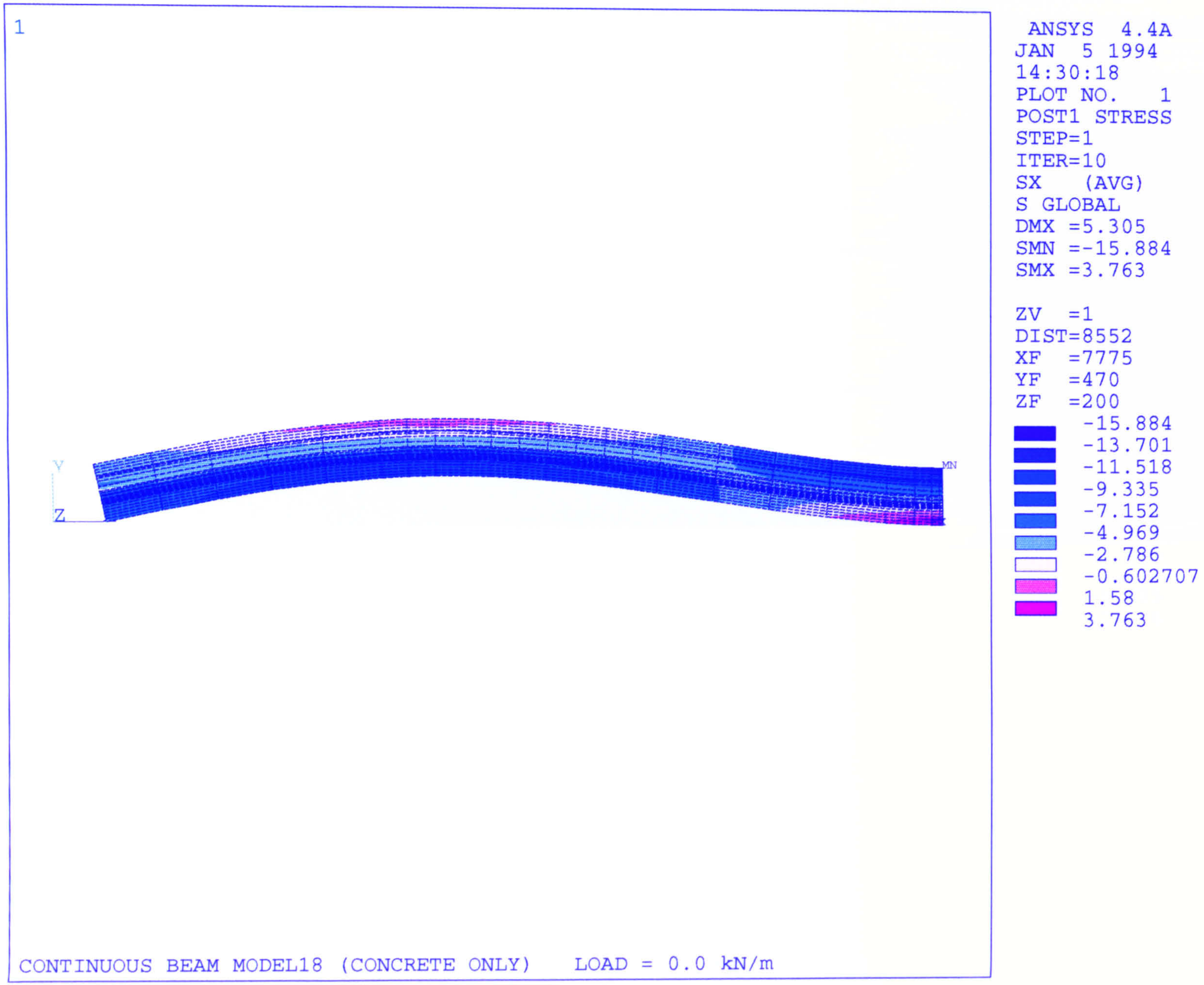
1
ANSYS 4.4A
JAN 5 1994
14:30:18
PLOT NO. 1
POST1 STRESS
STEP=1
ITER=10
SX (AVG)
S GLOBAL
DMX =5.305
SMN =-15.884
SMX =3.763
ZV =1
DIST=8552
XF =7775
YF =470
ZF =200
-15.884
-13.701
-11.518
-9.335
-7.152
-4.969
-2.786
-0.602707
1.58
3.763
Y
Z
MN
CONTINUOUS BEAM MODEL18 (CONCRETE ONLY) LOAD = 0.0 kN/m

Figure 4.4.11.

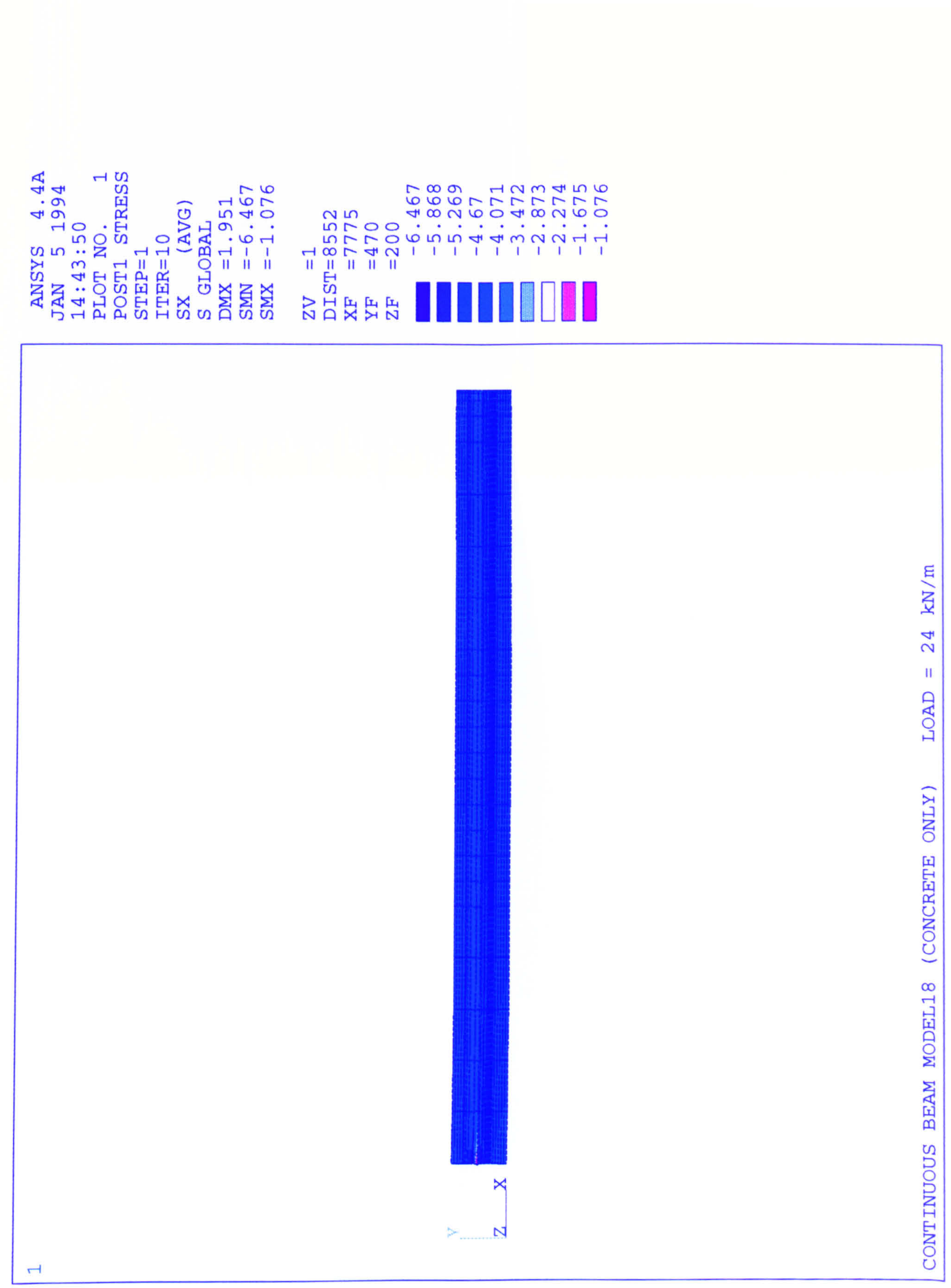
ANSYS 4.4A
JAN 5 1994
14:43:50
PLOT NO. 1
POST1 STRESS
STEP=1
ITER=10
SX (AVG)
S GLOBAL
DMX =1.951
SMN =-6.467
SMX =-1.076
ZV =1
DIST=8552
XF =7775
YF =470
ZF =200
-6.467
-5.868
-5.269
-4.67
-4.071
-3.472
-2.873
-2.274
-1.675
-1.076
LOAD = 24 kN/m
CONTINUOUS BEAM MODEL18 (CONCRETE ONLY)
Y
Z
X
1

Figure 4.4.12.

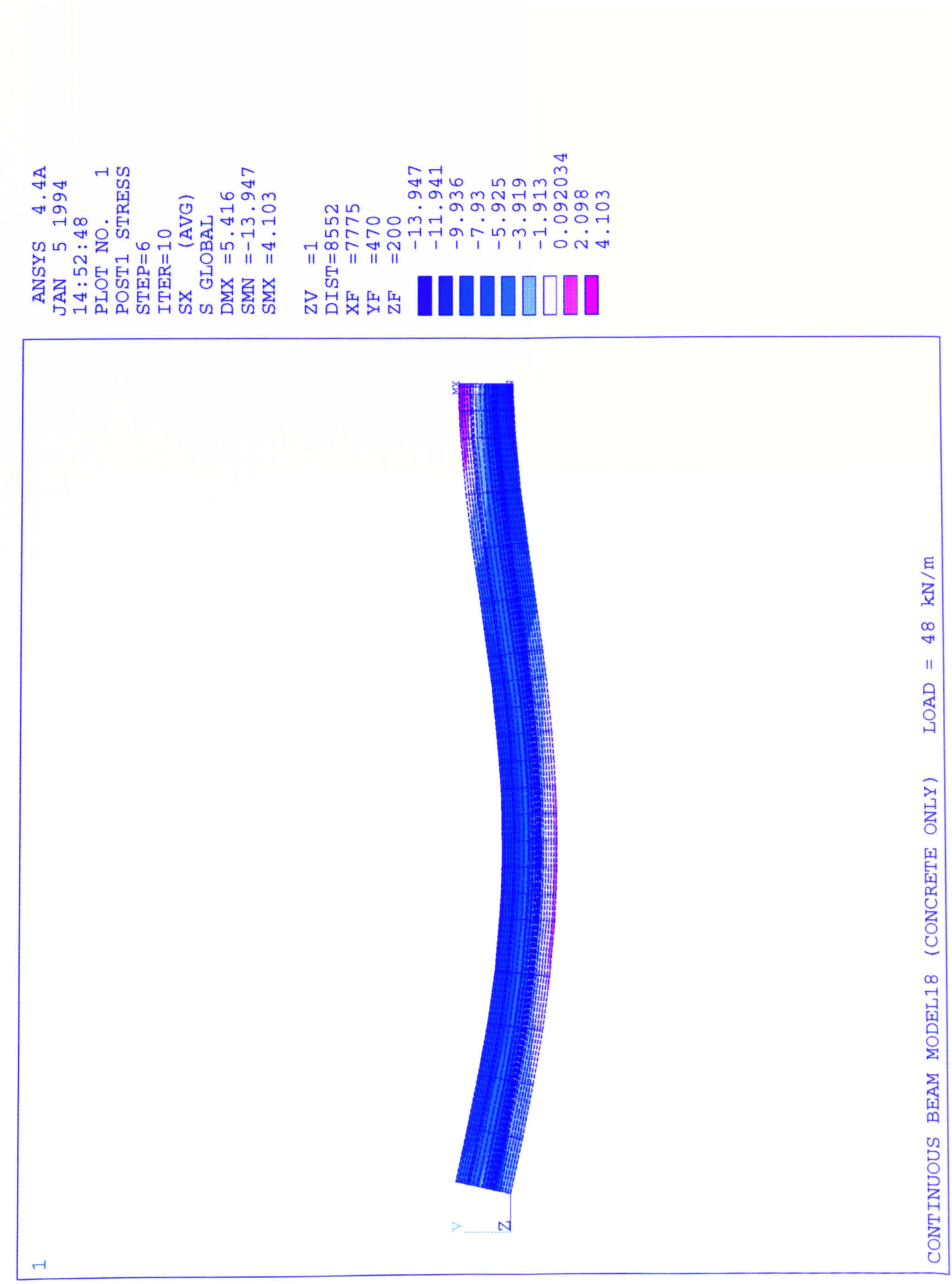
ANSYS 4.4A
JAN 5 1994
14:52:48
PLOT NO. 1
POST1 STRESS
STEP=6
ITER=10
SX (AVG)
S GLOBAL
DMX =5.416
SMN =-13.947
SMX =4.103
ZV =1
DIST=8552
XF =7775
YF =470
ZF =200
-13.947
-11.941
-9.936
-7.93
-5.925
-3.919
-1.913
0.092034
2.098
4.103
MX
Y
Z
1
CONTINUOUS BEAM MODEL18 (CONCRETE ONLY) LOAD = 48 kN/m

Figure 4.4.13.

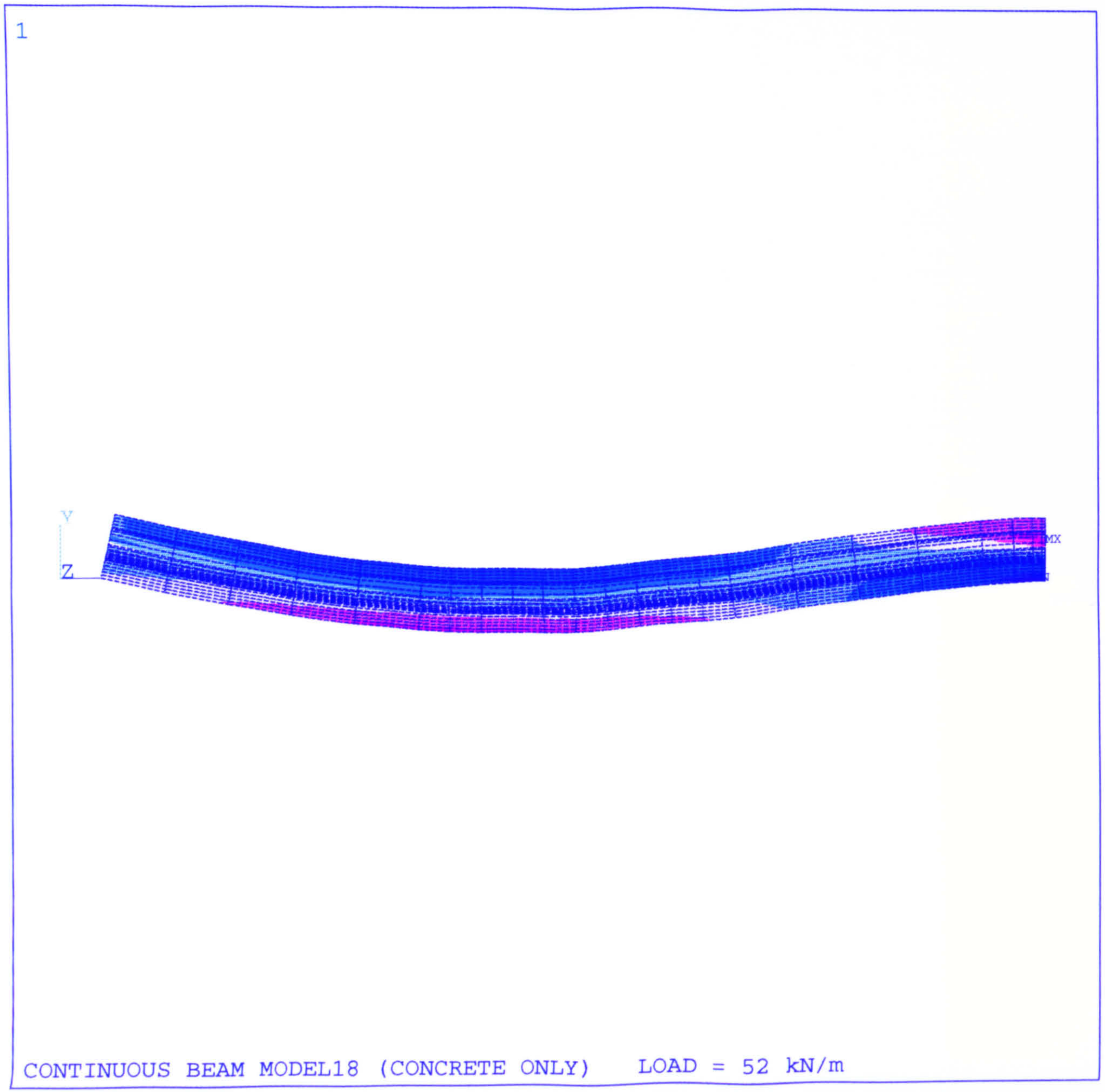
1
ANSYS 4.4A
JAN 5 1994
14:59:22
PLOT NO. 1
POST1 STRESS
STEP=7
ITER=10
SX (AVG)
S GLOBAL
DMX =6.644
SMN =-17.107
SMX =3.278
ZV =1
DIST=8552
XF =7775
YF =470
ZF =200
-17.107
-14.842
-12.577
-10.312
-8.047
-5.782
-3.517
-1.252
1.013
3.278
Y
Z
MX
CONTINUOUS BEAM MODEL18 (CONCRETE ONLY) LOAD = 52 kN/m

Figure 4.4.14.

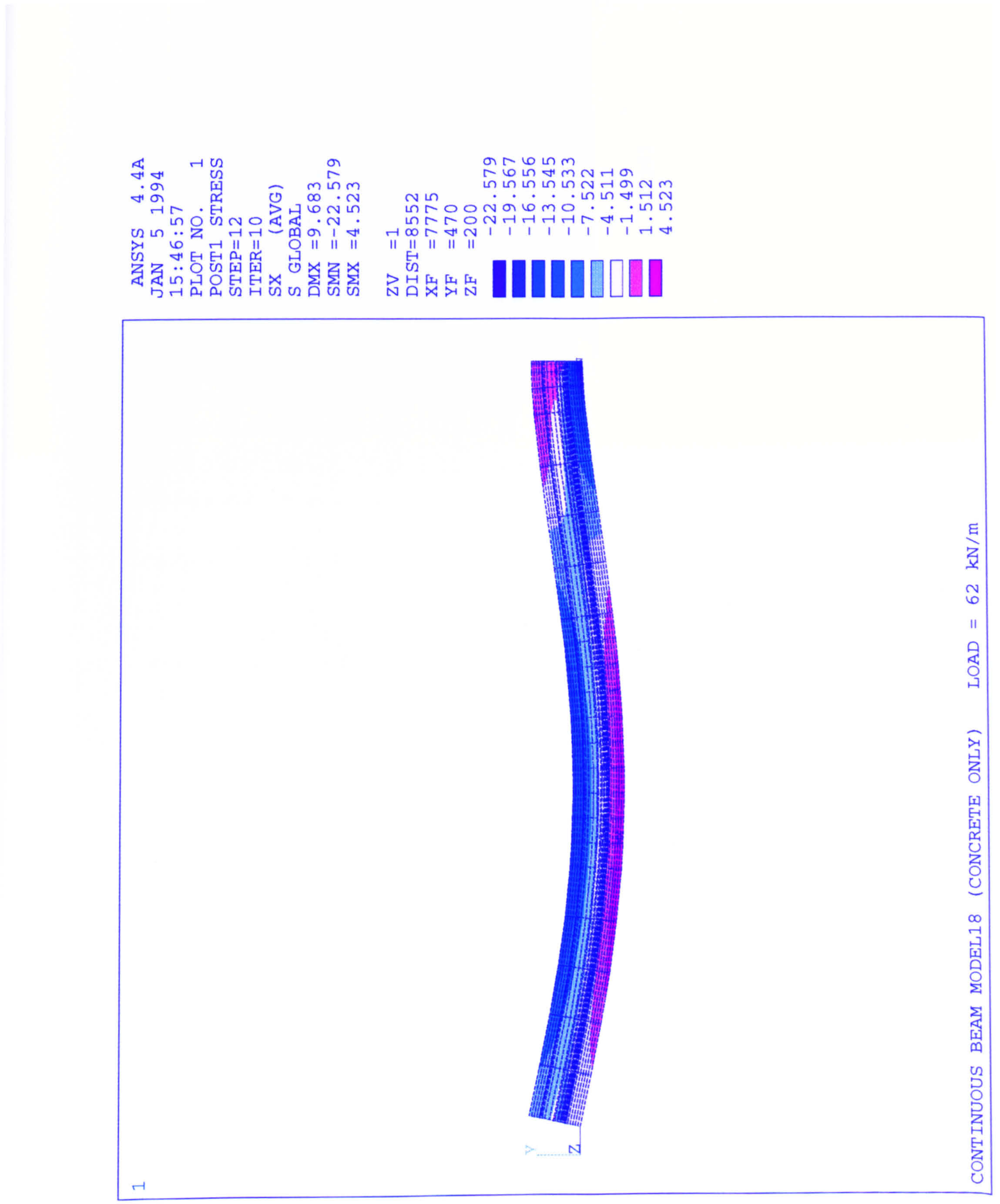
ANSYS 4.4A
JAN 5 1994
15:46:57
PLOT NO. 1
POST1 STRESS
STEP=12
ITER=10
SX (AVG)
S GLOBAL
DMX =9.683
SMN =-22.579
SMX =4.523
ZV =1
DIST=8552
XF =7775
YF =470
ZF =200
-22.579
-19.567
-16.556
-13.545
-10.533
-7.522
-4.511
-1.499
1.512
4.523
Y
Z
1
CONTINUOUS BEAM MODEL18 (CONCRETE ONLY) LOAD = 62 kN/m

Figure 4.4.15.

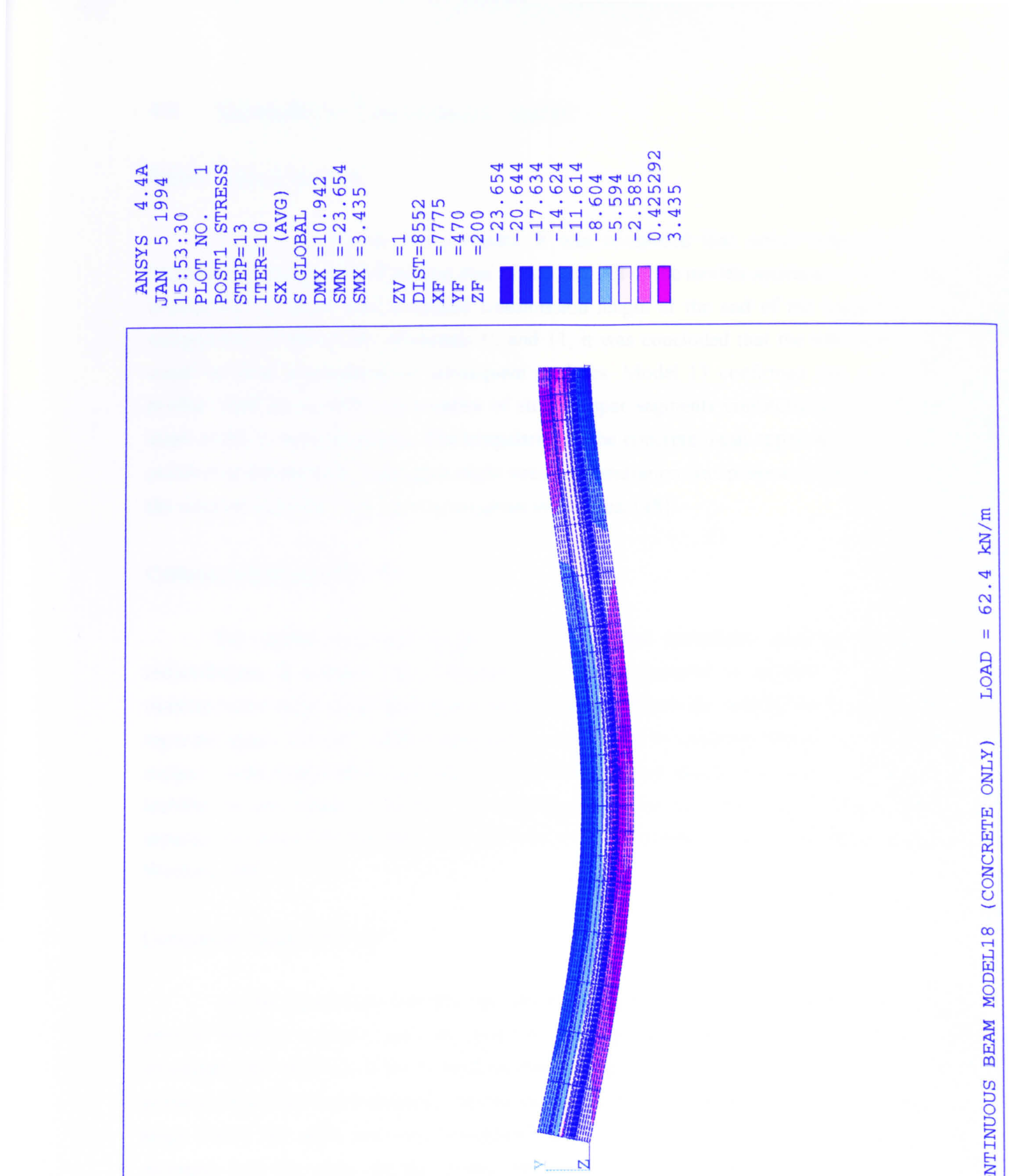
ANSYS 4.4A
JAN 5 1994
15:53:30
PLOT NO. 1
POST1 STRESS
STEP=13
ITER=10
SX (AVG)
S GLOBAL
DMX =10.942
SMN =-23.654
SMX =3.435
ZV =1
DIST=8552
XF =7775
YF =470
ZF =200
-23.654
-20.644
-17.634
-14.624
-11.614
-8.604
-5.594
-2.585
0.425292
3.435
CONTINUOUS BEAM MODEL18 (CONCRETE ONLY) LOAD = 62.4 kN/m
Y
Z
1

Figure 4.4.16.

4.5/ Conclusion to Finite Element Analyses

Simply Supported Beams

From an overview of the results, it was concluded that actual behaviour up to ultimate was modelled with a great deal of success. All of the models appeared to behave in a pretensioned manner with a marked transmission length at the end of the beams. From a comparuson of the results of models 10 and 11, it was concluded that the half beam model could be used successfully for subsequent analyses. Model 13 confirmed that a parabolic profile could be modelled as a series of straight spar segments connected to the concrete mesh at the correct loacations. The irregularity of the concrete mesh appeared to cause little problem in the analysis, although a slight stress concentration was present at the centreline at the support location. More details are given in Weekes, [48].

Continuous Beam Model 12

The tendon profile of model 12 was somewhat unrealistic, although about 50% redistribution of moments was obtained. The beam appeared to develop a large crack running to the level of the steel at the centre support, effectively dividing the beam into two separate spans. Ultimate failure appeared to be caused by cracking through at the centre support, indicating a shear type failure. The main problem arising from this model was the inability by any means to monitor the secondary moment into the cracking stage, and to separate the secondary moment from the total internal bending moment. Details are given in Weekes, [48].

Continuous beam Model 18

In the knowledge that the secondary moment could not be seperated from the internal bending moment past the onset of cracking, the purpose of model 18 was to investigate the variation of the internal bending moments at various sections along the beam as the applied load was increased. The centre support section was designed to reach a plastic hinge before the span, and was theoretically given the ductility to rotate and redistribute moments into the span. As the results indicate, the ultimate load behaviour was not as desired. Failure of the beam occurred without any plastic hinges developing, and this was due to the tendon force not being of the desired value at the centre support during the cracked stage.

The most probable cause of the problem was the shape of the tendon profile. In an earlier unsuccessful model, a reversed tendon curvature was used over the centre support. This produced a downwards equivalent load over a short length, and the angle at which the final spar elements were attached to the concrete nodes at the centre support was as close to the horizontal as possible. The problem with this layout was that the elastically calculated secondary moment was vastly different to that produced by the model. This was most likely due to the way in which the equivalent loads, taken as U.D.L.s, were being modelled as point loads at the connection of the steel spar elements. Refinements of the concrete and steel layout at the point of inflexion and at the support had little effect, so this model was abandoned. Model 18 had no reversed curvature, therefore the U.D.L., modelled as point loads was uniformly acting upwards along the length of the beam, so the secondary moment was as predicted by an equivalent load analysis. The problem with the continuously curved tendon is that at the centre support, the tendon joins the concrete at an angle to the horizontal, which may be the cause of stress concentrations. The concrete elements were particularly narrow in this area so that the lengths of the spar elements adjacent to the support were reduced, and the effect of having a uniform stress along the length of the spar element was reduced, so that a continuous change in tendon force could be modelled as correctly as possible. For simply supported beam model 13, this is also the case at the midspan location, that a stress concentration occurs at the location where the tendon joins to the centreline nodes, although for this case, the tendon angle to the horizontal at the centreline is very small. This supports the idea that the angling of the tendon at the ends of the beam models is the probable cause for stress concentrations and undesireable changes in the tendon force. It may also be true that the support section may be partly responsible for having caused a stress concentration. Another possibility is that the half beam models were experiencing a kind of transmission length effect, with local elastic shortening about the centreline section, effectively behaving as two separate tendons. Theoretically this should not be the case as the tendon is fixed from movement in the longitudinal direction, as well as the concrete elements at this location.

With hindsight, perhaps a linear harped tendon profile which would naturally produce point equivalent loads should have been modelled, eliminating the need for major refinements in the concrete mesh. This may still have caused stress concentrations at the centre support section due to the angling of the tendon. With a lengthy analysis such as this finite element approach, it is necessary to have ironed out as many possible problems in the model before starting the final analysis. This was the case for model 18, although it was always likely that stress concentrations and other factors would have an influence, factors which are difficult to assess in the basic theory. It can be said that finite elements model the actual behaviour better

than was at first anticipated, but causing complications when making comparisons with idealised theories about the behaviour.

Secondary Moment

Regardless of the success of model 18, the nature of the problem was such that the secondary moment could not be monitored once cracking had begun. It was possible to monitor the total internal bending moment, so the results may have been useful for studying the amount of moment redistribution available (although this was not the case). It was clear at this stage that an alternative approach was necessary to determine the influence of secondary moments on moment redistribution. Most of the previous work on the subject deals with how the inclusion of the elastically calculated secondary moment would affect the ultimate load, with provision for moment redistribution. The fact that the secondary moment may be changing in the stages leading up to the point of statical determinacy seems to have been somewhat neglected. This is a very important issue in the design of continuous prestressed concrete beams, as the inclusion or exclusion of the secondary moment at various stages in the design process may have a bearing on whether or by how much a design is conservative. If the secondary moment is changing, then this would dramatically complicate how the secondary moment should be treated in the design. The next step in the investigation was to find a means of separating the secondary moments from the total internal bending moment, up to a point where the beam is rendered statically determinate. After this, the secondary moment will of course be zero, but the amount of rotation available for moment redistribution may be affected by the behaviour of the secondary moment prior to this.

The next chapter (5) explains the method devised for achieving an estimate of the secondary moments through the cracking stage by an equivalent load analysis.

5/ Equivalent Load Analysis at Overload

5.1/ The SMAREL Algorithm

From the results of the finite element analyses of the continuous prestressed concrete beams, it is evident that there are a number of complications involved with regard to the correct way in which to model the tendon profile, the separation of secondary moments from the internal moments, and determination of the amount of moment redistribution which can take place at the ultimate limit state. Ordinary linear methods of calculating the secondary moment cannot be used due to the nonlinear behaviour in the post cracking stage. Various studies involving nonlinear analyses, as discussed in section 1.1, have attempted to shed light on the effects of secondary moments on the amount of redistribution available at plastic hinge formation, with suggestions on how they might be included in design. Many of these studies have performed nonlinear analyses of continuous prestressed concrete structures with regard to the overall behaviour up to the ultimate limit state, and have then attempted to relate the elastic secondary moment to the amount of rotation available. Others have recognised that the secondary moment may alter between the stages of first cracking and ultimate limit state, and suggest a number of alternatives to the effects of this. However, none of the previous work has attempted to separate the secondary moment from the internal moment during the nonlinear phase, a situation which appears to be logical if the effects of the secondary moment are to be included at ultimate limit state.

A number of methods such as equivalent load analysis are available to separate the secondary moment from the internal moment during the elastic phase. Nilson, [2], points out that such an analysis is dependent on the superposition of stresses, which is valid only if the beam is operating in a linear elastic manner. He also rightly suggests that the task of applying such a method into the nonlinear stage would be complicated by various factors such as increases in the tendon force at locations such as cracks, along with flexural stiffness changes.

Taking into account the extra complications required to perform such an analysis, it was decided to attempt a nonlinear analysis incorporating the equivalent load method to separate the secondary moment from the overall internal moment. Attention was paid to the correct representation of crack formation, tendon force, and stiffness variations along a particular beam span.

Computer programs were subsequently written to analyse two and three span continuous beams with rectangular, I, or T sections, and parabolic tendon profiles present at

one level in the beam only. These were given the name SMAREL which stands for Secondary Moments and Redistribution by Equivalent Load. The core elements fundamental to the operation of the program are now described in detail.

Main Procedures

The fundamental procedures used in the SMAREL algorithm for the calculation of secondary moments by equivalent loads using a nonlinear approach, break down into three main categories, as mentioned in section 2.2.6:-

1/ A double numerical differentiation to obtain equivalent loads from the primary moment.

2/ Calculation of stiffness, carry-over factors, and fixed end moments for a member of variable stiffness (created by the formation of cracks), for an equivalent load analysis

3/ A cracked section analysis of a prestressed concrete section, to determine the properties of the cracked sections.

For these procedures to be used in a computer program, it is necessary to somehow divide the beam into sections or elements. The finite difference procedure used in the numerical differentiation dictates that a nodal system at regular intervals be used. Hence the program would take in data relating to material properties, beam dimensions, and profile layout, and divide each span into nodes which were of equal spacing. The properties of the sections at each node could then be determined for different loading conditions, cracked section analyses performed, with tendon force and stiffness variations present over a particular length of nodes. The correct way in which to model the flexural stiffness changes and tendon force along the length of the beam was of paramount importance. At cracks, definite values for the tendon force and flexural stiffness can be ascertained, but at nodes adjacent to the crack, these will vary in some manner, depending on whether there are cracks immediately to the left, right, both sides or neither side of the crack in question. The representation of these variations is discussed in section 5.1.4.

5.1.1/ The Numerical Differentiation

To calculate the equivalent load, a numerical differentiation of the primary moment function must be incorporated due to the alteration of the tendon force after cracking, as this

will be more suited to solution by computer than an analytical method. Finite difference techniques are well suited for the solution of problems requiring either numerical integration or differentiation. For integration, the Trapezoidal and Simpson's rule can be derived from Bessels and Stirling's interpolation formulae, each having increased accuracy as the 'width' of the interval or differences are made smaller, creating more nodes in the range to be integrated. Numerical differentiation is a less 'stable' problem as far as finite differences are concerned, as the accuracy will only be optimised at particular interval sizes. Taking the general finite-difference formula for the derivative of a function $f(x)$ as :

$$\frac{df}{dx} = \lim_{h \to 0} \frac{f(x+h) - f(x-h)}{2h} \qquad (1)$$

it would appear at first that if h were made smaller, the accuracy of the derivative would improve. This is not the case as equation 1 is a ratio of h values, which, when h decreases, becomes numerically unstable. Various finite difference formulae are suited to different numerical tasks, and in this case, Stirlings interpolation formula is used.

Stirling's Interpolation Formula

Stirlings finite-difference interpolation formula is best suited for numerical differentiation, and is described in detail in Spencer et.al. [7]. It is derived from Gauss's central difference interpolation formula, and has the form:

$$P(x) = f_0 + S_1\left(\delta f_{-1/2} + \delta f_{1/2}\right) + S_2\delta^2 f_0 + S_3\left(\delta^3 f_{-1/2} + \delta^3 f_{1/2}\right) + S_4\delta^4 f_0 + \ldots\ldots, \quad (2)$$

Where $P(x)$ is the polynomial approximation to the function, f is the actual function value at points defined by the subscript, and δf's are the central differences, with the superscript representing the difference level, and the subscript representing the particular domain data point. The coefficients S are the Stirling coefficients, and are defined as follows:

$$S_1 = \frac{1}{2}u,\ S_2 = \frac{1}{2}u^2,\ S_3 = \frac{1}{2}u\left(u^2-1\right)\Big/3!,\ S_4 = u^2\left(u^2-1\right)\Big/4!,\ S_5 = \frac{1}{2}u\left(u^2-1\right)\left(u^2-2^2\right)\Big/5!,\ldots$$

where $u = (x - x_0)/h$, h is the interval between data points, and x is the interpolated point.

To obtain the formula for the derivative of the function, the approximating polynomial is simply differentiated to the required level. In this case, the chain rule may be used to differentiate the polynomial with respect to u, i.e.,

$$\frac{df}{dx} \approx \frac{dP}{dx} = \frac{du}{dx}\frac{dP}{du} = \frac{1}{h}\frac{dP}{du} \qquad \text{as} \quad u = (x - x_0)/h$$

In this case we are interested in the second differential, therefore the series solution of this will be:

$$\frac{d^2 f}{dx^2} \approx \frac{1}{h^2}\frac{d^2 P}{du^2} = \frac{1}{h^2}\left[\delta^2 f_0 + \frac{1}{2}u\left(\delta^3 f_{-1/2} + \delta^3 f_{1/2}\right) + \frac{1}{12}\left(6u^2 - 1\right)\delta^4 f_0 + \ldots\right] \quad (3)$$

For derivatives at the data points, x is put equal to x_0, and therefore u will be zero. The series solution of the second derivative of $f(x)$ becomes :

$$\frac{d^2 f_0}{dx^2} = \frac{1}{h^2}\left[\delta^2 f_0 - \frac{1}{12}\delta^4 f_0 + \frac{1}{90}\delta^6 f_0 - \ldots\ldots\right] \quad (4)$$

With a value of h between 0.01 and 0.1, the formula appears sufficiently accurate for most functions, but the accuracy is also dependant on the level of differences taken, i.e. the number of terms in the series solution, and also the number of decimal places of the numbers in the calculation. A continuous function of the primary moment will be adequately differentiated using this formula.

Extrapolation

At points where the function alters or becomes discontinuous, it follows that the derivatives must also be discontinuous at the same locations. When cracks appear, the primary moment function will exhibit such discontinuities. Where the function changes abruptly, this 'step' change cannot be dealt with by the finite difference procedure directly, as large oscillating spikes in the derivatives occur due to the numerical method involved. Therefore it is necessary to flag any points where the function alters, and treat each individual function separately. Changes in the primary moment function will occur at the ends of the beams, at cracks, between cracks, and where the tendon force begins to deviate from its effective prestress value. At the points where each function becomes discontinuous, to obtain the required level of finite difference values, an extrapolation of the function must be carried out past each end, so that step changes may be modelled correctly.

Newton-Gregory Interpolation Formula

This extrapolation is carried out using the Newton-Gregory forward and backward difference formulae, using the backward difference formula, equation (5), to extrapolate forwards, and the forward difference formula, equation(6), to extrapolate backwards, thus

$$P(x) = P(x_0 + hu) = f_0 + u\nabla f_0 + \frac{1}{2}u(u+1)\nabla^2 f_0 + \ldots\ldots + \frac{1}{n!}u(u+1)\ldots(u+n-1)\nabla^n f_0 \qquad (5)$$

$$P(x) = P(x_0 + hu) = f_0 + u\Delta f_0 + \frac{1}{2}u(u-1)\Delta^2 f_0 + \ldots\ldots + \frac{1}{n!}u(u-1)\ldots(u-n+1)\Delta^n f_0 \qquad (6)$$

where ∇ and Δ are backward and forward differences respectively. Details are given in Spencer et.al. [7].

5.1.2/ Stiffness and Carry-Over factors

Stiffness Changes in the Beam

Whilst behaving in an uncracked elastic manner, the flexural stiffness E_cI may be treated as constant along the length of a member, where E_c is the effective elastic modulus of concrete and I is the second moment of area of the uncracked section about the centroidal $x-x$ axis. As load is applied to the beam, the curvature ϕ will increase linearly with the bending moment, assuming the beam is uncracked. Typical approximate moment-curvature relationships for different percentages of tendon steel, together with the corresponding neutral axis depth at ultimate moment are shown in figure 5.1.1. It can be seen from this diagram that higher neutral axis depths at ultimate moment, and the lower the percentage of reinforcement tends to form a more ductile section, indicated by the shallower curve, which is more suitable for moment redistribution. The curvatureϕ, is given by $1/R$ where R is the radius of curvature of the beam section. When a particular section of the beam cracks, the curvature increases locally as the flexural stiffness E_cI has decreased. It can be shown by linear elastic theory that the bending moment is related to the deflection of the beam by the second derivative, $M = E_cI\,d^2y/dx^2$, and as the curvature is equal to the second derivative of the deflection function, the moment-curvature relationship becomes $\phi = M/E_cI$. When a particular section of the beam cracks, the curvature increases locally as the flexural stiffness E_cI has decreased and the linear relationship between moment and curvature no longer holds true. The direct relationship between bending moment and curvature is now given accurately by$M = E_cI\,d^2y/dx^2$, so that E_cI_g is the flexural stiffness of the gross cross-section of the beam, and is now equal to the gradient of the moment-curvature relationship.

Hence, for an accurate calculation of flexural stiffness, the moment-curvature relationships for each section of the beam should be known, as each section will have different properties especially after the onset of cracking.

Having ascertained these relationships, there are a number of methods available which can use them for the analysis of continuous beams, such as compatibility of deformations, Priestley et.al. [20]. El-Dib, [49], has produced a method for calculating stiffness factors, carry-over factors, and fixed-end moments of steel rectangular, I, and T section members subject to transverse and longitudinal loads. This method is extended here to reinforced and prestressed concrete sections. The evolution of the following calculations is given in detail in El-Dib [49].

A beam shown in figure 5.1.2 is simply supported at the left hand end and encastred at the right hand end. If a moment M_1 is applied to the left end, causing a rotation θ_1 of magnitude of 1 radian, a moment M_2 occurs at the right hand encastred end, where the rotation θ_2 is zero. The first moment-area theorem, with this information, is given by equation(7). The general equation for the bending moment is given by equation (8). Substitution of equation (7) into equation (8) yields equation (9). Two parameters R_1 and R_2 , given by equation (9a) are then used to simplify equation (9) to equation (10).

$$\theta_1 - \theta_2 = \int_0^L \frac{M}{EI}\, dx \tag{7}$$

$$M = \left(\frac{L-x}{L}\right)M_1 - \left(\frac{x}{L}\right)M_2 \tag{8}$$

$$1 = \int_0^L \frac{M_1}{EI}\frac{(L-x)}{L}\, dx - \int_0^L \frac{M_2}{EI}\frac{x}{L}\, dx \tag{9}$$

Let $R_1 = \int_0^L \frac{1}{EI}\left(\frac{L-x}{L}\right) dx$ and $R_2 = \int_0^L \frac{1}{EI}\left(\frac{x}{L}\right) dx$ (9a)

Then $$R_1 M_1 - R_2 M_2 = 1 \tag{10}$$

The second moment area theorem, given by equation (11) is then substituted into equation (8), yielding equation (12). Parameters R_{x1} and R_{x2} are introduced in equation (12a), so that equation (12) can be simplified to equation (13).

$$x_2\theta_2 - x_1\theta_1 = L\theta_2 - 0.\theta_1 = \int_0^L \frac{Mx}{EI}\ dx\ = 0 \qquad (11)$$

$$\int_0^L \frac{M_1}{EI}\left(\frac{L-x}{L}\right)x\ dx - \int_0^L \frac{M_2}{EI}\left(\frac{x}{L}\right)x\ dx\ = 0 \qquad (12)$$

Let $R_{x1} = \int_0^L \frac{1}{EI}\left(\frac{L-x}{L}\right)x\ dx$ and $R_{x2} = \int_0^L \frac{1}{EI}\left(\frac{x}{L}\right)x\ dx$ (12a)

Then $$R_{x1}M_1 - R_{x2}M_2 = 0 \qquad (13)$$

Solving the simultaneous equations (10) and (13) gives:

$$M_1 = \frac{1}{R_1 - R_{x1}\dfrac{R_2}{R_{x2}}} \quad \text{and} \quad M_2 = \frac{1}{R_{x2}\dfrac{R_1}{R_{x1}} - R_2} \qquad (14)$$

As the rotation θ_1 is equal to 1 radian, the stiffness factor s becomes:

$$s = \frac{M_1 L}{EI} \qquad (15)$$

The carry-over factor c becomes:

$$c = \frac{M_2}{M_1} \qquad (16)$$

The calculation of these factors requires the integration in equations (9a) and (12a) for the determination of the coefficients R_1, R_2, R_{x1}, and R_{x2}. Assuming that the EI values along the length of the beam may alter as a function of x, these integrations must be carried out numerically. There are a number of methods available for this, although one method in particular, based on the conversion of the required terms into curvatures, and representing them as 'equivalent concentrated loads' for integration, is best suited for reasons which will become apparent when the beam stiffness changes due to cracking. This procedure is analogous to the 'conjugate beam' method, and is described in detail in Allen [5].

The Numerical Integration

Assuming the beam is divided into 'n' nodes, the curvature of the beam at node 'i' will be :

$$\Phi_i = \frac{M_i}{EI_i} \tag{17}$$

The total curvature is the combination of the curvatures caused by the couples M_1 and M_2 as dictated by equation (8), hence :

$$\Phi_i = \Phi_{1i} - \Phi_{2i} = \frac{M_{1i}}{EI_i} - \frac{M_{2i}}{EI_i} \tag{18}$$

For convenience, the curvatures are altered such that:

$$\phi_{1i} = \frac{\Phi_{1i}}{|M_1|} \qquad \text{and} \qquad \phi_{2i} = \frac{\Phi_{2i}}{|M_2|} \tag{19}$$

These curvatures are then represented as equivalent point loads W located at nodes, as detailed in Allen [5]. The moment due solely to M_1 gives the following equivalent point loads.

$$\begin{aligned}
W_{11} &= \frac{h}{24}(7\phi_{11} + 6\phi_{12} - \phi_{13}) \\
&\vdots \\
W_{1i} &= \frac{h}{12}\left(\phi_{1(i-1)} + 10\phi_{1i} + \phi_{1(i+1)}\right) \\
&\vdots \\
W_{1n} &= \frac{h}{24}\left(7\phi_{1n} + 6\phi_{1(n-1)} - \phi_{1(n-2)}\right)
\end{aligned} \tag{20}$$

The coefficients R_1 and R_{x1} now become:

$$R_1 = \sum_{i=1}^{n} W_{1i} \qquad \text{and} \qquad R_{x1} = \sum_{i=1}^{n} W_{1i} x_i \tag{21}$$

Similarly, for the moments due to M_2, the equivalent point loads are :

$$W_{21} = \frac{h}{24}(7\phi_{21} + 6\phi_{22} - \phi_{23})$$

$$\vdots$$

$$W_{2i} = \frac{h}{12}\left(\phi_{2(i-1)} + 10\phi_{2i} + \phi_{2(i+1)}\right) \qquad (22)$$

$$\vdots$$

$$W_{2n} = \frac{h}{24}\left(7\phi_{2n} + 6\phi_{2(n-1)} - \phi_{2(n-2)}\right)$$

and the coefficients R_2 and R_{x2} are :

$$R_2 = \sum_{i=1}^{n} W_{2i} \qquad \text{and} \qquad R_{x2} = \sum_{i=1}^{n} W_{2i} x_i \qquad (23)$$

The results for the calculation of stiffness and carry-over factors of elastic prismatic members elastic members in El-Dib [49], using this procedure were excellent, and the method was applied to elastic-plastic non-prismatic members, also with good results.

Elastic-Plastic Non-Prismatic Members

The main feature of non-prismatic members is the variation of the flexural rigidity, EI. The effects of plasticity can be included by modelling the member as a pseudo non-prismatic member, as discussed in El-Dib [49]. Exact calculation of the flexural rigidity requires knowledge of moment curvature relationships at each nodal section, then the EI values may be obtained from the gradient of the graph, $dM/d\phi$. In this case, the curvature at a particular applied moment can be found directly from a cracked section analysis by dividing the extreme compressive fibre strain by the neutral axis depth, i.e., ε_c/x. Therefore, the specific point on the curve is known, and not the whole relationship required for exact calculation of EI. However it is sufficient to define an effective flexural rigidity as $EI_{eff} = M/\phi$, equal to the gradient of the secant at the point, as these values are to be used to calculate curvatures used for the integration procedure previously defined.

Fixed End Moments of a Variable Distributed Load

Details of a similar procedure for finding the fixed end moments of a member subject to a uniformly distributed load are given in El-Dib [49]. To calculate the fixed end moments of a beam subject to a varying load a similar procedure to that used for calculating stiffness and carry-over factors was used, based on the theory in El-Dib [49]. The total curvature at

node 'i' is the addition of the curvatures calculated by equation (19), and the curvature due to the transverse load:-

$$\Phi_{qi} = \frac{M_{qi}}{EI_i} \tag{24}$$

Where M_{qi} is the free bending moment function. The integration processes involved for calculating the free bending moment for a varying distributed load are described in appendix D, (the common method for calculating fixed end moments for an elastic prismatic beam is also included). The equivalent concentrated loads W_{qi} obtained from the curvature are calculated as before. Using the first moment area theorem gives :-

$$-M_1R_1 - M_2R_2 + R_q = 0 \tag{25}$$

Note that M_1 has changed sign from equation (10), as it is now a fixed end moment, rather than an applied clockwise positive moment. The end rotations are also zero. R_q is calculated from $\sum_{i=1}^{n} W_{qi}$ using the same procedure as in the previous section, and R_1 and R_2 are as before. The second moment area theorem leads to :-

$$-M_1R_{x1} - M_2R_{x2} + R_{qx} = 0 \tag{26}$$

Where $R_{qx} = \sum_{i=1}^{n} W_{qi}x_i$, and R_{x1} and R_{x2} are as before. Solving the simultaneous equations (25) and (26) for M_1 and M_2 gives :-

$$M_1 = \frac{\frac{R_2}{R_{x2}}R_{qx} - R_q}{R_{x1}\frac{R_2}{R_{x2}} - R_1} \quad \text{and} \quad M_2 = \frac{\frac{R_1}{R_{x1}}R_{qx} - R_q}{R_{x2}\frac{R_1}{R_{x1}} - R_2} \tag{27}$$

Which are the fixed end moments at the left and right hand ends respectively.

It should be stressed that to calculate relevant curvatures for the calculation of stiffness and carry over factors, it is necessary to include the equivalent load with any applied load when calculating the free bending moment. The primary as well as secondary moments, and those due to the applied load are to be included in the calculation for the stiffness, carry-overs, and fixed end moments, as it is the total moments which affect the curvature.

5.1.3/ Cracked Section Analysis

It is necessary for the calculation of curvatures, stiffnesses and general section properties that a cracked section analysis of prestressed concrete members be performed. Appendix B describes in detail the required calculations for such an analysis of rectangular, I, and T sections, in a separate module CSA. The prestressed reinforcement is at one level in the beam only, and at present there is no option for the inclusion of non-prestressed reinforcement. In the CSA algorithm, the prestress effects manifest themselves as a resistance component. Therefore the cracking moment is calculated using a superposition of stress, with the prestress effects included. This does not, however, include secondary moments, as these are internal moments created by restraining the beam from deforming at the internal support, i.e. the support acts as an external transverse load. The secondary moments must therefore be included with the internal moment caused by the applied loads. Once the internal moment in the beam has surpassed the cracking moment, the cracked section analysis balances the forces in the steel and the concrete for equilibrium, iterating the concrete extreme compressive fibre until the correct internal moment is reached.

The neutral axis depth and concrete fibre strain can then be used directly to calculate the local curvature at the section. Of course, not all of the sections where the resultant bending moment envelope exceeds the cracking moment envelope will actually be cracked, therefore a procedure based on the bond length is incorporated to calculate an effective crack spacing.

5.1.4/ Tendon Force and Stiffness Variations

When the internal bending moment envelope exceeds the cracking moment envelope at a particular location, the beam must crack to a certain extent in the zone where the cracking moment has been exceeded. If the primary crack forms at the node where the maximum difference between the cracking and internal bending moment envelopes occurs, a cracked section analysis will yield a number of useful properties at the particular node, such as curvature, which can be related to the flexural stiffness, and the tendon force. The location of other cracks in the cracked moment zone need to be determined, cracked section analyses performed at the cracked nodes, and the variation of the tendon force and flexural stiffness between and either side of cracks must then be addressed.

Bond length and Crack Spacing

Let the primary crack be the only crack to occur in a particular moment zone which exceeds the cracking moment envelope. At the crack the tension is taken all by the steel tendon. At some distance away from the crack, there will be a section which has been unaffected by the formation of the crack. Moving from the cracked section to the unaffected section, the bond between the steel and the concrete increases so that the steel gradually transfers tension back to the concrete. The bond length l_b is defined as the length between these two sections over which sufficient tension can be transferred to the concrete so as to cause the cracking moment (modulus of rupture) to be reached at the unaffected section.

The bond length can be estimated from the following equation (28):

$$l_b = \frac{P_1 - P_2}{u_{av} \sum O} \qquad (28)$$

Where:
- P_1 Tendon Force at section just after cracking when the applied moment equals the cracking moment.
- P_2 Tendon Force at section just before cracking when the applied moment equals the cracking moment.
- u_{av} Average bond stress between the steel and the concrete
- $\sum O$ Total surface area of the prestressing steel per unit length.

A value for the average bond stress was taken as half that of the ultimate bond stress. This is obtained from the ultimate anchorage bond stress, given in B.S.8110: clause 3.12.8.4., as $\beta\sqrt{f_{cu}}$, where β is a bond coefficient. Values for the bond coefficient for various bar types are given in B.S.8110: table 6.6-1. In this case, the value for plain bars in tension was used, i.e. 0.28. The values for the bond coefficient all include a partial factor of safety of 1.4, which must be multiplied out to obtain an actual bond stress. Thus, an approximation to the average bond stress used in the SMAREL programs is given by equation (29) as:

$$\frac{0.28 \times 1.4 \times \sqrt{f_{cu}}}{2} \qquad (29)$$

In an actual prestressed concrete beam, the first primary crack will occur at the section which has the weakest modulus of rupture, assuming the beam is subject to a constant moment zone. Subsequent cracks will then form at sections with higher moduli of rupture. The nearest distance an adjacent crack can be to the primary crack is equal to the

bond length. Assuming that cracks form at a further distance apart than the bond length, then the nearest distance apart that two cracks may be from each other so that another crack may form in between them, is a distance equal to twice the bond length. This is so that there will be a distance equal to the bond length either side of the new crack, allowing the build up of enough tension in the concrete for it to form. Hence this means that the crack spacing can vary between values of l_b and $2l_b$, so that the average crack spacing is taken as $1.5l_b$. In the program, the primary crack forms at the node where the internal bending moment envelope exceeds the cracking moment envelope by the greatest amount. Either side of this crack, at a distance of $1.5l_b$, the nearest nodes to this distance are scanned to see if the cracking moment envelope has been exceeded. If this is the case then the node is deemed to have cracked, if not then the node remains uncracked. This process is repeated until all of the nodes which have cracked have been ascertained.

Variations of Tendon Force and Stiffness Between Cracks

The flexural bond stress distribution between cracks is complex and a vast amount of experimental and theoretical work related to the subject has been produced. Nilson and Winter [4] explain how the bond stress is actually distributed in a flexural reinforced concrete member, and Priestley et. al. [19] produced a simplified version to correspond with the average crack spacing of $1.5l_b$. This simplified version is used here and gives rise to methods of modelling the variation of tendon force and flexural stiffness between and either side of cracks.

Figure 5.3a shows two isolated cracks, spaced a distance of $1.5l_b$ apart. The bond stress distribution between the cracks can be seen in figure 5.3b, with the maximum bond stress u_m occurring at the cracks, and decreasing linearly to a value of $0.25u_m$ midway between the cracks. On the other side of the cracks the bond stress is assumed to fall to zero. Assuming a constant effective prestress before any cracking has occurred, the tendon force at the cracks is increased from this to the values calculated from the cracked section analyses. Priestley et. al. [19] suggest a relationship between the bond stress and the reduction of the stress in the steel away from the crack. However to reduce the complications involved with this, it was decided to fit a continuous curved function for the tendon force reduction, rather than a linear one as for the bond stress. A cosine function appeared suitable for this purpose, figure 5.3c. The value of the tendon force midway between the cracks was calculated from the following formula:-

$$0.25\left(\frac{P_1 + P_2 - 2P_{eff}}{2}\right) + P_{eff}$$

The cosine function was then fitted between the values at the cracks and the midway value calculated with this formula. Where there is no adjacent crack, the cosine function was fitted between the value at the crack and the effective prestress force at a distance of l_b away from the crack. Therefore, after the cracked section analysis of all of the cracked nodes has been performed, then the tendon force variations are fitted to the relevant nodes in the vicinity of the cracked zone.

A similar procedure was used for the effective flexural stiffness variation. The effective stiffnesses at the cracked nodes was calculated from the curvature obtained from the cracked section analyses. Again, a cosine function was applied to the stiffness variation in exactly the same manner as for the tendon force. In this case it was then decided to perform a parametric study on the effects of altering the stiffness variation from the cosine function to a series of three linear variations symmetrical about each particular crack. The form of these variations is shown in figure 5.3d.

5.1.5/ SMAREL Solution Algorithm

A general outline of the steps involved in the SMAREL algorithm is as follows:-

1/ Input Model Data, giving an initial applied U.D.L. (elastic), and an estimate of the corresponding net internal moments at the supports (SM's).

2/ Calculate the primary moment, the product of the tendon force and eccentricity.

3/ Calculate the equivalent load, the second differential of the primary moment.

4/ Add the applied and equivalent loads, giving the total load.

5/ Calculate the free bending moment for the total load.

6/ Calculate the fixed end moments, stiffness, and carry-over factors.

7/ Perform moment distribution on the continuous beam system to calculate the total support moments.

8/ Calculate the net internal support moments (SM1's) by subtracting the primary moments from the total moments (i.e. reactant moments).

9/ Recalculate the free bending moment for the applied load only (any secondary moment is included in the reactant moments calculated in step 8, as they are linear between supports).

10/ Add the free and reactant moments at supports to obtain the actual net internal bending moment envelope.

11/ Calculate the cracking moment envelope (positive and negative regions of the cracking envelope are calculated based on the sign of the net internal bending moment envelope) .

12/ Compare cracking and actual internal moment envelopes to obtain zones (nodes) where the cracking moment has been exceeded, and isolate the node(s) in both the positive and negative regions at which the maximum difference occurs (if any). These are the primary cracked nodes, and there can be only one in any cracked region, positive or negative.

13/ Calculate the ultimate moment envelopes(positive and negative regions of the ultimate envelope are calculated based on the sign of the net internal bending moment envelope) .

14/ Calculate the section properties (effective stiffness, tendon force etc.) at the primary cracked nodes by carrying out a cracked section analysis at the node(s) in question.

15/ Calculate the corresponding bond length for the negative and positive moment zones where cracking has occurred. This will relate to the crack spacing in these cracked zones.

16/ Obtain all other secondary cracked nodes using the bond length calculated in step 15, spaced from the primary cracked node across the length of the cracked zone.

17/ At all secondary cracked nodes, calculate the section properties (effective stiffness, tendon force etc.) using a cracked section analysis. Functions to represent changes in the Stiffness and tendon force between cracks are fitted to the relevant nodes.

18/ Recalculate the primary moment from the new tendon force.

19/ Recalculate the new equivalent load.

20/ Add the equivalent and applied loads to give the total load.

21/ Calculate the free bending moment for the total load.

22/ Calculate the fixed end moments, stiffness, and carry-over factors.

23/ Perform moment distribution on the continuous beam system to calculate the total support moments.

24/ Calculate the net internal support moments (SM2's) by subtracting the primary moments from the total moments (i.e. reactant moments).

25/ If the support moments are such that ((SM2's-SM1's)/SM2's) are greater than a predetermined criterion, then the cycle is repeated from step 2, else step 26

26/ If the support moments are such that ((SM's-SM2's)/SM's) are greater than a predetermined criterion, then the origional estimate to the internal support moments are altered to the mean of the old estimate and the new, i.e. SM's=(SM's+SM2's)/2, and the cycle is repeated from step 2, else step 27.

27/ Recalculate the equivalent load from the primary moment.

28/ Recalculate the free bending moment due to the equivalent load only.

29/ Calculate the fixed end moments, stiffness, and carry-over factors due to the equivalent load only (i.e. the curvature contribution from the equivalent load is considered only). The effective stiffness values (EI's) used in the calculation are those for the actual beam with the total loads applied.

30/ Perform moment distribution on the continuous beam system to calculate the total support moments (in the case the resulting moments).

31/ Subtract the primary moment from the resultant moment to give the secondary moments at the supports.

32/ Check if the ultimate moment envelope has been violated at any point along the length of the beam. If not, add the next increment of load , and cycle from step 2. If so, then the analysis is complete up to first plastic hinge formation.

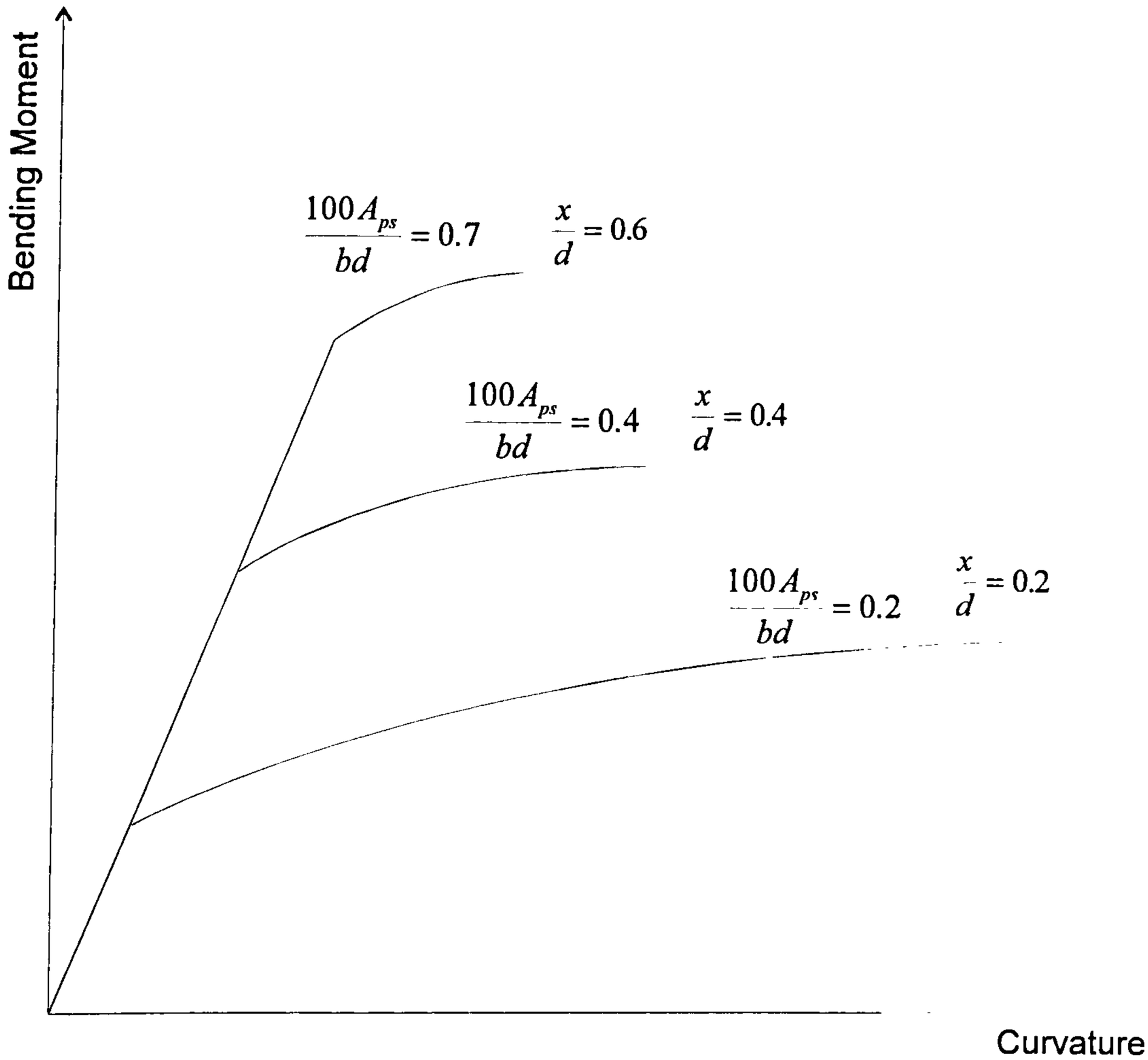

Figure 5.1.1 Moment Curvature Relationships for Prestressed Concrete Sections with varying percentages of Prestressed Reinforcement and varying Neutral Axis Depths at Ultimate Moment

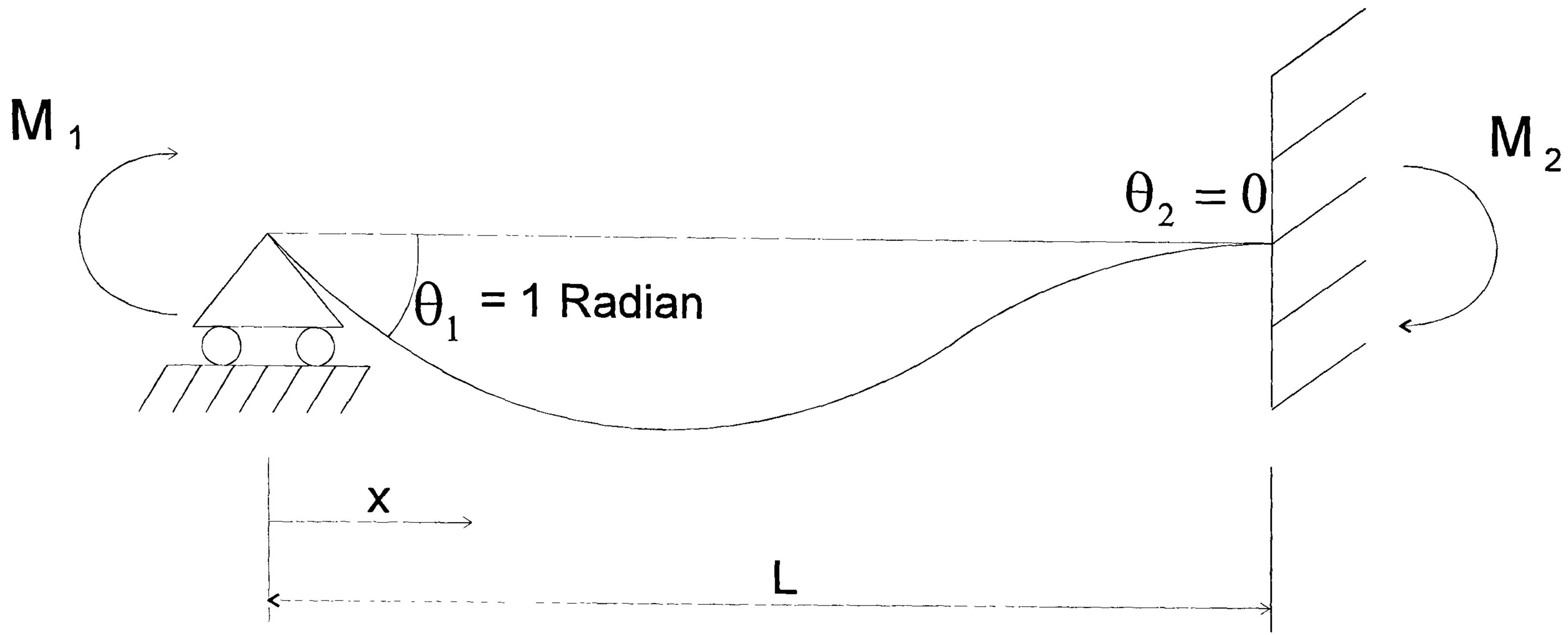

Figure 5.1.2. Beam, Simply Supported at left hand end and Encastred at right hand end.

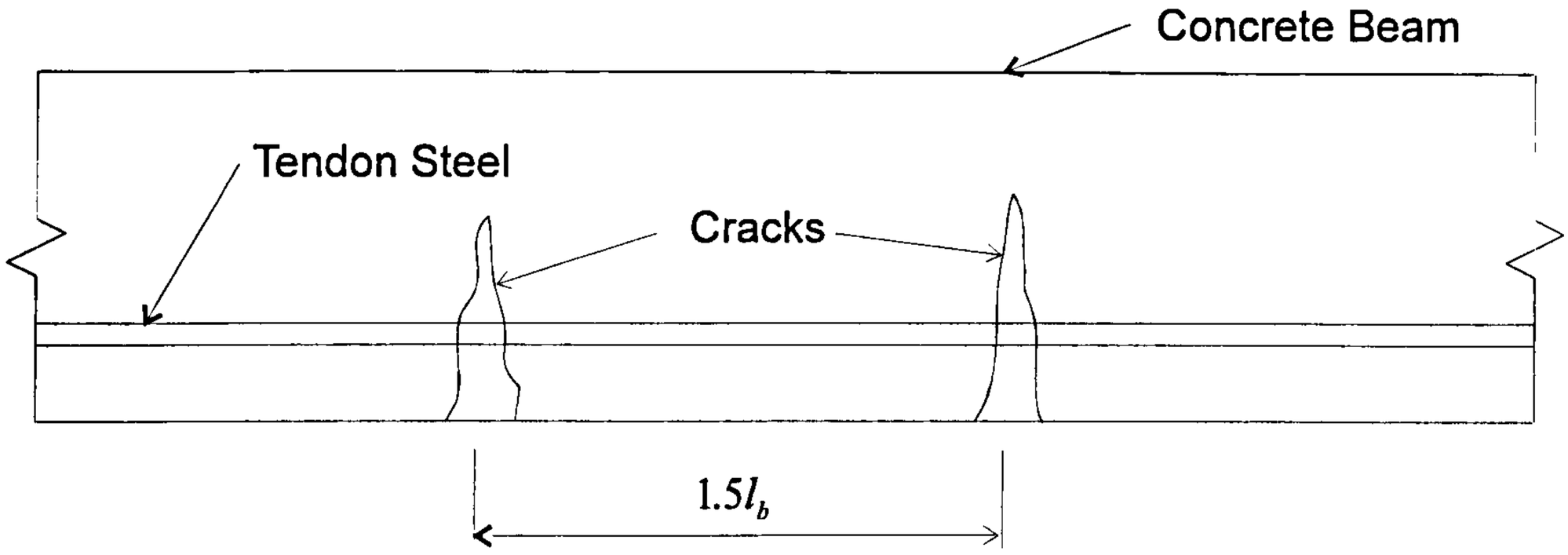

5.1.3a Prestressed Concrete Beam Cracked at Two Locations

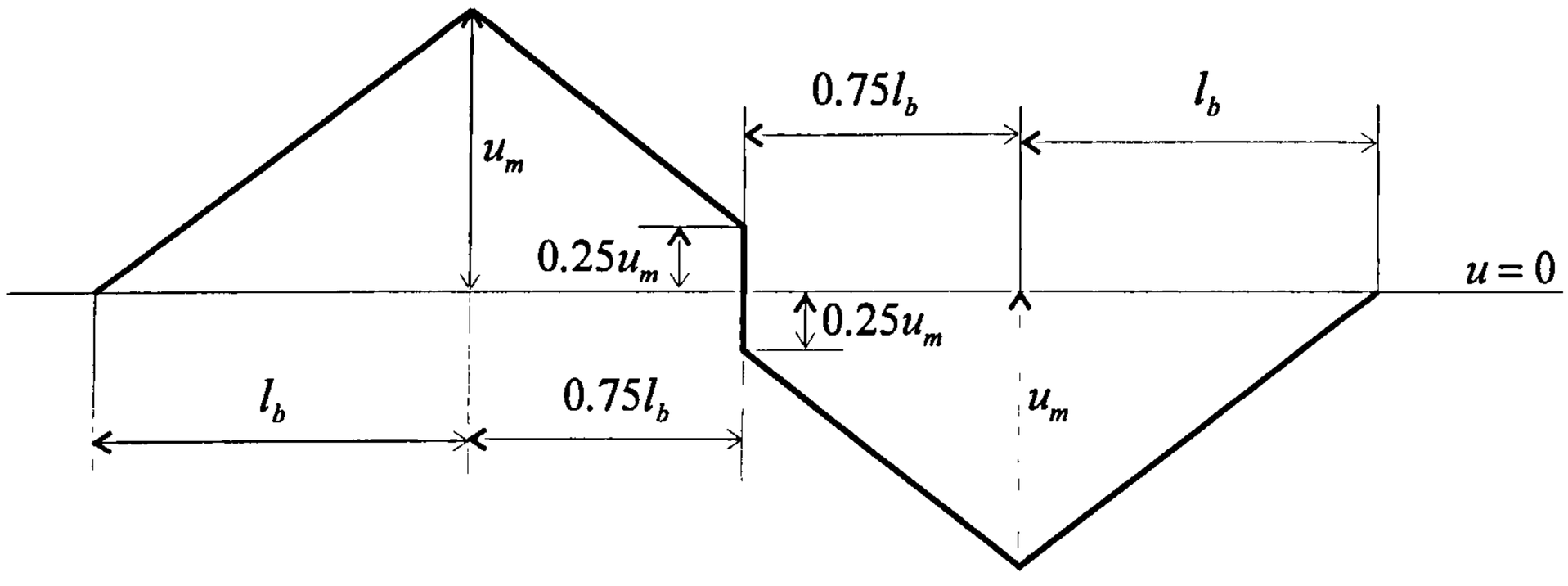

5.1.3b Idealised Distribution of Bond Stress

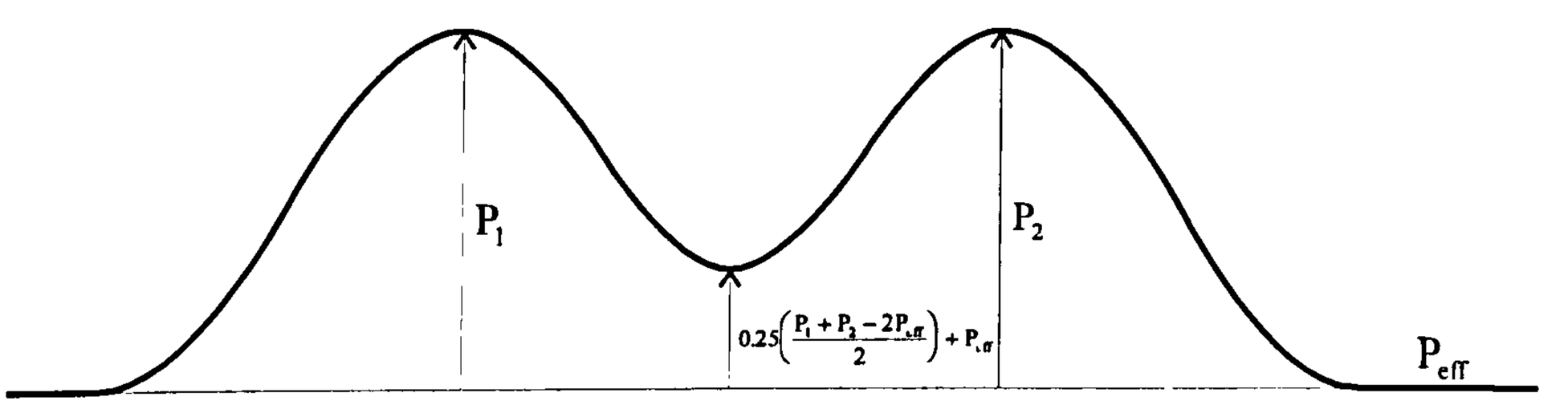

5.1.3c Idealised Distribution of Tendon Force

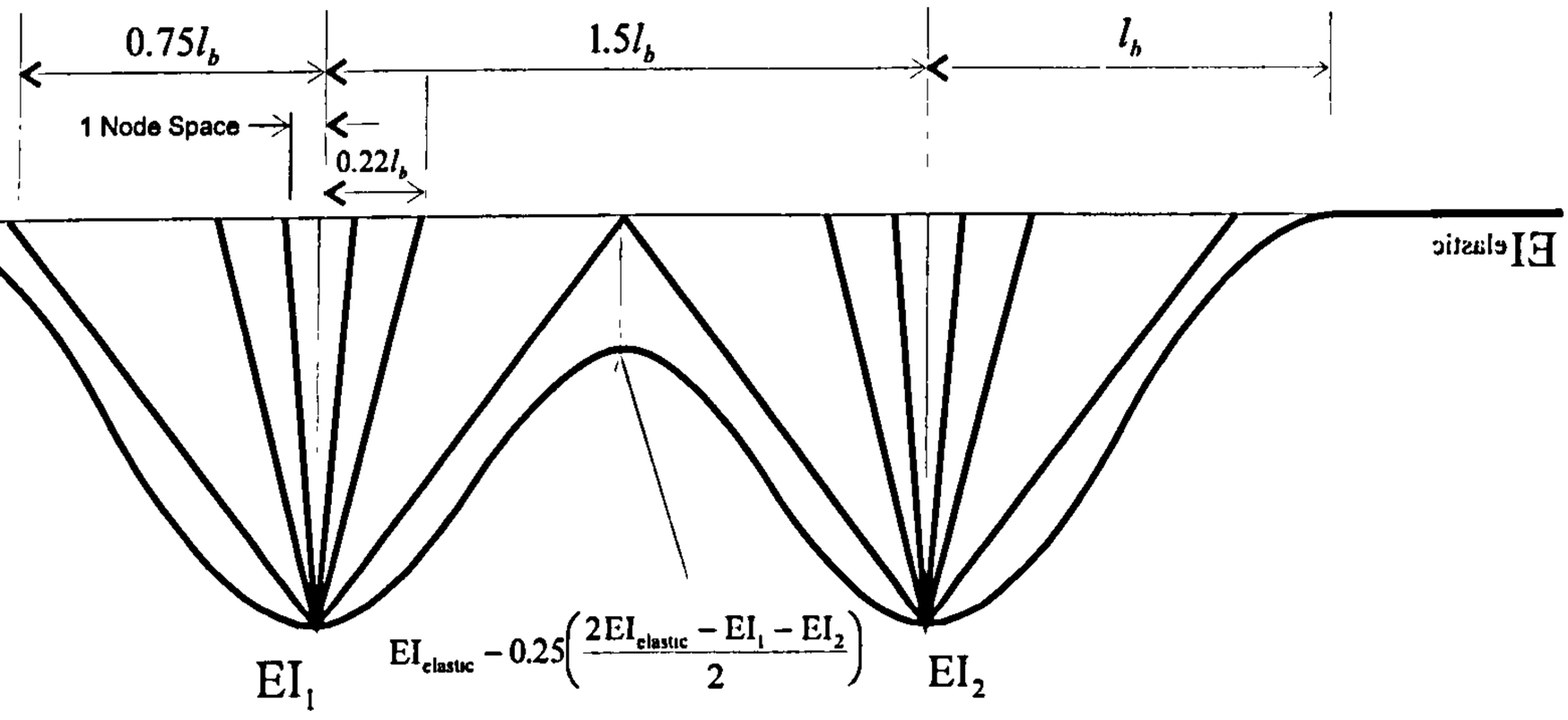

5.1.3d Idealised Distribution of Effective Flexural Stiffness

5.2/ Two Span Beam Examples with SMAREL30

Program SMAREL30 was written to analyse two-span continuous beams with continuously curved tendon profiles at one level in the beam. Two models were used, Twospan 1 and Twospan 2, with the properties listed in Table 5.1.

Twospan 1

Twospan 1 had exactly the dimensions and tendon layout as for finite element model, Model 18, shown in figure 4.2.1. The calculations for the equivalent load and elastic secondary moment at the centre support were exactly the same, i.e. 24 kN/m and 75 kNm respectively. The program reads in the data from Table 5.1 stored in the file INPUT.DAT, and then prompts the user for an applied U.D.L., and a corresponding value for the internal bending moment for the centre support. On the first load step, a load and internal support moment which are below the cracking value are chosen. After these values have been entered, the program proceeds to alter the internal support moment specified by the user until it agrees with the value calculated by the program using a moment distribution procedure. Only the left hand span is used in the calculation, assuming symmetry about the centre support. The internal bending moment and secondary moment at the centre support are then written to an output file SEC.DAT, and the next load increment of 0.1 kN/m is added to the applied load. The internal bending moment at the centre support for the last load step is used as an estimate for the value at the next load step, hence the load increments must be small, as any cracking can affect the stiffness and carry-over factors greatly. This process is repeated for each load step, with successive results written to SEC.DAT. If the program begins to oscillate between two cracked states whilst it tries to find a solution, this requires an exit after a number of attempts. This value was set to thirty, after which the results are again written to SEC.DAT, and the next load increment applied.

When the ultimate moment at a particular section (namely the centre support) is reached, a plastic hinge is deemed to have formed. At this stage, the envelopes of internal bending moment, tendon force, effective flexural stiffness, and equivalent load are written to four separate data files for later analysis. The program is then terminated.

Parametric Study of Effective Flexural Stiffness

Four separate runs of the program were performed with different stiffness variations between cracks. These were namely a cosine variation, and linear variations between

effective flexural stiffness values at cracks and the elastic flexural stiffness value, at nodal distances of $0.75l_b$, $0.22l_b$, and 1 node spacing away from the cracks.

Twospan 2

Twospan 2 was similar to Twospan 1 but with an altered drape of the tendon profile, and an eccentricity of the tendon above the section centroid at the centre support of 400mm. This had the effect of altering the equivalent load and primary moment so that the secondary moment was of opposite sign and identical magnitude to that for Twospan 1. The calculations for the equivalent load and secondary moment at the centre support are :

$$M_1 = 0.4 \times 2000 = 800\text{kNm}$$

The equivalent U.D.L. is :

$$-\frac{0.3625 \times 2000 \times 8}{15^2} = -25.78\text{kN/m}$$

This equivalent load produces fixed end moments of :

$$\mp\frac{25.78 \times 15^2}{12} = \mp 483.33\text{kNm}$$

From moment distribution, the resultant moment over the centre support is the fixed end moment plus a carry over of half the value of the fixed end moment at the end support with a reversed sign, i.e.

$$M_3 = 483.33 + (0.5 \times 483.33) = 725\text{kNm}$$

Hence the magnitude of the secondary moment over the centre support is :

$$M_2 = M_3 - M_1 = 725 - 800 = -75\text{kNm}$$

The information in table5.1 was used in the data file INPUT.DAT, and the program procedure was the same as for Twospan 1. The parametric study for the stiffness variation was also carried out.

In both instances, the program was terminated at the formation of the first plastic hinge. Therefore no analysis of the available rotation and moment distribution is carried out by the program.

5.3/ Three Span BeamExample with SMARELIT

The SMARELIT program was used to analyse a three span beam example prepared by the Consulting Engineers Roughton and Partners for the A127 Durham Western Bypass, Club Lane Bridge. Calculations and relevant design information of the T-section prestressed concrete bridge are given in Roughton and Partners [51] and the idealised dimensions of the bridge and tendon layout are also shown in figures 5.3.1 and 5.3.2. All of the relevant data for the file INPUT.DAT are listed in table 5.2, and information relating to each of the spans, files SPAN.DAT, are listed in table 5.3.

Elastic Secondary Moments

To calculate the elastic secondary moments at the internal supports an equivalent load analysis using moment distribution can be performed. The notation in figure 5.2a. is used :-

Equivalent Loads:-

Equation for the calculation of the equivalent U.D.L. for a parabolic profile is:

$$-\frac{8 \times P \times e}{L^2}$$

For Span A, equivalent load = $-\frac{8 \times 13600 \times 0.171}{12.5^2} = -119.1\ \text{kN/m}$

For Span B, equivalent load = $-\frac{8 \times 13600 \times 0.739}{26.0^2} = -118.9\ \text{kN/m}$

For Span C, equivalent load = $-\frac{8 \times 13600 \times 0.249}{15.1^2} = -118.8\ \text{kN/m}$

Distribution Factors:

Joint	Member	Stiffness	∑Stiffness	Distribution Factor δ
1	A	$4EI/12.5 = 0.32EI$	$0.32EI$	1.0
2	A	$3EI/12.5 = 0.24EI$	0.39EI	0.61
	B	$4EI/26.0 = 0.15EI$		0.39
3	B	$4EI/26.0 = 0.15EI$	$0.35EI$	0.44
	C	$3EI/15.1 = 0.2EI$		0.56
4	C	$4EI/15.1 = 0.26EI$	$0.26EI$	1.0

Fixed End Moments:

Member	Joint	Formula	Value
A	1	$qL^2/12$	-1549.5
	2	$-qL^2/12$	1549.5
B	2	$qL^2/12$	-6703.7
	3	$-qL^2/12$	6703.7
C	3	$qL^2/12$	-2261.1
	4	$-qL^2/12$	2261.1

Moment Distribution for Resultant Moments M_3:

Member/Joint	A1	A2	B2	B3	C3	C4
δ	1	0.61	0.39	0.44	0.56	1
Initial State	-1549.5	1549.5	-6703.7	6703.7	-2261.1	2261.1
Relax	1549.5	3144.1	2010.1	-1954.7	-2487.9	-2261.1
Carry-Over	0	774.8	-977.35	1005.1	-1130.6	0
Relax		123.6	79.0	55.2	70.3	
Carry-Over	0	0	27.6	39.5	0	0
Relax		-16.8	-10.8	-17.4	-22.1	
Carry-Over	0	0	-8.7	-5.4	0	0
Relax		5.3	3.4	2.4	3.0	
Carry-Over	0	0	1.2	1.7	0	0
Relax		-0.7	-0.5	-0.7	-1.0	
Carry-Over	0	0	-0.4	-0.3	0	0
Relax		0.2	0.2	0.1	0.2	
Total	0	5580.0	-5580.0	5829.2	-5829.2	0

Primary Moment at Support 2 : $M_1 = P \times e = 13600 \times 0.274 = 3726.4$ kNm

Primary Moment at Support 3 : $M_1 = P \times e = 13600 \times 0.274 = 3726.4$ kNm

Secondary moment at Support 2: $M_2 = M_3 - M_1 = 5580 - 3726.4 = 1853.6$ kNm

Secondary moment at Support 3: $M_2 = M_3 - M_1 = 5829.2 - 3726.4 = 2102.8$ kNm

Analysis Procedure

The load was applied uniformly to all spans simultaneously, with the first load application being the approximate balanced load of 120 kN/m. At first, the load steps were quite large whilst the beam was behaving elastically, up to the point of first cracking at a critical section. Subsequent load steps were applied at intervals of 0.1 kN/m, and the program allowed to iterate until the net internal bending moments at supports 2 and 3 had stabilised to within the required accuracy. A maximum number of iterations of 30 per load step was introduced to avoid non-convergence at particular load steps, hence after 30 iterations at one load level, the next load step would be applied. After each load step, the internal bending moment and the secondary moments at supports 2 and 3 are recorded in a data file for analysis. The ultimate bending moment envelope is compared with the internal moment envelope after each load step to see if it has been exceeded at any location long the length of the beam. Once this has occurred, a plastic hinge is deemed to have formed at the critical section, and the tendon force, stiffness, equivalent load, and internal bending moment envelopes are all written to the appropriate data files. A normal exit is then made from the program. At the stage of the formation of one plastic hinge, unlike the 2-span beam, the 3-span beam will still be statically indeterminate, but the program cannot be continued past one plastic hinge due to the physical alterations of the structure which effects the analysis procedure.

Stiffness Variation

As for the Twospan models four separate runs of the program were performed with different stiffness variations between cracks. These were namely a cosine variation, and linear variations between effective flexural stiffness values at cracks and the elastic flexural stiffness value, at nodal distances of $0.75l_b$, $0.22l_b$, and 1 node spacing away from the cracks.

Output

The internal and secondary bending moments for each load step were recorded for comparison of each analysis. At plastic hinge formation of each run, the envelopes of internal bending moment, equivalent load, effective flexural stiffness, and tendon force can be compared for each stiffness variation.

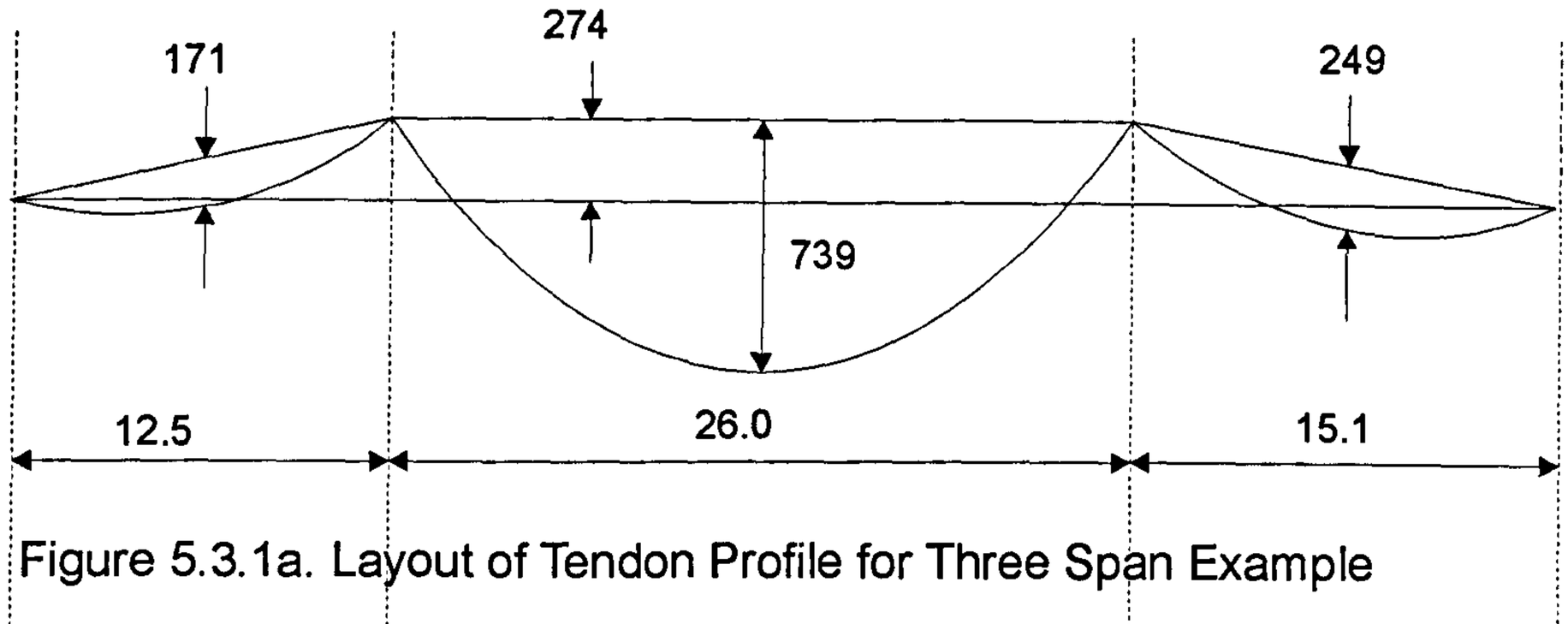

Figure 5.3.1a. Layout of Tendon Profile for Three Span Example

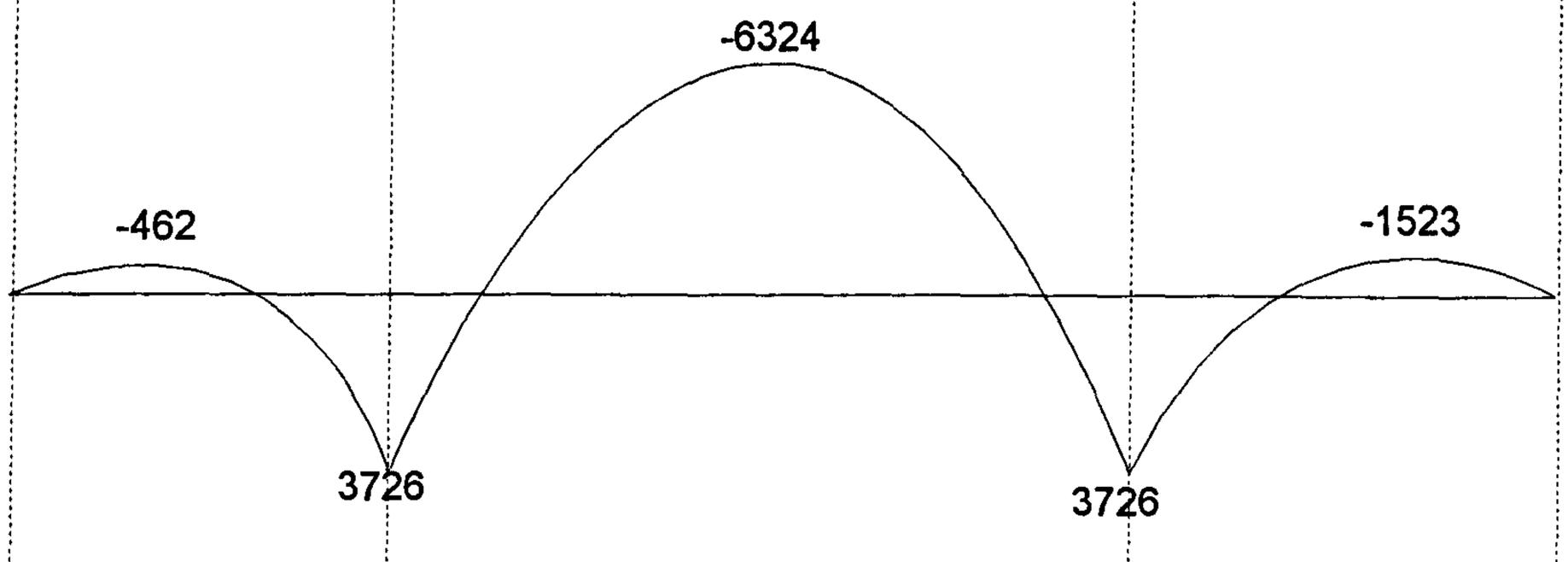

Figure 5.3.1b. Primary Bending Moment Envelope (M1)

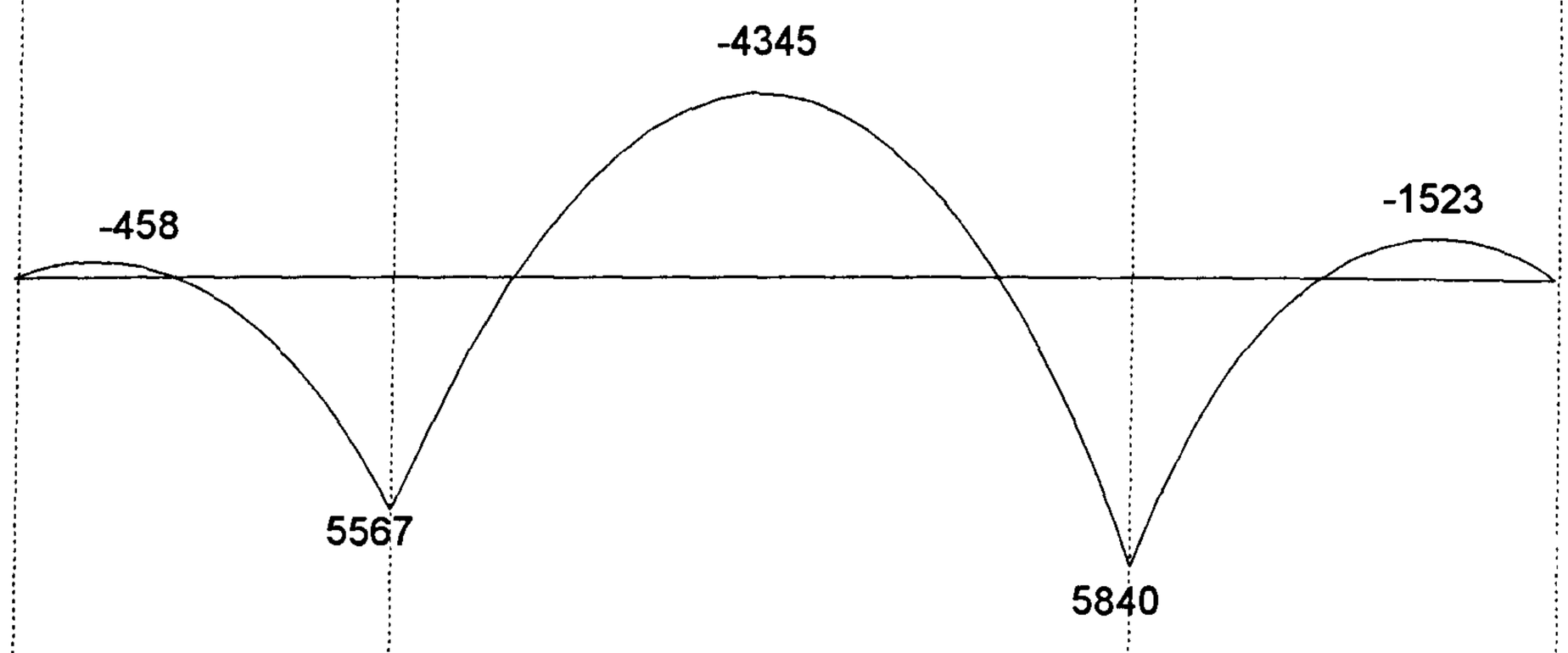

Figure 5.3.1c. Resulting Bending Moment Envelope (M3)

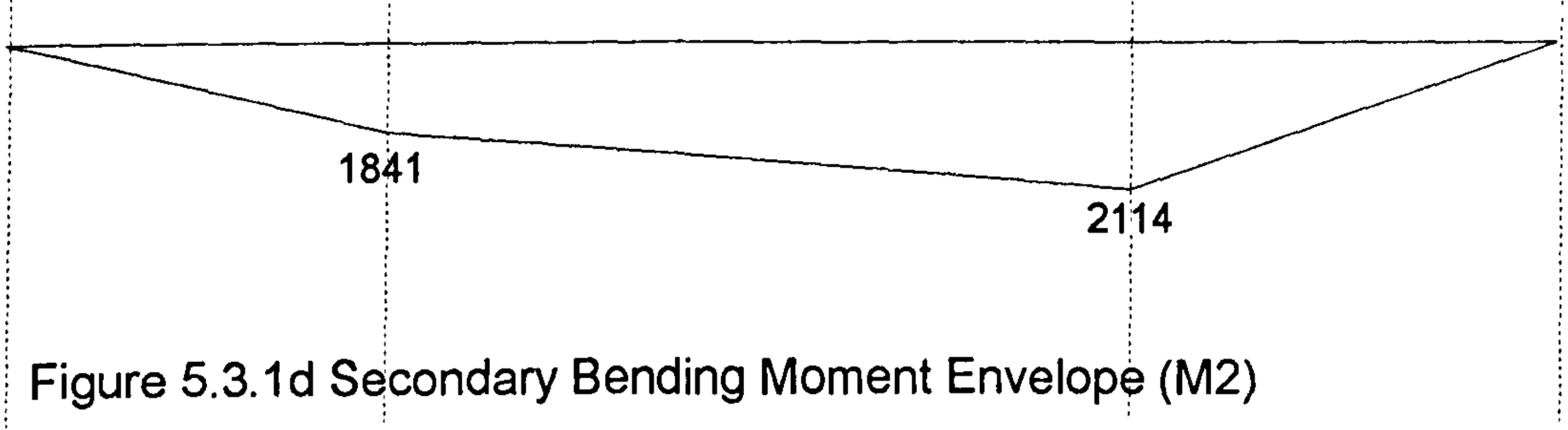

Figure 5.3.1d Secondary Bending Moment Envelope (M2)

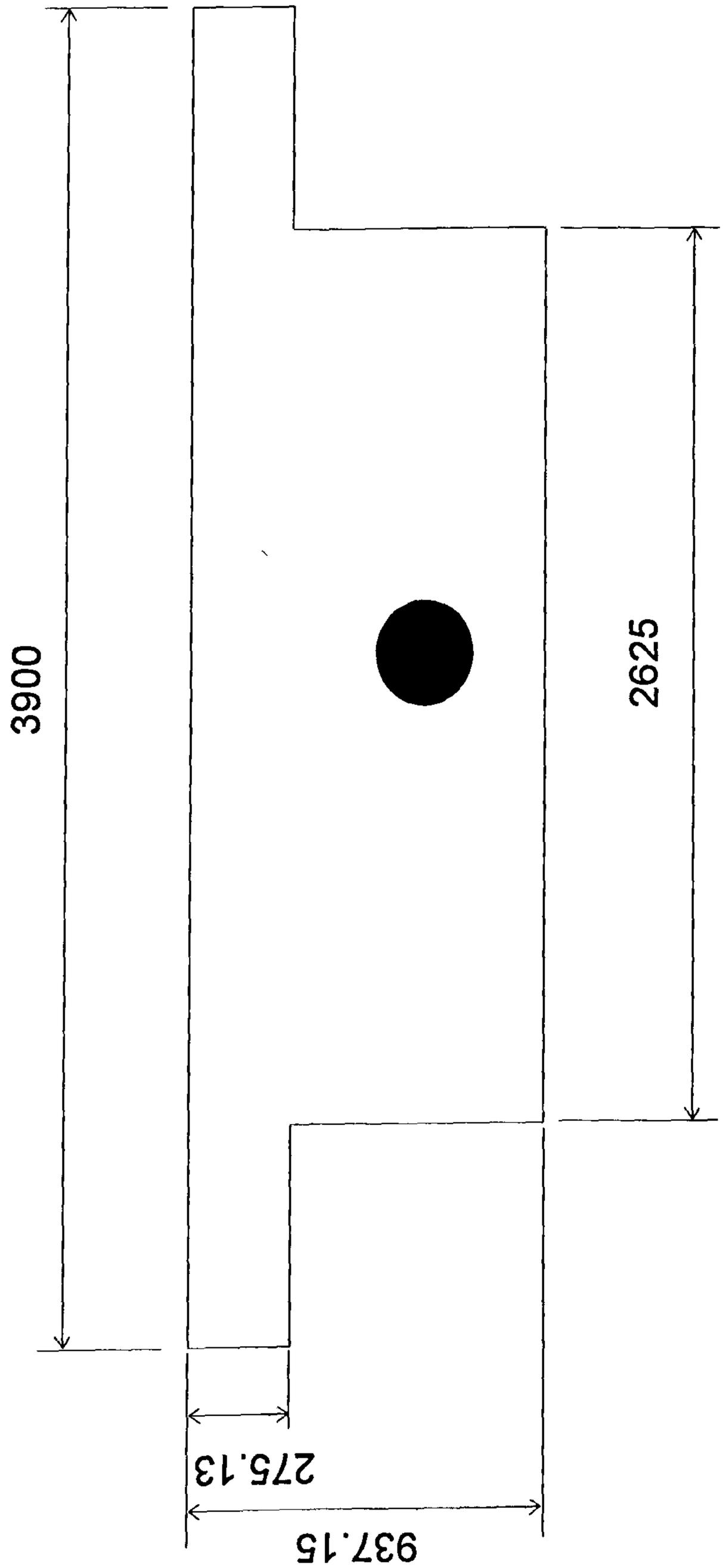

Figure 5.3.2. Cross-Sectional Dimensions for Three Span Beam

Table 5.1

Input Data for Two-Span Models for SMAREL30, Twospan 1 and 2

		Twospan 1	Twospan 2
AS	Area of Steel (mm^2)	1700.0	1700.0
DE	Overall Depth (mm)	1000.0	1000.0
ES	Elastic Modulus of Steel (kN/mm^2)	200.0	200.0
EC	Elastic Modulus of Concrete (kN/mm^2)	37.83	37.83
E1	Drape of Parabolic Profile (mm)	337.5	362.5
FCU	Characteristic Strength of Concrete (N/mm^2)	60.0	60.0
FPU	Characteristic Strength of Prestressing Steel (N/mm^2)	1750.0	1750.0
PF	Prestress Force (kN)	2000.0	2000.0
L	Span Length (m)	15.0	15.0
GAM1	γ_1	1.0	1.0
GAM2	γ_2	1.0	1.0
BW	Breadth of Web (mm)	400.0	400.0
BF1	Breadth of top Flange (mm)	400.0	400.0
BF2	Breadth of bottom Flange (mm)	400.0	400.0
DF1	Depth of top Flange (mm)	200.0	200.0
DF2	Depth of bottom Flange (mm)	200.0	200.0

Table 5.2

Input Data for Three-Span Model for SMARELIT, Beam 3
(File INPUT.DAT)

		Threespan
AS	Area of Steel (mm^2)	12000.0
DE	Overall Depth (mm)	937.15
ES	Elastic Modulus of Steel (kN/mm^2)	200.0
EC	Elastic Modulus of Concrete (kN/mm^2)	34.7
FCU	Characteristic Strength of Concrete (N/mm^2)	40.0
FPU	Characteristic Strength of Prestressing Steel (N/mm^2)	1750.0
PF	Prestress Force (kN)	13600.0
GAM1	γ_1	1.0
GAM2	γ_2	1.0
BW	Breadth of Web (mm)	2625.0
BF1	Breadth of top Flange (mm)	3900.0
BF2	Breadth of bottom Flange (mm)	2625.0
DF1	Depth of top Flange (mm)	275.13
DF2	Depth of bottom Flange (mm)	100.0
STRAND	Number of Prestressing Strands	3

Table 5.3

Input Span Data for Three-Span Model for SMARELIT, Threespan
(Files:- SPAN1.DAT, SPAN2.DAT, SPAN3.DAT)

		Span1	Span2	Span3
L	Length of Span (m)	12.5	26.0	15.1
ELH	Eccentricity (mm)	0.0	274.0	274.0
ERH	Eccentricity (mm)	274.0	274.0	0.0
EN	Eccentricity (mm)	171.0	739.0	249.0

5.4/ Results for SMAREL Programs

5.4.1/ Twospan Beam Models

The first model analysed using the SMAREL30 program, Twospan 1, had the same specifications as ANSYS model 18. This was so that both sets of results might be compared.

Figure 5.4.1. shows the variation of internal bending moment at the centre support versus the applied U.D.L., for the four different cases of flexural stiffness variation between cracks. In each case, cracking was initiated at the centre support at an internal bending moment value of -1239 kNm. The lines are linear and coincident up to this point. After cracking, the gradients of all of the lines decrease slightly as the flexural stiffness at the support decreases, causing a redistribution of moment from the support into the span. Once cracking has begun in the span, the lines increase in gradient approximately to the values of when they were behaving linearly, as the moment redistributes back from the span to the support.

It can be seen that after first cracking in the span, the greatest decrease in gradient is associated with the stiffness representation which causes the widest variation (reduction) in the stiffness over the largest range of nodes, i.e. the cosine variation will have the greatest influence, followed by the linear $0.75l_b$, and $0.22l_b$ variations, and the linear variation over one node spacing has virtually no recognisable effect.

The moment at which the plastic hinge is formed at the centre support is -2090 kNm, and is obtained by all the stiffness models. Again, from figure 5.4.1., it can be seen that the applied U.D.L. at which this occurs will be greater for the widest stiffness reduction between cracks, i.e. the cosine variation.

The estimated secondary bending moments for each stiffness case are plotted against applied load in figure 5.4.2. In each case, the value remains constant at 75 kNm up to the point where cracking is initiated. After cracking has begun at the centre support, the secondary moments can be seen to curve downwards with a negative gradient. As the cracks widen in the negative zone, the gradient becomes steeper, and the formation of new cracks in the negative moment zone causes a step decrease in the secondary moment. As the span starts to crack, a series of smaller steps which increase the secondary moment appear. The cracks in the positive moment zone in the span, although they may be greater in number, are not as large (wide) as the cracks in the negative moment zone over the centre support, and will not have as much influence on the overall flexural stiffness and distribution of moments

in the beam, as those in the negative zone. Hence the secondary moment decreases in magnitude from its originally positive value, and may become negative, as seen with the cosine stiffness variation. Also, the secondary moments could not be monitored after the plastic hinge had formed at the centre support, as the structure had become statically determinate.

Internal bending moment envelopes for the left hand span are shown in figure 5.4.3., illustrating the parabolic form in each case. The effective flexural stiffness envelopes in each case are shown in figure 5.4.4., illustrating the pattern of cracking, and the different forms of the stiffness variation between cracks. Figure 5.4.5. shows how the tendon force varies in a cosine fashion along the span, with the greatest increases in the negative moment zone. The form of the equivalent load is shown in figure 5.4.6., and clearly shows a form similar to that for the tendon force, i.e. a cosine function. This is to be expected, as the primary moment will be a combination of cosine functions superimposed (added) to the elastic parabolic function. When this is differentiated twice, the parabolic function becomes linear, and the cosine function will remain of the same form. Hence in the regions where the tendon force changes from the parabolic form to the cosine plus parabolic form, the second differential will be of cosine form, superimposed on a linear function. Referring to figure 5.4.6, the horizontal portions between the cracked zones are not zero, but actually correspond to an equivalent load of -24 kN/m. The large fluctuation of equivalent load is such that this does not show clearly on the graph.

For Twospan 2, the same response can be seen from a plot of internal bending moment versus applied load, shown in figure 5.4.7. In this case cracking is initiated at a value of -1470 kNm over the centre support, and a plastic hinge forms at the centre support at a value of -2390 kNm. Similar trends as for Twospan 1 for the distribution of bending moments occur for the four different stiffness models.

The secondary moments are shown in figure 5.4.8.. The elastic value of -75 kNm is held up to the point of first cracking, after which the secondary moments decrease in a manner similar to that described for Twospan 1. However, as the secondary moment is negative to start with, this means that the secondary moment becomes even more negative, i.e. larger in magnitude. In the case of the cosine stiffness variation, this decreases to -220 kNm at the formation of the plastic hinge.

Envelopes of internal bending moment, effective flexural stiffness, tendon force, and equivalents load are shown in figures 5.4.9., 5.4.10., 5.4.11., 5.4.12., respectively, and are similar in form to that for Twospan1.

5.4.2/ Threespan model

Although a limit of 30 iterations per load step was specified for the three span example, the analysis passed through a number of stages in which the solution would oscillate between a number of different cracked states. Even so the results show a general trend similar to that for the twospan examples. Support 3 cracked first at a moment of -7853 kNm, followed by support 2 at a moment of -8080 kNm (at loads of 207 and 218 kN/m respectively), and finally the centre span developed a few cracks before a plastic hinge formed at support 3, at a load of approximately 300 kN/m

Figures 5.4.13. and 5.4.14. show the variation of internal bending moment with applied load at supports 2 and 3 respectively. Concentrating on the cosine stiffness variation model, it can be seen that the onset of cracking at support 3 causes a small step decrease in the bending moment at this location due to the local softening, and redistributes moment to support 2. Once support 2 begins to crack, the reverse happens, where the moment redistributes back to support 3. As the load at which the plastic hinge forms is approached, the cosine stiffness variation has a pronounced decrease in gradient, more so than for the other stiffness models.

The variation of secondary moment with applied load is shown for support 2 and 3 in figures 5.4.15. and 5.4.16 respectively. It can be seen that when support 3 cracks, the secondary moment reduces here in a step fashion, corresponding to an increase at support 2. Once support 2 begins to crack, the situation is reversed, with the secondary moment increasing again at support 3 and reducing at support 2. The secondary moment then passes through a series of stages where the crack pattern cannot settle and the solution has not converged. However, there appears to be a general increase in both of the secondary moment values at the supports, accompanied by the onset of cracking in the centre span. Towards the load at which the plastic hinge forms at support 3, the secondary moment tends to remain fairly constant at support 2, at values higher than the origional elastically calculated value, whilst the secondary moment at support 3 is reducing to values below the elastic value. All of the stiffness models show similar results with the widest stiffness reductions having the greatest effect.

The internal bending moment envelopes at plastic hinge formation for all four stiffness models are shown in figure 5.4.17. This shows only very slight differences between the internal bending moments at this stage, due to slight differences in the applied load. The maximum positive bending moment occurs in the centre span as this is the longest of the

three spans. Envelopes of effective flexural stiffness, tendon force and equivalent load are shown in figures 5.4.18., 5.4.19., and 5.4.20. respectively. These clearly show the expected forms and reveal the crack pattern. Three cracks are present over each support section, with three cracks in the centre span. Also the effects of the cracks at the supports appear to be greater than those in the span, probably due the cross sectional properties in the cracked section analysis at these locations.

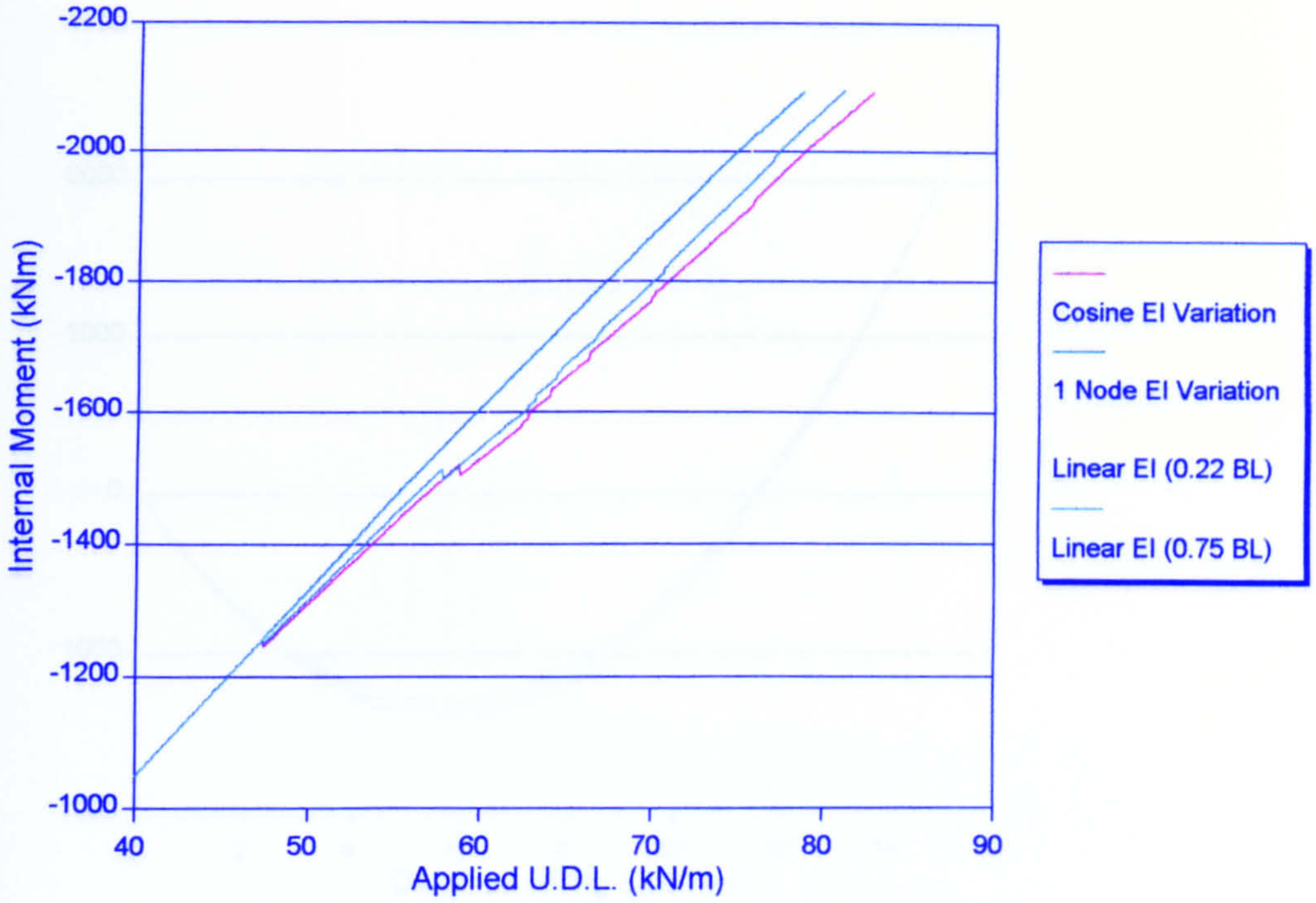

Figure 5.4.1. Internal Moment vs Applied Load, SMAREL30, Twospan1

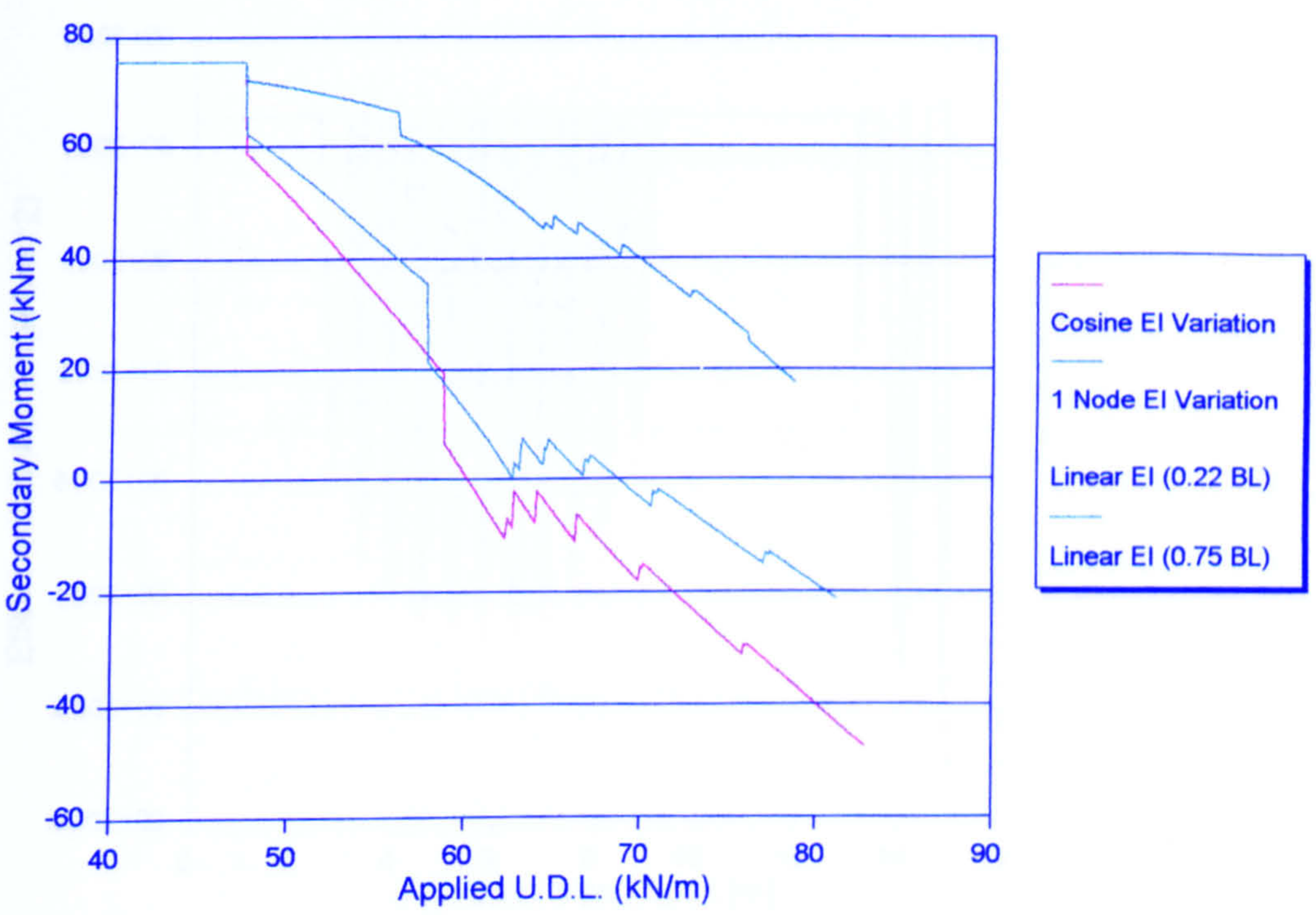

Figure 5.4.2. Secondary Moment vs Applied Load, SMAREL30, Twospan1

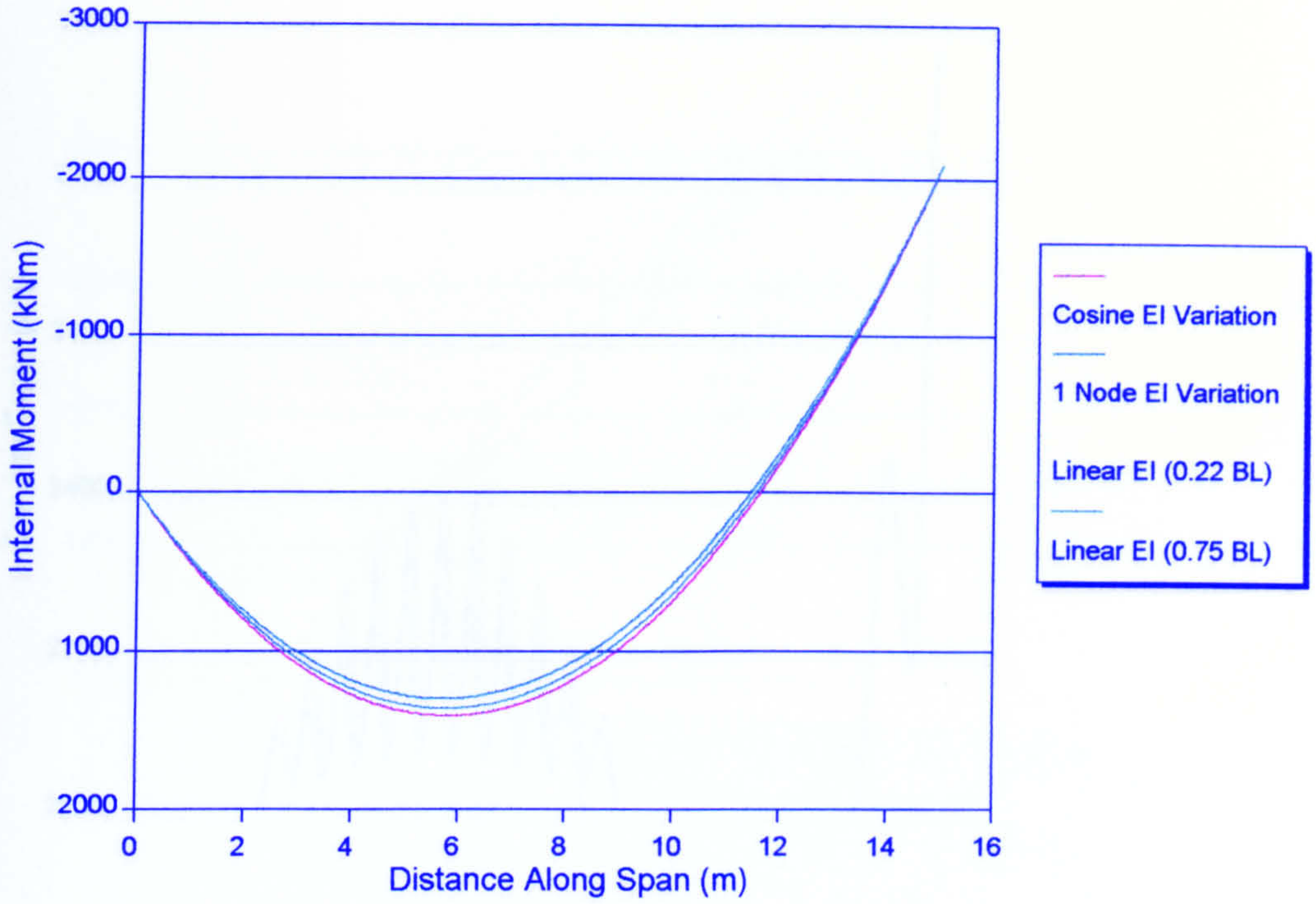

Figure 5.4.3. Internal Moment Envelopes, SMAREL30, Twospan1

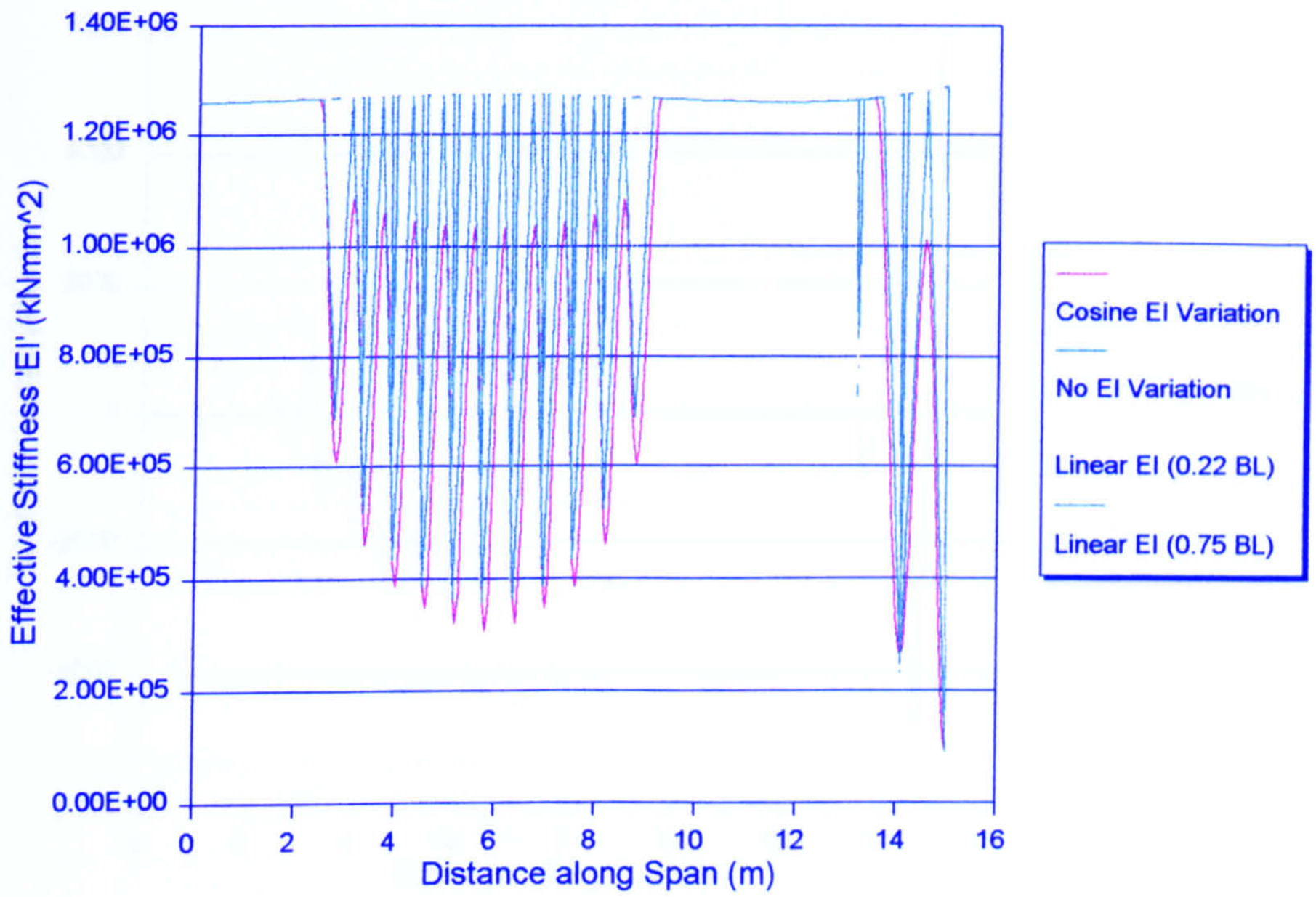

Figure 5.4.4. Effective Flexural Stiffness Envelopes, SMAREL30, Twospan1

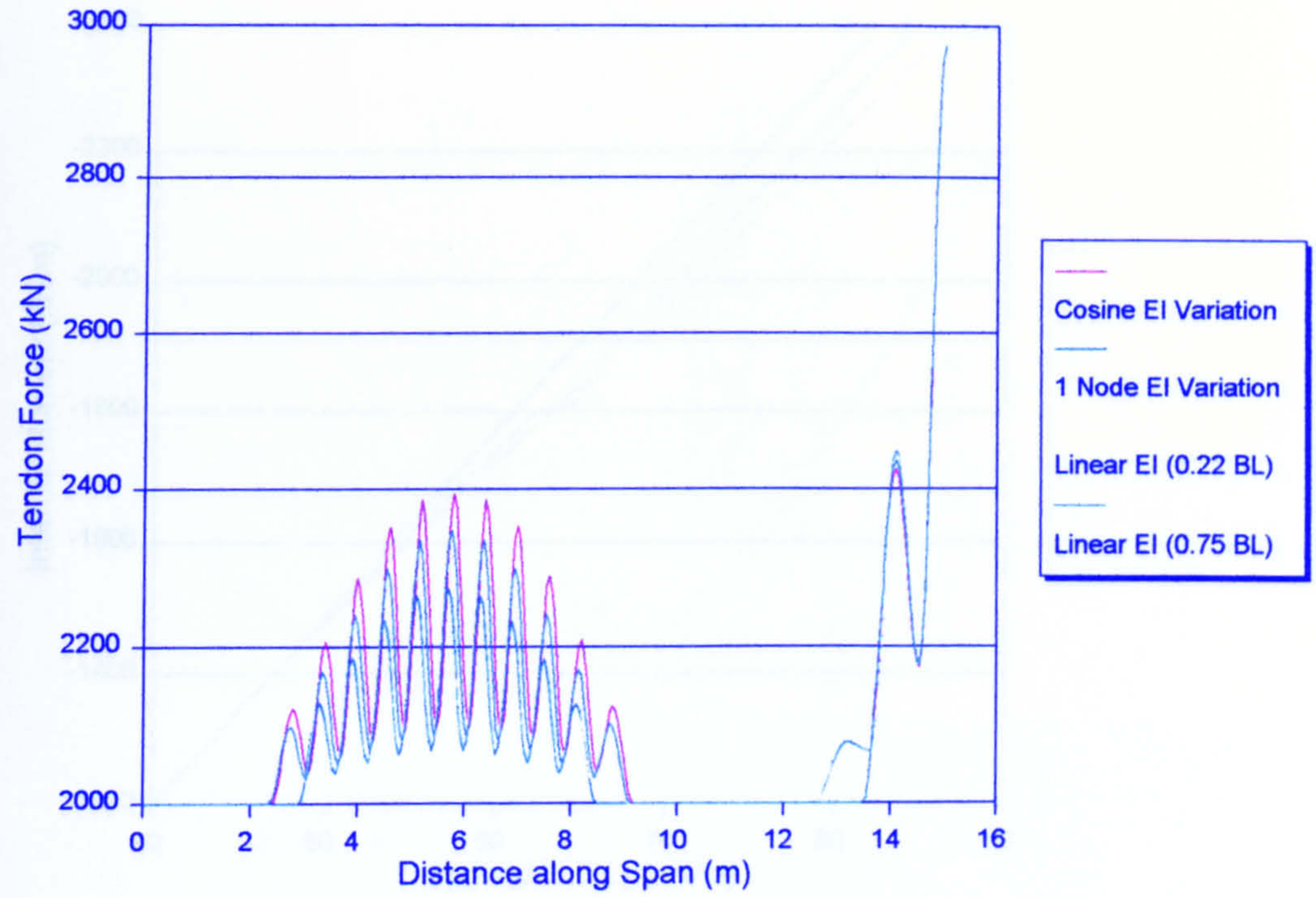

Figure 5.4.5. Tendon Force Envelope, SMAREL30, Twospan1

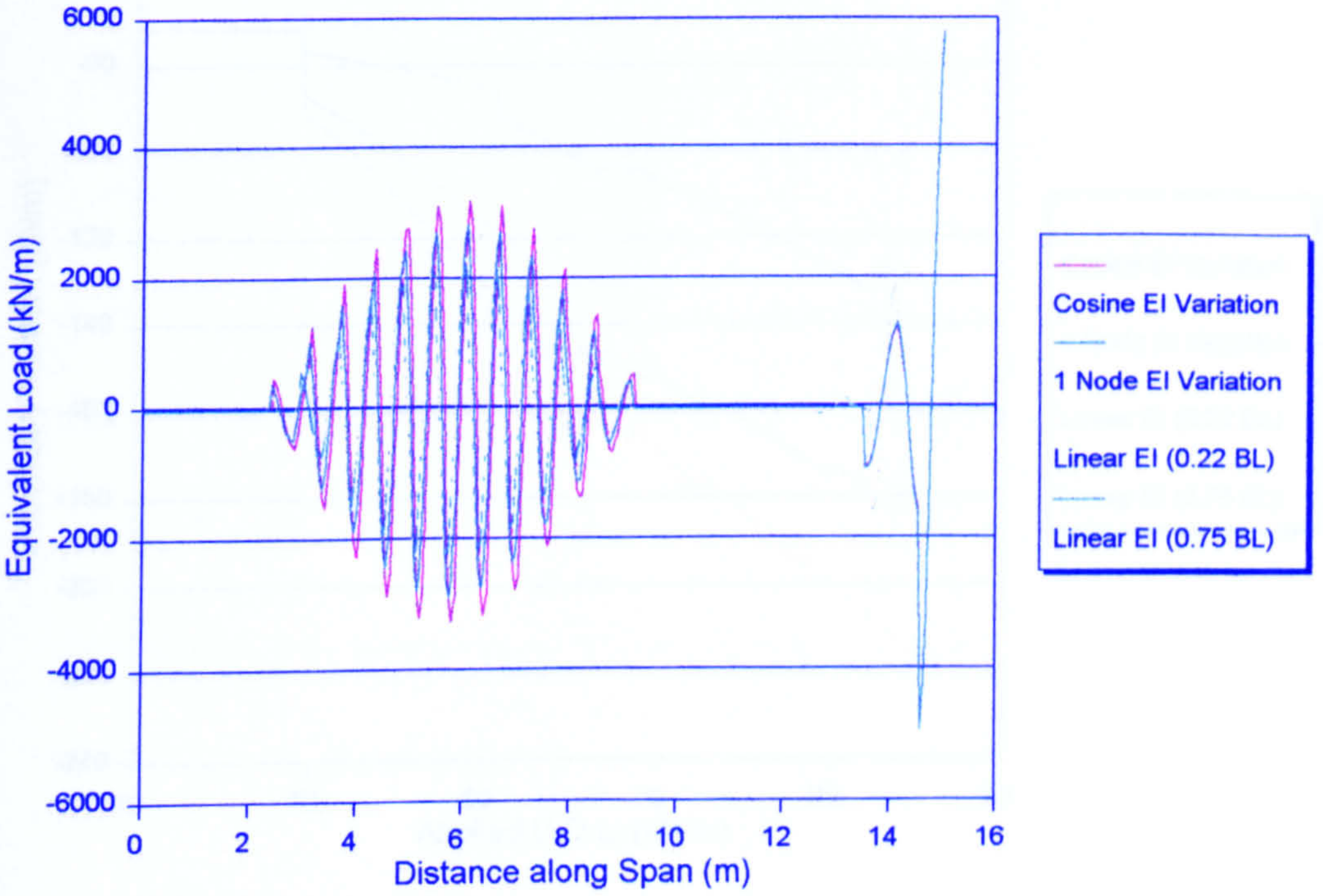

Figure 5.4.6. Equivalent Load Envelope, SMAREL30, Twospan1

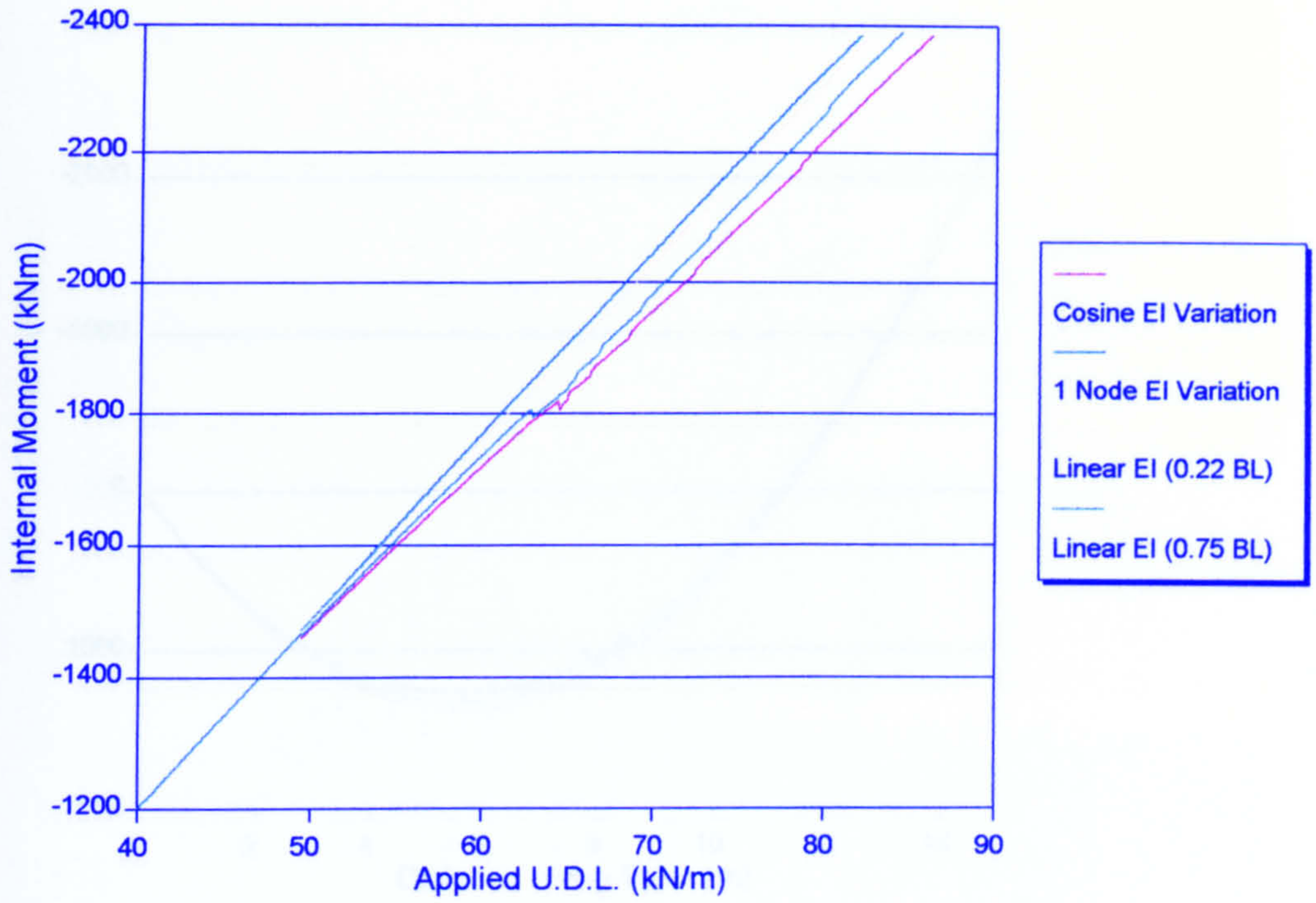

Figure 5.4.7. Internal Moment vs Applied Load, SMAREL30, Twospan2

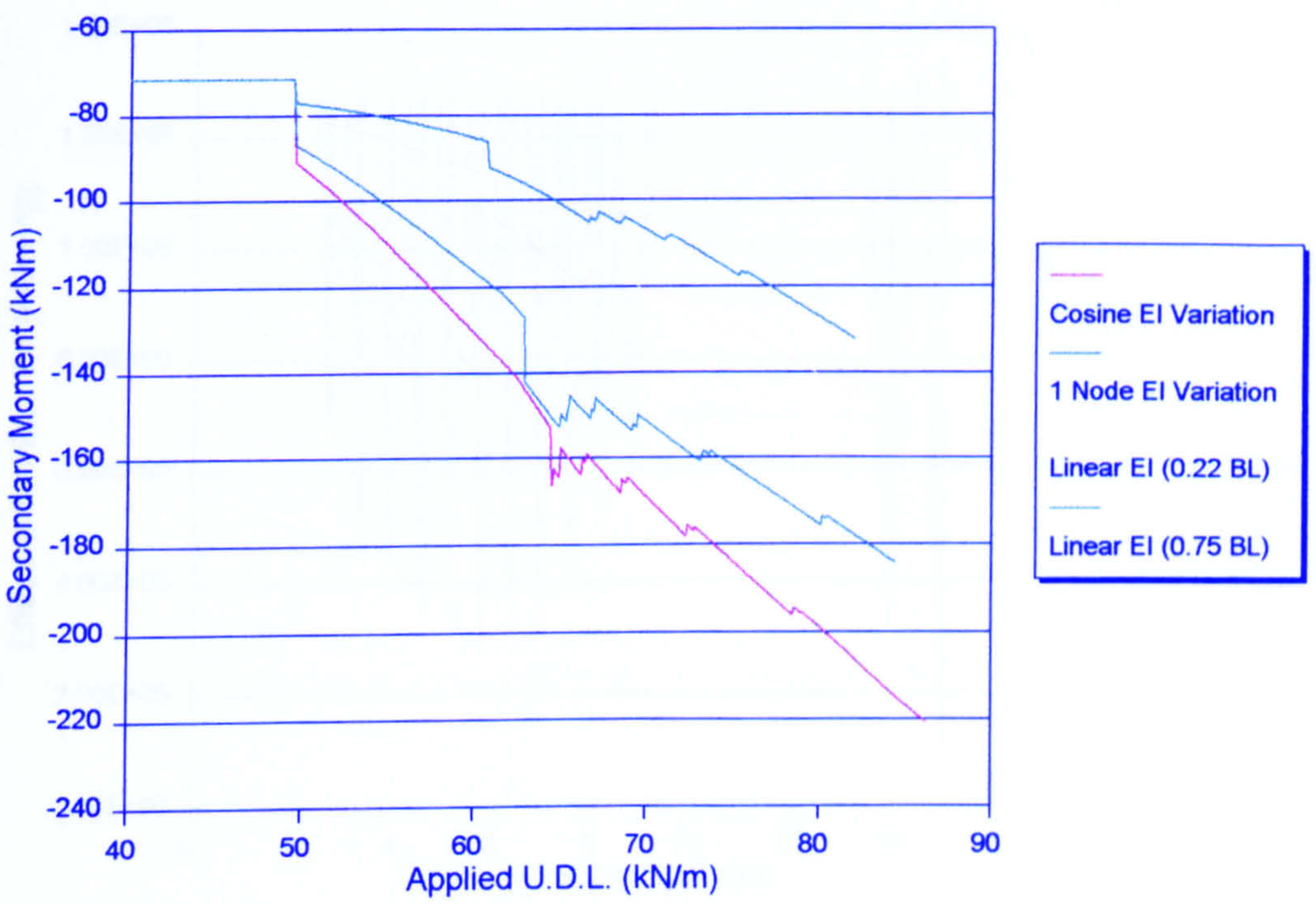

Figure 5.4.8. Secondary Moment vs Applied Load, SMAREL30, Twospan2

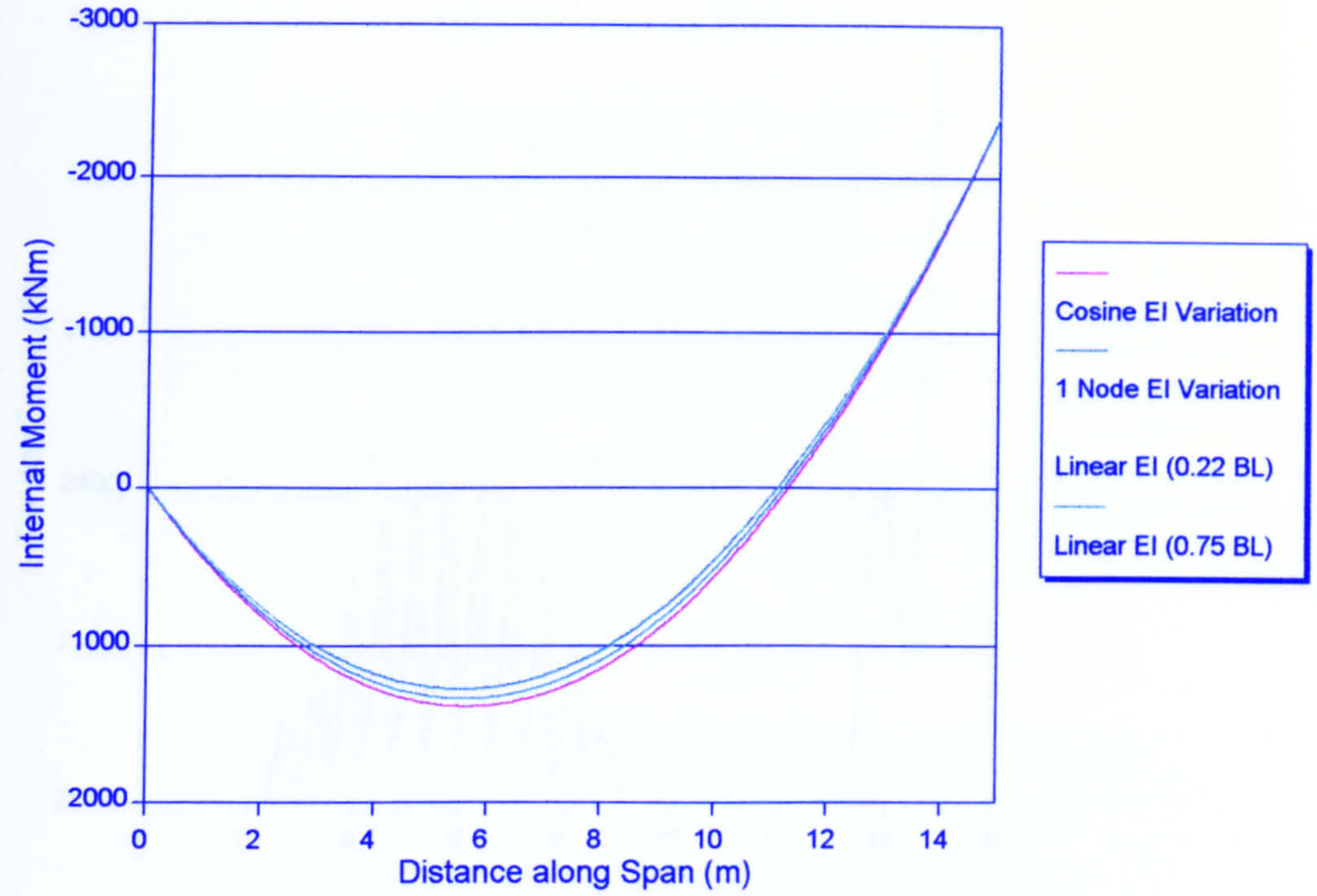

Figure 5.4.9. Internal Moment Envelopes, SMAREL30, Twospan2

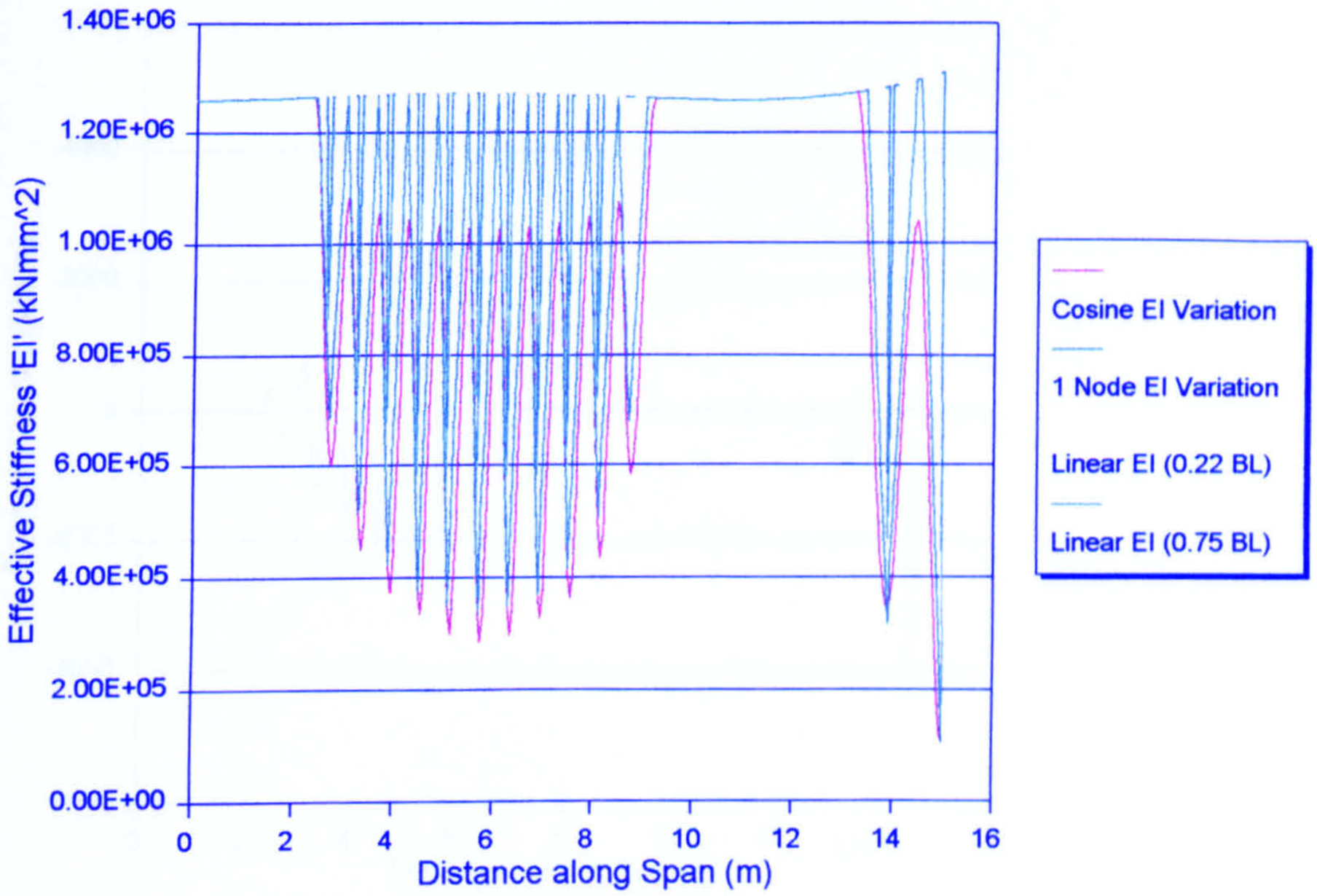

Figure 5.4.10. Effective Flexural Stiffness Envelopes, SMAREL30, Twospan2

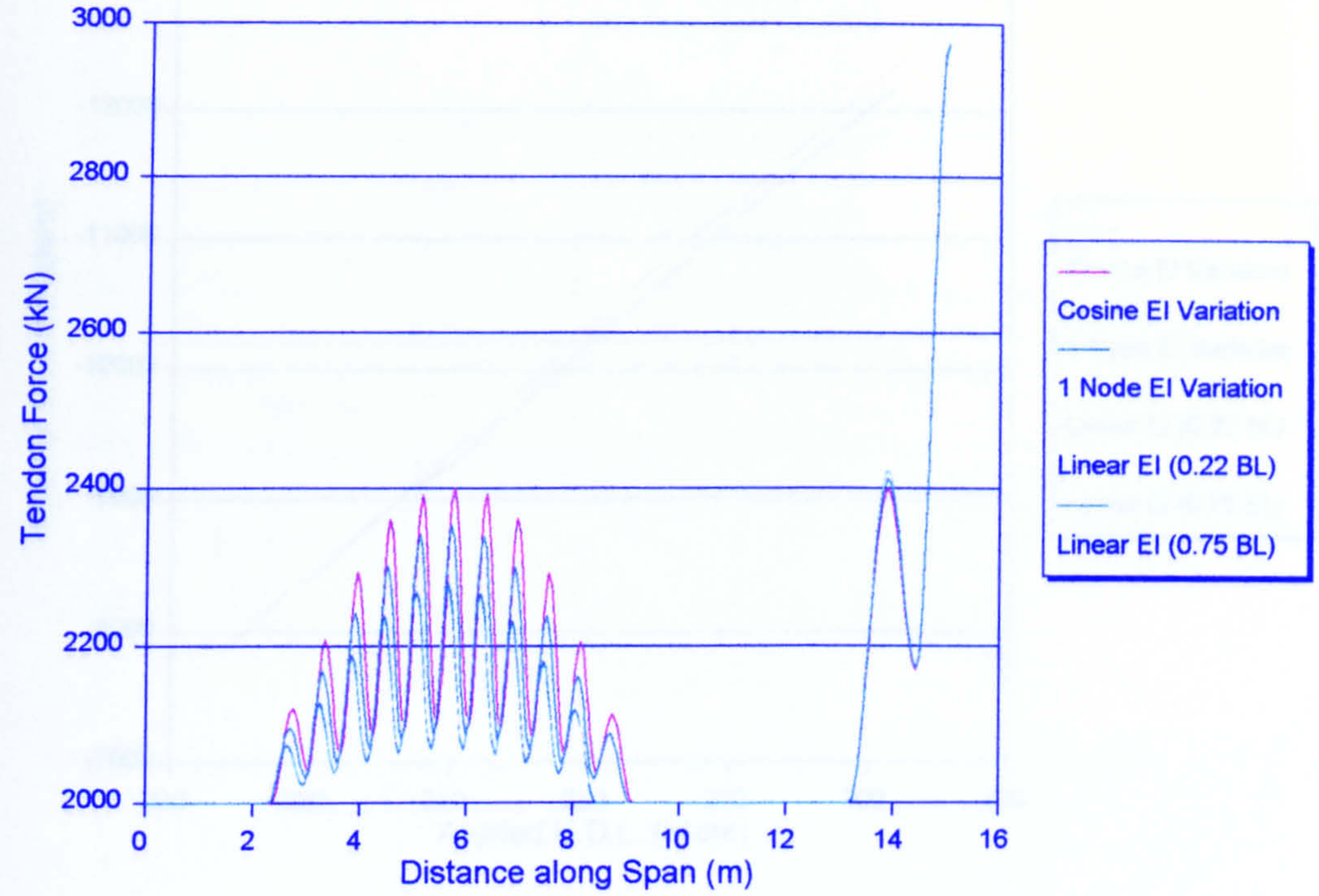

Figure 5.4.11. Tendon Force Envelopes, SMAREL30, Twospan2

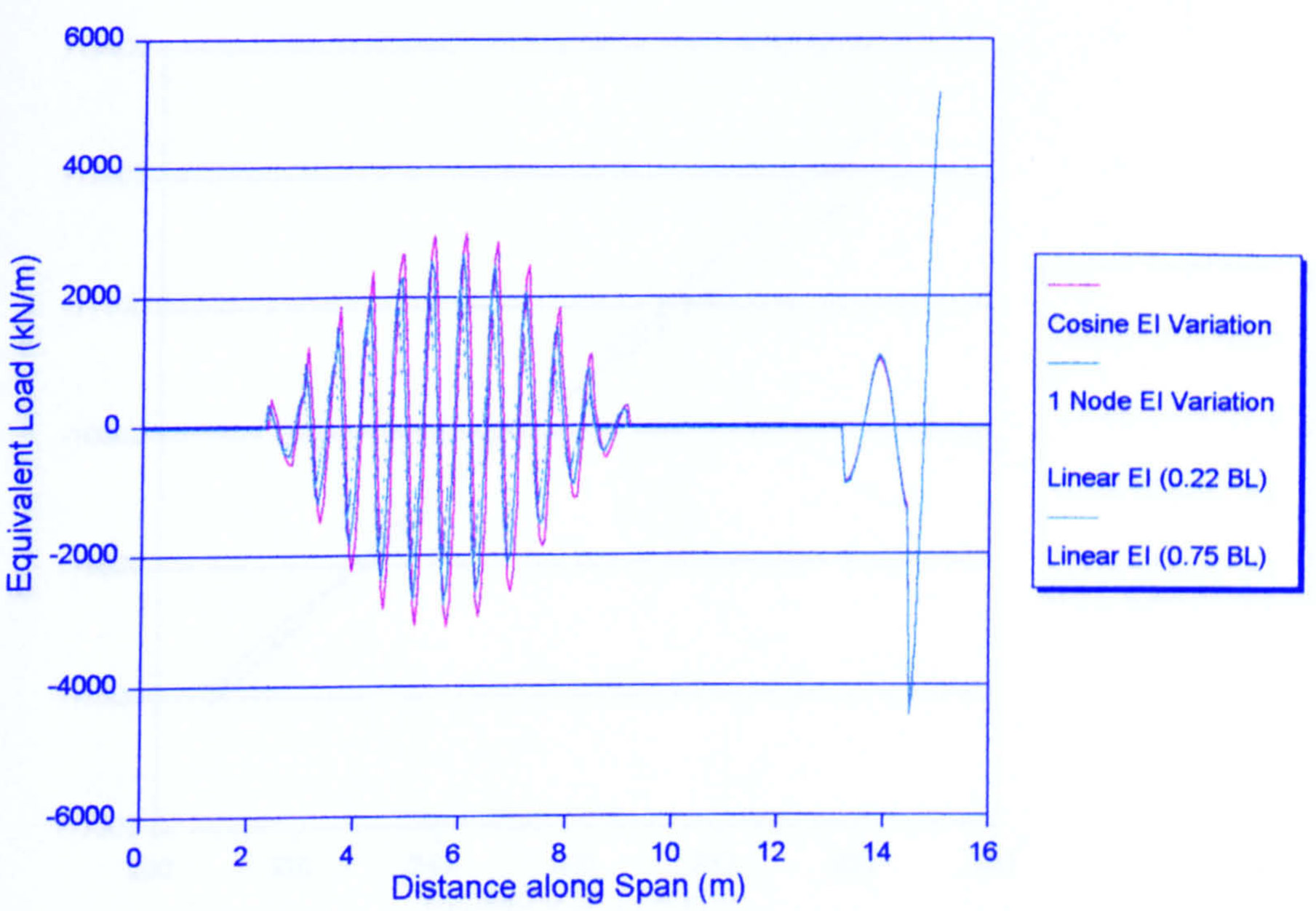

Figure 5.4.12. Equivalent Load Envelopes, SMAREL30, Twospan2

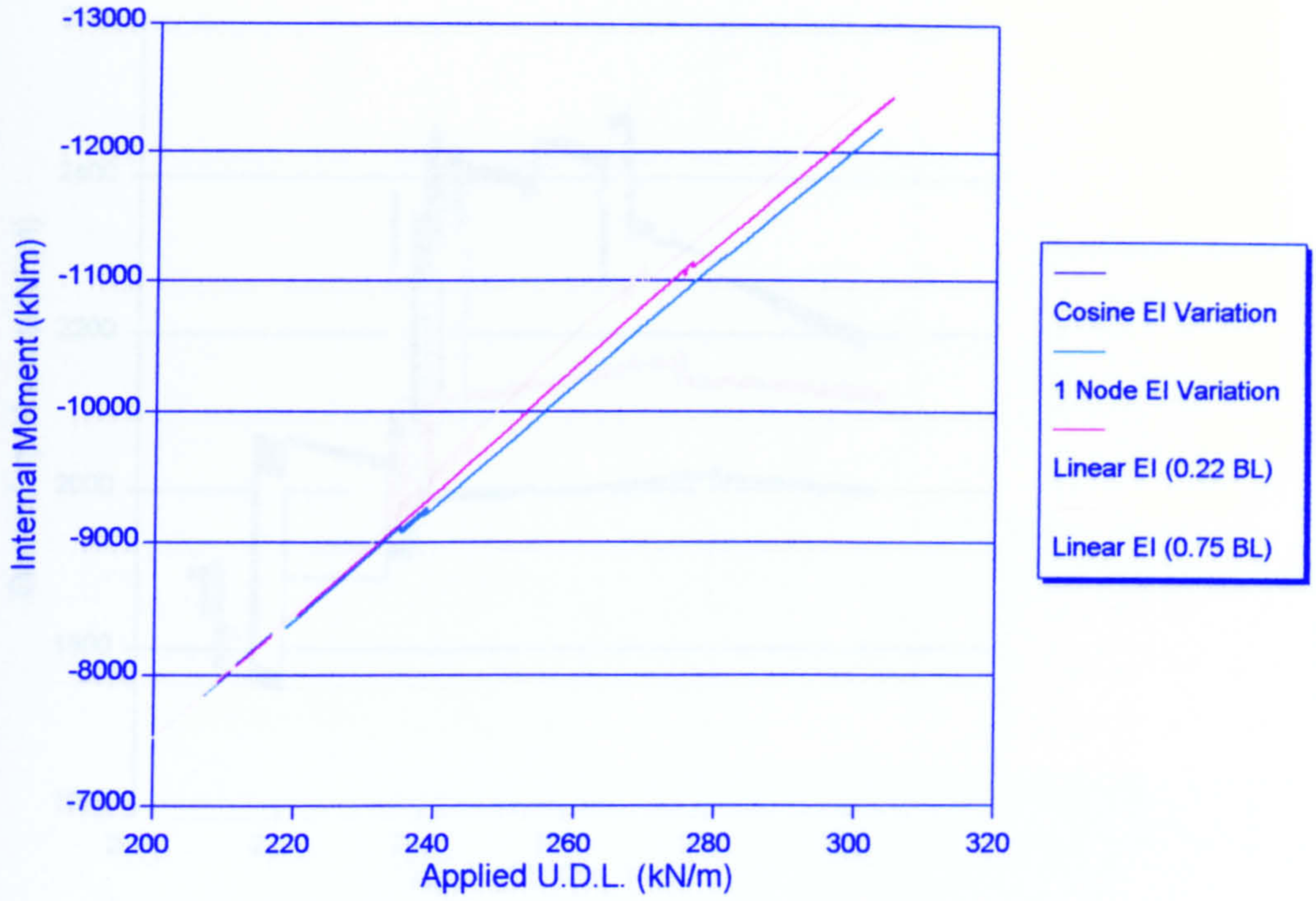

Figure 5.4.13. Internal Moment vs Applied Load at Support 2, SMARELIT, Threespan

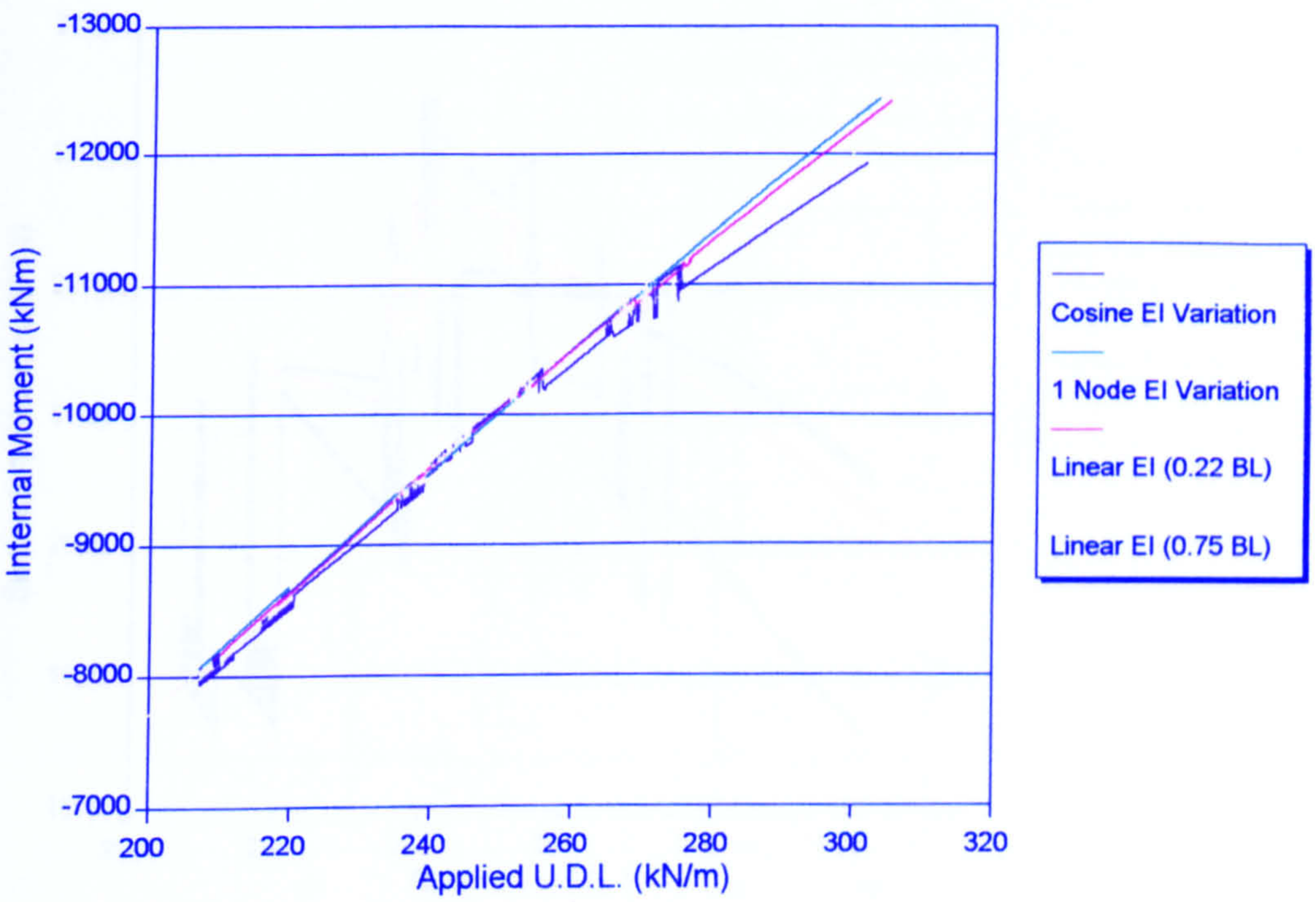

Figure 5.4.14. Internal Moment vs Applied Load at Support 3, SMARELIT, Threespan

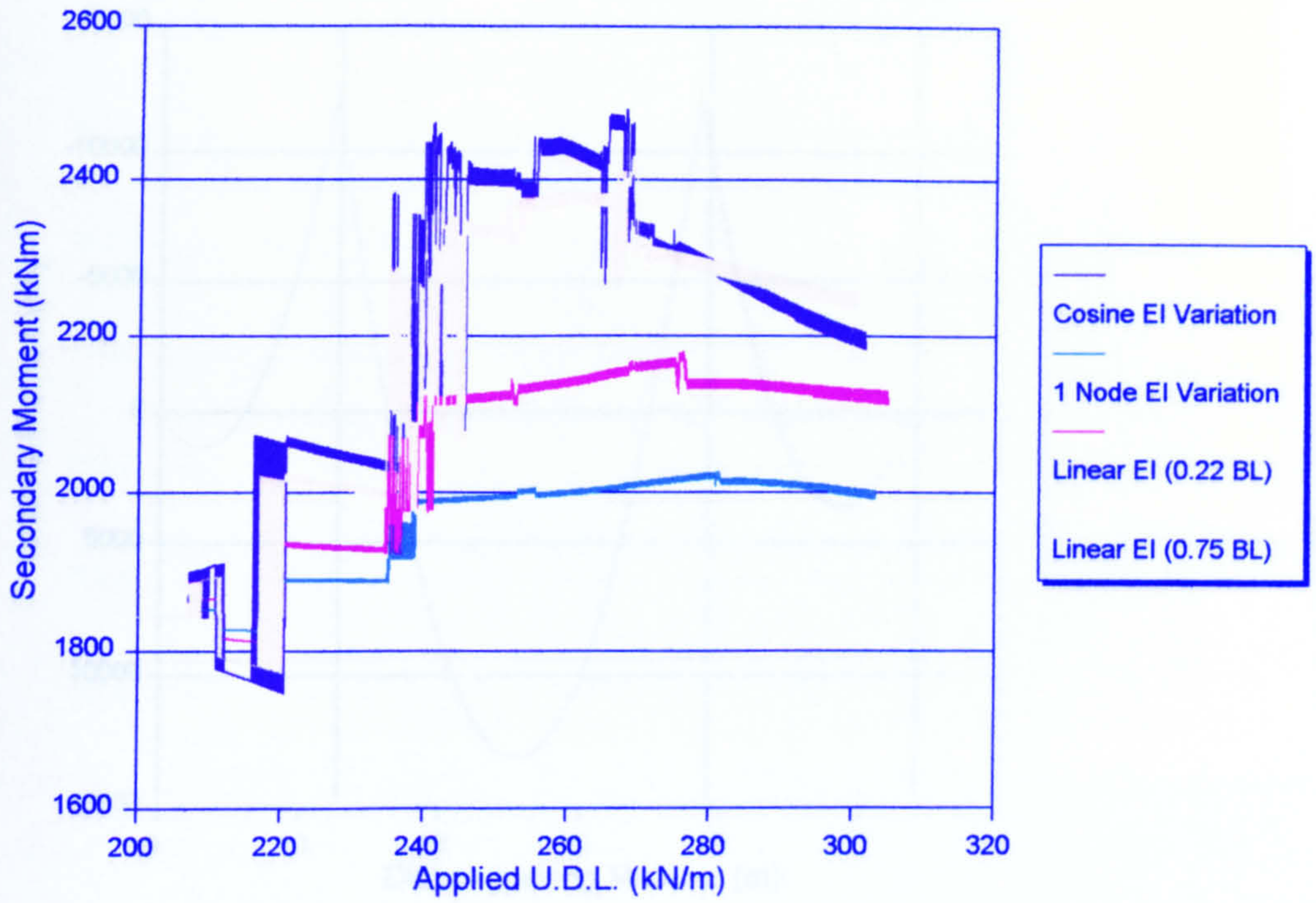

Figure 5.4.15. Secondary Moment vs Applied Load at Support 2, SMARELIT, Threespan

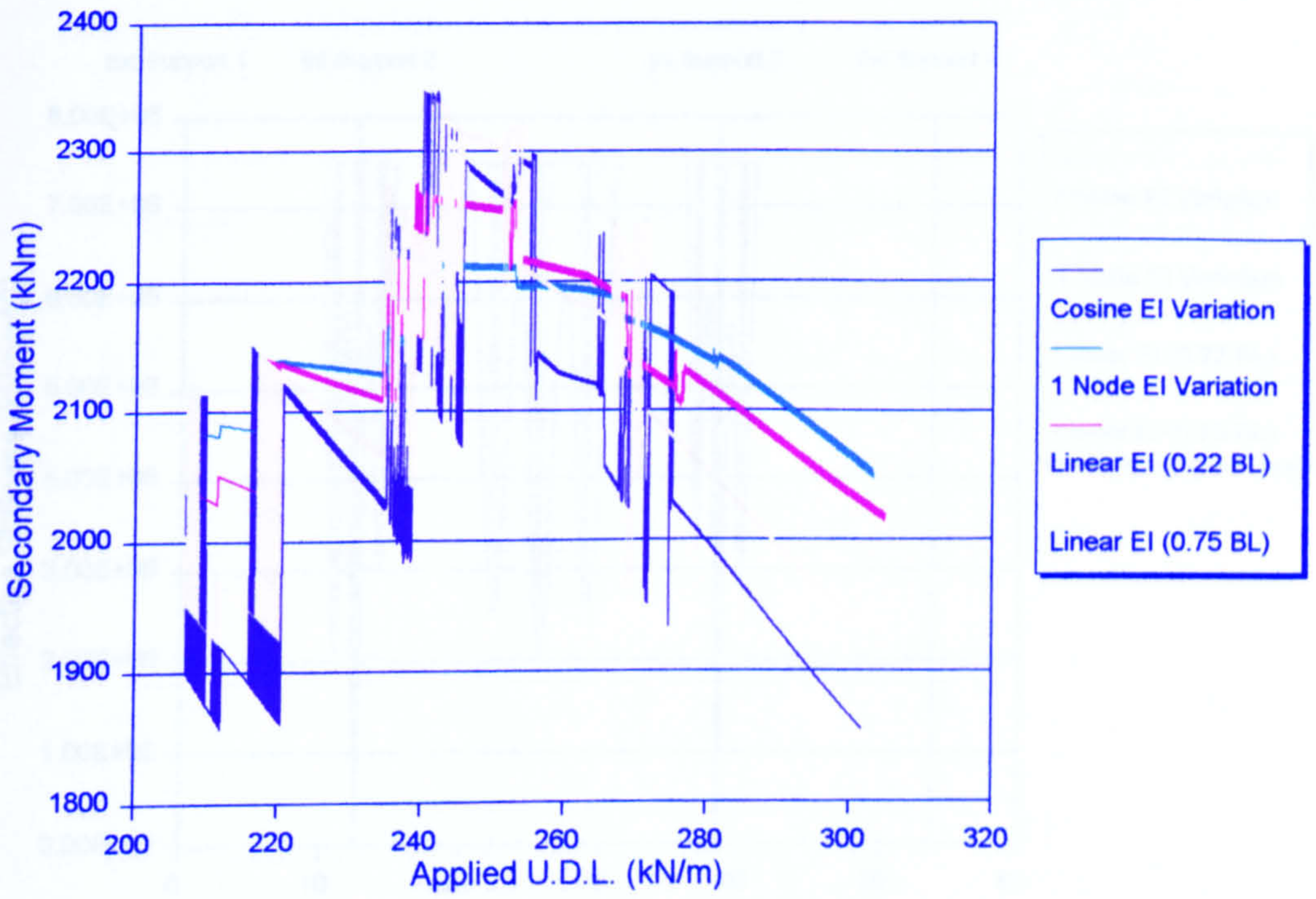

Figure 5.4.16. Secondary Moment vs Applied Load at Support 3, SMARELIT, Threespan

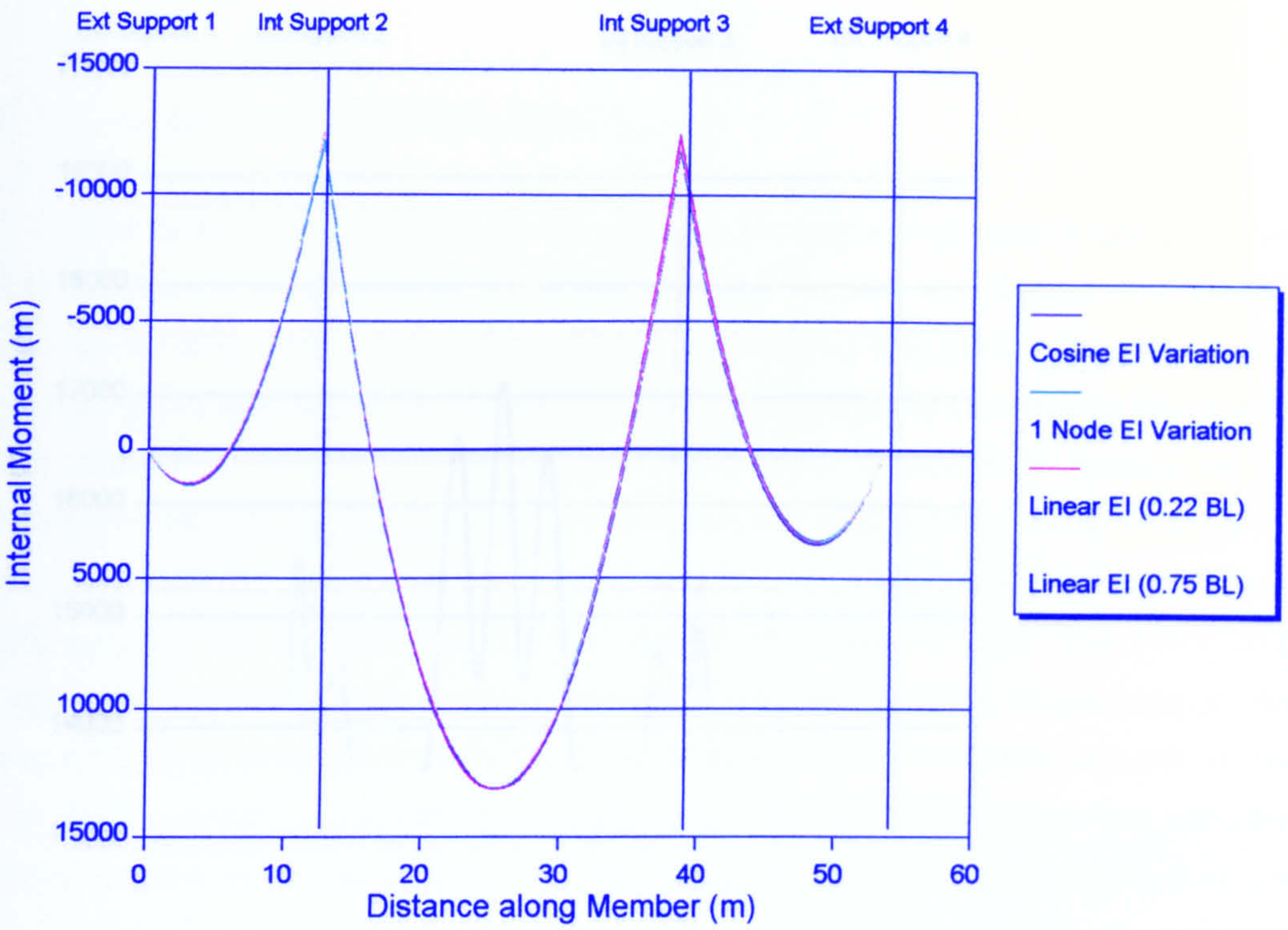

Figure 5.4.17. Internal Moment Envelopes, SMARELIT, Threespan

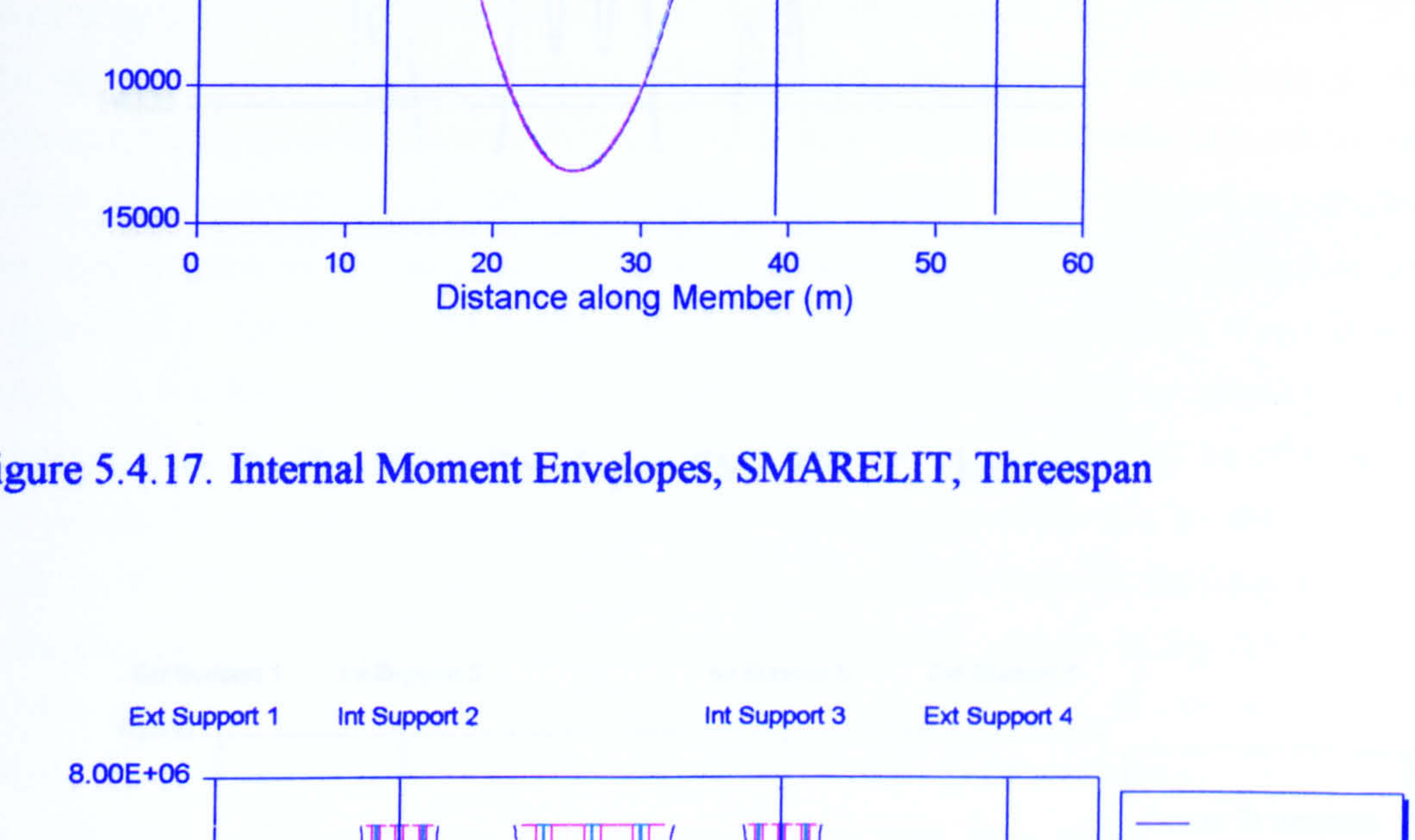

Figure 5.4.18. Effective Flexural Stiffness Envelopes, SMARELIT, Threespan

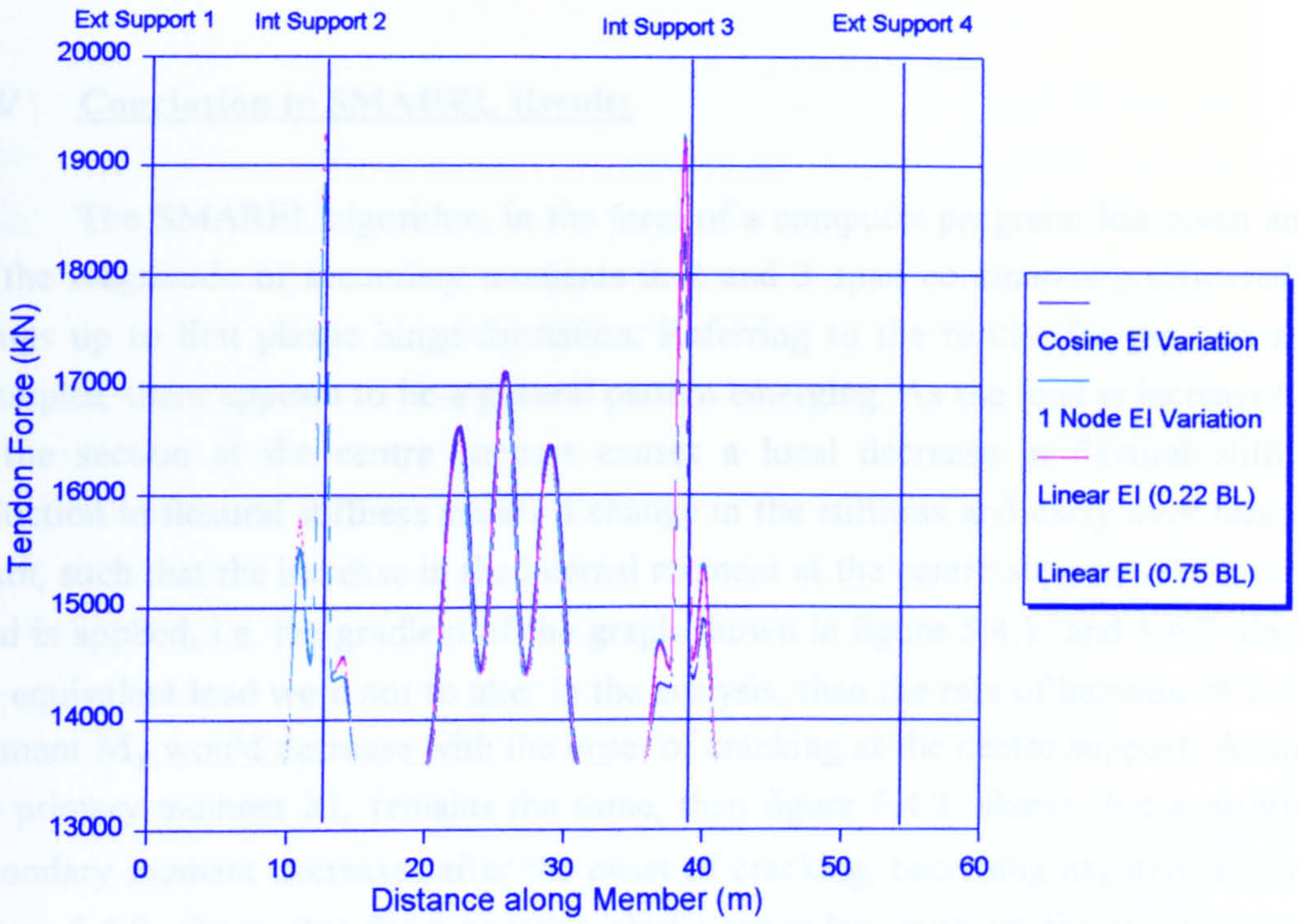

Figure 5.4.19. Tendon Force Envelopes, SMARELIT, Threespan

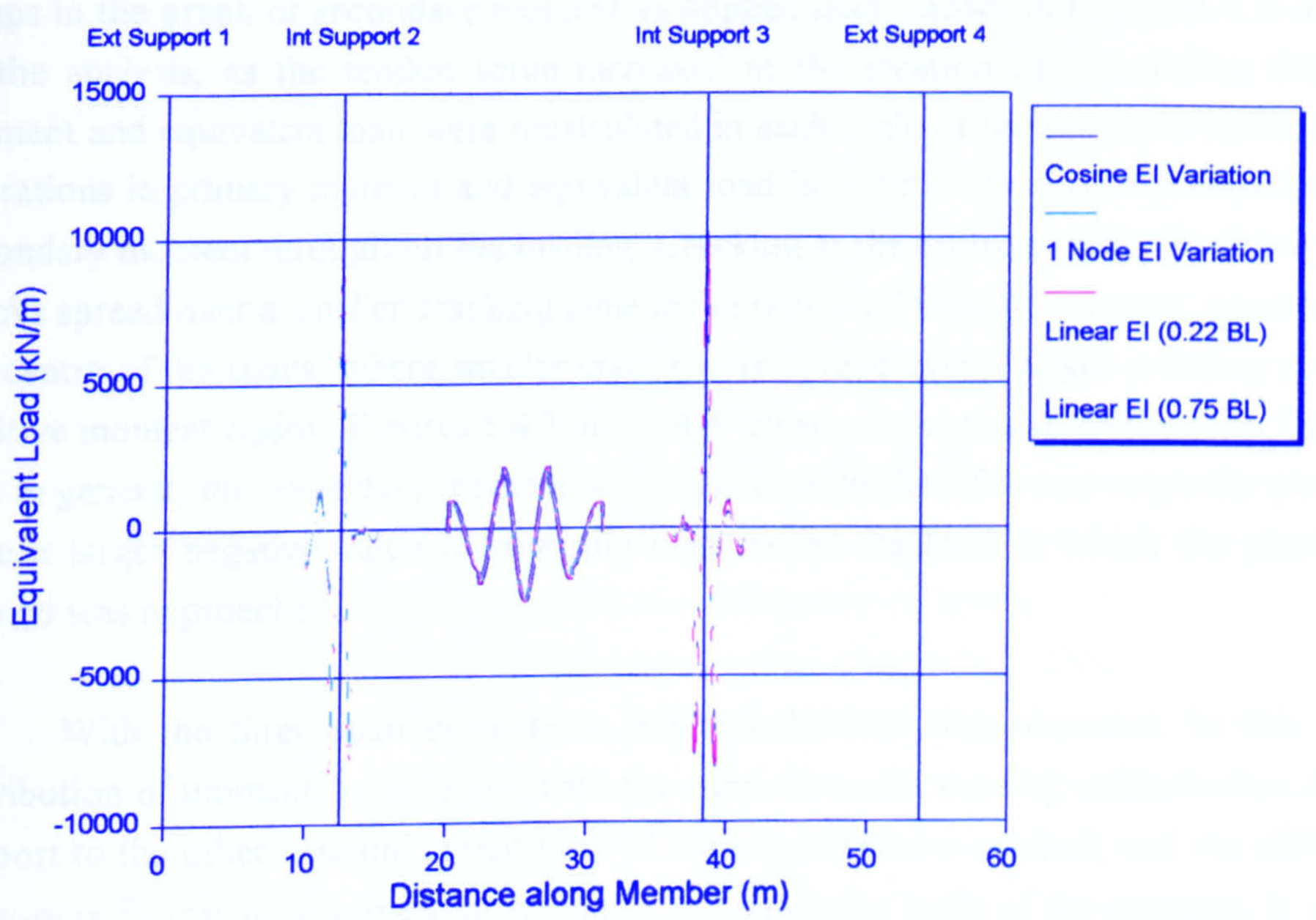

Figure 5.4.20. Equivalent Load Envelopes, SMARELIT, Threespan

5.5/ Conclusion to SMAREL Results

The SMAREL algorithm, in the form of a computer program, has given an estimate of the magnitude of secondary moments in 2 and 3 span continuous prestressed concrete beams up to first plastic hinge formation. Referring to the results for the two span beam examples, there appears to be a general pattern emerging. As the load is increased, cracking in the section at the centre support causes a local decrease in flexural stiffness. This reduction in flexural stiffness causes a change in the stiffness and carry over factors for the beam, such that the increase in the internal moment at the centre support is reduced as more load is applied, i.e. the gradient of the graph shown in figure 5.4.1. and 5.4.7. decreases. If the equivalent load were not to alter in the analysis, then the rate of increase of the resultant moment M_3 would decrease with the onset of cracking at the centre support. Assuming that the primary moment M_1 remains the same, then figure 5.4.2. shows that a positive elastic secondary moment decreases after the onset of cracking, becoming negative at some stage. Figure 5.4.8. shows that for a negative elastic secondary moment the trend is similar after cracking has begun, having a larger negative value as the load is applied. The onset of cracking in the span causes the stiffness and carry-over factors to alter so that the gradient of the graph of internal moment vs applied load is increased. This can be seen in figures 5.4.1 and 5.4.7. This has the opposite effect on the secondary moment, causing a series of small jumps in the graph of secondary moment vs applied load, shown in figures 5.4.2. and 5.4.8. In the analysis, as the tendon force increased at the location of the cracks, the primary moment and equivalent load were recalculated in each cycle of the program. However, these alterations in primary moment and equivalent load have little effect on the behaviour of the secondary moment throughout the loading. Cracking at the centre support consisted of larger cracks spread over a smaller cracking zone in the region of negative moment, as compared to the centre of the spans, where smaller cracks were spread over a larger cracking zone in the positive moment region. Figures 5.4.3 and 5.4.4. clearly show this to be the case. This meant that in general, the secondary moment would become smaller if it was originally positive, or have a larger negative value if originally negative as the load at which the plastic hinge formed was approached.

With the three span example, a similar behaviour was observed. In this case the distribution of moments is different, with the support cracks causing redistribution from one support to the other. Assuming that both of the supports have cracked, and the stiffness and carry-over factors have somewhat stabilised at a particular cycle of the program, it would be fair to assume that the internal moments would continue to increase with load at a constant gradient. The secondary moments both continue to redistribute from one support to the other until the centre span cracks, and then both increase positively with applied load. This effect

can be seen clearly from figures 5.4.15. and 5.4.16. As the load is increased further, at support 2 the secondary moment reaches a stage where it is fairly constant, whilst the secondary moment at support 3 decreases until the plastic hinge is reached here.

It should be stressed that some of the factors used in the SMAREL program are based on empirical data, and a number of details assumed, e.g. the form of the variation of tendon force between cracks was assumed to follow a cosine function. The cracked section analysis has been idealised to comply with information from BS8110, and bond lengths and crack spacing based on data for beams subject to constant moment zones. Regardless of the specification for items such as crack spacing etc. the general trend has emerged, and it is clear that the secondary moment will alter due to the changes in stiffness and tendon force caused by cracking. Experiments (for parameters such as stiffness variations and tendon force changes between cracks) may shed light on the correct values to use in the program to give a better model of the actual beam behaviour.

Rotation Capacity

An attempt was made to analyse the beam Twospan1 for rotation capacity once the plastic hinge had formed at the centre support. Two subroutines were written to continue the analysis up to ultimate. A.L.L.Bakers method was used in one subroutine to calculate the maximum rotation available at the plastic hinge, described in Massonet and Save [8], and the other subroutine made an attempt to calculate the rotation which was occurring at successive load steps by using an integration procedure involving the flexural stiffnesses at the node locations, explained in Matheson [6]. The idea was to compare the calculated rotation with the rotation capacity, and terminate the analysis when the rotation capacity had been reached. Unfortunately the calculated hinge rotation predicted by the subroutine was greater than the calculated rotation capacity, therefore these routines were abandoned. One possible explanation for the problem could have been that the stiffnesses used were effective flexural stiffnesses (secant stiffnesses) rather than the actual stiffnesses (tangent stiffnesses). To calculate actual stiffnesses would require the calculation of moment curvature relationships at each node for the full range up to ultimate moment, a procedure which would be very time consuming. This approach is currently being pursued by Ove Arup and Partners with the program ADSEC, for the analysis and design of reinforced and prestressed concrete sections.

Moment Redistribution

The general design procedure for moment redistribution at the ultimate limit state has been explained in section 2. How to include secondary moments in the analysis has been a problem in a number of design codes, and there are conflicting methods of design. Concentrating on the design to BS8110, this can be broken down into specific problem areas. The idea is to provide enough ductility at plastic hinges so that full specified redistribution of moments can be attained. If this can be achieved, then the secondary moments need not be included in the analysis, as the ultimate moments and load will be insensitive to their inclusion, according to plastic theory.

Taking the example of a two span beam, we will assume that the designer has calculated the ultimate load and the elastic bending moment envelope associated with this, and wishes to reduce the ultimate moment at the centre support by the allowable limit of 20%. Let us also assume that the designer has attempted to ensure that the required amount of rotation capacity for full redistribution has been supplied at the centre support so that full redistribution occurs into the span. He has checked that the limit to the neutral axis depth at the centre support section meets the requirements stipulated in BS8110, and highlighted in section 2.1.1. The code requires that the ultimate moments before redistribution should include any secondary moment present multiplied by a factor of 1.0, hence if the limit of 20% redistribution is in force, this means that the secondary moments must also be included in the redistributed envelope with a factor of 1.0. If it could be ensured that the elastic secondary moments remained constant up to plastic hinge formation, then this procedure is adequate to ensure the required ductility needed for the full specified redistribution, ensuring that the secondary moments need not be included in the redistribution process.

As mentioned earlier, if the ductility of the section cannot be guaranteed, then the complications arise as to how to include the secondary moment. As the results of the program showed, the secondary moment is altering, in some instances going from positive to negative. It is the elastically calculated secondary moment which is used in the design for ductility, and if it is changing as the program predicts, the design will clearly be erroneous. If an erroneous design for ductility of a plastic hinge occurs, this may lead to only partial moment redistribution, compared to the full specified redistribution. Regardless of the fact that the secondary moment disappears once the beam becomes statically determinate, the changing secondary moments have affected the load at which the first plastic hinge forms, and hence the available rotation capacity left in the hinge. So if the full specified redistribution cannot be realised, then the secondary moment will have had some influence on the failure of the beam. If the ductility of the hinge which depends on the secondary moment

has altered and full specified redistribution cannot be achieved, the secondary moments have influenced the redistribution process.

The results of the program cannot in anyway suggest a change to design procedures as they stand. They only serve the purpose, like the majority of other research on the subject, of highlighting problems in the design procedure. Patterns in the results have emerged, but these would need to be reinforced by experimental studies before positive steps could be taken to test changes in design.

6/ General Conclusion

A method for estimating how the elastic secondary moments change with respect to applied loads in continuous prestressed concrete beams has been presented in the SMAREL algorithm. The effects of cracking have been explicitly modelled, rather than to smear the cracks (altered section properties) over 'a cracked zone' in the beam. This was done in order to search for an improvement in the accuracy of the results, as the program strives to model the cracks as realistically as possible. It should be stressed that this only provides an estimate, and can really only be used to highlight patterns in the secondary moment change, as the quantitative measurements are subject to interpretation

Trends in the Secondary Moment, SMAREL Results

The results of the two span beams highlight the effects of the flexural stiffness variation along the length of the beam. All show similar trends in the patterns of change in the internal and secondary moments throughout the loading. The greater stiffness variations have greater effects on both of these moments, significantly the secondary moments.

In general, cracking at the support causes the secondary moment to become more negative, and cracking in the span causes the secondary moment to become more positive, highlighted in figures 5.4.2. and 5.4.8. Comparing the effects of cracking in the negative moment regions over internal supports, with cracking in the positive moment regions in the span, it can be seen that the results are more significant. Cracking at the supports produces larger (deeper) cracks over a smaller length than those which occur in the span. They therefore have a greater overall effect on the flexural stiffness than those cracks occurring in the span. For the two-span beams, the result of this is an overall change in the negative direction of the secondary moment, as load is applied, as discussed in section 5.5.

This change in the secondary moment with applied load would at first appear detrimental, as a negative secondary moment over the centre support might decrease the load at which a plastic hinge forms. Any negative secondary moment would add to the negative internal moment at the centre support caused by the applied load, which in turn might cause a greater extent of cracking at the centre support. This effect would tend to alter the tendon force, stiffness, and carry over factors in a manner which would make the secondary moment even more negative. Also, the effect of the negative secondary moment in the span would be to decrease the extent of cracking in the positive moment region in the span, hence the step changes which make the secondary moment more positive (highlighted in figures 5.4.2. and 5.4.8) would be smaller. The main conclusion from this would be that a secondary moment

which is tending to become more negative as load is applied, is having an effect on the beam which will enhance this alteration of the secondary moment becoming more negative.

However, when looking at the overall effect, and examining what is happening to the total internal moment, it can be seen that the conclusion in the previous paragraph is not correct. From figures 5.4.1. and 5.4.7., the results clearly show that with the models with a more severe flexural stiffness variation between cracks, the applied load at which the plastic hinge forms at the centre support is slightly greater, which obviously contradicts the previous statements. These results can be explained by looking at the portion of the internal moment caused by the applied loads only (i.e. subtracting the secondary moment from the internal moment, so that prestress effects are ignored). The effects of the cracking at the centre support are such that the internal moment due to the applied loads only, redistributes to the span. With the increase in applied load, the relative amount by which the internal moment is magnified over the support appears to be less with the greater flexural stiffness variations between cracks, as more moment is redistributed to the span with increased load and cracking. This effect on the portion of internal moment due to applied loads only, when compared to the effect caused by the changing secondary moment, has a greater influence on the total internal moment. It is also significant that the secondary moment becomes a smaller percentage of the total internal bending moment as the applied load is increased. Hence, the load at which the plastic hinge forms will be larger for the more severe flexural stiffness variations between cracks.

Moment Redistribution

How to handle secondary moments in the design process is now of concern. The present method of including the secondary moments with a factor of 1.0 was described in section 5. Concentrating on the two span beam problem, it is normally required that redistribution if any will occur from the internal support into the span section. The designer would normally take account of any elastic secondary moment by adding this to the elastic bending moment envelope calculated from the ultimate loads before the redistribution process.

The change in total internal moment with applied load for the two span beams, shown in figures 5.4.1. and 5.4.7. give clues as to the effect of the secondary moment on the redistribution process. During the load stage before cracking, it can be seen that in both cases, the relationships between total internal moment and applied load are linear, as expected. Once cracking has commenced, the relationships deviate somewhat from this linear relationship, with a slightly reduced gradient, with the more severe stiffness variations

between cracks causing a greater gradient reduction. If the secondary moment is subtracted from the total internal moment, and the resulting internal moment due to applied load only plotted against applied load, then any deviations from linearity after cracking are slightly more exaggerated than in figure 5.4.1. and 5.4.7., but the graphs will essentially be of the same form, and a higher applied load would eventually be necessary for plastic hinge formation. This is true for the two possible cases where the elastic secondary moment is initially positive or negative. Regardless of how the secondary moment is changing with applied load, it seems reasonable to assume that the secondary moment should be included in the analysis, as the internal moments due to applied load only, and the secondary moment change to complement one another. It also appears reasonable that a factor of 1.0 should be applied to the secondary moment. The ultimate loads are factored in any case, therefore producing a larger elastic bending moment with respect to the secondary moment. The main conclusion which can be drawn from this is that the present approach adopted in BS8110 appears to be adequate. But the reasons for this are more complex than the simplified approach adopted in the code. A similar conclusion can be drawn for the results of the three span model.

Rotation Capacity

In the SMAREL program for the two span beams, two subroutines were written with the aim of continuing the analysis past first plastic hinge formation, up to formation of a collapse mechanism. One subroutine would calculate the rotation of the hinge at the internal support, updating the effective flexural stiffnesses at each load step. The actual rotation thus obtained would be compared with the rotation capacity (maximum rotation) at each load step, and the analysis terminated when either rotation capacity of the hinge (partial redistribution) is reached, or a plastic hinge forms in the span (full redistribution). The methods used for these subroutines are described briefly here.

Maximum Rotation Capacity

A method proposed by A.L.L.Baker for calculating the maximum allowable rotation (rotation capacity) of a plastic hinge in reinforced or prestressed concrete is described in Massonet and Save, [8]. The maximum allowable rotation is given as :-

$$\theta = \frac{S_p l_p}{n_h d}$$

Where S_p is the difference between the ultimate strain in the concrete at fracture and the strain in the concrete when the steel starts to yield, l_p is the length of the plastic region which is replaced by a hinge at one section, and $n_n d$ is the depth of the neutral axis. This method assumes that the curvature is distributed over a plastic hinging length l_p.

Available Rotation

A procedure involving the integration of stiffness along the length of the beam was used to calculate the actual rotation at a particular load level. The calculations involved in the process were taken from Matheson [6], and will not be dealt with here. A stand alone program was first written to analyse the end rotations for different combinations of applied load and end moments on a particular single span beam. This was then incorporated as a subroutine, so that the left hand span of the two span beam system could be analysed as a single span. This single span was then treated as a simply supported beam with end moments of zero at the left hand end, and a moment equal to the plastic moment (at the centre support in the actual two span beam), at the right hand end.

When the model with the cosine stiffness variation was used, after the plastic hinge was reached, the analysis terminated with the maximum rotation capacity having been exceeded. After this attempt, the relevant subroutines were abandoned for improvement and use at a later stage.

Subsequent (stand alone) analysis of the left hand span has shown that the rotations at the right hand end where the plastic moment is applied, are highly dependant upon the model of the flexural stiffness variation used. The more severe the stiffness variation the less actual rotation occurs for a particular applied load, and the actual rotation can be less than the predicted rotation capacity. In some cases, namely with the cosine stiffness variation, the predicted rotation can be in the opposite direction, which is clearly erroneous, and indicates that this model may be incorrect. This perhaps gives an indication of the better stiffness models which should be used in the analysis.

Alternatively, if the method of calculation of the maximum and actual rotations are studied, it can be seen that there is a discrepancy in the treatment of the plastic hinge. For the rotation capacity, the curvature and rotation of the hinge is assumed to be distributed over a plastic hinging length, giving an average rotation over this length. For the calculation for the actual rotation at a particular applied load, the hinge rotation is assumed to be concentrated at a single nodal location over the centre support. Hence the values for actual rotation and rotation capacity may be in conflict as a result of the calculation methods.

The correct way to approach the problem of available redistribution is to study the rotations at the hinges. Due to the aforementioned complications, it is not appropriate to give any quantitative values (for rotations etc.) to any of the analyses at this stage.

Comparison with Finite Element Analysis Results

The finite element analysis results of model 18 were affected to an extent by unexpected reduction in predicted tendon force at the centre support. This may be due to a number of factors as previously explained in section 4.5. The most probable causes may be the sharp angling of the tendon at the centre support, or the cracking of the thin concrete element at the level of the tendon. The effect appears similar to that at the end of the beam where a transmission length is occurring, as would be present in a pretensioned member. At the centre support, all of the elements on the vertical centreline have been restrained from movement in the longitudinal horizontal direction, including the tendon spar element, so the transmission length analogy is an unlikely cause of this problem.

The internal moment at the centre support of model 18 appears similar in form to that obtained from the SMAREL program for Twospan 1. The gradients do not match exactly, but behaviour is comparable with the beams with smaller flexural stiffness variations. Improvement in the finite element models would be necessary to continue the analyses further. The choice of continuous beam model would also need to be looked at carefully

Improvements in the SMAREL Algorithm

At present, the SMAREL program code can deal with two and three span continuous prestressed concrete beams, and takes the analysis up to the formation of the first plastic hinge. As previously explained, a subroutine to continue the analysis for the two span beam program was written, with the aim of comparing the actual rotation at a particular load with the rotation capacity. The idea was to update the effective flexural stiffnesses at each increment of load and to calculate the rotation of the hinge over the support. The analysis would then ideally terminate when either a plastic hinge formed in the span, thereby creating a mechanism (full redistribution), or when the plastic hinge at the support reaches its rotation capacity (partial redistribution). However when this subroutine was 'tied' in to the rest of the program (for the cosine stiffness variation), the analysis would not continue due to the rotation capacity being surpassed immediately after the plastic hinge has formed at the internal support. As the two methods for calculating the maximum and available rotations are based on different principles, alternative ways for calculating these rotations based on similar

basic principles need to be applied. In the case of the three span beam, when a plastic hinge forms at an internal support, the program will terminate, although the beam is still statically indeterminate, and requires the formation of two hinges to become statically determinate, three to form a mechanism (assuming all hinges have adequate rotation capacity). For continuous beam systems with more than three spans, the failure modes become more complicated and there are more of them, each depending on how the load is applied. So perhaps the program could be modified to encompass some of these failure modes, and analyse the beam up to the stage at which a mechanism forms.

Actual (tangent) flexural stiffnesses rather than effective (secant) flexural stiffnesses should ideally be used in any such calculations. These can only be obtained by calculation of the moment-curvature relationships at each node along the beam. This is possible, but could be demanding on both computer time and storage space. The moment-curvature relationships at a large number of load levels would be required, and would need to be stored in a database before the main SMAREL program is executed. In any calculation for rotations, given the bending moment diagram, the consideration of compatibility requirements is useful. Moment-area methods and the 'conjugate beam' method which treats the curvatures as applied loads, requires the integration of the curvatures along the beam length. Whichever method is used, knowledge of the stiffness or curvature variation along the beam is necessary. Each moment-curvature relationship would require storage, and some kind of iterative method of solution.

The solution algorithm for SMAREL has something of a trial and error convergence process, and it is possible for the solution at a particular load to oscillate between a number of states, never reaching a stable solution. This was particularly evident with the three span program. There are more stiffness and carry-over factors involved in the moment distribution, and therefore there are more unconverged states which may be obtained whilst the program searches for a stable solution. In a number of cases, the program cycles through the unconverged states and will never reach a stable one. The cracking pattern and final state of the beam depends heavily on the load path, and any analysis must have an incremental loading procedure. Therefore a better means of assessing whether the beam has reached a stable cracked condition is required.

So far, only continuously curved tendon profiles that yield distributed equivalent loads can be input into the program (tendons exhibiting reversed curvature over supports may be used), and the applied loads are also uniformly distributed across the spans. It would be desirable to be able to apply point loads in combination with distributed loads, and to have a facility to enable sharp changes in the tendon profile to be modelled (i.e. harped tendons).

The program has a large number of arrays to handle, with double precision accuracy required for the finite difference method used for the double differentiation. In some cases it might be possible to improve the code throughout the program so that the execution is faster. A large amount of array ordering processes could be made redundant by simplifying the source code in certain areas.

After the program has been improved, as far as required, a user interface for the input of data would allow people who are not familiar with the workings to use it. At present, the data is inserted by means of pre prepared data files.

Further Study

Improvements required in the SMAREL algorithm for the prediction of secondary moments up to statical determinacy have been presented. With regard to the amount of moment redistribution available, SMAREL has not adequately addressed the problem, and it appears that an alternative approach would be necessary. The effects of secondary moments and how they change throughout loading have been estimated, but this does not appear to give a many clues as to how the moments should be redistributed in the design process. A better approach to the design of prestressed concrete continuous beams at the ultimate limit state would be to look at the overall problem, by applying section property analysis at small increments in load using moment-curvature relationships, rather than separate out the various bending moments. Analysis of continuous beam systems with different elastic secondary moments, and how they behave at the ultimate limit state, might produce relations that could be used to incorporate the elastic secondary moment in a better way into the design. The designer would like the design process to be as simple as possible, and therefore does not want to be dealing with complicated methods or analyses of continuous beam systems. Hence it appears that nonlinear methods such as finite elements (backed up with empirical work) would be more useful in the long term research, and concentration on reaching the desired failure loads with various elastic secondary moments, should be the aim.

References

1/ M.K.Hurst, Prestressed Concrete Design, Chapman and Hall 1988.

2/ A.H.Nilson, Design of Prestressed Concrete, 2nd Edition, John Wiley and Sons 1987.

3/ T.Y.Lin and N.H.Burns, Design of Prestressed Concrete Structures, 3rd Edition, John Wiley and Sons 1982.

4/ A.H.Nilson and G.Winter, Design of Concrete Structures, 11th Edition, McGraw-Hill International, 1991.

5/ H.G.Allen and P.S.Bulson, Background to Buckling, McGraw-Hill 1980.

6/ J.A.L.Matheson, N.W.Murray, and R.K.Livesley, Hyperstatic Structures Volume 1: An Introduction to the Theory of Statically Indeterminate Structures, Butterworths 1959.

7/ Spencer et al, Engineering Mathematics, Volume 1,Van Nostrand Reinhold 1987.

8/ C.E.Massonet and M.A.Save, Plastic Analysis and Design Volume 1: Beams and Frames, Blaisdell Publishing Co. 1965.

9/ R.F.Warner and K.A.Faulkes, Prestressed Concrete, Pitman (Australia) 1979.

10/ A.L.L.Baker, Ultimate Load Theory applied to the Design of Reinforced and Prestressed Concrete Frames, Concrete Publications Ltd. 1956.

11/ S.S.J.Moy, Plastic Methods for Steel and Concrete Structures, Macmillan 1989.

12/ F.K.Kong and R.H.Evans, Reinforced and Prestressed Concrete, 3rd Edition, Van Nostrand Reinhold 1987.

13/ W.M.Jenkins, Structural Analysis Using Computers, Longman Scientific and Technical 1990.

14/ R.C.Coates, M.G.Coutie, and F.K.Kong, Structural Analysis, 3rd Edition, Van Nostrand Reinhold 1988.

15/ R.D.Cook, D.S.Malkus, M.E.Plesha, Concepts and Applications of Finite Element Analysis, 3rd Edition, John Wiley and Sons 1989.

16/ N.H.Burns, Moment-Curvature Relationships for Partially Prestressed Concrete Beams, Journal of the P.C.I., Vol 9, Part1, pp 52-63, 1964.

17/ S.K.Mallick, Redistribuition of Moments in Two Span Prestressed Concrete Beams, Magazine of Concrete Research, Vol 14, No 42, pp 171-183, Nov. 1962.

18/ T.Y.Lin, K.Thornton, Secondary Moment and Moment Redistribution in Continuous Prestressed Concrete Beams, Journal of the P.C.I., pp 8-20, Jan.-Feb. 1972.

19/ M.J.N.Priestley, R.Park, and F.P.S.Lu, Moment-Curvature Relationships for Prestressed Concrete in Constant Moment Zones, Magazine of Concrete Research, Vol 23, No 75-76, June-Sept. 1971.

20/ M.J.N.Priestley and R.Park, Moment Redistribution in Prestressed Concrete Beams, Magazine of Concrete Research, Vol 24, No 80, Sept. 1972.

21/ A.A.Mufti, M.S.Mirza, J.O.McCutcheon, and J.Houde, A Study of the Behaviour of Reinforced Concrete Elements using Finite Elements, Structural Concrete Series No70-5, Dept. of Civil Engineering and Applied Mechanics, McGill University, Canada, Sept. 1970.

22/ S.M.Seraj, M.D.Kotsovos, and M.N.Pavlovic, Non-Linear Finite Element Analysis of Prestressed Conctrete Members, Proceedings of the Institution of Civil Engineers, Structures and Buildings, Paper 9885, pp 403-418, Nov. 1992.

23/ T.I.Campbell and A.Moucessian, Prediction of the Load Capacity of Two-Span Continuous Prestressed Concrete Beams, Journal of the P.C.I., pp 131-151, March-April 1988.

24/ P.B.Morice and H.E.Lewis, The Strength of Prestressed Concrete Continuous Beams and Simple Plane Frames, Symposium on The Strength of Concrete Structures, Session C, Paper 3, pp 377-400, 1956.

25/ P.B.Morice, A Direct Design Method for Statically Indeterminate Prestressed Concrete Structures, World Conference on Prestressed Concrete, Paper 22.

26/ P.B.Morice, The Analysis of Prestressed Concrete Structures and the Application of Recent Research, Proceedings of the Instituion of Civil Engineers, Vol 6, pp 445-497, March 1957.

27/ P.Marro, Optimal Limit State Design with Unbonded Prestressing Tendons, Magazine of Concrete Research, Vol 32, No 113, pp 227-240, Dec. 1980.

28/ A.H.Mattock, J.Yamazaki, and B.T.Kattula, Comparitive Study of Prestressed Concrete Beams With and Without Bond, Part 1, Journal of the A.C.I., pp 116-125, Feb. 1971.

29/ T.I.Campbell and V.K.R.Kodur, Deformation Controlled Non-Linear Analysis of Prestressed Concrete Continuous Beams, Journal of the P.C.I., pp 42-55, Sept.-Oct. 1990.

30/ J.W.Kelly, T.Y.Lin, A.C.Scordelis, and C.C.Zollman, Proceedings of World Conference on Prestressed Concrete, July 1957.

31/ E.W.Bennet, N.Cooke, and L.P.Naughton, Deformation of Continuous Prestressed Concrete Beams and its effect on the Ultimate Load, Proceedings of the Institution of Civil Engineers, Paper No.6997, 1967.

32/ A.Huber, Effect of Hyperstatic Prestressing Moments and the Carrying Capacity of Continuous Beams, Journal of the A.C.I., pp 561-566, July-Aug 1986.

33/ P.J.Wyche, J.G.Uren, G.C.Reynolds, Interaction between Prestress Secondary Moments, Moment Redistribution, and Ductility - A Treatise on the Australian Concrete Codes, A.C.I. Structural Journal, Vol 89, pp 57-70, Jan-Feb 1992.

34/ H.Scholz, Ductility, Redistribution, and Hyperstatic Moments in Partially Prestressed Members, A.C.I. Structural Journal, Vol. 87, pp 341-349, May-June 1990.

35/ A.H.Mattock, Secondary Moments and Moment Redistribution in ACI-318-77 Code, International Symposium on Nonlinearity and Continuity in Prestressed Concrete, Preliminary Publication, Vol. 3: Hyperstatic Structures; Nonlinear Design, codes and Practice. University of Waterloo, July 4-6, 1983.

36/ A.Aguado, A.C.Aparicio, and J.Murcia, Nonlinear Behaviour of Statically Indeterminate Prestressed Concrete Structures :- Application to Glatt Bridge, International Symposium on Nonlinearity and Continuity in Prestressed Concrete, Preliminary Publication, Vol. 3: Hyperstatic Structures; Nonlinear Design, codes and Practice. University of Waterloo, July 4-6, 1983.

37/ A.Rösli and H.Hofacker, Tests on the Glatt Bridge at Opfikon (Switzerland), Cement and Concrete Association, Library Translation No. 106, 1963

38/ R.F.Warner and K.A.Faulkes, Overload Behaviour and design of Continuous Prestressed Concrete Beams, International Symposium on Nonlinearity and Continuity in Prestressed Concrete, Preliminary Publication, Vol. 3: Hyperstatic Structures; Nonlinear Design, Codes and Practice. University of Waterloo, July 4-6, 1983.

39/ A.C.Scordelis, Computer Models for the Nonlinear Analysis of Reinforced and Prestressed Concrete Structures, Journal of the P.C.I., pp 116-135, Nov-Dec 1984.

40/ A.S.C.E. Task Commitee on Finite Element Analysis of R.C. Structures, State of the Art Report on Finite Element Analysis of R.C., A.S.C.E. Special Publications, 1982.

41/ F.Levi, G. Mancini, and D.Munari, Hyperstatic Effect of Prestressing Between Serviceability and Ultimate Limit States, International Symposium on Nonlinearity and Continuity in Prestressed Concrete, Preliminary Publication, Vol. 2: Hyperstatic Structures; Nonlinear Analysis. University of Waterloo, July 4-6, 1983.

42/ A.Cauvin, Nonlinear Analysis of Continuous Prestressed Concrete Beams, International Symposium on Nonlinearity and Continuity in Prestressed Concrete, Preliminary Publication, Vol. 2: Hyperstatic Structures; Nonlinear Analysis. University of Waterloo, July 4-6, 1983.

43/ A.C.Scordelis, Analytical Models for Nonlinear Material, Geometricand Time-Dependant Effects, International Symposium on Nonlinearity and Continuity in Prestressed Concrete, Preliminary Publication, Vol. 2: Hyperstatic Structures; Nonlinear Analysis. University of Waterloo, July 4-6, 1983.

44/ A.H.Mattock, Prediction of the Load Capacity of Two-Span Continuous Prestressed Concrete Beams, Reader Comment, P.C.I. Journal, pp 157-159, Sept-Oct 1988.

45/ N.El-Mezaini, and E.Citipitioglu, Finite Element Analysis of Prestressed and Reinforced Concrete Structures, A.S.C.E. Journal of Structural Engineering, Vol. 117, pp 2851-2864, Oct 1991.

46/ G.J.Desalvo, and R.W.Gorman, ANSYS Engineering Analysis Users Manual, Revision 4.4a, Swanson Analysis Systems INC., Houston, Pennsylvania.

47/ M.Suidan, and W.C.Schnobrich, Finite Element Analysis of Reinforced Concrete, Journal of the Structural Division, Proceedings of the A.S.C.E., Vol 99, No. ST10, Oct 1973.

48/ L.Weekes, A Study of Secondary Moments and Moment Redistribution in Prestressed Concrete Continuous Structures by Finite Element Analysis, Transfer Document, University of Southampton, March 1992.

49/ El-Dib, A theoretical and Experimental Study of the effect of the Spread of Plasticity on the Behaviour of Beam-Columns, and on the Non-Linear Analysis of Steel Frames, Ph.D Thesis, University of Southampton, January 1988.

50/ BS 8110, Structural use of Concrete: Part1. Code of Practice for Design and Construction: 1985

51/ Roughton and Partners, Design Calculations for A127 Durham Western Bypass Club Lane Bridge.

AppendixA

SMAREL Program Procedure

Two programmes, SMAREL30 and SMARELIT were written in Fortran77, the former for the analysis of two span prestressed concrete beams, and the latter for three span. Their purpose is to produce an estimate of the magnitude of secondary moments through serviceability and up to the stage at which a plastic hinge forms. Both programmes have a cracked section analysis module, details of which are given in appendix B, which can handle rectangular, I, or T sections, with prestressed reinforcement with a parabolic profile, present at one level only in the beam. The two span version analyses the left hand span only, therefore all models have to be symmetrical about the central support, with identical tendon profiles, and uniformly distributed loading level. With the three span version, all data for the spans are read into the programme separately, catering for unsymmetrical beam systems. At present, the transverse load can only be applied as a uniformly distributed along the spans, although it should not be a hard task to upgrade the programme to cope with individual loadings on spans. Non-prestressed reinforcement has been excluded in the cracked section analysis, and the prestressed reinforcement is assumed to be fully bonded to the concrete. The program flow for SMARELIT is described here.

Program Flow

Relevant model data are read into the programme from the file 'INPUT.DAT', containing the following information :-

AS	=>	Area of prestressing steel	mm^2
DE	=>	Overall depth of section	m
ES	=>	Elastic modulus of steel	kN/mm^2
EC	=>	Initial elastic modulus of concrete	kN/mm^2
FCU	=>	Characteristic strength of concrete	N/mm^2
FPU	=>	Characteristic strength of steel	N/mm^2
PF	=>	Prestress force	kN
GAM1	=>	Material factor for concrete	----
GAM2	=>	Material factor for steel	----
BW	=>	Breadth of web	m
BF1	=>	Breadth of top flange	m
BF2	=>	Breadth of bottom flange	m
DF1	=>	Depth of top flange	m

DF2	=>	Depth of bottom flange	*m*
STRAND	=>	Number of prestressing tendons	----

Individual span data are then read into the programme from files 'SPAN1.DAT', 'SPAN2.DAT', and 'SPAN3.DAT', corresponding with the spans working from left to right. Each of these data files contains the following information:-

L*	=>	Length of span	*m*
ELH	=>	Eccentricity of tendon at left hand end	*m*
ERH	=>	Eccentricity of tendon at right hand end	*m*
EN	=>	Drape of tendon at midspan	*m*

('*' is a number associated with the corresponding span number)

After each one of these data files is read, the information is processed by the subroutine SPANSET where nodes, cross sectional areas, second moments of area, eccentricity arrays and prestress force arrays are calculated for each span. A nodal interval of 0.05 m is used for each span, as dictated by the subsequent numerical differentiation required to calculate the equivalent load. A number of variables and arrays involved with flagging and allocation of cracks are initialised by the subroutine INITIAL1 for the uncracked state, therefore only points where the tendon eccentricity and prestress forces (the primary moment function) alters are flagged and recorded, i.e. at the ends of each span.

The primary moment envelope for each span is calculated by the subroutine PRIMARY by direct multiplication of the eccentricity array E*(I) with the prestress force array P*(I), and the applied load set into the matrix AL(I). This process is given a label for loop back at the end of the programme. The primary moment is stored in the first column of a seven column wide matrix FD*(I,J), which is passed to the subroutine EQUIV, along with the crack flags. This takes the first column and calculates the finite differences between the values in each row, placing these in the next column. This process is repeated six times so that the required six levels of differences are obtained for the series solution given by Stirlings interpolation formula to find the second differential, i.e. the equivalent load. Extrapolation procedures are used at function change points to obtain the correct difference values in the last column. This requires that no adjacent changes in primary moment function be within six nodes of one another unless they are coincident. Therefore care is needed to ensure that this does not occur, as cracks may appear near to where tendons change in curvature along the beam. This may be a problem when the curvature of the tendon profile is reversed near the supports. The equivalent load is stored in the array C*(I), and the first

value of a particular length of continuous function is stored in the array C1*(I), so that two values are stored for a particular node at which the function change occurs (the last value of a function is stored in the C*(I) matrix). The theory is detailed in section 5.1.

The equivalent load is passed back to the main programme, and added to any applied uniformly distributed load by the subroutine LOADSUM. This combination of load is passed to subroutine FREEBM which carries out an integration procedure to determine the free bending moment envelope on the span in question, taking into account any function discontinuities. The matrix D*(I) is returned with the correct bending moment values. Next, the stiffness, carry-over factors, and fixed-end moments are obtained using the method described in section 5.1, by subroutine FEM. Curvatures are calculated from EI effective (secant) flexural stiffness values using the free bending moment envelope calculated from the total load, and two unit end couples. These curvatures are integrated along the beam to obtain the necessary values for the determination of stiffness factors, carry-over factors, and fixed-end moments. For each span this process must be carried out twice for the determination of the relevant factors for each end of the span, so in between the calls of the FEM subroutine, a procedure to reverse the direction in which the x co-ordinate traverses the length of the span, the EI values, and the free bending moment is carried out by subroutine REVERSE to facilitate this.

The fixed end moments, carry-over factors, and relative stiffnesses are passed to the subroutine MDIST which carries out a moment distribution on a three span beam with simply supported external supports. The resulting moments at the four supports are stored in the array TOTAL(I) which is returned to the main routine. Another small subroutine calculates the internal moment at the supports from these total moments by subtracting the primary moment at these points. Hence we have the reactant internal moments at the internal supports, with those at the outer supports being zero.

The free bending moment is calculated for each span again, this time with the applied load only. The reason for this is that the algorithm for the cracked section analysis takes into account any initial strain in the steel and concrete caused by the prestress, and therefore gives the internal moment at which the section will crack. If the equivalent load is used in conjunction with the applied load, the effects of the prestress are effectively being used twice in the calculation, and will obviously cause erroneous results. The free bending moment envelope is added to the reactant internal moment envelope, calculated from the internal support moments, carried out by the subroutine RESM, to calculate the resultant internal moment envelope, and store it in the matrix RES*(I) for each span.

The cracking moment envelope is then calculated by subroutine MCRACK, and stored in the matrix CR*(I). This is carried out at this stage of the programme, rather than at the beginning, as a precaution for the change in length of the negative and positive moment zones. The resultant moment is checked for its sign, and the cracking moment of the same sign is calculated for comparison purposes at a later stage, albeit that the range of the change in the position of zero moment is unlikely to encroach upon the zones of major cracking.

Subroutine ENDS and CENTRE perform a comparison of the cracking and resultant moment envelopes for each span, and stores the values of the differences where the resultant moment envelope exceeds the cracking moment envelope. The nodes at which the maximum differences in both negative and positive moments occur are then also isolated, and the difference values stored. Subroutine BONDS then calculates a value for the bond stress based on the concrete characteristic strength, Kong [12].

The ultimate moment envelope is calculated for each span next, so that the maximum compressed concrete fibre strain values at the two extremes of cracking and ultimate moment are known for iteration purposes of calculating section properties at intermediate moments. Again, as a precaution this is carried out at this stage rather than at the beginning of the programme.

Maximum difference values of resultant and cracking moment in each moment zone of each span are checked to see if they are non-zero, i.e. to check if cracking has occurred. Any non-zero differences cause the programme to enter an IF loop which calls the subroutine BICHOP. This routine performs a binary chop process as described for the algorithm in Appendix B, iterating the extreme compressed concrete fibre strain until the correct moment is obtained from the subroutine MCALC. In this case the applied moment is made equal to the cracking moment, so that the bond lengths for use in determining crack spacing may be calculated from the difference between the effective prestress, and the tendon force immediately cracking has occurred. Subroutine BONDL is used for this purpose, using a calculation formulated from the analysis of constant moment zones, Priestley et.al. [19].

Tendon force is set to the effective prestress value, and various items associated with crack flagging are initialised in the subroutines INITIAL2 for the end spans, and INITIAL2A for the centre span, for subsequent procedures. Using the bond lengths calculated for each moment zone (assuming cracking has occurred), subroutines CRACKS1 and CRACKS2 ascertain other cracked nodes by scanning the area over which the differences between the resultant and cracking moment envelopes are non-zero. If any non zero differences occur at

1.5 times the bond length away from the primary or other cracks, these nodes at 1.5 times the bond length are also deemed to have cracked.

Subroutines TFORCEP and TFORCEN then take each individual moment zone of each span and call subroutine BICHOP to perform cracked section analyses at cracked nodes in the positive and negative moment regions respectively. The change of tendon force between cracks and at the end of the cracked zones are modelled using a cosine function. Assuming the crack is question is the first or last in a series of cracks, the tendon force will drop to its effective prestress force value at a distance equal to the bond length away from the cracked zone, described by a cosine function. As the distance between cracks is equal to 1.5 times the bond length, the tendon force halfway between cracks is taken as the effective prestress force plus one quarter of the difference between the average of the tendon forces of the adjacent cracks and the effective prestress force. The cosine function is then fitted appropriately between the peaks and troughs of the tendon force. A similar procedure is applied to the EI stiffness values along the beam, although the functions and lengths over which stiffnesses change are the subject of a parametric study.

Next, the crack flags need to be ordered and tidied after the new tendon forces and EI values have been created, and this is done by subroutines BUBBLE, which performs an ordinary bubble sort, and RESET, which checks and sets the location of the cracked node numbers in the CRACK(I) matrix.

The primary moment and equivalent load are then recalculated with the new tendon force. The equivalent load is added to the applied load, the free bending moment recalculated, and the fixed end moments established, as before. The moment distribution is performed to obtain the resultant moments, and the primary moment is again subtracted to give the internal moments at the supports. Hence, two cycles are performed in one 'loop' of the programme. These moments are compared with those calculated from the first cycle, and if they are outside the prescribed convergence criterion, a counter for crack control is increased by one, and looped back to where the first primary moment was calculated. If the counter is set to anything other than one, then the crack pattern formed on the first run is kept to for subsequent iterations. When the internal support moments obtained at the end of the programme after the second cycle are in agreement with those from the first cycle, the values which were input at the start of the programme for the internal support moments are then compared with those from the second cycle. If they are not within the desired criterion, the averages of these two moment values at the internal supports is taken, and are made equal to the input moment values. The programme loops back with the counter reset to one

to initiate a new crack pattern. Once these moments agree, the secondary moment may then be calculated.

The equivalent load is recalculated, but this time it is not added to the applied load. The corresponding free bending moment envelope, fixed-end moments, stiffness, and carry-over factors are obtained, ready for the moment distribution. After this has been carried out, the result is the total moments at the supports due to equivalent load only, then the primary moment is subtracted from these to give the secondary moments. A check for failure is then carried out by comparing the resultant internal moment (due to the total load) with the ultimate bending moment envelope. If at any section the ultimate envelope has been exceeded, a plastic hinge is deemed to have formed, and the programme is terminated. If this is not the case, a variety of information is written to an output file SEC1.DAT, and a small increment is added to the applied U.D.L. The program reruns with this new load.

Depending on the convergence criteria, the load increment, and the initial support moment estimate gives a bearing on the results obtained. If the number of full repeats of the core of the programme exceeds a pre-set value, the next load step is initiated, as it is possible for the process to oscillate between a number of unstable states.

Flow Chart:- For Main Program

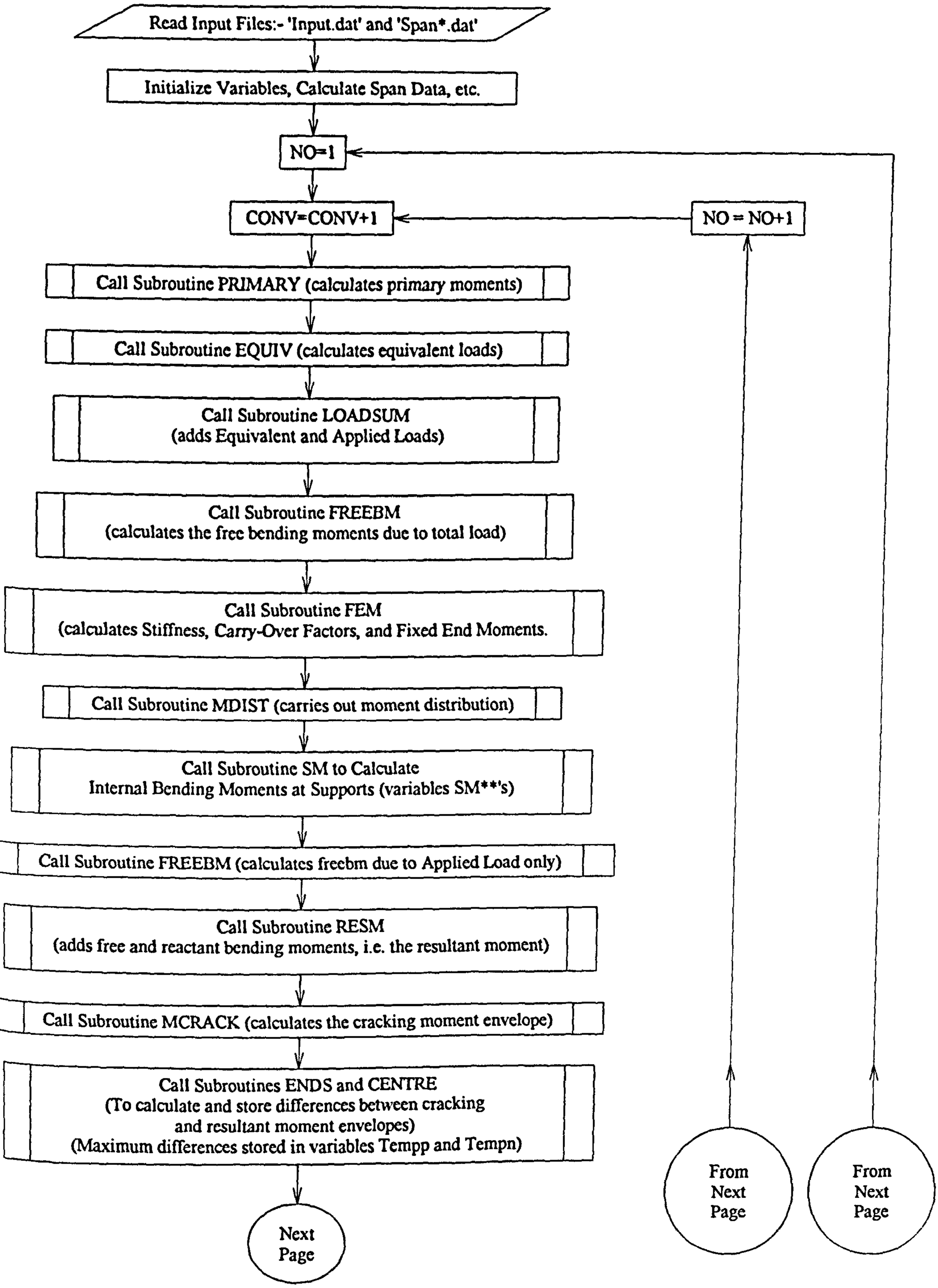

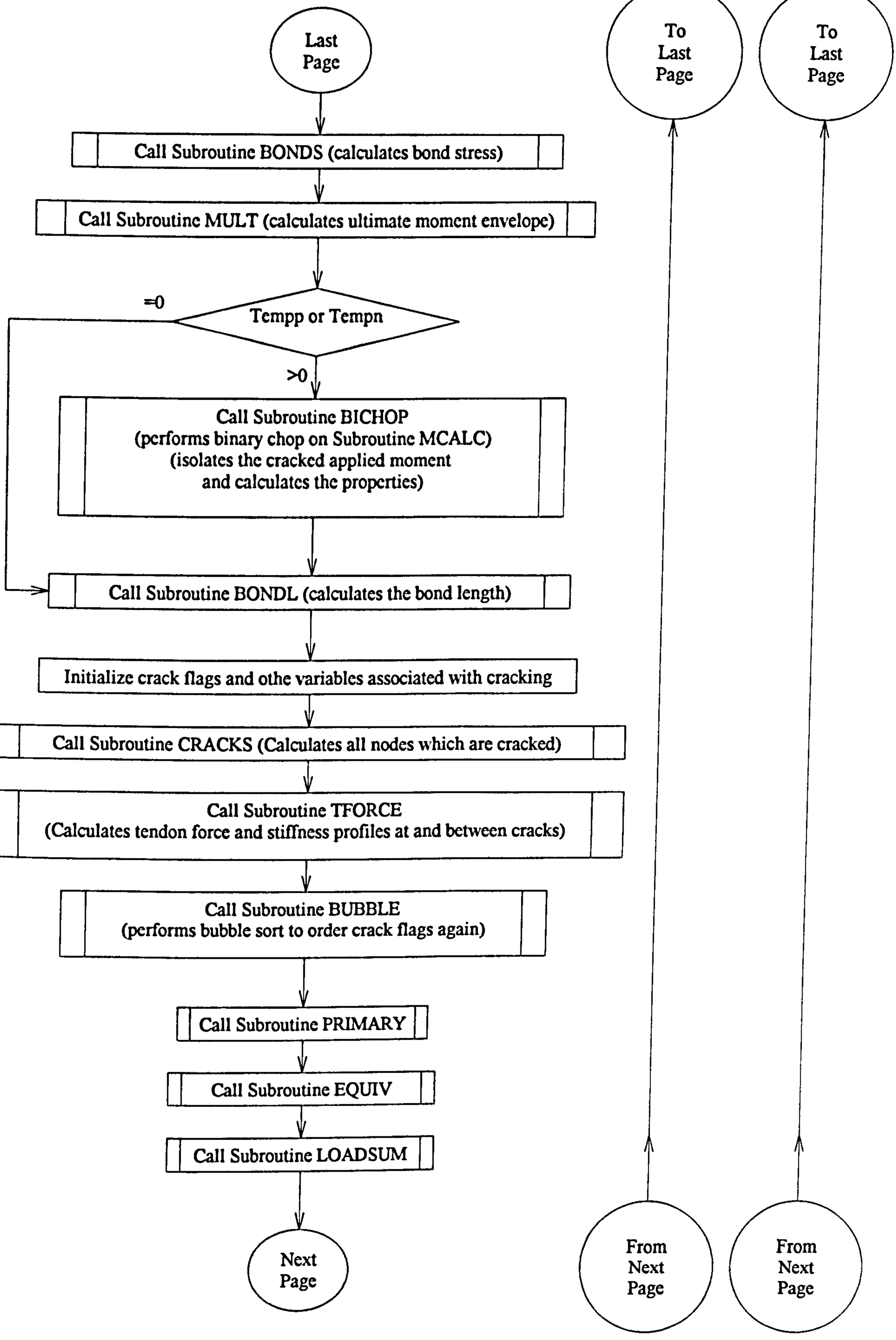
Last Page
Call Subroutine BONDS (calculates bond stress)
Call Subroutine MULT (calculates ultimate moment envelope)
=0
Tempp or Tempn
>0
Call Subroutine BICHOP
(performs binary chop on Subroutine MCALC)
(isolates the cracked applied moment
and calculates the properties)
Call Subroutine BONDL (calculates the bond length)
Initialize crack flags and othe variables associated with cracking
Call Subroutine CRACKS (Calculates all nodes which are cracked)
Call Subroutine TFORCE
(Calculates tendon force and stiffness profiles at and between cracks)
Call Subroutine BUBBLE
(performs bubble sort to order crack flags again)
Call Subroutine PRIMARY
Call Subroutine EQUIV
Call Subroutine LOADSUM
Next Page
To Last Page
To Last Page
From Next Page
From Next Page

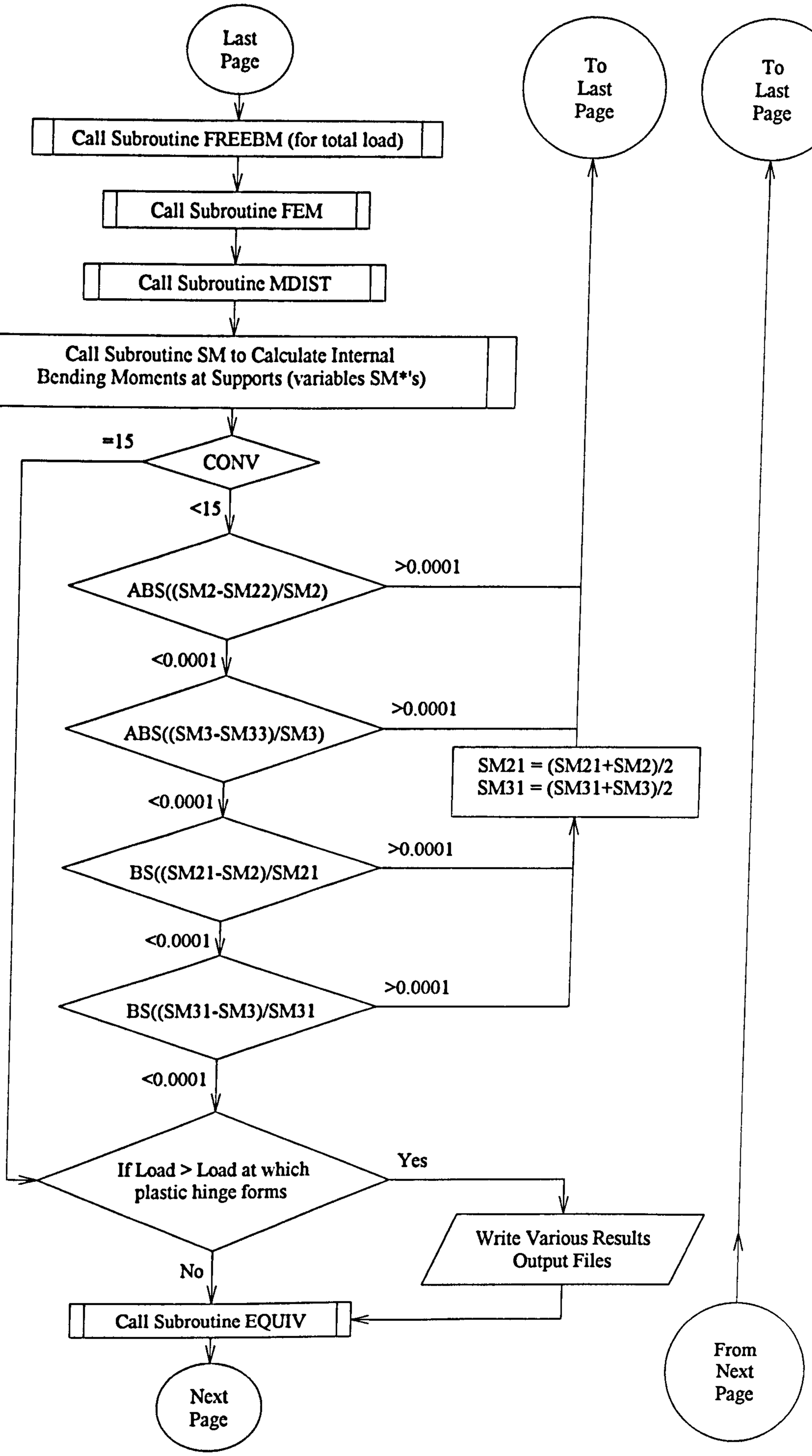
Last Page
Call Subroutine FREEBM (for total load)
Call Subroutine FEM
Call Subroutine MDIST
Call Subroutine SM to Calculate Internal Bending Moments at Supports (variables SM*'s)
=15
CONV
<15
ABS((SM2-SM22)/SM2)
>0.0001
<0.0001
ABS((SM3-SM33)/SM3)
>0.0001
SM21 = (SM21+SM2)/2
SM31 = (SM31+SM3)/2
<0.0001
BS((SM21-SM2)/SM21
>0.0001
<0.0001
BS((SM31-SM3)/SM31
>0.0001
<0.0001
If Load > Load at which plastic hinge forms
Yes
No
Write Various Results Output Files
Call Subroutine EQUIV
Next Page
To Last Page
To Last Page
From Next Page

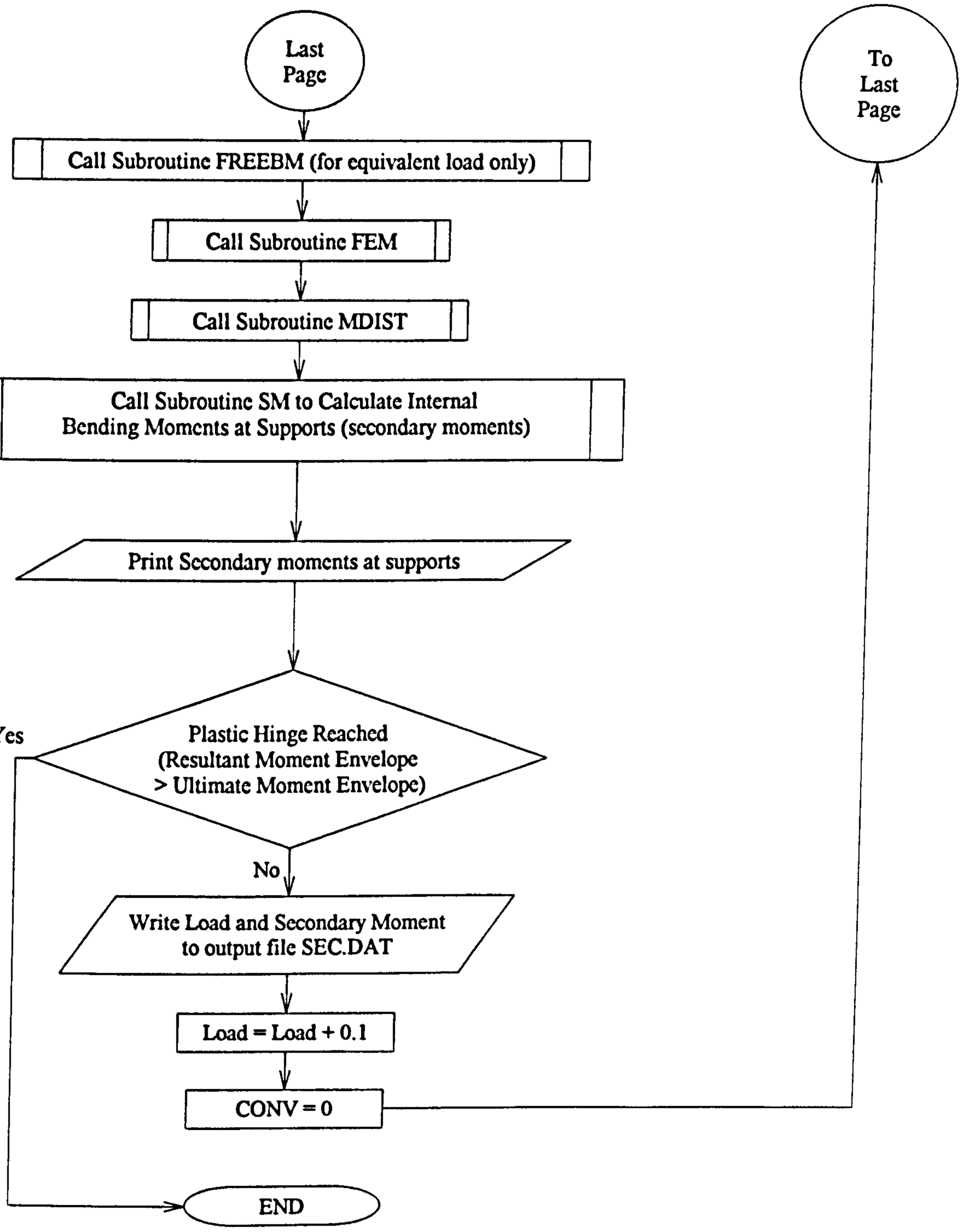
Last Page
Call Subroutine FREEBM (for equivalent load only)
Call Subroutine FEM
Call Subroutine MDIST
Call Subroutine SM to Calculate Internal Bending Moments at Supports (secondary moments)
Print Secondary moments at supports
Yes
Plastic Hinge Reached (Resultant Moment Envelope > Ultimate Moment Envelope)
No
Write Load and Secondary Moment to output file SEC.DAT
Load = Load + 0.1
CONV = 0
END
To Last Page

Flow Chart:- For Subroutine BICHOP

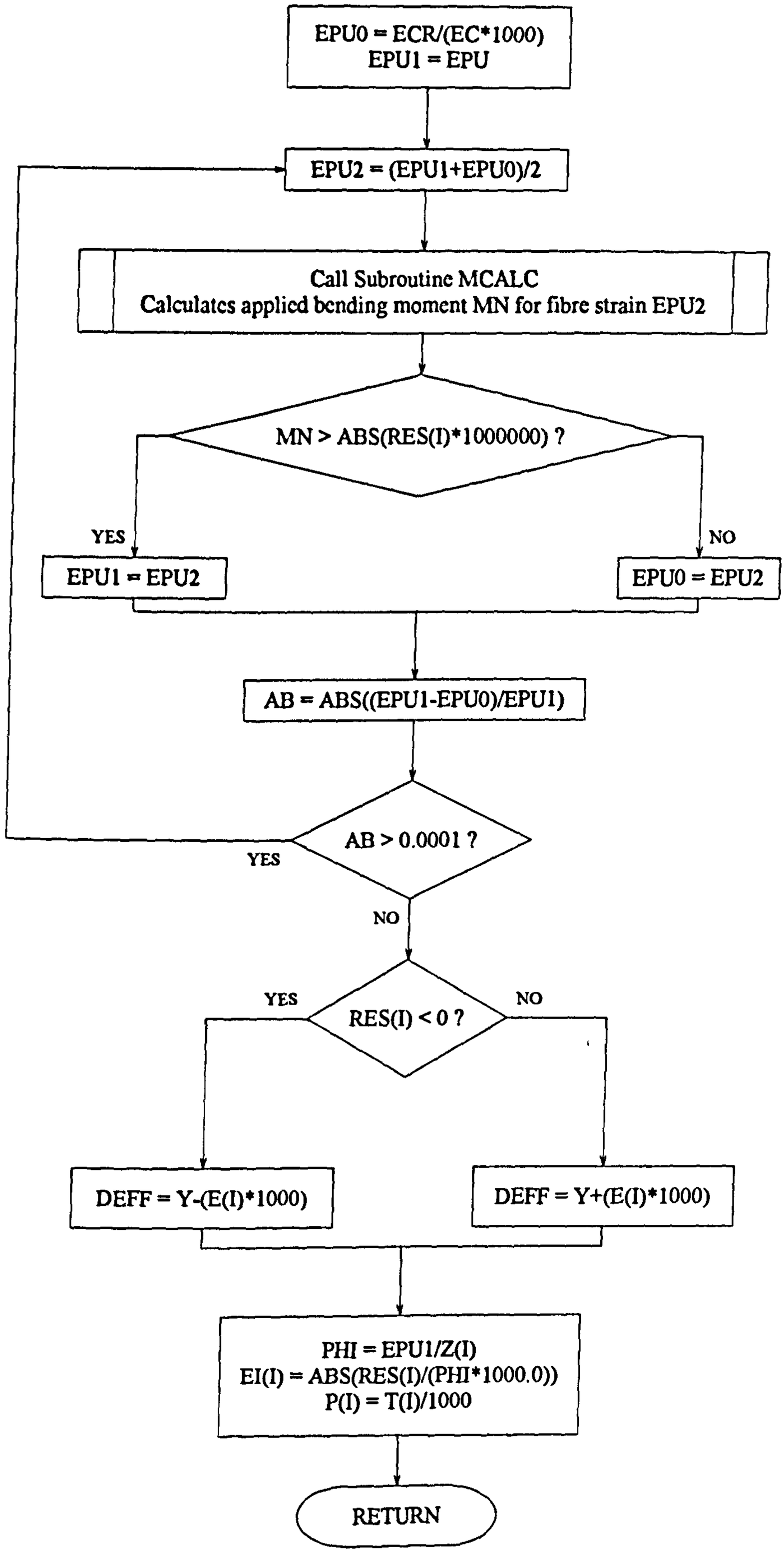

General Flow Chart :- For Subroutine MCALC

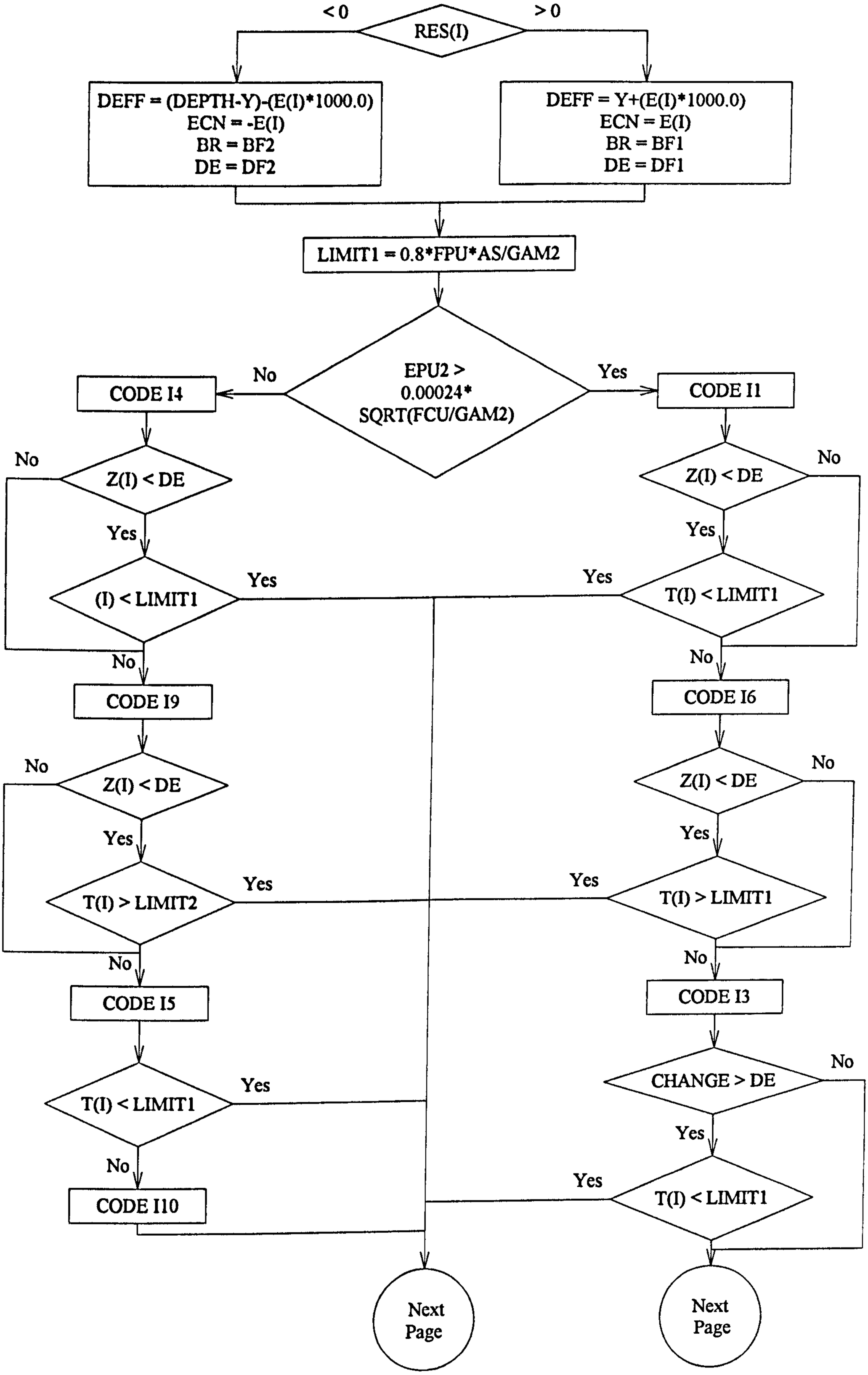

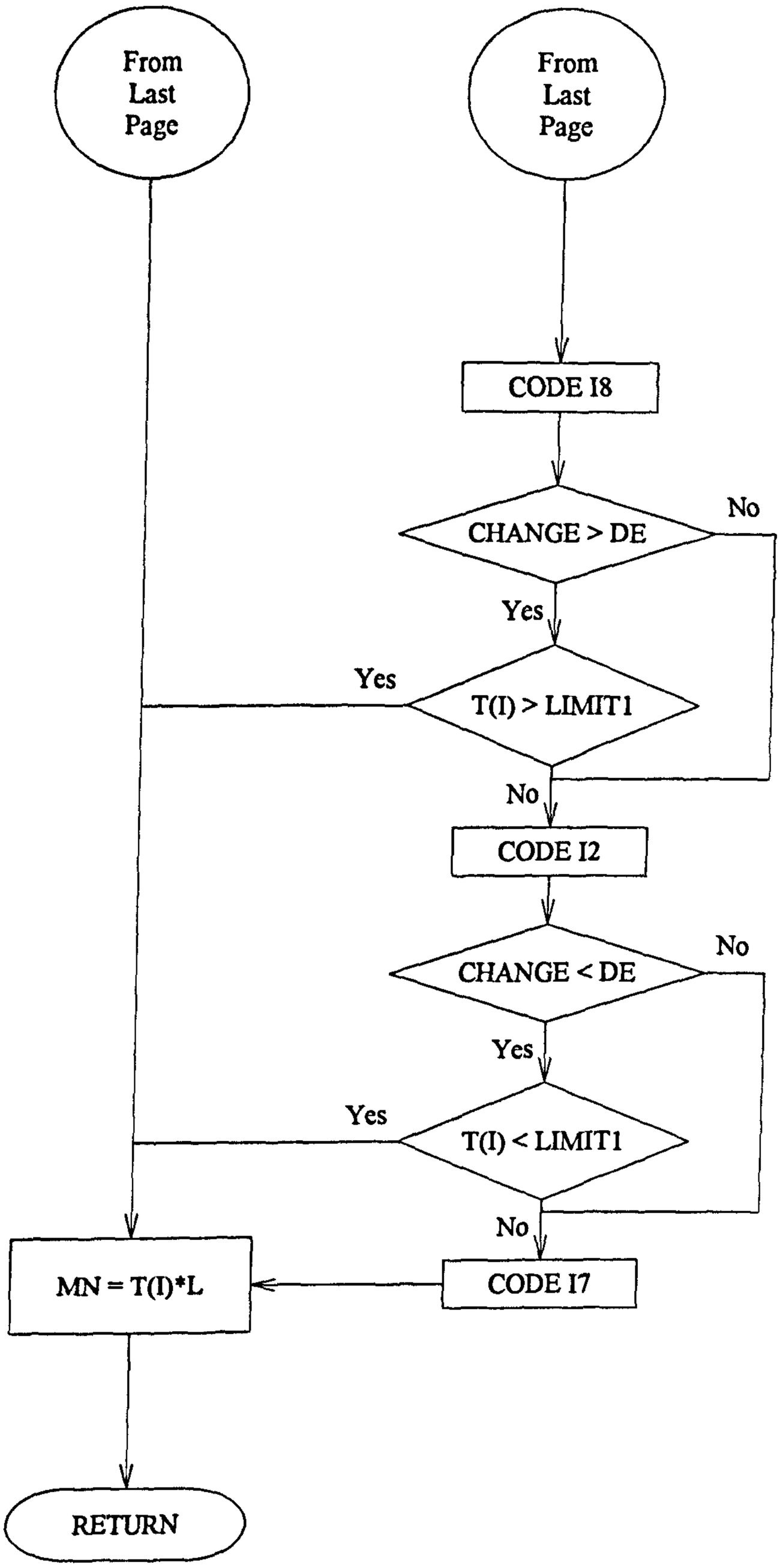
From Last Page
From Last Page
CODE I8
CHANGE > DE
No
Yes
Yes
T(I) > LIMIT1
No
CODE I2
CHANGE < DE
No
Yes
Yes
T(I) < LIMIT1
No
MN = T(I)*L
CODE I7
RETURN

General Flow Chart :- For Subroutine MULT

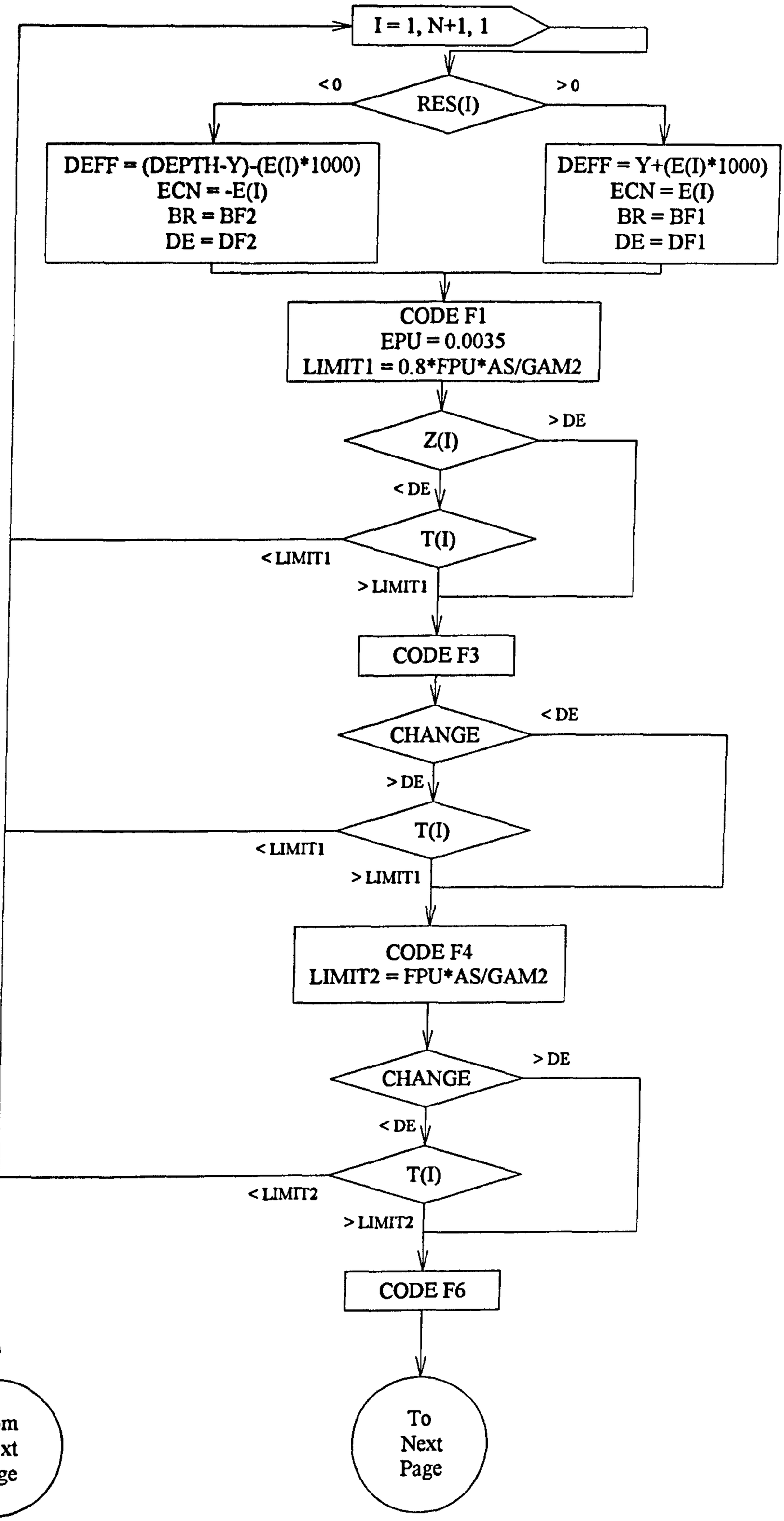

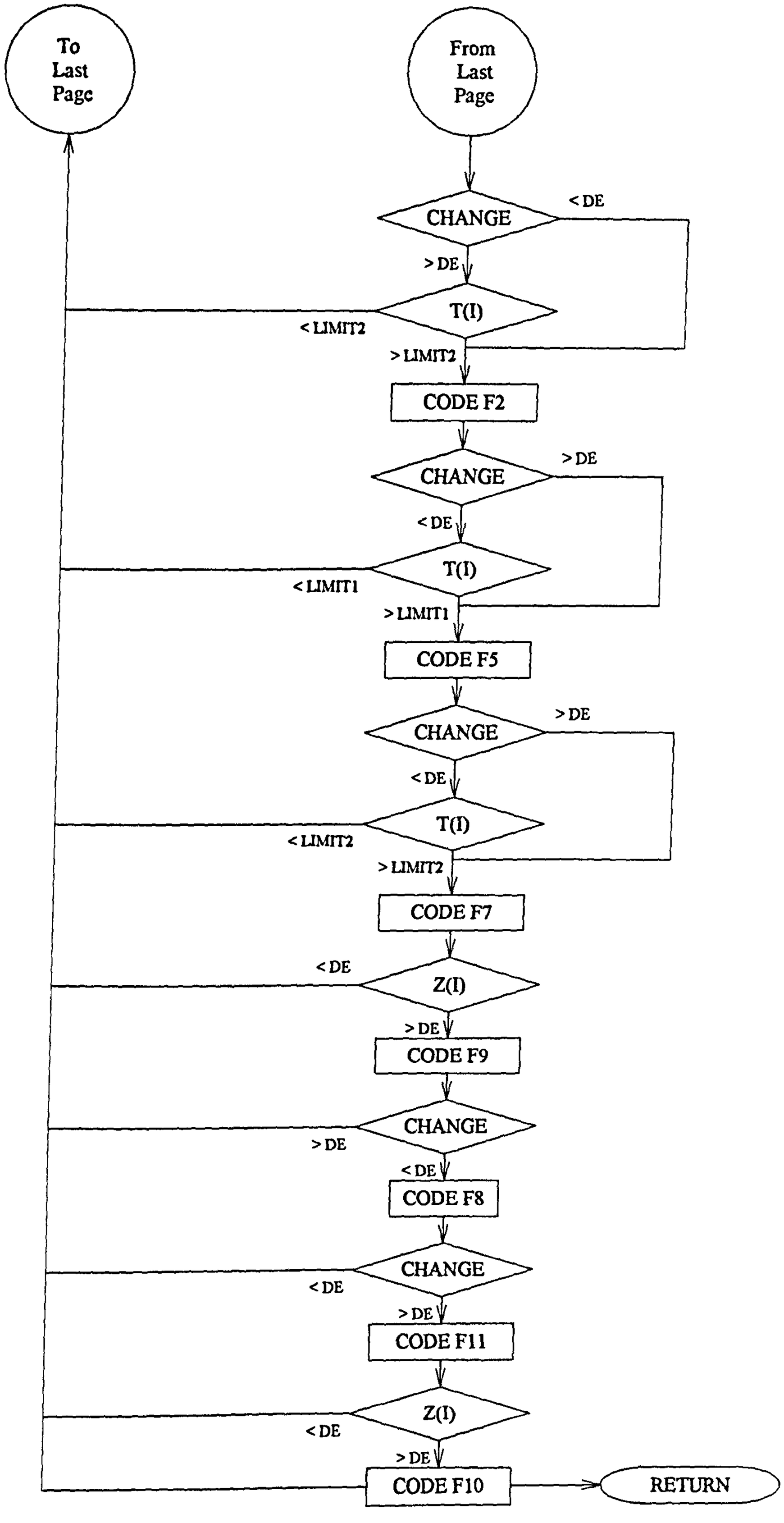
To Last Page
From Last Page
CHANGE
< DE
> DE
T(I)
< LIMIT2
> LIMIT2
CODE F2
CHANGE
> DE
< DE
T(I)
< LIMIT1
> LIMIT1
CODE F5
CHANGE
> DE
< DE
T(I)
< LIMIT2
> LIMIT2
CODE F7
Z(I)
< DE
> DE
CODE F9
CHANGE
> DE
< DE
CODE F8
CHANGE
< DE
> DE
CODE F11
Z(I)
< DE
> DE
CODE F10
RETURN

Flow Chart :-
For Subroutine FREEBM

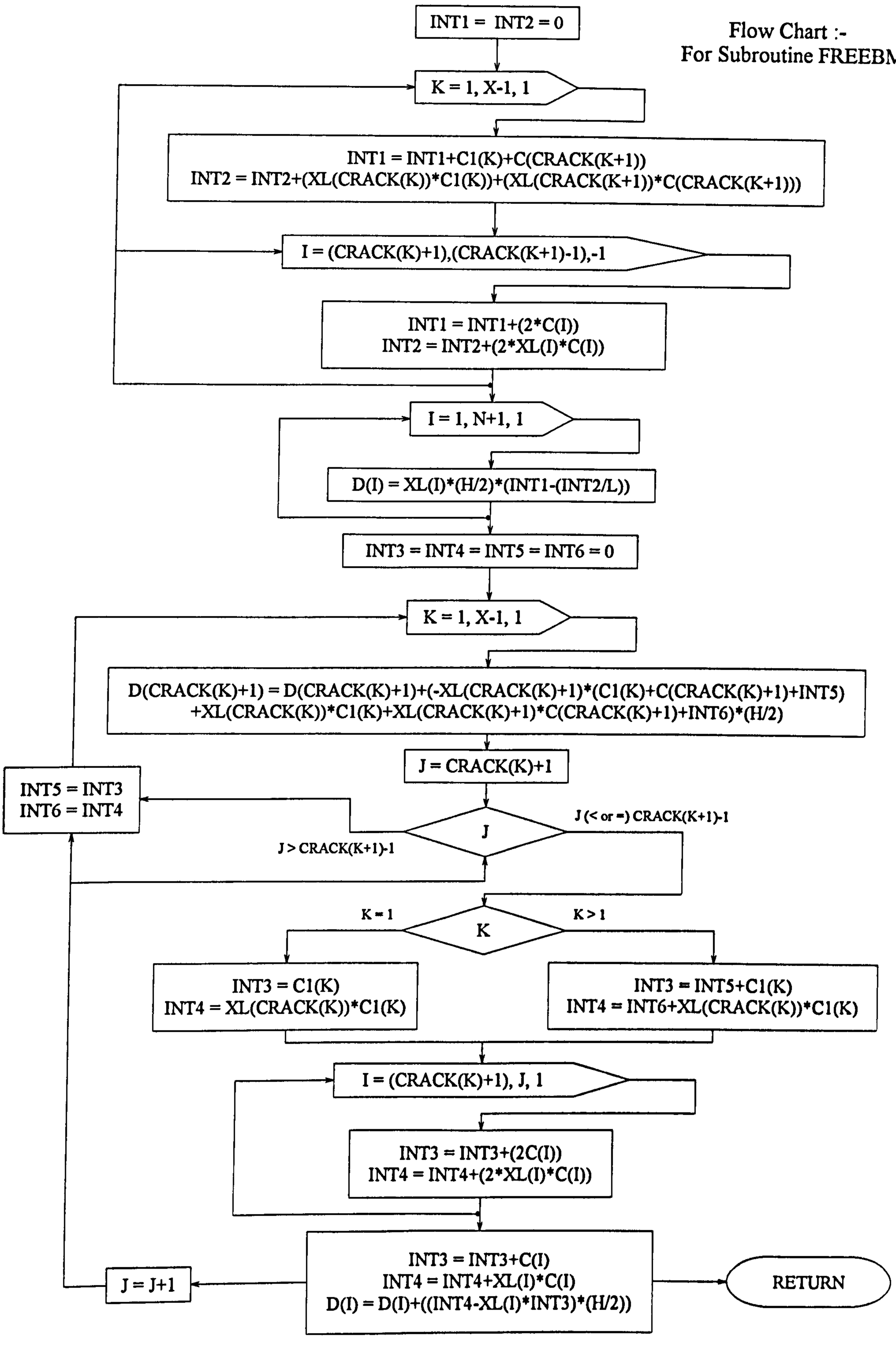

Flow Chart :- For Subroutine FEM

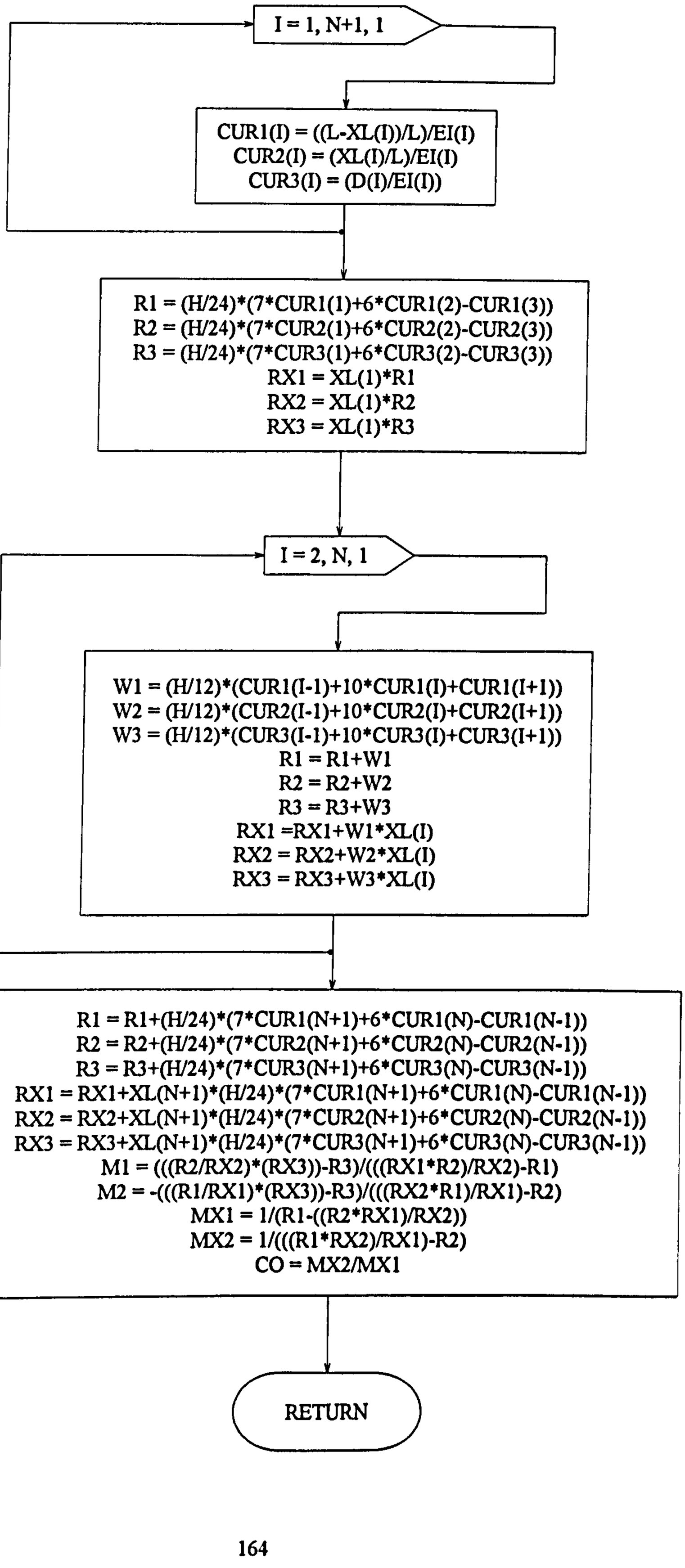

Flow Chart :- For Subroutine EQUIV

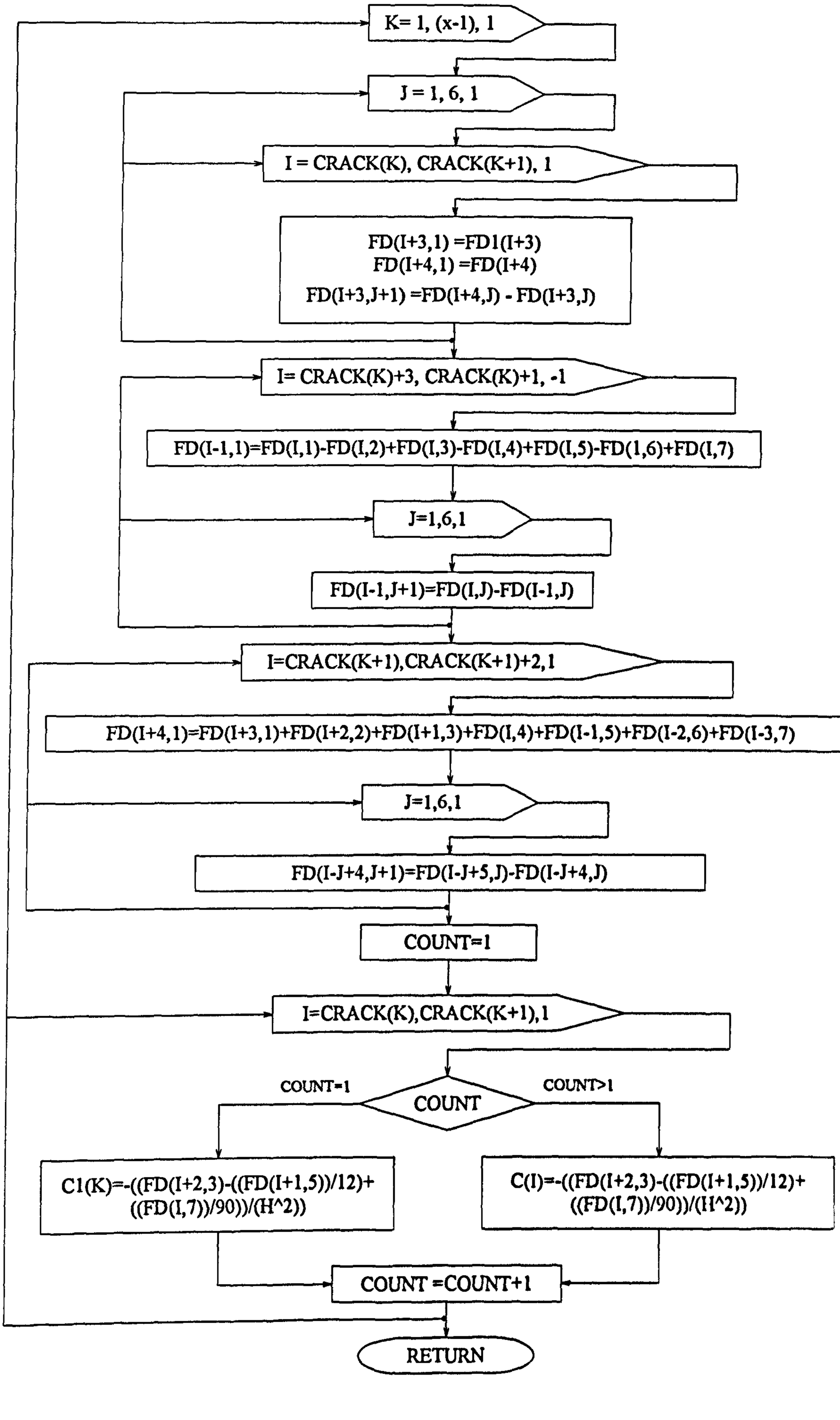

Flow Chart :-
For Subroutine MDIST

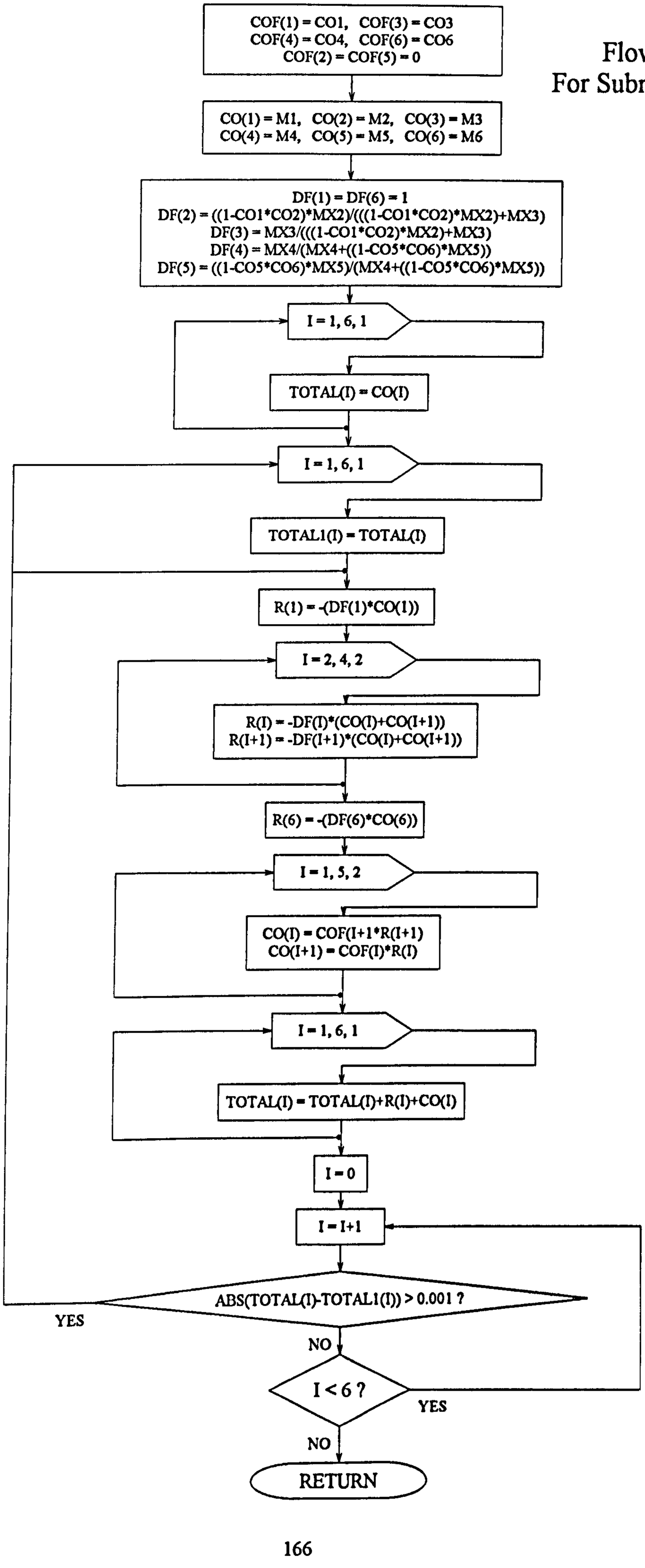

Flow Chart :- For Subroutine TFORCEP

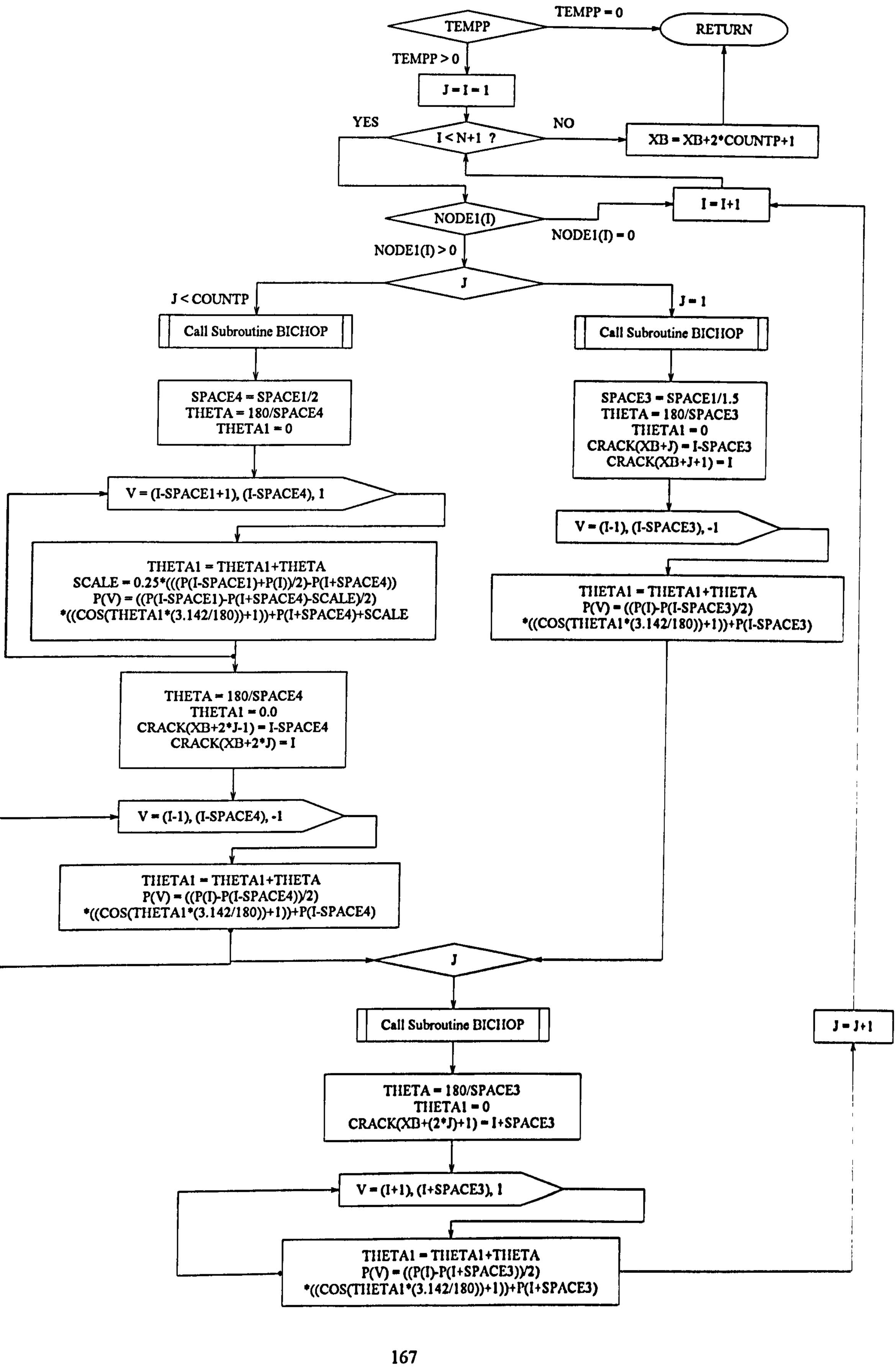

Appendix B

Cracked-Section Analysis of Reinforced and Prestressed Concrete I and T Sections

The SMAREL algorithm requires the program to perform cracked-section analyses of various prestressed and reinforced concrete sections. In Weekes, [48], a procedure has been described for the calculation of cracked-section properties of rectangular P.C. or R.C. sections, with a fully bonded single tendon and no non-prestressed reinforcement, a process which can be time consuming if carried out by hand, and is therefore best solved using a programmable calculator or computer programme.

The analysis is performed by three subroutines, MCRACK, MULT, and MCALC. MCRACK and MULT calculate the applied bending moment at which cracking of the concrete section occurs, and the ultimate moment of resistance of the section respectively. Having ascertained the two 'boundary' bending moments of the cracked stage, together with the corresponding values of strain at the extreme compressed concrete fibre, bending moments between these two boundary values are applied to the section. Subroutine MCALC calculates an applied bending moment for a particular extreme concrete fibre strain, and a binary chop process is used to alter the strain until a moment is obtained that is equal to the applied moment.

The calculations for the cracked section properties of I and T sections follow similar procedures, with a number of refinements.

Modes of Cracked I and T Sections

The material stress-strain relationships for steel and concrete are shown in figures B1a and B1b respectively, extracted from B.S.8110, and are used here for the calculation of the cracked section properties. The steel is represented by a conventional multilinear stress-strain relationship, and the concrete has a parabolic-linear form, representative of concrete compression in flexure.

Failure and Intermediate Modes

Subroutine MULT consists of eleven possible failure conditions, shown in figure B2a, and are listed in Table B1. Assuming that the steel reaches its ultimate stress of f_{pu}/γ_m, and the concrete compressive fibre strain is less than $2.4\times10^{-4}\sqrt{f_{cu}/\gamma_m}$, the profile of the concrete compression zone will be parabolic. The depth of the neutral axis will decide whether the profile resides within the flange only, or in both flange and web. If the concrete

compressive fibre strain is in the range $2.4\times10^{-4}\sqrt{f_{cu}/\gamma_m} < \varepsilon_c < 0.0035$, then the stress profile is of parabolic-linear form. Again, the value of the neutral axis depth will decide the prescence of the profile in the flange only, or in both flange and web. The location of the position where the stress profile changes from parabolic to linear is also of importance, i.e, either in the flange or web. When the concrete compressive fibre strain reaches 0.0035, the concrete is deemed to have crushed. In this instance, the concrete stress profile is of parabolic-linear form, either entirely within the flange, or in both flange and web, with function changeover from parabolic to linear in flange or web. The steel stress in this case is less than the ultimate value, and there are two cases to consider, where the stress is less than $0.8f_{pu}/\gamma_m$, or in the range $0.8f_{pu}/\gamma_m < \sigma_p < f_{pu}/\gamma_m$.

Having ascertained the various failure modes, the intermediate modes which the section may experience as the bending moment increases from the cracking to the ultimate stage must be considered, and these are implemented in subroutine MCALC. With regards to the state of the stress in the steel, the two aforementioned ranges apply. The concrete compressive fibre strain, ε_c, will be less than 0.0035, therefore the profile may be parabolic or parabolic-linear, with five possible profile variations. This gives rise to ten modes in all, as shown in figure B2a, and listed in table B2.

Calculation of the Cracking Moment

To ascertain the bending moment at which the onset of cracking occurs, the tensile strength of the concrete in flexure (modulus of rupture) is calculated as approximately :-

$$f_{tu} = 0.59\sqrt{f_{cu}/\gamma_m} \qquad \text{(b1)}$$

The ultimate tensile stress and the bending moment at which cracking occurs either in rectangular, I, or T sections is given by :-

$$f_{tu} = \frac{P}{A_c} + \frac{Pe}{Z} + \frac{M_{cr}}{Z} \qquad \text{(b2)}$$

This equation can easily be rearanged to give the cracking moment M_{cr} in terms of the concrete tensile strength. The section modulus Z is calculated from I/y for either top or bottom.

Cracked Sections

The dimensions of the I and T sections are shown in figure B3. From the design stress-strain curve for concrete shown in figure B1a, values 'a' and 'b' are assigned such that 'a' represents the ultimate stress, and 'b' represents the strain at which the curve changes from parabolic to linear, i.e.

$$a = 0.67\frac{f_{cu}}{\gamma_m} \quad \text{and} \quad b = 2.4\times10^{-4}\sqrt{\frac{f_{cu}}{\gamma_m}} \tag{b3}$$

1/ Concrete Parabolic, Steel Elastic

Assuming that the concrete section has cracked, and that the extreme concrete fibre strain is less than b, the concrete compressive stress profile will be parabolic, either entirely within the flange, or in both flange and web. In this instance we will consider the stress in the steel when it is less than $0.8 f_{pu}/\gamma_m$.

a/ Concrete profile in flange only .

The equation of the parabola for $0 < \varepsilon_c < 2.4\times10^{-4}\sqrt{f_{cu}/\gamma_m}$ is:

$$\sigma = a - a\left(\frac{\varepsilon - b}{b}\right)^2 \tag{b4}$$

Given the applied moment M, we will also assume that the extreme concrete fibre strain ε_c is also known, and the neutral axis depth x is to be calculated from this. The concrete strain at a distance x_1 from the neutral axis is :

$$\varepsilon = \frac{\varepsilon_c . x_1}{x} \tag{b5}$$

Substitution for ε from equation (b5) into equation (b4), yields an equation for the stress as:

$$\sigma = a - a\left(\frac{\varepsilon_c . x_1}{x_1 . b} - 1\right)^2 \tag{b6}$$

The total compressive force is the the product of the area within the compression profile and the breadth of the flange, Bf_1 :

$$C = Bf_1 \int_0^x \sigma \, dx_1 \tag{b7}$$

Substituting equation (b6) into this integral (b7) and solving, the compressive force in the concrete becomes:

$$C = Bf_1\left(\frac{3ab\varepsilon_c - a\varepsilon_c^2}{3b^2}\right)x \tag{b8}$$

For the tendon steel stress-strain curve shown in figure B1b, the steel is deemed to be in the 'elastic' or first stage when the stress is less than $0.8 f_{pu}/\gamma_m$. In this range, the concrete prestrain is :

$$\frac{1}{E_c}\left(\frac{p.A_{ps}}{A_c} + \frac{p.A_{ps}.e^2}{I}\right) \tag{b9}$$

The concrete strain at the tendon level is equal to :

$$\left(\frac{d\varepsilon_c}{x} - \varepsilon_c\right) \tag{b10}$$

Tendon prestrain is :

$$\frac{p}{E_c} \tag{b11}$$

The addition of equations, (b9), (b10), and (b11), leads to the total force in the steel :

$$T = A_{ps}E_s\left(\frac{pA_{ps}}{E_cA_c} + \frac{pA_{ps}e^2}{IE_c} + \frac{d\varepsilon_c}{x} - \varepsilon_c + \frac{p}{E_s}\right) \tag{b12}$$

Equating the concrete compression (b8), the steel tension (b12), and rearranging gives a quadratic equation in x :

$$Bf_1\left(\frac{3ab\varepsilon_c - a\varepsilon_c^2}{3b^2}\right)x^2 - \left(A_{ps}E_s\left(\frac{pA_{ps}}{E_cA_c} + \frac{pA_{ps}e^2}{IE_c} - \varepsilon_c + \frac{p}{E_c}\right)\right)x - \left(A_{ps}E_s d\varepsilon_c\right) = 0 \tag{b13}$$

This equation can be solved to yield a value x for the neutral axis depth. The internal moment which produces this value of x is calculated as :

$$M = C.z = T.z \tag{b14}$$

where z is the internal lever arm between the centre of compression and tension :

$$z = d - x - \bar{x} \tag{b15}$$

The distance from the neutral axis to the centroid of the parabolic profile is :

$$\bar{x} = \frac{(8b - 3\varepsilon_c)x}{4(3b - \varepsilon_c)} \tag{b16}$$

b/ Concrete profile in web and flange.

The total compressive force in this case is the addition of the areas of the parabolic compression profile within the web and flange, multiplied by the corresponding breadths. The required integrals are :

$$B_w \int_0^{x-df_1} \sigma \, dx_1 + Bf_1 \int_{x-df_1}^{x} \sigma \, dx_1 \tag{b17}$$

Substituting equation (b6) into (b17), and performing the integration gives a compressive force of :

$$C = Bf_1\left(\frac{3ab\varepsilon_c - a\varepsilon_c^2}{3b^2}\right)x + (B_w - Bf_1)\left(\frac{a\varepsilon_c^2(x-df_1)^3 - 3abx\varepsilon_c(x-df_1)^2}{3x^2b^2}\right) \tag{b18}$$

Equating the compressive force C, equation (b18), and the tendon force T in equation (b12), rearrangement gives a cubic equation in x of the form:

$$\left[Bf_1\left(\frac{3ab\varepsilon_c - a\varepsilon_c^2}{3b^2}\right) + (B_w - Bf_1)\left(\frac{a\varepsilon_c^2}{3b^2}\right)\right]x^3$$
$$+\left[A_{ps}E_s\left(\varepsilon_c - \frac{p}{E_c} - \frac{pA_{ps}e^2}{IE_c} - \frac{pA_{ps}}{E_cA_c}\right) + (Bf_1 - B_w)\left(\frac{a\varepsilon_c^2 df_1}{b^2} + \frac{a\varepsilon_c}{b}\right)\right]x^2$$
$$+\left[(B_w - Bf_1)\left(\frac{a\varepsilon_c^2 df_1^2}{b^2} + \frac{a\varepsilon_c df_1}{b}\right) - A_{ps}E_s d\varepsilon_c\right]x$$
$$+\left[(Bf_1 - B_w)\left(\frac{a\varepsilon_c^2 df_1^3}{3b^2}\right)\right] = 0 \tag{b19}$$

Once this cubic has been solved to give the neutral axis depth x, the bending moment is calculated as in equation (b14). The distance from the neutral axis to the centroid of the parabolic profile is :

$$\bar{x} = \frac{(B_w - Bf_1)(8abx\varepsilon_c(x-df_1)^3 - 3a\varepsilon_c(x-df_1)^4) + Bf_1(8ab\varepsilon_c x^4 - 3a\varepsilon_c^2 x^4)}{4(B_w - Bf_1)(a\varepsilon_c^2(x-df_1)^3 - 3abx\varepsilon_c(x-df_1)^2) + Bf_1 x^3(3ab\varepsilon_c - a\varepsilon_c^2)} \qquad \text{(b20)}$$

2/ Concrete Parabolic, Steel Inelastic

The stress in the steel in this case lies in the range $0.8F_{pu}/\gamma_m < \sigma_p < F_{pu}/\gamma_m$

a/ Concrete profile in flange only.

The concrete compressive force C is given by equation (b8). When calculating the tendon force T, the concrete prestrain, concrete strain at the tendon level, and tendon prstrain are given by equations (b9), (b10), (b11) respectively. The slope of the steel stress strain curve in the range $0.8F_{pu}/\gamma_m < \sigma_p < F_{pu}/\gamma_m$ is assigned the value E_{s1}. The tensile force in the tendon becomes :

$$T = A_{ps}E_{s1}\left(\frac{pA_{ps}}{E_cA_c} + \frac{pA_{ps}e^2}{IE_c} + \frac{d\varepsilon_c}{x} - \varepsilon_c + \frac{p}{E_s}\frac{0.8f_{pu}}{E_s\gamma_m}\right) + \frac{0.8f_{pu}A_{ps}}{\gamma_m} \qquad \text{(b21)}$$

Where :

$$E_{s1} = \left(\frac{0.2f_{pu}}{\gamma_m}\right) + \left(\frac{0.2f_{pu}}{\gamma_m E_s} + 0.005\right) \qquad \text{(b22)}$$

Equating the concrete compressive force, equation (b18), and the steel tension equation (b21), gives a quadratic in x of the form :

$$Bf_1\left(\frac{3ab\varepsilon_c - a\varepsilon_c^2}{3b^2}\right)x^2 - \left(A_{ps}E_{s1}\left(\frac{pA_{ps}}{E_cA_c} + \frac{pA_{ps}e^2}{IE_c}\varepsilon_c + \frac{p}{E_c}\frac{0.8f_{pu}}{\gamma_m E_s}\right) + \frac{0.8f_{pu}A_{ps}}{\gamma_m}\right)x - (A_{ps}E_{s1}d\varepsilon_c) = 0 \qquad \text{(b23)}$$

This can be solved to give the neutral axis depth, and the distance from the neutral axis to the centroid of the compression profile, internal lever arm, and bending moment are calculated from (b16), (b15), and (b14) respectively.

b/ Concrete profile in flange and web.

The concrete compressive force C and the steel tensile force T are given by equations (b18) and (b21) respectively . Equating these two, the resultant cubic equation in x is :

$$\left[Bf_1\left(\frac{3ab\varepsilon_c-a\varepsilon_c^2}{3b^2}\right)+(B_w-Bf_1)\left(\frac{a\varepsilon_c^2}{3b^2}\right)\right]x^3$$
$$+\left[A_{ps}E_{s1}\left(\varepsilon_c-\frac{p}{E_c}-\frac{pA_{ps}e^2}{IE_c}-\frac{pA_{ps}}{E_cA_c}+\frac{0.8f_{pu}}{\gamma_mE_s}\right)-\frac{0.8f_{pu}A_{ps}}{\gamma_m}+(Bf_1-B_w)\left(\frac{a\varepsilon_c^2df_1}{b^2}+\frac{a\varepsilon_c}{b}\right)\right]x^2$$
$$+\left[(B_w-Bf_1)\left(\frac{a\varepsilon_c^2df_1^2}{b^2}+\frac{a\varepsilon_cdf_1}{b}\right)-A_{ps}E_{s1}d\varepsilon_c\right]x$$
$$+\left[(Bf_1-B_w)\left(\frac{a\varepsilon_c^2df_1^3}{3b^2}\right)\right]=0 \qquad \text{(b24)}$$

Once the neutral axis depth is obtained, the distance from the neutral axis to the centroid of the compression profile, internal lever arm, and bending moment are given by equations (b20), (b15), and (b14) respectively.

3/ Concrete Parabolic, Steel Broken

a/ Concrete profile in flange only.

The steel tensile force T in this case is $f_{pu}A_{ps}/\gamma_m$, (at this value the steel is deemed to have failed). The concrete compressive force C given by equation (b8) is set equal to the ultimate tensile force T, and the resulting equation rearranged to make x the subject in terms of the concrete fibre strain ε_c. The steel tensile force given by equation (b21) is set to the ultimate value, and a straight substitution for x performed. A cubic equation in terms of ε_c can then be solved :

$$(adBf_1)\varepsilon_c^3-(3abdBf_1)\varepsilon_c^2+\left(\frac{3f_{pu}A_{ps}b^2}{\gamma_m}\right)\varepsilon_c+\left(\frac{3f_{pu}A_{ps}b^2F_1}{\gamma_m}\right)=0 \qquad \text{(b25)}$$

Where :

$$F_1=\left(\frac{0.2f_{pu}}{\gamma_mE_{s1}}-\frac{pA_{ps}}{E_cA_c}-\frac{pA_{ps}e^2}{IE_c}-\frac{p}{E_s}+\frac{0.8f_{pu}}{\gamma_mE_s}\right) \qquad \text{(b26)}$$

The neutral axis is :

$$x = \frac{d\varepsilon_c}{(F_1 + \varepsilon_c)} \tag{b27}$$

The distance from the neutral axis to the centroid of the compression profile, internal lever arm, and bending moment are given by equations (b16), (b15), and (b14) respectively.

b/ Concrete profile in flange and web.

The concrete compressive force C given in equation (b18) is set equal to the ultimate tensile force T. The substitution of equation (b21) for either x or ε_c will result in a cubic in either x or ε_c . In this case, the cubic in x has the form :

$$\begin{aligned}
&\left[(B_w - Bf_1)(aF_1^2) - Bf_1(3abF_1 + aF_1^2)\right]x^3 \\
&+\left[(3abF_1 dBf_1) + (B_w - Bf_1)(3abF_1 - 3aF_1^2 d)\right]x^2 \\
&+\left[(B_w - Bf_1)(3aF_1)(F_1 df_1^2 - bd - bdf_1) + 6Tdb^2\right]x \\
&+\left[(B_w - Bf_1)(3abdf_1 F_1 d - aF_1^2 df_1^3) + (3Tb^2 d^2)\right] = 0
\end{aligned} \tag{b28}$$

The distance from the neutral axis to the centroid of the compression profile, internal lever arm, and bending moment are given by equations (b20), (b15), and (b14) respectively.

4/ Concrete Parabolic-Linear, Steel Elastic

a/ Concrete profile in flange only.

The equation for the parabolic portion of the stress profile in the range$0 < \varepsilon_c < 2.4\times10^{-4}\sqrt{f_{cu}/\gamma_m}$ is given by equation (b4). For the linear portion in the range$2.4\times10^{-4}\sqrt{f_{cu}/\gamma_m} < \varepsilon_c < 0.0035$, then $\sigma = a$. The area under the parabolic portion of the compression profile is :

$$\int_0^{\frac{bx}{\alpha}} \sigma \, dx_1 = \int_0^{\frac{bx}{\alpha}} \frac{2ax_1\varepsilon_c}{xb} - \frac{ax_1^2\varepsilon_c^2}{b^2x^2} \, dx_1 \tag{b29}$$

This integral is solved as :

$$\frac{2abx}{3\varepsilon_c} \tag{b30}$$

The area under the linear portion of the profile is :

$$ax\left(1-\frac{b}{\varepsilon_c}\right) \qquad \text{(b31)}$$

Therefore the total area is the addition of expressions (b30), and (b31), and the compressive force in the concrete becomes :

$$C = ax\left(1-\frac{b}{3\varepsilon_c}\right)Bf_1 \qquad \text{(b32)}$$

The tensile force in the steel is given by equation (b12), and equating with equation (b32), gives a quadratic equation of the form:

$$Bf_1\left(a\left(1-\frac{b}{3\varepsilon_c}\right)\right)x^2-\left(A_{ps}E_s\left(\frac{pA_{ps}}{E_cA_c}+\frac{pA_{ps}e^2}{IE_c}-\varepsilon_c+\frac{p}{E_c}\right)\right)x-\left(A_{ps}E_sd\varepsilon_c\right)=0 \qquad \text{(b33)}$$

The distance from the neutral axis to centroid of the compression profile is:

$$\bar{x}=\frac{\frac{5b^2x}{12\varepsilon_c^2}+\frac{x}{2}\left(1-\frac{b^2}{\varepsilon_c^2}\right)}{\left(1-\frac{b}{3\varepsilon_c}\right)} \qquad \text{(b34)}$$

The internal lever-arm, and internal bending moment are given by equations (b15), and (b14) respectively.

b/ Concrete profile in flange and web, function change in web.

The area under the parabolic portion of the compression profile is given by equation (b4), and the contribution to the compressive force is :

$$B_w\left(\frac{2abx}{3\varepsilon_c}\right) \qquad \text{(b35)}$$

For the linear portion of the profile, the contribution to the compressive force is :

$$B_w\int_{\frac{bx}{a}}^{x-df_1} a\,dx_1 \;+Bf_1\int_{x-df_1}^{x} a\,dx_1 \qquad \text{(b36)}$$

Solving this integral and adding the result to the parabolic portion, equation (b35), gives the total compression as :

$$C = B_w\left(\mathrm{a}x - \mathrm{a}df_1 - \frac{\mathrm{a}bx}{3\varepsilon_c}\right) + Bf_1(\mathrm{a}df_1) \qquad \text{(b37)}$$

The tension in the steel is given by equation (b12), and equating compression and tension gives a quadratic in x as :

$$B_w\left(\mathrm{a} - \frac{\mathrm{a}b}{3\varepsilon_c}\right)x^2 + \left\{(Bf_1 - B_w)(\mathrm{a}df_1) + (A_{ps}E_s)\left(\varepsilon_c - \frac{pA_{ps}}{E_cA_c} - \frac{pA_{ps}e^2}{IE_c} - \frac{p}{E_s}\right)\right\}x - A_{ps}E_sd\varepsilon_c = 0$$

(b38)

The distance from the neutral axis to the centroid of the compression profile is calculated as :

$$\bar{x} = \frac{B_w\left(\frac{\mathrm{a}(x-df_1)^2}{2} - \frac{\mathrm{a}b^2x^2}{12\varepsilon_c^2}\right) + Bf_1\left(\frac{\mathrm{a}x^2}{2} - \frac{\mathrm{a}(x-df_1)^2}{2}\right)}{B_w\left(\mathrm{a}x - \mathrm{a}df_1 - \frac{\mathrm{a}bx}{3}\right)} \qquad \text{(b39)}$$

The lever arm and internal bending moment are calculated as in equations (b15), and (b14).

c/ Concrete profile in flange and web, function change in flange.

The contribution to the total compression by the parabolic portion of the profile is:

$$B_w\int_0^{x-df_1}\sigma\,dx_1 + Bf_1\int_{x-df_1}^{\frac{bx}{a}}\sigma\,dx_1 \qquad \text{(b40)}$$

Where σ is given by equation (b4). The contribution from the linear portion of the compression profile is :

$$Bf_1\int_{\frac{bx}{a}}^{x}\mathrm{a}\,dx_1 \qquad \text{(b41)}$$

Adding integrals (b40), and (b41), and solving gives the total compressive force :

$$C = (B_w - Bf_1)\left\{\frac{a(x-df_1)^2\varepsilon_c}{xb} - \frac{a(x-df_1)^3\varepsilon_c{}^2}{3b^2x^2}\right\} + Bf_1\left(ax - \frac{abx}{3\varepsilon_c}\right) \qquad \text{(b42)}$$

Equating the compression and tension given by equations (b42), and (b12) gives a cubic equation in x :

$$\left\{Bf_1\left(\frac{2ab}{3\varepsilon_c} + a\left(1-\frac{b}{\varepsilon_c}\right)\right) + (B_w - Bf_1)\left(\frac{a\varepsilon_c}{b} - \frac{a\varepsilon_c{}^2}{3b^2}\right)\right\}x^3$$
$$+\left\{(B_w - Bf_1)\left(\frac{a\varepsilon_c{}^2 df_1}{b^2} - \frac{2a\varepsilon_c df_1}{b}\right) - A_{ps}E_s\left(\frac{pA_{ps}}{E_cA_c} + \frac{pA_{ps}e^2}{IE_c} - \varepsilon_c + \frac{p}{E_s}\right)\right\}x^2$$
$$+\left\{(B_w - Bf_1)\left(\frac{a\varepsilon_c df_1{}^2}{b} - \frac{a\varepsilon_c{}^2 df_1{}^2}{b^2}\right) - A_{ps}E_s d\varepsilon_c\right\}x \qquad \text{(b43)}$$
$$+\left\{(Bf_1 - B_w)\left(\frac{adf_1{}^3\varepsilon_c{}^2}{3b^2}\right)\right\} = 0$$

The distance from the neutral axis to the centroid of the compression profile is calculated as :

$$\bar{x} = \frac{(B_w - Bf_1)\left(\frac{2a\varepsilon_c(x-df_1)^3}{3bx} - \frac{a\varepsilon_c{}^2(x-df_1)^4}{4b^2x^2}\right) + Bf_1\left(\frac{ax^2}{2} - \frac{ab^2x^2}{12\varepsilon_c{}^2}\right)}{(B_w - Bf_1)\left(\frac{a\varepsilon_c(x-df_1)^2}{bx} - \frac{a\varepsilon_c{}^2(x-df_1)^3}{3b^2x^2}\right) + Bf_1\left(\frac{2abx}{3\varepsilon_c} + ax\left(1-\frac{b}{\varepsilon_c}\right)\right)} \qquad \text{(b44)}$$

The lever arm and internal bending moment are calculated as in equations (b15), and (b14) respectively.

5/ Concrete Parabolic-Linear , Steel Inelastic

a/ Concrete profile in flange only.

The compressive force in the concrete is given by equation (b32), and is equated to the steel tension in equation (b21). The resulting quadratic equation in x is :

$$Bf_1\left(a - \frac{ab}{3\varepsilon_c}\right)x^2 - \left(A_{ps}E_{s1}\left(\frac{pA_{ps}}{E_cA_c} + \frac{pA_{ps}e^2}{IE_c} - \varepsilon_c + \frac{p}{E_c} - \frac{0.8f_{pu}}{\gamma_m E_s}\right) + \frac{0.8f_{pu}A_{ps}}{\gamma_m}\right)x - d\varepsilon_c A_{ps}E_{s1} = 0 \qquad \text{(b45)}$$

The distance from the neutral axis to the centroid of the compression profile, the lever arm, and the internal bending moment are given by equations (b34), (b15), and (b14) respectively.

b/ Concrete profile in flange and web, function change in web.

The compressive force in the concrete is given by equation (b37), and is equated to the steel tension in equation (b21). The resulting quadratic equation in x is :

$$B_w\left(a-\frac{ab}{3\varepsilon_c}\right)x^2+\left\{(Bf_1-B_w)(adf_1)-\frac{0.8f_{pu}A_{ps}}{\gamma_m}+(A_{ps}E_{s1})\left(\varepsilon_c-\frac{pA_{ps}}{E_cA_c}-\frac{pA_{ps}e^2}{IE_c}-\frac{p}{E_s}-\frac{0.8f_{pu}}{\gamma_mE_s}\right)\right\}x-A_{ps}E_{s1}d\varepsilon_c=0 \qquad \text{(b46)}$$

The distance from the neutral axis to the centroid of the compression profile, the lever arm, and the internal bending moment are given by equations (b39), (b15), and (b14) respectively.

c/ Concrete profile in flange and web, function change in flange.

The compressive force in the concrete is given by equation (b42), and is equated to the steel tension in equation (b21). The resulting cubic equation in x is :

$$\left\{Bf_1\left(\frac{2ab}{3\varepsilon_c}+a\left(1-\frac{b}{\varepsilon_c}\right)\right)+(B_w-Bf_1)\left(\frac{a\varepsilon_c}{b}-\frac{a\varepsilon_c^2}{3b^2}\right)\right\}x^3$$

$$+\left\{(B_w-Bf_1)\left(\frac{a\varepsilon_c^2df_1}{b^2}-\frac{2a\varepsilon_cdf_1}{b}\right)-A_{ps}E_{s1}\left(\frac{pA_{ps}}{E_cA_c}+\frac{pA_{ps}e^2}{IE_c}-\varepsilon_c+\frac{p}{E_s}-\frac{0.8f_{pu}}{\gamma_mE_s}\right)-\frac{0.8f_{pu}A_{ps}}{\gamma_m}\right\}x^2$$

$$+\left\{(B_w-Bf_1)\left(\frac{a\varepsilon_cdf_1^2}{b}-\frac{a\varepsilon_c^2df_1^2}{b^2}\right)-A_{ps}E_{s1}d\varepsilon_c\right\}x$$

$$+\left\{(Bf_1-B_w)\left(\frac{adf_1^3\varepsilon_c^2}{3b^2}\right)\right\}=0 \qquad \text{(b47)}$$

The distance from the neutral axis to the centroid of the compression profile, the lever arm, and the internal bending moment are given by equations (b44), (b15), and (b14) respectively.

6/ Concrete Parabolic-Linear, Steel Broken

a/ Concrete profile in flange only.

The steel tensile force in this case is $T=f_{pu}A_{ps}/\gamma_m$, and this is equated to the concrete compressive force given in equation (b32). Following a similar procedure as in section 3a/, the value of ε_c is calculated as :

$$\varepsilon_c = \frac{bd\gamma_m + 3f_{pu}A_{ps}F_1}{3aBf_1 d\gamma_m - 3f_{pu}A_{ps}} \qquad \text{(b48)}$$

The neutral axis depth, the distance from the neutral axis to the centroid of the compression profile, internal lever arm, and bending moment are given by equations (b45), (b34), (b15), and (b14) respectively.

b/ Concrete profile in web and flange, function change in web.

The concrete compressive force C given by equation (b37), is set equal to the ultimate tensile force $T=f_{pu}A_{ps}/\gamma_m$. Substitution for ε_c from equation (b27) is performed, and the neutral axis depth becomes:

$$x = \frac{T - Bf_1 adf_1 + B_w\left(\frac{abd}{3F_1} + adf_1\right)}{B_w\left(a + \frac{ab}{3F_1}\right)} \qquad \text{(b49)}$$

The extreme compressive fibre strain, distance from the neutral axis to the centroid of the compression profile, lever arm, and internal bending moment are given by equations (b46), (b39), (b15), and (b14), respectively.

c/ Concrete profile in web and flange, function change in flange.

The concrete compressive force C given by equation (b42), is set equal to the ultimate tensile force $T=f_{pu}A_{ps}/\gamma_m$. Substitution for ε_c from equation (b27) is performed, and a cubic equation for the neutral axis depth is obtained :

$$\left\{(Bf_1 - B_w)\left(3abF_1 + aF_1^2\right) + Bf_1\left(\frac{ab^3}{F_1} + 3ab^2\right)\right\}x^3$$
$$+\left\{(B_w - Bf_1)\left(3abF_1 d + 6abF_1 df_1 + 3adf_1 F_1^2\right) - Bf_1\left(\frac{3ab^3 d}{F_1} + 6ab^2 d\right) - 3b^2 T\right\}x^2$$
$$+\left\{(Bf_1 - B_w)\left(6abdf_1 F_1 d + 3abF_1 df_1^2 + 3aF_1^2 df_1^2\right) + Bf_1\left(3ab^2 d^2 + \frac{3ab^3 d^2}{F_1}\right) + 6Tb^2 d\right\}x$$
$$+\left\{(B_w - Bf_1)\left(3abdf_1^2 F_1 d + aF_1^2 df_1^3\right) - \frac{Bf_1 ab^3 d^3}{F_1} - 3Tb^2 d^2\right\} = 0 \qquad \text{(b50)}$$

The extreme compressive fibre strain, distance from the neutral axis to the centroid of the compression profile, lever arm, and internal bending moment are given by equations (b27), (b44), (b15), and (b14), respectively.

7/ Concrete Extreme Compressive Fibre reaches Ultimate Strain

a/ Steel elastic.

All of the equations in section 4 apply, with the concrete fibre strain ε_c set to 0.0035.

b/ Steel inelastic.

All of the equations in section 5 apply, with the concrete fibre strain ε_c set to 0.0035.

Table B1 : Failure Modes of Prestressed Concrete I and T Sections

State of Concrete Stress	State of Steel Stress	Failure Code
$\varepsilon_c = 0.0035$ Parabolic-Linear, all within flange.	$T < 0.8 f_{pu}/\gamma_m$	Code F1
$\varepsilon_c = 0.0035$ Parabolic-Linear, within web and flange, function changeover in flange.	$T < 0.8 f_{pu}/\gamma_m$	Code F2
$\varepsilon_c = 0.0035$ Parabolic-Linear, within web and flange, function changeover in web.	$T < 0.8 f_{pu}/\gamma_m$	Code F3
$\varepsilon_c = 0.0035$ Parabolic-Linear, all within flange.	$0.8 f_{pu}/\gamma_m < T < f_{pu}/\gamma_m$	Code F4
$\varepsilon_c = 0.0035$ Parabolic-Linear, within web and flange, function changeover in flange.	$0.8 f_{pu}/\gamma_m < T < f_{pu}/\gamma_m$	Code F5
$\varepsilon_c = 0.0035$ Parabolic-Linear, within web and flange, function changeover in web.	$0.8 f_{pu}/\gamma_m < T < f_{pu}/\gamma_m$	Code F6
$2.4 \times 10^{-4} < \varepsilon_c < 0.0035$ Parabolic-Linear, all within flange.	$T = f_{pu}/\gamma_m$	Code F7
$2.4 \times 10^{-4} < \varepsilon_c < 0.0035$ Parabolic-Linear within web and flange, function changeover in flange.	$T = f_{pu}/\gamma_m$	Code F8
$2.4 \times 10^{-4} < \varepsilon_c < 0.0035$ Parabolic-Linear within web and flange, function changeover in web.	$T = f_{pu}/\gamma_m$	Code F9
$\varepsilon_c < 2.4 \times 10^{-4}$ Parabolic within flange only.	$T = f_{pu}/\gamma_m$	Code F10
$\varepsilon_c < 2.4 \times 10^{-4}$ Parabolic within flange and web.	$T = f_{pu}/\gamma_m$	Code F11

Table B2 : Intermediate Cracked Modes of Prestressed Concrete I and T Sections

State of Concrete Stress	State of Steel Stress	Cracked Section Code
$2.4\times10^{-4}<\varepsilon_c<0.0035$ Parabolic-Linear, all within flange	$T<0.8f_{pu}/\gamma_m$	Code I1
$2.4\times10^{-4}<\varepsilon_c<0.0035$ Parabolic-Linear within web and flange, function changeover in flange	$T<0.8f_{pu}/\gamma_m$	Code I2
$2.4\times10^{-4}<\varepsilon_c<0.0035$ Parabolic-Linear within web and flange, function changeover in web	$T<0.8f_{pu}/\gamma_m$	Code I3
$\varepsilon_c<2.4\times10^{-4}$ Parabolic within flange only	$T<0.8f_{pu}/\gamma_m$	Code I4
$\varepsilon_c<2.4\times10^{-4}$ Parabolic within flange and web	$T<0.8f_{pu}/\gamma_m$	Code I5
$2.4\times10^{-4}<\varepsilon_c<0.0035$ Parabolic-Linear, all within flange	$0.8f_{pu}/\gamma_m<T<f_{pu}/\gamma_m$	Code I6
$2.4\times10^{-4}<\varepsilon_c<0.0035$ Parabolic-Linear within web and flange, function changeover in flange	$0.8f_{pu}/\gamma_m<T<f_{pu}/\gamma_m$	Code I7
$2.4\times10^{-4}<\varepsilon_c<0.0035$ Parabolic-Linear within web and flange, function changeover in web	$0.8f_{pu}/\gamma_m<T<f_{pu}/\gamma_m$	Code I8
$\varepsilon_c<2.4\times10^{-4}$ Parabolic within flange only	$0.8f_{pu}/\gamma_m<T<f_{pu}/\gamma_m$	Code I9
$\varepsilon_c<2.4\times10^{-4}$ Parabolic within flange and web	$0.8f_{pu}/\gamma_m<T<f_{pu}/\gamma_m$	Code I10

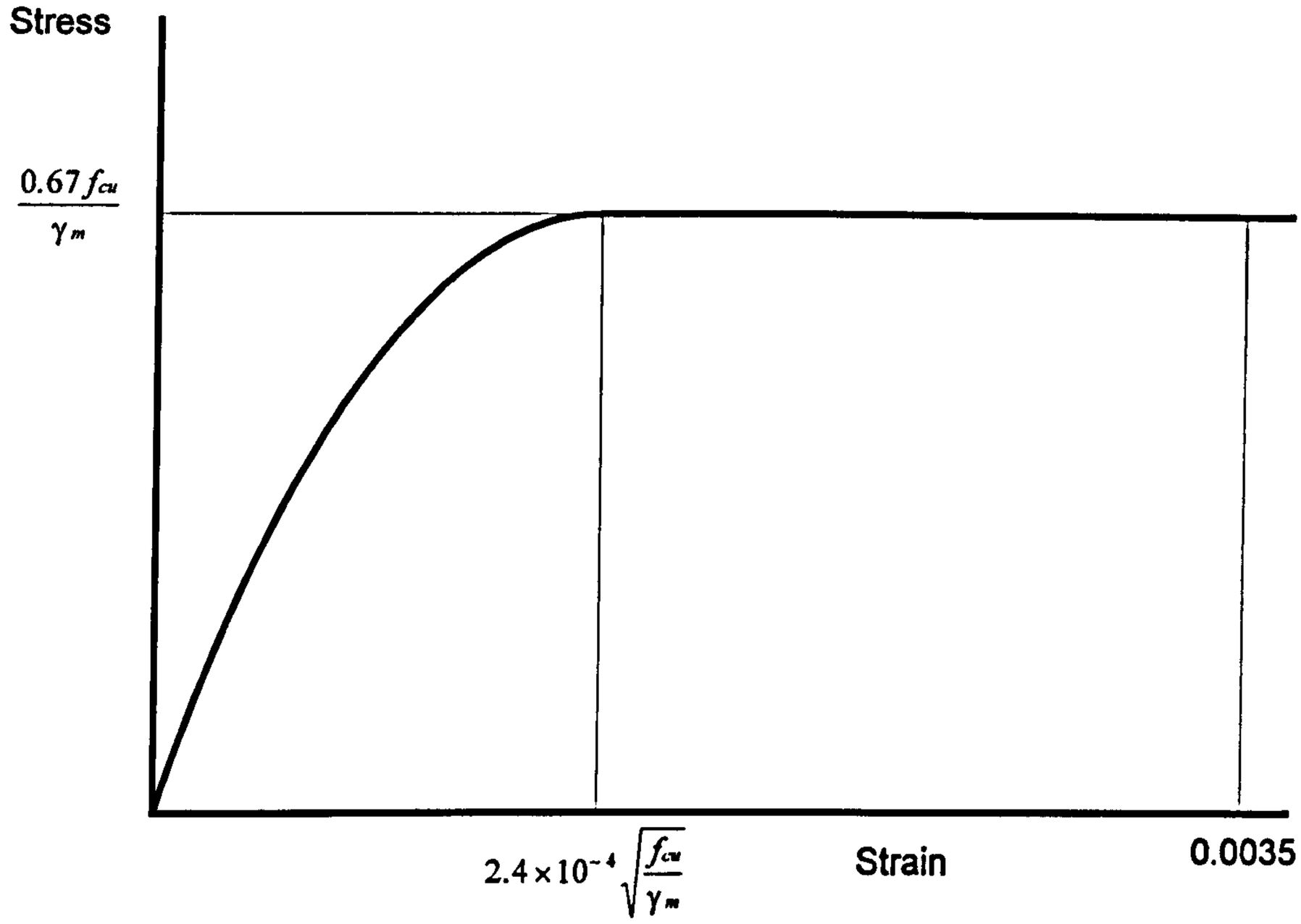

Figure B1.a. Design Stress-Strain Curve for Normal-Weight Concrete

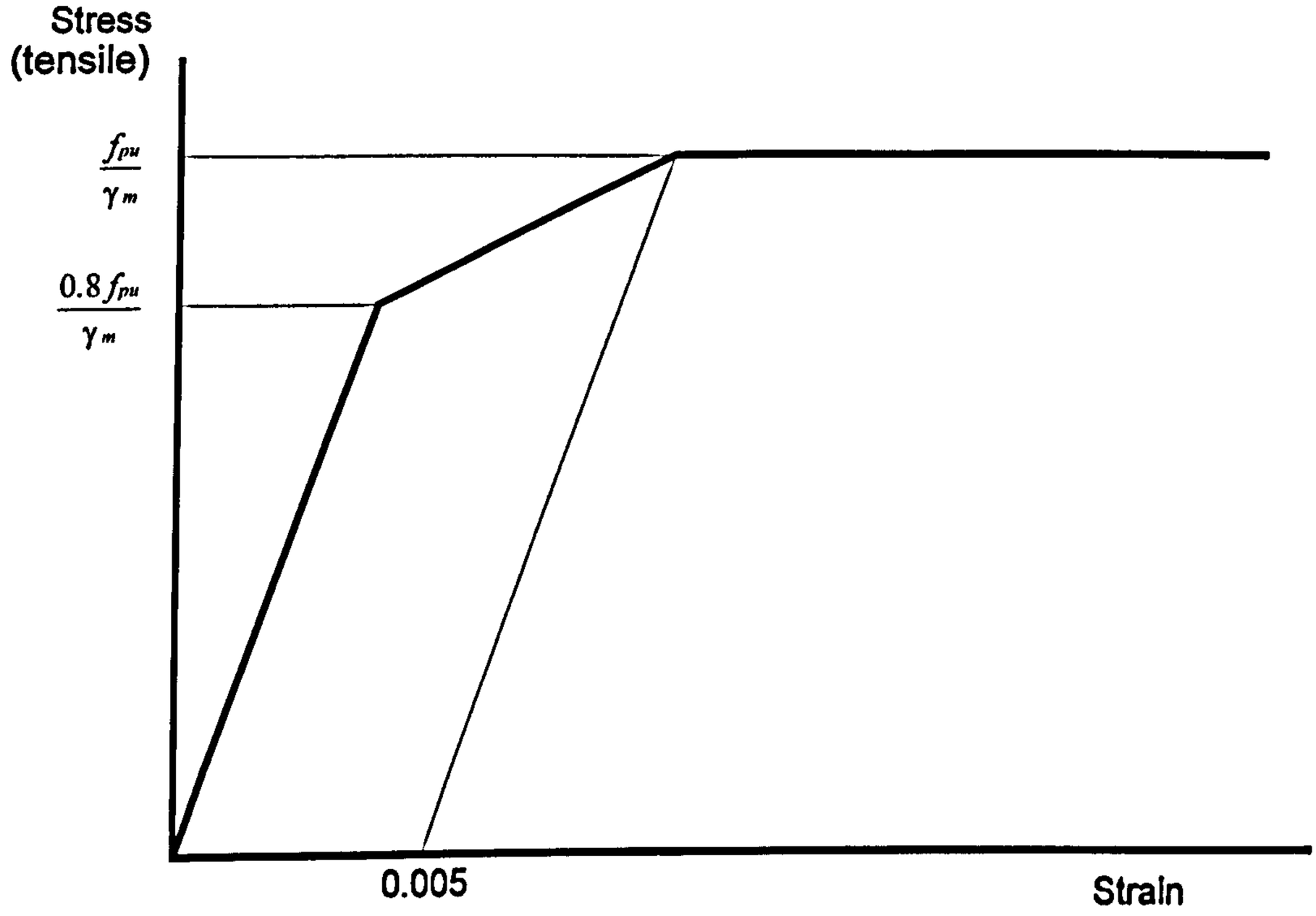

Figure B1.b. Design Stress-Strain Curve for Prestressing Tendons

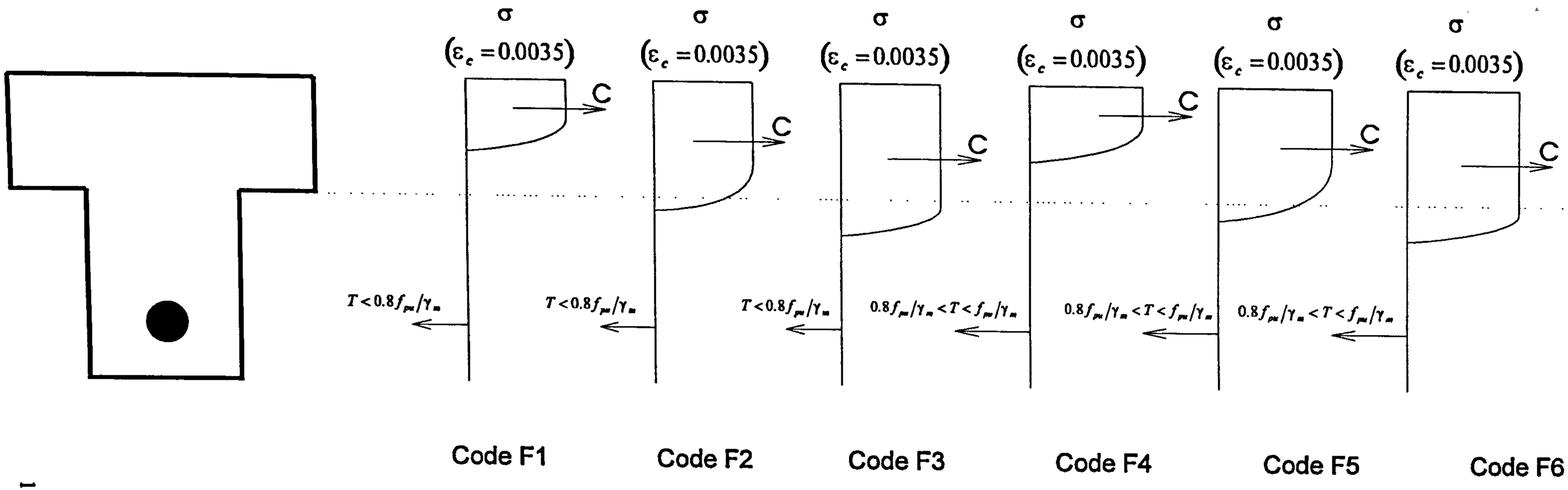

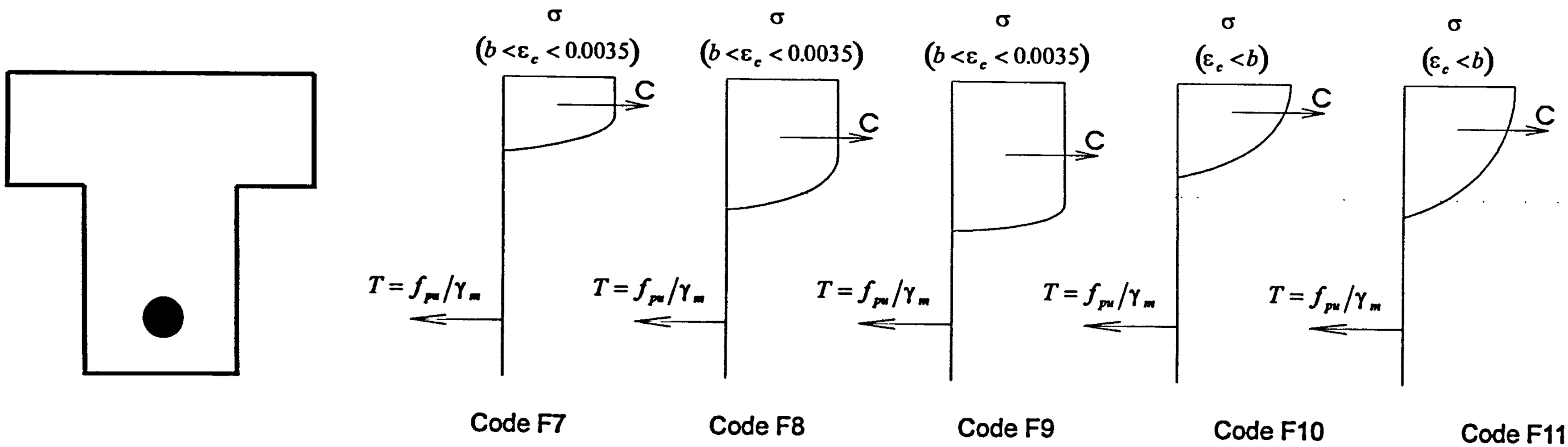

Figure B2a. Failure Modes of prestressed Concrete I and T Sections

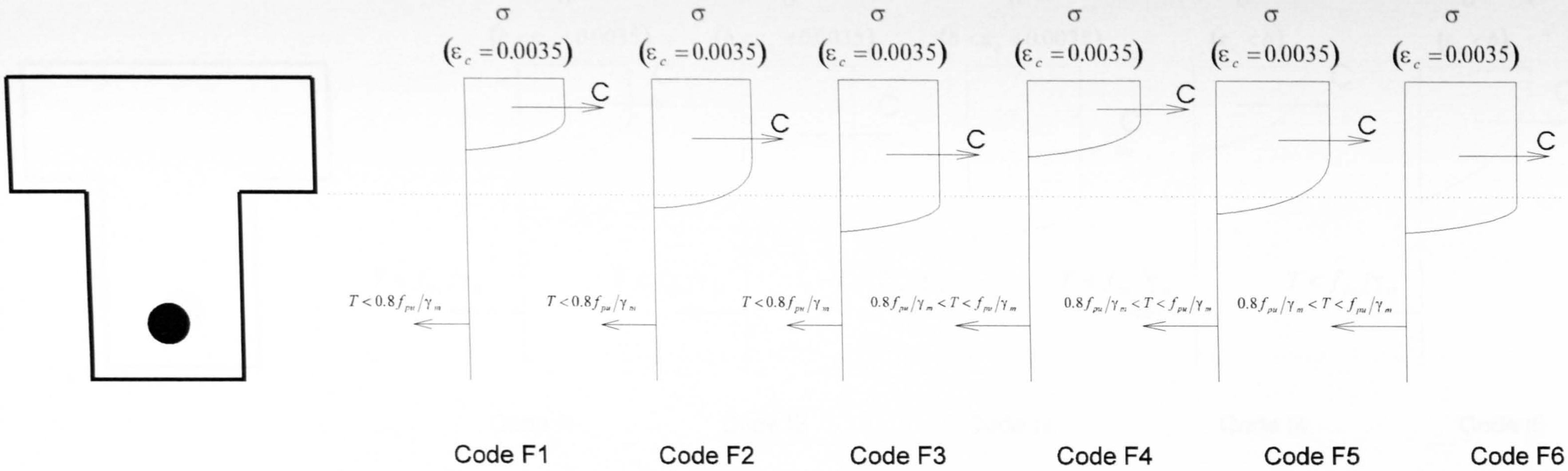

Figure B2a. Failure Modes of prestressed Concrete I and T Sections

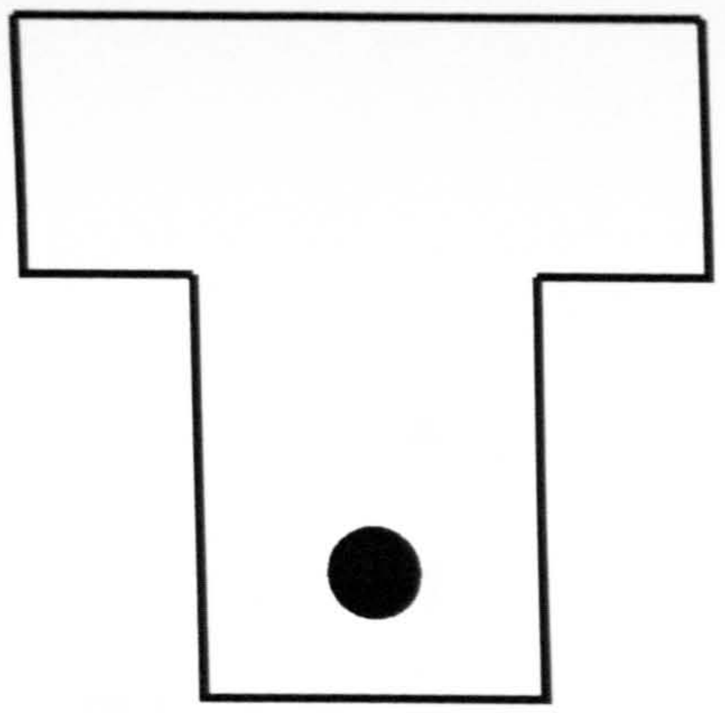

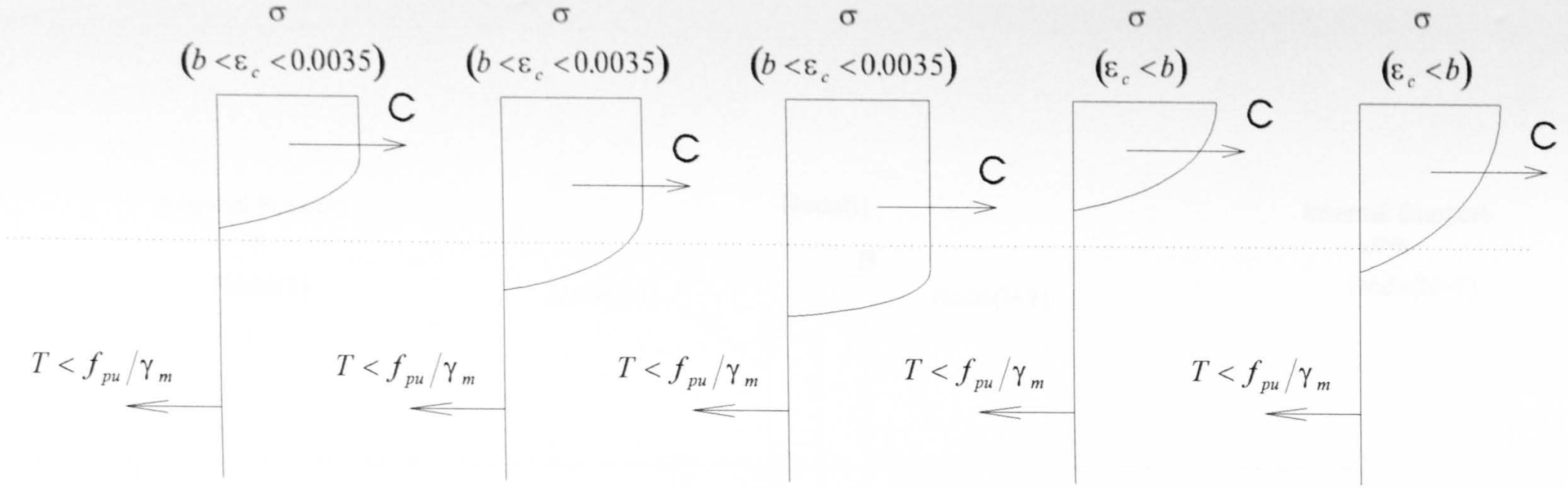

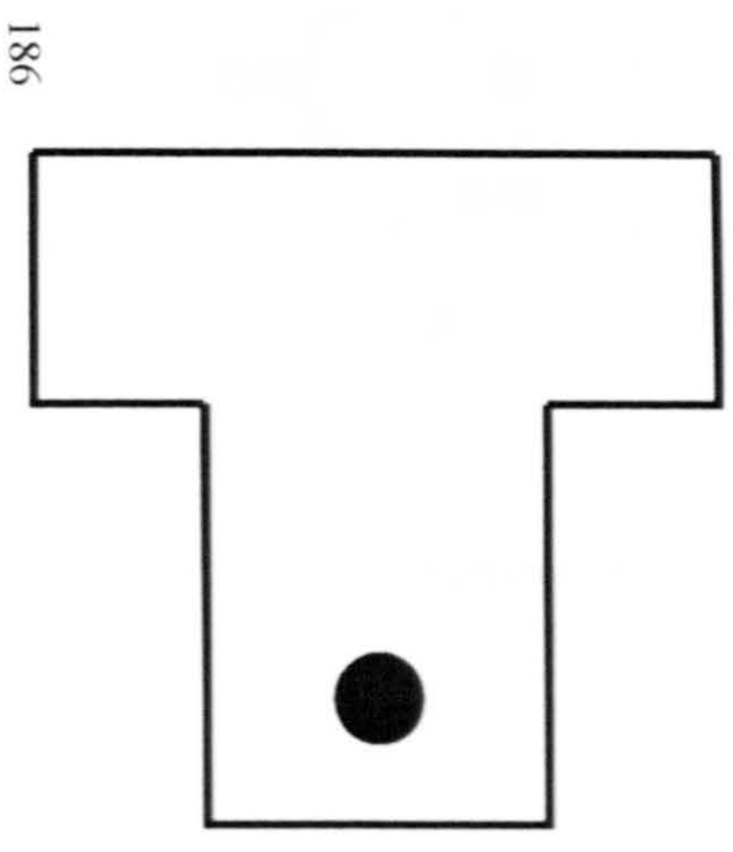

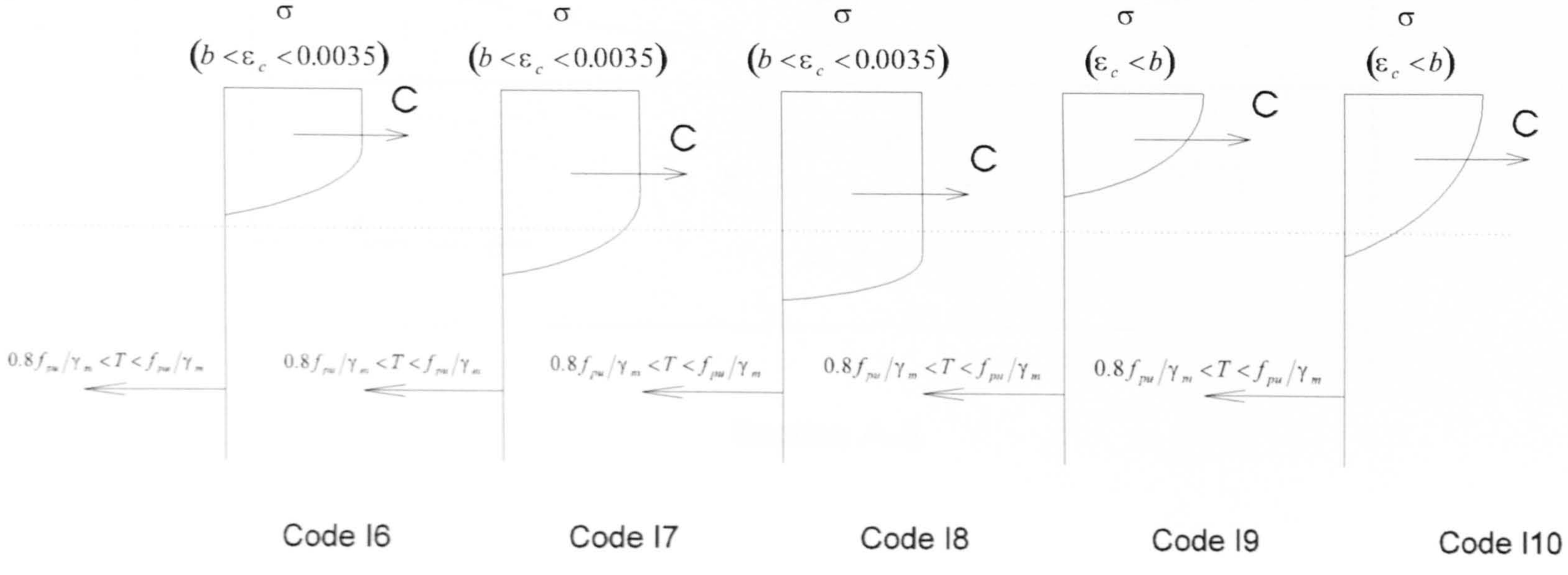

Figure B2b. Intermediate Cracked Modes of Prestressed Concrete I and T Sections

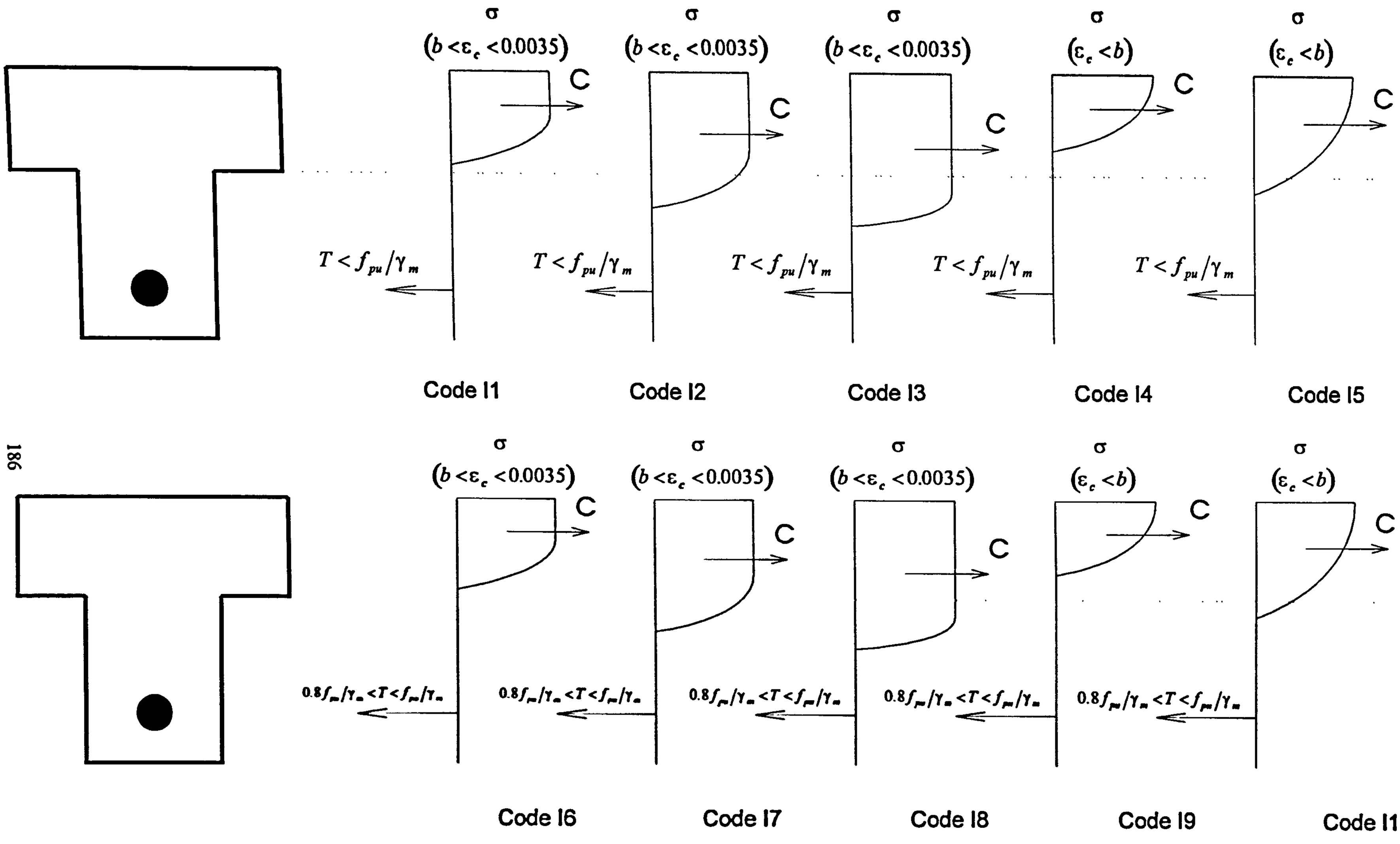

Figure B2b. Intermediate Cracked Modes of Prestressed Concrete I and T Sections

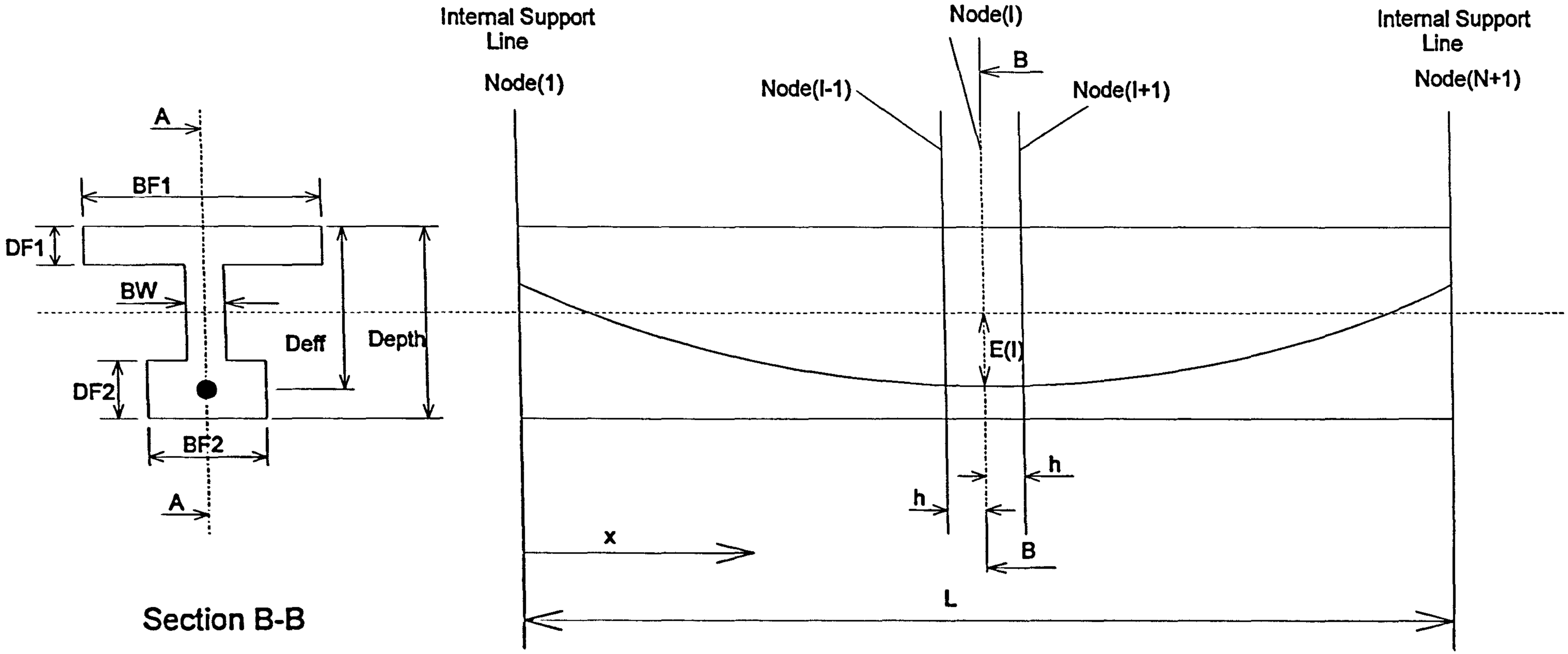

Figure B.3. Beam Dimensions as Used in the Cracked Section Analysis for SMARELIT

Appendix C

Free Bending Moment and Fixed End Moments due to Varying Distributed Load

A simply supported beam with a varying distributed load $q = q(x)$ is shown in figure C1. The free bending moment may be calculated by using the conventional method, by cutting the beam at a general point x, and ensuring that the moments about this point are in equilibrium

First the reactions R_A and R_B must be established, taking vertical and moment equilibrium :

$$\sum \uparrow \qquad R_A + R_B = \int_0^L q(x) \quad dx \tag{c1}$$

$$\sum M_A \qquad R_B L = \bar{x} \int_0^L q(x) \quad dx \tag{c2}$$

where
$$\bar{x} = \frac{\int_0^L q(x)x \quad dx}{\int_0^L q(x) \quad dx} \tag{c3}$$

Therefore $$R_B = \frac{1}{L}\int_0^L q(x)x \quad dx \qquad R_A = \int_0^L q(x) \quad dx - \frac{1}{L}\int_0^L q(x)x \quad dx \tag{c4}$$

Cut the beam at point x, and take moments about this point, figure.C2 :

$$M = R_A x - (x - \bar{x}_1)\int_0^x q(x) \quad dx \tag{c5}$$

where
$$\bar{x}_1 = \frac{\int_0^x q(x)x \quad dx}{\int_0^x q(x) \quad dx} \tag{c6}$$

Substituting for R_A and $\bar{x}$ gives the full moment equation in terms of x :

$$M = \left(\int_0^L q(x)\,dx - \frac{1}{L}\int_0^L q(x)x\,dx - \int_0^x q(x)\,dx \right) x + \int_0^x q(x)x\,dx \qquad \text{(c7)}$$

Hence there are four different integrals to be evaluated numerically, which can be done readily using Simpsons rule, Spencer et al, [7]. The last two integrals in equation (c7) need to be updated at each node as the x value is increased by the nodal interval h, causing an increase in the number of strips on each cycle to calculate the next moment value.

Elastic Fixed-End Moments

The details of the general calculation with the required steps is given by T.R.Graves-Smith, Linear Analysis of Frameworks, Ellis Horwood. The general equation for the fixed-end moments is :

$$P_F = -kd_Q \qquad \text{(c8)}$$

where k = member stiffness matrix $= \left\{\frac{EI}{L}\right\}\begin{bmatrix} 4.0 & 2.0 \\ 2.0 & 4.0 \end{bmatrix}$ (c9)

and $$d_Q = \left\{\frac{1}{EI}\right\}\begin{bmatrix} -\int_0^L M\,dx + \frac{x}{L}\int_0^L M\,dx \\ \frac{x}{L}\int_0^L M\,dx \end{bmatrix} \qquad \text{(c10)}$$

are the end rotations of the simply supported member due to transverse loads Q, with M being the free bending moment. Multiplying (c8) through by the member stiffness matrix gives the fixed end moments :

$$P_{F1} = \frac{1}{L}\left(6\int_0^L \frac{Mx}{L}\,dx - 4\int_0^L M\,dx \right) \qquad \text{(c11)}$$

$$P_{F2} = \frac{1}{L}\left(6\int_0^L \frac{Mx}{L}\,dx - 2\int_0^L M\,dx \right) \qquad \text{(c12)}$$

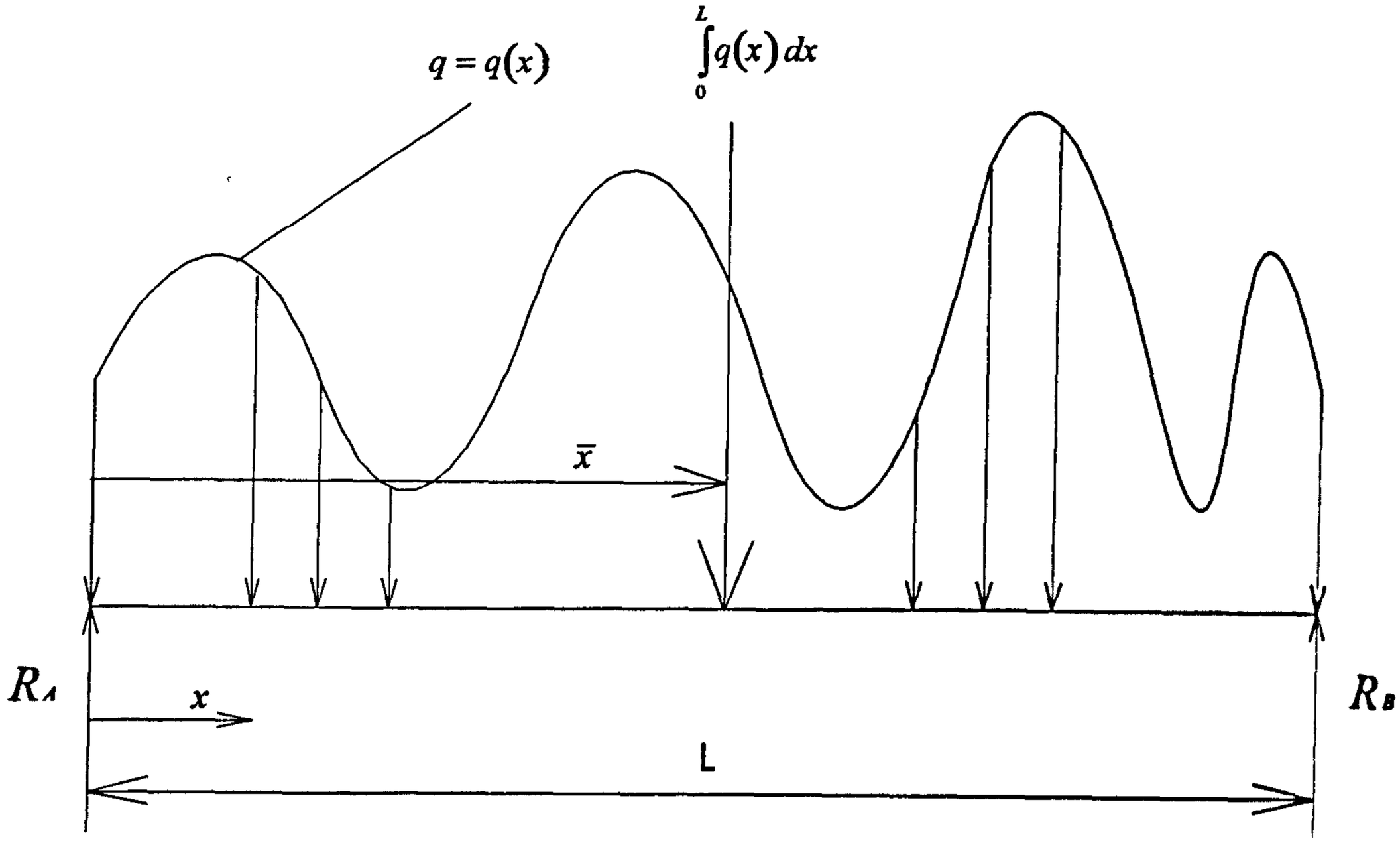

Figure C1. Simply Supported Beam with Varying Distributed Load

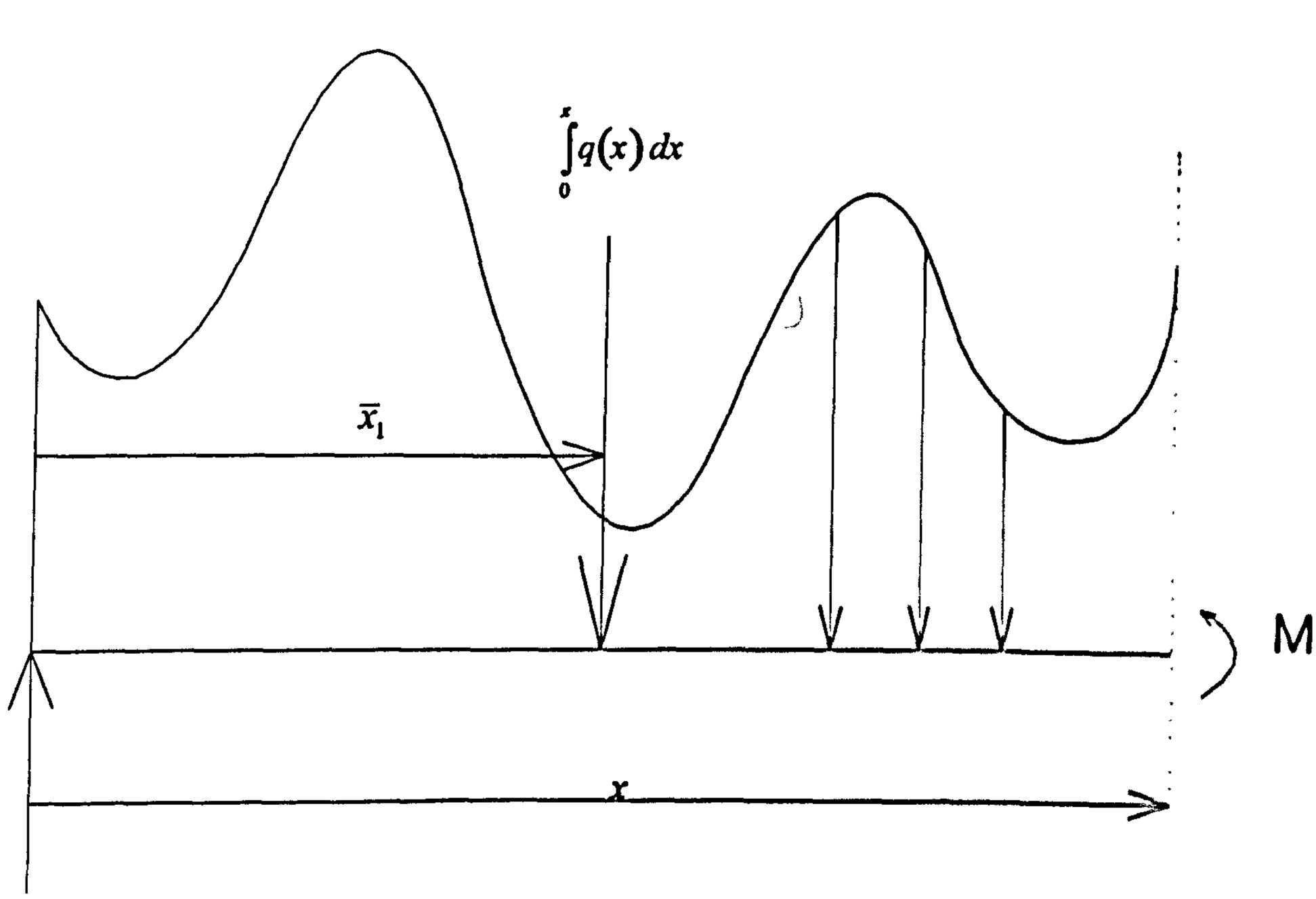

Figure C2. Beam cut at Point x for Moment Equilibrium

Appendix D

ANSYS Input Data File (Model 18)

```
/prep7
c ***********************************************************************
/title,CONTINUOUS BEAM MODEL16
C ***********************************************************************
kan,0
c ***********************************************************************
c ***********************************************************************
et,1,65,0,0,0,0,2,3          *Concrete element main body
et,2,45,0,0,0,1,2,3          *3D-isoparametric solid (for embedded tendon) N.A.
et,3,23,0,1,0,1,0,2          *2D-plastic beam N.A.
et,4,12,0,0,1,0,0,2          *2D-interface element (for bond)
et,5,45,0,0,0,0,0,0          *3D-isoparametric solid (for end support conc.)
et,6,1,0,0,0,0,0,0           *Spar element (for prestressing steel)
c ***********************************************************************
r,1,0,0,0,0,0,0,0
r,2,7.979,                   *Radius of tendon steel  N.A.
r,3,0,5e12,0.1,0,5e12        *Interface Stiffness
r,4,850,5.882e-3             *Initial prestrain of tendon steel
r,5,7,0,0,0                  *no Rebar
r,6,600,0                    *end shear
r,7,600,0                     *shear
r,8,850,0.00                 *c.s.tendon
c ***********************************************************************
c ******Concrete multilinear (non-linear) material properties********
c ***********************************************************************
knl,1
mp,ex,1,37827
mp,nuxy,1,0.2
mp,gxy,1,15761
mp,dens,1,2.3544e-5
nltab,1,0
nl,1,13,17,0.465e-3,0.93e-3,0.140e-2,0.186e-2,0.35e-2
nl,1,19,0,17.59,30.15,37.74,40.2,40.2
nl,1,55,1
nl,1,61,1
nl,1,67,4.473
nl,1,73,-1
c ***********************************************************************
c ******Concrete multilinear (non-linear) material properties********
c ***********************************************************************
knl,8
mp,ex,8,37827
mp,nuxy,8,0.2
mp,gxy,8,15761
mp,dens,8,2.3544e-5
nltab,8,0
nl,8,13,17,0.465e-3,0.93e-3,0.140e-2,0.186e-2,0.35e-2
nl,8,19,0,17.59,30.15,37.74,40.2,40.2
nl,8,55,1
nl,8,61,1
nl,8,67,-1
nl,8,73,-1
```

```
c ***********************************************************************
c ******Tendon bilinear (non-linear) material properties*************
c ***********************************************************************
mp,ex,2,0.2e6
mp,nuxy,2,0.3
mp,gxy,2,76923
nltab,2,0
nl,2,13,17,0.7e-2,0.1375e-1,0.35e-1
nl,2,19,0,1400,1750,1750
c ***********************************************************************
c ************shear reinforcement material props *********************
c ***********************************************************************
mp,ex,7,0.2e6
mp,nuxy,7,0.3
mp,gxy,7,76923
c ***********************************************************************
c ************end anchorage steel*************************************
c ***********************************************************************
mp,ex,6,0.2e6
mp,nuxy,6,0.3
mp,gxy,6,77000
c ***********************************************************************
c ******End support concrete linear material properties**************
c ***********************************************************************
mp,ex,4,25232
mp,nuxy,4,0.2
mp,gxy,4,10513
c ***********************************************************************
c ******Interface friction material property**************************
c ***********************************************************************
mp,mu,5,4e10
c ***********************************************************************
c ******Node generation***********************************************
c ***********************************************************************
n,1,0,0,0
n,2,0,0,400
ngen,6,2,1,2,1,0,50,0
ngen,2,2,11,12,1,0,36,0
ngen,2,2,13,14,1,0,0.5,0
ngen,2,2,15,16,1,0,2,0
ngen,2,2,17,18,1,0,11.5,0
ngen,2,2,19,20,1,0,4,0
ngen,2,2,21,22,1,0,8.5,0
ngen,2,2,23,24,1,0,3.5,0
ngen,2,2,25,26,1,0,8,0
ngen,2,2,27,28,1,0,14.5,0
ngen,2,2,29,30,1,0,5.5,0
ngen,2,2,31,32,1,0,12,0
ngen,2,2,33,34,1,0,20.5,0
ngen,2,2,35,36,1,0,7.5,0
ngen,2,2,37,38,1,0,16,0
ngen,2,2,39,40,1,0,36,0
ngen,2,2,41,42,1,0,20,0
ngen,2,2,43,44,1,0,44,0
ngen,2,2,45,46,1,0,25,0
ngen,2,2,47,48,1,0,79,0
ngen,2,2,49,50,1,0,92,0
ngen,2,2,51,52,1,0,51,0
```

```
ngen,2,2,53,54,1,0,31,0
ngen,2,2,55,56,1,0,16.5,0
ngen,2,2,57,58,1,0,5.5,0
ngen,5,2,59,60,1,0,50,0
ngen,2,68,1,68,1,500,0,0
ngen,6,68,69,136,1,1000,0,0
ngen,11,68,409,476,1,500,0,0
ngen,5,68,1089,1156,1,1000,0,0
ngen,2,68,1361,1428,1,500,0,0
ngen,2,68,1429,1496,1,300,0,0
ngen,2,68,1497,1564,1,150,0,0
ngen,3,68,1565,1632,1,50,0,0
n,1769,0,525,0
n,1770,0,525,400
n,1771,500,500,0
n,1772,500,500,400
n,1773,1500,436,0
n,1774,1500,436,400
n,1775,2500,384,0
n,1776,2500,384,400
n,1777,3500,344,0
n,1778,3500,344,400
n,1779,4500,316,0
n,1780,4500,316,400
n,1781,5500,300,0
n,1782,5500,300,400
n,1783,6000,286.5,0
n,1784,6000,286.5,400
n,1785,6500,286,0
n,1786,6500,286,400
n,1787,7000,288.5,0
n,1788,7000,288.5,400
n,1789,7500,304,0
n,1790,7500,304,400
n,1791,8000,312.5,0
n,1792,8000,312.5,400
n,1793,8500,324,0
n,1794,8500,324,400
n,1795,9000,338.5,0
n,1796,9000,338.5,400
n,1797,9500,356,0
n,1798,9500,356,400
n,1799,10000,376.5,0
n,1800,10000,376.5,400
n,1801,10500,400,0
n,1802,10500,400,400
n,1803,11500,456,0
n,1804,11500,456,400
n,1805,12500,525,0
n,1806,12500,525,400
n,1807,13500,604,0
n,1808,13500,604,400
n,1809,14500,696,0
n,1810,14500,696,400
n,1811,15000,747,0
n,1812,15000,747,400
n,1813,15300,778,0
n,1814,15300,778,400
```

```
n,1815,15450,794.5,0
n,1816,15450,794.5,400
n,1817,15500,800,0
n,1818,15500,800,400
c ***********************************************************************
c ******Concrete element generation*************************************
c ***********************************************************************
mat,6
real,1
type,5
e,1,2,4,3,69,70,72,71
egen,33,2,1
mat,1
real,5
type,1
e,69,70,72,71,137,138,140,139
egen,33,2,34
egen,20,68,34,66
mat,8
e,1429,1430,1432,1431,1497,1498,1500,1499
egen,9,2,694
mat,1
e,1447,1448,1450,1449,1515,1516,1518,1517
egen,24,2,703
egen,4,68,694,726
c ***********************************************************************
c ******Steel generation*************************************************
c ***********************************************************************
mat,2
real,4
type,6
e,1769,1771
e,1770,1772
egen,24,2,826,827
c ***********************************************************************
c ******Interface bond element generation*******************************
c ***********************************************************************
mat,5
real,3
type,4
e,47,1769
e,48,1770
e,113,1771
e,114,1772
e,177,1773
e,178,1774
e,241,1775
e,242,1776
e,303,1777
e,304,1778
e,365,1779
e,366,1780
e,427,1781
e,428,1782
e,491,1783
e,492,1784
e,557,1785
e,558,1786
```

```
e,629,1787
e,630,1788
e,701,1789
e,702,1790
e,771,1791
e,772,1792
e,843,1793
e,844,1794
e,913,1795
e,914,1796
e,985,1797
e,986,1798
e,1055,1799
e,1056,1800
e,1127,1801
e,1128,1802
e,1199,1803
e,1200,1804
e,1271,1805
e,1272,1806
e,1341,1807
e,1342,1808
e,1411,1809
e,1412,1810
e,1481,1811
e,1482,1812
e,1551,1813
e,1552,1814
e,1621,1815
e,1622,1816
e,1691,1817
e,1692,1818
c ***********************************************************************
c ************end support*************************************************
c ***********************************************************************
n,1819,0,-30,0
n,1820,0,-30,400
n,1821,500,-30,0
n,1822,500,-30,400
n,1823,1500,-30,0
n,1824,1500,-30,400
mat,4
real,1
type,5
e,1819,1820,2,1,1821,1822,70,69
e,1821,1822,70,69,1823,1824,138,137
c ***********************************************************************
n,1825,15500,-20,0
n,1826,15500,-20,400
n,1827,15500,-40,0
n,1828,15500,-40,400
n,1829,15500,-60,0
n,1830,15500,-60,400
n,1831,15550,-20,0
n,1832,15550,-20,400
n,1833,15550,-40,0
n,1834,15550,-40,400
n,1835,15550,-60,0
```

```
n,1836,15550,-60,400
e,1565,1633,1825,1825,1566,1634,1826,1826
e,1497,1498,1566,1565,1827,1828,1826,1825
e,1429,1430,1498,1497,1829,1830,1828,1827
e,1825,1826,1634,1633,1831,1832,1702,1701
e,1827,1828,1826,1825,1833,1834,1832,1831
e,1829,1830,1828,1827,1835,1836,1834,1833
c ***********************************************************
c ***** spar elements for shear ***************************
c ***********************************************************
mat,7
real,7
type,6
e,69,135
e,70,136
egen,6,68,932,933
egen,6,136,942,943
egen,8,68,952,953
c ***********************************************************
c ****** Boundary conditions ******************************
c ***********************************************************
d,1821,uy,0,,1822,1
d,1821,uz,0,,1821,1
d,1829,uy,0,,1830,1
d,1825,ux,0,,1830,1
d,1633,ux,0,,1700,1
d,1749,ux,0,,1750,1
c ***********************************************************
c ****** Applied pressure *********************************
c ***********************************************************
ep,66,4,0.0,,792,33
c ***********************************************************
c ****** Output control ***********************************
c ***********************************************************
wsort
iter,-10,10,10
postrs,,1,6,3,5,4,3
afwrite
finish
```

Appendix E

SMARELIT Fortran Source Code

```
      PROGRAM SMARELIT
C     ****************************************************************
      DOUBLE PRECISION A,B,AC,AS,FCU,FPU,ECR,EPU,EPU1,EPU2,EC,ES,PF,BOND
      DOUBLE PRECISION BW,BF1,BF2,DF1,DF2,DE,ELH,ERH,EN,H,MN,M
      DOUBLE PRECISION CO1,CO2,CO3,CO4,CO5,CO6
      DOUBLE PRECISION AL1(2001),AL2(2001),AL3(2001)
      DOUBLE PRECISION C1(2001),C2(2001),C3(2001)
      DOUBLE PRECISION C11(2001),C12(2001),C13(2001)
      DOUBLE PRECISION CR1(2001),CR2(2001),CR3(2001)
      DOUBLE PRECISION D1(2001),D2(2001),D3(2001)
      DOUBLE PRECISION DEF1(2001),DEF2(2001),DEF3(2001)
      DOUBLE PRECISION EPUA,EPUB,EPUC
      DOUBLE PRECISION E1(2001),E2(2001),E3(2001)
      DOUBLE PRECISION EI1(2001),EI2(2001),EI3(2001)
      DOUBLE PRECISION FD1(2007,7),FD2(2007,7),FD3(2007,7)
      DOUBLE PRECISION GAM1,GAM2,L1,L2,L3,LOAD,LOAD1
      DOUBLE PRECISION LB1,LB2,LB3,LB4,LB5,LB6,LB7
      DOUBLE PRECISION M1,M2,M3,M4,M5,M6,MX1,MX2,MX3,MX4,MX5,MX6
      DOUBLE PRECISION MCRP1(2001),MCRP2(2001),MCRP3(2001),MCRN1(2001)
      DOUBLE PRECISION MCRN2A(2001),MCRN2B(2001),MCRN3(2001)
      DOUBLE PRECISION P1(2001),P2(2001),P3(2001)
      DOUBLE PRECISION P11(2001),P12(2001),P13(2001)
      DOUBLE PRECISION RES1(2001),RES2(2001),RES3(2001)
      DOUBLE PRECISION RES11(2001),RES21(2001),RES31(2001)
      DOUBLE PRECISION SEC1(2001),SEC2(2001),SEC3(2001)
      DOUBLE PRECISION SEM1,SEM2,SEM3,SEM4
      DOUBLE PRECISION SM1,SM2,SM3,SM4,SM11,SM21,SM31,SM41
      DOUBLE PRECISION SM12,SM22,SM32,SM42,STRAND
      DOUBLE PRECISION TEMPP1,TEMPP2,TEMPP3,TEMPN1
      DOUBLE PRECISION TEMPN2A,TEMPN2B,TEMPN3,TOTAL(6)
      DOUBLE PRECISION T1(2001),T2(2001),T3(2001)
      DOUBLE PRECISION ULT1(2001),ULT2(2001),ULT3(2001)
      DOUBLE PRECISION XL1(2001),XL2(2001),XL3(2001)
      DOUBLE PRECISION X4,Y,Z1(2001),Z2(2001),Z3(2001)
C
      INTEGER I,NO,CONV
      INTEGER COUNTP1,COUNTP2,COUNTP3
      INTEGER COUNTN1,COUNTN2A,COUNTN2B,COUNTN3
      INTEGER N1,N2,N3,CRACK1(2001),CRACK2(2001),CRACK3(2001)
      INTEGER NODE1(2001),NODE2(2001),NODE3(2001),NODE4A(2001)
      INTEGER NODE4B(2001),NODE5(2001),NODE6(2001)
      INTEGER SPACE11,SPACE21,SPACE12,SPACE22A,SPACE22B
      INTEGER SPACE13,SPACE23
      INTEGER XB1,XB2,XB3,J1,J2,J3,J4A,J4B,J5,J6
C     ****************************************************************
      OPEN (UNIT=10,FILE='INPUT.DAT',STATUS='OLD')
      OPEN (UNIT=13,FILE='EQUIV.DAT',STATUS='NEW')
      OPEN (UNIT=14,FILE='STIF.DAT',STATUS='NEW')
      OPEN (UNIT=15,FILE='TFORCE.DAT',STATUS='NEW')
      OPEN (UNIT=16,FILE='RES.DAT',STATUS='NEW')
      OPEN (UNIT=21,FILE='SPAN1.DAT',STATUS='OLD')
      OPEN (UNIT=22,FILE='SPAN2.DAT',STATUS='OLD')
      OPEN (UNIT=23,FILE='SPAN3.DAT',STATUS='OLD')
      OPEN (UNIT=12,FILE='SEC1.DAT',STATUS='NEW')
      READ (10,*) AS,DE,ES,EC,FCU,FPU,PF,GAM1,GAM2,BW,BF1,BF2,DF1,
     &DF2,STRAND
C     ****************************************************************
      PRINT*,'INPUT MOMENT VALUES'
      READ*,SM11,SM21,SM31,SM41
      PRINT*,'INPUT APPLIED LOAD'
      READ*,LOAD
      LOAD1=1190
C
      TEMPP1=0.0
      TEMPP2=0.0
      TEMPP3=0.0
      TEMPN1=0.0
      TEMPN2A=0.0
      TEMPN2B=0.0
      TEMPN3=0.0
C
      M=ES/EC
      H=0.05
      NO=1
C     ****************************************************************
      READ (21,*) L1,ELH,ERH,EN
      CALL SPANSET(A,B,N1,L1,H,BW,BF1,BF2,DF1,DF2,DE,AC,Y,FCU,
     &ECR,GAM1,XL1,ELH,ERH,EN,E1,PF,P11,P1,DEF1,SEC1,EI1,EC)
      READ (22,*) L2,ELH,ERH,EN
      CALL SPANSET(A,B,N2,L2,H,BW,BF1,BF2,DF1,DF2,DE,AC,Y,FCU,
     &ECR,GAM1,XL2,ELH,ERH,EN,E2,PF,P12,P2,DEF2,SEC2,EI2,EC)
      READ (23,*) L3,ELH,ERH,EN
      CALL SPANSET(A,B,N3,L3,H,BW,BF1,BF2,DF1,DF2,DE,AC,Y,FCU,
     &ECR,GAM1,XL3,ELH,ERH,EN,E3,PF,P13,P3,DEF3,SEC3,EI3,EC)
C     ****************************************************************
      CALL INITIAL1(N1,N2,N3,XB1,XB2,XB3,CRACK1,CRACK2,CRACK3,
     &MCRP1,MCRP2,MCRP3,MCRN1,MCRN2A,MCRN2B,MCRN3)
      CONV=1
30    NO=1
40    CONV=CONV+1
      CALL PRIMARY(AL1,LOAD,FD1,P1,E1,N1)
      CALL PRIMARY(AL2,LOAD,FD2,P2,E2,N2)
      CALL PRIMARY(AL3,LOAD,FD3,P3,E3,N3)
      CALL EQUIV(FD1,C1,H,N1,L1,XB1,CRACK1,C11)
      CALL EQUIV(FD2,C2,H,N2,L2,XB2,CRACK2,C12)
      CALL EQUIV(FD3,C3,H,N3,L3,XB3,CRACK3,C13)
      CALL LOADSUM(N1,LOAD,AL1,C1,XB1,C11)
      CALL LOADSUM(N2,LOAD,AL2,C2,XB2,C12)
      CALL LOADSUM(N3,LOAD,AL3,C3,XB3,C13)
      CALL FREEBM(XL1,C1,D1,H,L1,N1,CRACK1,XB1,C11)
      CALL FREEBM(XL2,C2,D2,H,L2,N2,CRACK2,XB2,C12)
      CALL FREEBM(XL3,C3,D3,H,L3,N3,CRACK3,XB3,C13)
      CALL FEM(XL1,CO1,D1,EI1,H,L1,N1,M1,M2,MX1)
      CALL REVERSE(EI1,D1,XL1,N1)
      CALL FEM(XL1,CO2,D1,EI1,H,L1,N1,M1,M2,MX2)
      CALL REVERSE(EI1,D1,XL1,N1)
      CALL FEM(XL2,CO3,D2,EI2,H,L2,N2,M3,M4,MX3)
      CALL REVERSE(EI2,D2,XL2,N2)
      CALL FEM(XL2,CO4,D2,EI2,H,L2,N2,M3,M4,MX4)
      CALL REVERSE(EI2,D2,XL2,N2)
      CALL FEM(XL3,CO5,D3,EI3,H,L3,N3,M5,M6,MX5)
      CALL REVERSE(EI3,D3,XL3,N3)
      CALL FEM(XL3,CO6,D3,EI3,H,L3,N3,M5,M6,MX6)
      CALL REVERSE(EI3,D3,XL3,N3)
      CALL MDIST(CO1,CO2,CO3,CO4,CO5,CO6,M1,M2,M3,M4,M5,M6,
     &MX1,MX2,MX3,MX4,MX5,MX6,TOTAL)
      CALL SM(SM1,SM2,SM3,SM4,TOTAL,E1,E2,P1,P2,N1,N2)
            SM12=SM1
            SM22=SM2
            SM32=SM3
            SM42=SM4
      CALL FREEBM(XL1,AL1,D1,H,L1,N1,CRACK1,XB1,C11)
      CALL FREEBM(XL2,AL2,D2,H,L2,N2,CRACK2,XB2,C12)
      CALL FREEBM(XL3,AL3,D3,H,L3,N3,CRACK3,XB3,C13)
      CALL RESM(XL1,D1,RES1,SM11,SM21,L1,N1)
      CALL RESM(XL2,D2,RES2,SM21,SM31,L2,N2)
      CALL RESM(XL3,D3,RES3,SM31,SM41,L3,N3)
      CALL INITRES(RES11,RES1)
      CALL INITRES(RES21,RES2)
      CALL INITRES(RES31,RES3)
```

```
100  CALL MCRACK(E1,ECR,SEC1,Y,P11,AS,AC,FCU,GAM1,CR1,RES11,N1,DE)
     CALL MCRACK(E2,ECR,SEC2,Y,P12,AS,AC,FCU,GAM1,CR2,RES21,N2,DE)
     CALL MCRACK(E3,ECR,SEC3,Y,P13,AS,AC,FCU,GAM1,CR3,RES31,N3,DE)
     CALL ENDS(NO,N1,RES1,RES11,CR1,TEMPP1,TEMPN1,J1,J2,MCRP1,MCRN1)
     CALL CENTRE(NO,N2,RES2,RES21,CR2,MCRP2,MCRN2A,
    &MCRN2B,TEMPP2,TEMPN2A,TEMPN2B,I3,I4A,I4B)
     CALL ENDS(NO,N3,RES3,RES31,CR3,TEMPP3,TEMPN3,I5,I6,MCRP3,MCRN3)
     CALL BONDS(BOND,FCU)
     CALL MULT(A,AC,AS,B,EC,E1,EPUA,ES,GAM2,P11,SEC1,RES11,
    &ULT1,Z1,T1,N1,Y,FPU,DF1,DF2,BF1,BF2,BW,DE)
     CALL MULT(A,AC,AS,B,EC,E2,EPUB,ES,GAM2,P12,SEC2,RES21,
    &ULT2,Z2,T2,N2,Y,FPU,DF1,DF2,BF1,BF2,BW,DE)
     CALL MULT(A,AC,AS,B,EC,E3,EPUC,ES,GAM2,P13,SEC3,RES31,
    &ULT3,Z3,T3,N3,Y,FPU,DF1,DF2,BF1,BF2,BW,DE)
     IF (TEMPP1.NE 0.0) THEN
              CALL BICHOP(A,AC,AS,B,EC,E1,EPUA,ES,GAM2,L1,P11,ULT1,Z1,
    &   FPU,MN,EPU2,EPU1,X4,Y,J1,T1,CR1,ECR,SEC1,M,EI1,P1,DF1,DF2,BF1,
    &   BF2,BW,DE)
     ELSE
              I1=1
     ENDIF
     IF (TEMPN1.NE.0 0) THEN
              CALL BICHOP(A,AC,AS,B,EC,E1,EPUA,ES,GAM2,L1,P11,ULT1,Z1,
    &   FPU,MN,EPU2,EPU1,X4,Y,J2,T1,CR1,ECR,SEC1,M,EI1,P1,DF1,DF2,BF1,
    &   BF2,BW,DE)
     ELSE
              I2=1
     ENDIF
     IF (TEMPP2.NE.0 0) THEN
              CALL BICHOP(A,AC,AS,B,EC,E2,EPUB,ES,GAM2,L2,P12,ULT2,Z2,
    &   FPU,MN,EPU2,EPU1,X4,Y,J3,T2,CR2,ECR,SEC2,M,EI2,P2,DF1,DF2,BF1,
    &   BF2,BW,DE)
     ELSE
              I3=1
     ENDIF
     IF (TEMPN2A.NE.0 0) THEN
              CALL BICHOP(A,AC,AS,B,EC,E2,EPUB,ES,GAM2,L2,P12,ULT2,Z2,
    &   FPU,MN,EPU2,EPU1,X4,Y,J4A,T2,CR2,ECR,SEC2,M,EI2,P2,DF1,DF2,BF1,
    &   BF2,BW,DE)
     ELSE
              I4A=1
     ENDIF
     IF (TEMPN2B.NE.0 0) THEN
              CALL BICHOP(A,AC,AS,B,EC,E2,EPUB,ES,GAM2,L2,P12,ULT2,Z2,
    &   FPU,MN,EPU2,EPU1,X4,Y,J4B,T2,CR2,ECR,SEC2,M,EI2,P2,DF1,DF2,BF1,
    &   BF2,BW,DE)
     ELSE
              I4B=1
     ENDIF
     IF (TEMPP3.NE.0 0) THEN
              CALL BICHOP(A,AC,AS,B,EC,E3,EPUC,ES,GAM2,L3,P13,ULT3,Z3,
    &   FPU,MN,EPU2,EPU1,X4,Y,J5,T3,CR3,ECR,SEC3,M,EI3,P3,DF1,DF2,BF1,
    &   BF2,BW,DE)
     ELSE
              I5=1
     ENDIF
     IF (TEMPN3.NE.0 0) THEN
              CALL BICHOP(A,AC,AS,B,EC,E3,EPUC,ES,GAM2,L3,P13,ULT3,Z3,
    &   FPU,MN,EPU2,EPU1,X4,Y,J6,T3,CR3,ECR,SEC3,M,EI3,P3,DF1,DF2,BF1,
    &   BF2,BW,DE)
     ELSE
              I6=1
     ENDIF
     CALL BONDL(LB1,P1,AS,BOND,I1,PF,STRAND)
     CALL BONDL(LB2,P1,AS,BOND,I2,PF,STRAND)
     CALL BONDL(LB3,P2,AS,BOND,I4A,PF,STRAND)
     CALL BONDL(LB4,P2,AS,BOND,I3,PF,STRAND)
     CALL BONDL(LB5,P2,AS,BOND,I4B,PF,STRAND)
     CALL BONDL(LB6,P3,AS,BOND,I5,PF,STRAND)
     CALL BONDL(LB7,P3,AS,BOND,I6,PF,STRAND)
     CALL INITIAL2(P1,NODE1,NODE2,CRACK1,XB1,N1,PF)
     CALL INITIAL2A(P2,NODE3,NODE4A,NODE4B,CRACK2,XB2,N2,PF)
     CALL INITIAL2(P3,NODE5,NODE6,CRACK3,XB3,N3,PF)
     CALL CRACKS1(TEMPP1,TEMPN1,NODE1,NODE2,LB1,LB2,
    &MCRP1,MCRN1,COUNTP1,COUNTN1,SPACE11,SPACE21,H,I1,I2)
     CALL CRACKS2(TEMPP2,TEMPN2A,TEMPN2B,NODE3,NODE4A,NODE4B,
    &LB4,LB3,LB5,MCRP2,MCRN2A,MCRN2B,COUNTP2,COUNTN2A,COUNTN2B,
    &SPACE12,SPACE22A,SPACE22B,H,I3,I4A,I4B)
     CALL CRACKS1(TEMPP3,TEMPN3,NODE5,NODE6,LB6,LB7,
    &MCRP3,MCRN3,COUNTP3,COUNTN3,SPACE13,SPACE23,H,I5,I6)
     DO 121 I=1,2001,1
       EI1(I)=(EC*SEC1(I))/(10 0**6)
       EI2(I)=(EC*SEC2(I))/(10 0**6)
       EI3(I)=(EC*SEC3(I))/(10 0**6)
121  CONTINUE
     CALL TFORCEP(N1,P1,EI1,XB1,CRACK1,NODE1,TEMPP1,SPACE11,
    &COUNTP1,A,AC,AS,B,EC,E1,EPUA,ES,GAM2,L1,P11,ULT1,Z1,FPU,Y,
    &RES11,ECR,SEC1,M,RES1,DF1,DF2,BF1,BF2,BW,DE)
     CALL TFORCEN(N1,P1,EI1,XB1,CRACK1,NODE2,TEMPN1,SPACE21,
    &COUNTN1,A,AC,AS,B,EC,E1,EPUA,ES,GAM2,L1,P11,ULT1,Z1,FPU,Y,
    &RES11,ECR,SEC1,M,RES1,DF1,DF2,BF1,BF2,BW,DE)
     CALL TFORCEN(N2,P2,EI2,XB2,CRACK2,NODE4A,TEMPN2A,SPACE22A,
    &COUNTN2A,A,AC,AS,B,EC,E2,EPUB,ES,GAM2,L2,P12,ULT2,Z2,FPU,Y,
    &RES21,ECR,SEC2,M,RES2,DF1,DF2,BF1,BF2,BW,DE)
     CALL TFORCEP(N2,P2,EI2,XB2,CRACK2,NODE3,TEMPP2,SPACE12,
    &COUNTP2,A,AC,AS,B,EC,E2,EPUB,ES,GAM2,L2,P12,ULT2,Z2,FPU,Y,
    &RES21,ECR,SEC2,M,RES2,DF1,DF2,BF1,BF2,BW,DE)
     CALL TFORCEN(N2,P2,EI2,XB2,CRACK2,NODE4B,TEMPN2B,SPACE22B,
    &COUNTN2B,A,AC,AS,B,EC,E2,EPUB,ES,GAM2,L2,P12,ULT2,Z2,FPU,Y,
    &RES21,ECR,SEC2,M,RES2,DF1,DF2,BF1,BF2,BW,DE)
     CALL TFORCEN(N3,P3,EI3,XB3,CRACK3,NODE6,TEMPN3,SPACE23,
    &COUNTN3,A,AC,AS,B,EC,E3,EPUC,ES,GAM2,L3,P13,ULT3,Z3,FPU,Y,
    &RES31,ECR,SEC3,M,RES3,DF1,DF2,BF1,BF2,BW,DE)
     CALL TFORCEP(N3,P3,EI3,XB3,CRACK3,NODE5,TEMPP3,SPACE13,
    &COUNTP3,A,AC,AS,B,EC,E3,EPUC,ES,GAM2,L3,P13,ULT3,Z3,FPU,Y,
    &RES31,ECR,SEC3,M,RES3,DF1,DF2,BF1,BF2,BW,DE)
     CALL BUBBLE(XB1,CRACK1)
     CALL BUBBLE(XB2,CRACK2)
     CALL BUBBLE(XB3,CRACK3)
     CALL RESET(XB1,CRACK1,N1)
     CALL RESET(XB2,CRACK2,N2)
     CALL RESET(XB3,CRACK3,N3)
     CALL PRIMARY(AL1,LOAD,FD1,P1,E1,N1)
     CALL PRIMARY(AL2,LOAD,FD2,P2,E2,N2)
     CALL PRIMARY(AL3,LOAD,FD3,P3,E3,N3)
     CALL EQUIV(FD1,C1,H,N1,L1,XB1,CRACK1,C11)
     CALL EQUIV(FD2,C2,H,N2,L2,XB2,CRACK2,C12)
     CALL EQUIV(FD3,C3,H,N3,L3,XB3,CRACK3,C13)
     CALL LOADSUM(N1,LOAD,AL1,C1,XB1,C11)
     CALL LOADSUM(N2,LOAD,AL2,C2,XB2,C12)
     CALL LOADSUM(N3,LOAD,AL3,C3,XB3,C13)
     CALL FREEBM(XL1,C1,D1,H,L1,N1,CRACK1,XB1,C11)
     CALL FREEBM(XL2,C2,D2,H,L2,N2,CRACK2,XB2,C12)
     CALL FREEBM(XL3,C3,D3,H,L3,N3,CRACK3,XB3,C13)
     CALL FEM(XL1,CO1,D1,EI1,H,L1,N1,M1,M2,MX1)
     CALL REVERSE(EI1,D1,XL1,N1)
     CALL FEM(XL1,CO2,D1,EI1,H,L1,N1,M1,M2,MX2)
     CALL REVERSE(EI1,D1,XL1,N1)
     CALL FEM(XL2,CO3,D2,EI2,H,L2,N2,M3,M4,MX3)
     CALL REVERSE(EI2,D2,XL2,N2)
```

```
CALL FEM(XL2,CO4,D2,EI2,H,L2,N2,M3,M4,MX4)
CALL REVERSE(EI2,D2,XL2,N2)
CALL FEM(XL3,CO5,D3,EI3,H,L3,N3,M5,M6,MX5)
CALL REVERSE(EI3,D3,XL3,N3)
CALL FEM(XL3,CO6,D3,EI3,H,L3,N3,M5,M6,MX6)
CALL REVERSE(EI3,D3,XL3,N3)
CALL MDIST(CO1,CO2,CO3,CO4,CO5,CO6,M1,M2,M3,M4,M5,M6,
&MX1,MX2,MX3,MX4,MX5,MX6,TOTAL)
CALL SM(SM1,SM2,SM3,SM4,TOTAL,E1,E2,P1,P2,N1,N2)
NO=NO+1
IF (CONV.LT.15) THEN
IF (ABS((SM2-SM22)/SM2) GT.0 0001) THEN
        NO=NO+1
        GO TO 40
ELSEIF (ABS((SM3-SM32)/SM3) GT.0.0001) THEN
        NO=NO+1
        GO TO 40
ENDIF
IF (ABS((SM21-SM2)/SM21).GT.0 0001) THEN
        SM21=(SM21+SM2)/2.0
  SM31=(SM31+SM3)/2.0
  GO TO 40
ELSEIF (ABS((SM31-SM3)/SM31) GT 0.0001) THEN
        SM21=(SM21+SM2)/2.0
  SM31=(SM31+SM3)/2.0
        GO TO 40
ENDIF
ENDIF
IF (LOAD GT.301.7) THEN
  DO 800 I=1,N1+1,1
    WRITE (13,*) 'EQUIV LOAD1@',I,'=',C1(I),'C11(I)=',C11(I)
    WRITE (14,*) 'STIFFNESS1@',I,'=',EI1(I)
    WRITE (15,*) 'TENDON FORCE1@',I,'=',P1(I)
    WRITE (16,*) 'RES1',I,'=',RES1(I)
800   CONTINUE
  DO 801 I=1,N2+1,1
    WRITE (13,*) 'EQUIV LOAD2@',I,'=',C2(I),'C12(I)=',C12(I)
    WRITE (14,*) 'STIFFNESS2@',I,'=',EI2(I)
    WRITE (15,*) 'TENDON FORCE2 @',I,'=',P2(I)
    WRITE (16,*) 'RES2',I,'=',RES2(I)
801   CONTINUE
  DO 802 I=1,N3+1,1
    WRITE (13,*) 'EQUIV LOAD3@',I,'=',C3(I),'C13(I)=',C13(I)
    WRITE (14,*) 'STIFFNESS3@',I,'=',EI3(I)
    WRITE (15,*) 'TENDON FORCE3 @',I,'=',P3(I)
    WRITE (16,*) 'RES3',I,'=',RES3(I)
802   CONTINUE
ENDIF
CALL EQUIV(FD1,C1,H,N1,L1,XB1,CRACK1,C11)
CALL EQUIV(FD2,C2,H,N2,L2,XB2,CRACK2,C12)
CALL EQUIV(FD3,C3,H,N3,L3,XB3,CRACK3,C13)
CALL FREEBM(XL1,C1,D1,H,L1,N1,CRACK1,XB1,C11)
CALL FREEBM(XL2,C2,D2,H,L2,N2,CRACK2,XB2,C12)
CALL FREEBM(XL3,C3,D3,H,L3,N3,CRACK3,XB3,C13)
CALL FEM(XL1,CO1,D1,EI1,H,L1,N1,M1,M2,MX1)
CALL REVERSE(EI1,D1,XL1,N1)
CALL FEM(XL1,CO2,D1,EI1,H,L1,N1,M1,M2,MX2)
CALL REVERSE(EI1,D1,XL1,N1)
CALL FEM(XL2,CO3,D2,EI2,H,L2,N2,M3,M4,MX3)
CALL REVERSE(EI2,D2,XL2,N2)
CALL FEM(XL2,CO4,D2,EI2,H,L2,N2,M3,M4,MX4)
CALL REVERSE(EI2,D2,XL2,N2)
CALL FEM(XL3,CO5,D3,EI3,H,L3,N3,M5,M6,MX5)
CALL REVERSE(EI3,D3,XL3,N3)
CALL FEM(XL3,CO6,D3,EI3,H,L3,N3,M5,M6,MX6)
CALL REVERSE(EI3,D3,XL3,N3)
CALL MDIST(CO1,CO2,CO3,CO4,CO5,CO6,M1,M2,M3,M4,M5,M6,
&MX1,MX2,MX3,MX4,MX5,MX6,TOTAL)
CALL SM(SEM1,SEM2,SEM3,SEM4,TOTAL,E1,E2,P1,P2,N1,N2)
PRINT*,'SECONDARY MOMENT A =',SEM2
PRINT*,'SECONDARY MOMENT B =',SEM3
CALL CHECK(RES1,ULT1,I,N1)
IF (I.NE (N1+2)) THEN
        GO TO 400
ENDIF
CALL CHECK(RES2,ULT2,I,N2)
IF (I.NE.(N2+2)) THEN
        GO TO 400
ENDIF
CALL CHECK(RES3,ULT3,I,N3)
IF (I.NE.(N3+2)) THEN
        GO TO 400
ENDIF
WRITE (12,*) 'LOAD=',LOAD,'SM2=',SM2,'SM3=',SM3,
&'SEM2=',SEM2,'SEM3=',SEM3,
&'XB1=',XB1,'XB2=',XB2,'XB3=',XB3,'CONV=',CONV
LOAD=LOAD+0.1
PRINT*,'NEXT LOAD=',LOAD
CONV=1
GO TO 30
400  END
*  ***********************************************************************
   SUBROUTINE BICHOP(A,AC,AS,B,EC,E,EPU,ES,GAM2,L,P1,ULT,Z,
   &FPU,MN,EPU2,EPU1,X4,Y,I,T,RES,ECR,SEC,M,EI,P,DF1,DF2,BF1,
   &BF2,BW,DE)
*  ***********************************************************************
*  SUBROUTINE BICHOP PERFORMS A BINARY CHOP PROCESS TO CALCULATE
*  THE CRACKED SECTION PROPERTIES @ NODE I, SUBJECT TO A BENDING
*  MOMENT RES(I)
*  ***********************************************************************
*
   DOUBLE PRECISION A,AB,AC,AS,B,ES,EC,EPU,EPU1,EPU2,FPU,GAM2
   DOUBLE PRECISION DF1,DF2,BF1,BF2,BW,DE,ECR,L,M,MN,PHI,Y,X4
   DOUBLE PRECISION DEFF,E(2001),RES(2001),P(2001),ULT(2001)
   DOUBLE PRECISION SEC(2001),T(2001),Z(2001),EI(2001),P1(2001)
   INTEGER I
*
            EPU0=ECR/(EC*1000.0)
            EPU1=EPU
11    EPU2=(EPU1+EPU0)/2.0
*
   CALL MCALC(A,AC,AS,B,EC,E,EPU,ES,GAM2,P1,SEC,ULT,Z,
   &FPU,MN,EPU2,X4,Y,I,T,RES,DF1,DF2,BF1,BF2,BW,DE)
*
            IF (MN GT.ABS(RES(I)*1000000 0)) THEN
              EPU1=EPU2
            ELSE
              EPU0=EPU2
            ENDIF
            AB=ABS((EPU1-EPU0)/EPU1)
            IF (AB GT 0 000001) THEN
              GO TO 11
            ELSE
              IF (RES(I) LT 0 0) THEN
                      DEFF=Y-(E(I)*1000 0)
              ELSE
                      DEFF=Y+(E(I)*1000 0)
              ENDIF
              PHI=EPU1/Z(I)
              EI(I)=ABS((ABS(RES(I))-ABS(T(I)*E(I)*1000 0))/(PHI*1000 0))
```

```
            P(I)=T(I)/1000 0
          ENDIF
  RETURN
  END
*  ****************************************************************
   SUBROUTINE EQUIV(FD1,C,H,N,L,X,CRACK,C1)
*  ****************************************************************
*  SUBROUTINE EQUIV CALCULATES THE EQIVALENT LOAD C(I) FROM THE
*  PRIMARY MOMENT B(I,1) USING STIRLINGS INTERPOLATION (FINITE
*  DIFFERENCE) FORMULA FOR THE NUMERICAL DIFFERENTIATION
*  ****************************************************************
*
   INTEGER I,J,K,X,COUNT,CRACK(2001),N
   DOUBLE PRECISION FD1(2007),H,L,C1(2001)
   DOUBLE PRECISION FD(2007,7),C(2001)
*
   DO 84 K=1,(X-1),1
            DO 24 J=1,6,1
              DO 14 I=CRACK(K),CRACK(K+1),1
                FD(I+3,1)=FD1(I+3)
                FD(I+4,1)=FD1(I+4)
                FD(I+3,J+1)=FD(I+4,J)-FD(I+3,J)
14      CONTINUE
24    CONTINUE
            DO 44 I=(CRACK(K)+3),(CRACK(K)+1),-1
              FD(I-1,1)=FD(I,1)-FD(I,2)+FD(I,3)-FD(I,4)+FD(I,5)-FD(I,6)
     &    +FD(I,7)
            DO 34 J=1,6,1
              FD(I-1,J+1)=FD(I,J)-FD(I-1,J)
34      CONTINUE
44    CONTINUE
            DO 64 I=CRACK(K+1),(CRACK(K+1)+2),1
              FD(I+4,1)=FD(I+3,1)+FD(I+2,2)+FD(I+1,3)+FD(I,4)+FD(I-1,5)
     &    +FD(I-2,6)+FD(I-3,7)
            DO 54 J=1,6,1
              FD(I-J+4,J+1)=FD(I-J+5,J)-FD(I-J+4,J)
54      CONTINUE
64    CONTINUE
            COUNT=1
            DO 74 I=CRACK(K),CRACK(K+1)
              IF (COUNT EQ 1) THEN
                C1(K)=-((FD(I+2,3)-((FD(I+1,5))/12 0)+((FD(I,7))
     &      /90 0))/(H*H))
              ELSE
                C(I)=-((FD(I+2,3)-((FD(I+1,5))/12 0)+((FD(I,7))
     &      /90 0))/(H*H))
              ENDIF
              COUNT=COUNT+1
74    CONTINUE
84  CONTINUE
    RETURN
    END
*
*  ****************************************************************
    SUBROUTINE FREEBM(XL,C,D,H,L,N,CRACK,X,C1)
*  ****************************************************************
*  SUBROUTINE FREEBM CALCULATES THE FREE BENDING MOMENT
*  ENVELOPE D(I) ON THE BEAM DUE TO THE EQUIVALENT AND
*  APPLIED LOADS
*  ****************************************************************
*
    INTEGER I,J,K,X,N,CRACK(2001)
    DOUBLE PRECISION XL(2001),C(2001),D(2001),INT1,INT2,INT3,INT4
    DOUBLE PRECISION H,L,INT5,INT6,C1(2001)
*
    INT1=0 0
    INT2=0.0
    DO 25 K=1,(X-1),1
              INT1=INT1+C1(K)+C(CRACK(K+1))
              INT2=INT2+(XL(CRACK(K))*C1(K))+(XL(CRACK(K+1))*C(CRACK(K+1)))
              DO 15 I=(CRACK(K)+1),(CRACK(K+1)-1),1
                INT1=INT1+(2 0*C(I))
                INT2=INT2+(2.0*XL(I)*C(I))
15    CONTINUE
25  CONTINUE
    DO 35 I=1,N+1,1
              D(I)=XL(I)*(H/2.0)*(INT1-(INT2/L))
35  CONTINUE
*  ****************************************************************
    INT3=0 0
    INT4=0 0
    INT5=0 0
    INT6=0.0
    DO 65 K=1,(X-1),1
              D(CRACK(K)+1)=D(CRACK(K)+1)+(-XL(CRACK(K)+1)*(C1(K)
    &  +C(CRACK(K)+1)+INT5)+XL(CRACK(K))*C1(K)
    &  +XL(CRACK(K)+1)*C(CRACK(K)+1)+INT6)*(H/2.0)
              J=CRACK(K)+1
45    IF (J LE (CRACK(K+1)-1)) THEN
                IF (K.EQ.1) THEN
                  INT3=C1(K)
                  INT4=XL(CRACK(K))*C1(K)
                ELSE
                  INT3=INT5+C1(K)
                  INT4=INT6+XL(CRACK(K))*C1(K)
                ENDIF
                DO 55 I=(CRACK(K)+1),J,1
                  INT3=INT3+(2 0*C(I))
                  INT4=INT4+(2.0*XL(I)*C(I))
55      CONTINUE
              INT3=INT3+C(I)
              INT4=INT4+XL(I)*C(I)
              D(I)=D(I)+((INT4-XL(I)*INT3)*(H/2 0))
              J=J+1
              GO TO 45
            ENDIF
            INT5=INT3
            INT6=INT4
65  CONTINUE
    RETURN
    END
*
*  ****************************************************************
    SUBROUTINE FEM(XL,CO,D,EI,H,L,N,M1,M2,MX1)
*  ****************************************************************
*  SUBROUTINE FEM CALCULATES THE FIXED END MOMENTS AND
*  CARRY-OVER FACTORS OF A SIMPLY SUPPORTED BEAM SUBJECT TO
*  THE LOADING C(I) AND THE FREE BM D(I) USING THE MOMENT
*  AREA METHODS AND CURVATURE OF THE BEAM
*  ****************************************************************
*
    INTEGER I,N
    DOUBLE PRECISION XL(2001),D(2001),CO,MX1,MX2,L,H
    DOUBLE PRECISION CUR1(2001),CUR2(2001),CUR3(2001),EI(2001)
    DOUBLE PRECISION R1,R2,R3,RX1,RX2,RX3,W1,W2,W3,M1,M2
*
    DO 16 I=1,(N+1)
              CUR1(I)=((L-XL(I))/L)/EI(I)
              CUR2(I)=(XL(I)/L)/EI(I)
              CUR3(I)=(D(I)/EI(I))
```

```
16  CONTINUE
    R1=(H/24.0)*(7.0*CUR1(1)+6.0*CUR1(2)-CUR1(3))
    R2=(H/24 0)*(7 0*CUR2(1)+6 0*CUR2(2)-CUR2(3))
    R3=(H/24.0)*(7.0*CUR3(1)+6.0*CUR3(2)-CUR3(3))
    RX1=XL(1)*R1
    RX2=XL(1)*R2
    RX3=XL(1)*R3
    DO 26 I=2,N
              W1=(H/12.0)*(CUR1(I-1)+10*CUR1(I)+CUR1(I+1))
              W2=(H/12 0)*(CUR2(I-1)+10*CUR2(I)+CUR2(I+1))
              W3=(H/12.0)*(CUR3(I-1)+10*CUR3(I)+CUR3(I+1))
              R1=R1+W1
              R2=R2+W2
              R3=R3+W3
              RX1=RX1+W1*XL(I)
              RX2=RX2+W2*XL(I)
              RX3=RX3+W3*XL(I)
 26  CONTINUE
    R1=R1+(H/24 0)*(7 0*CUR1(N+1)+6 0*CUR1(N)-CUR1(N-1))
    R2=R2+(H/24 0)*(7 0*CUR2(N+1)+6 0*CUR2(N)-CUR2(N-1))
    R3=R3+(H/24 0)*(7 0*CUR3(N+1)+6 0*CUR3(N)-CUR3(N-1))
    RX1=RX1+XL(N+1)*(H/24 0)*(7 0*CUR1(N+1)+6 0*CUR1(N)-CUR1(N-1))
    RX2=RX2+XL(N+1)*(H/24 0)*(7.0*CUR2(N+1)+6 0*CUR2(N)-CUR2(N-1))
    RX3=RX3+XL(N+1)*(H/24 0)*(7.0*CUR3(N+1)+6 0*CUR3(N)-CUR3(N-1))
    M1=(((R2/RX2)*(RX3))-R3)/(((RX1*R2)/RX2)-R1)
    M2=-(((R1/RX1)*(RX3))-R3)/(((RX2*R1)/RX1)-R2)
    MX1=1 0/(R1-((R2*RX1)/RX2))
    MX2=1 0/(((R1*RX2)/RX1)-R2)
    CO=MX2/MX1
    RETURN
    END
*
*  ***************************************************************
    SUBROUTINE RESM(XL,D,RES,SMA,SMB,L,N)
*  ***************************************************************
*  SUBROUTINE RES CALCULATES THE RESULTANT INTERNAL BENDING
*  MOMENT IN THE PRESTRESSED CONCRETE BEAM
*  ***************************************************************
*
    DOUBLE PRECISION XL(2001),D(2001),RES(2001),L,SMA,SMB
    INTEGER I,N

    DO 17 I=1,(N+1)
              RES(I)=SMA-(SMA*XL(I)/L)-(SMB*XL(I)/L)+D(I)
17  CONTINUE
    RETURN
    END
*
*  ***************************************************************
    SUBROUTINE MCRACK(E,ECR,SEC1,Y,P,AS,AC,FCU,GAM1,CR,RES,N,DE)
*  ***************************************************************
*  SUBROUTINE MCRACK CALCULATES THE CRACKING MOMENT OF THE
*  PRESTRESSED CONCRETE SECTION
*  ***************************************************************
*
    INTEGER I,N
    DOUBLE PRECISION E(2001),ECR,SEC1(2001),Y,P(2001),AS,AC,FCU,GAM1
    DOUBLE PRECISION RES(2001),CR(2001),DE
*
    DO 18 I=1,(N+1),1
    IF (RES(I).GE.0.0) THEN
              CR(I)=(SEC1(I)*(DE-Y))-((P(I)*1000 0/AC)+(P(I)*(1/1000000 0)*E(I)*
   &  (DE-Y)/SEC1(I))+ECR)/1000000 0
    ELSE
              CR(I)=(SEC1(I)*Y)-((P(I)*1000 0/AC)+(P(I)*(1/1000000 0)*E(I)*
   &  Y/SEC1(I))+ECR)/1000000.0
    ENDIF
18  CONTINUE
    RETURN
    END
*
*  ***************************************************************
    SUBROUTINE MULT(A,AC,AS,B,EC,E,EPU,ES,GAM2,P,SEC1,RES,
   &ULT,Z,T,N,Y,FPU,DF1,DF2,BF1,BF2,BW,DEPTH)
*  ***************************************************************
*  SUBROUTINE MULT CALCULATES THE ULTIMATE MOMENT OF RESISTANCE
*  OF THE PRESTRESSED CONCRETE SECTION
*  ***************************************************************
*
    INTEGER I,N
    DOUBLE PRECISION DEFF,E(2001),RES(2001),P(2001),ULT(2001),T(2001)
    DOUBLE PRECISION A,AB,AC,AS,A1,A2,A3,A4,A5,B,B1,BR,C1,E5,EC,ES
    DOUBLE PRECISION ENEW,EPU,FPU,G,GAM2,K2,LIMIT1,LIMIT2
    DOUBLE PRECISION PS,X1,X2,X3,X4,Z(2001),Y
    DOUBLE PRECISION ECN,SEC1(2001),L,BW,F1,DF1,DF2,BF1,BF2
    DOUBLE PRECISION AA,BB,CC,DD,ROOT1,ROOT2,ROOT3,DEPTH,DE
    DOUBLE PRECISION FUNCX1,FUNCX2,FUNCX3,NUM,DEN,CHANGE
*
    DO 59 I=1,(N+1),1
    IF (RES(I).LT.0 0) THEN
              DEFF=(DEPTH-Y)-(E(I)*1000.0)
              ECN=-E(I)
              BR=BF2
              DE=DF2
    ELSE
              DEFF=Y+(E(I)*1000.0)
              ECN=E(I)
              BR=BF1
              DE=DF1
    ENDIF
C
C   CONCRETE REACHES ULTIMATE STRAIN, PARABOLIC-LINEAR PROFILE
C   IS ENTIRELY WITHIN FLANGE, STEEL ELASTIC
C
    EPU=0.0035
    K2=A*(1 0-(B/(3 0*EPU)))
    A1=K2*BR
    A2=AS*ES*1000 0
    PS=P(I)*1000 0/AS
    A3=(PS*AS)/(EC*AC*1000 0)
    A4=(PS*AS*(ECN*1000 0)**2)/(SEC1(I)*EC*1000 0)
    A5=(PS/(ES*1000 0))
    B1=A2*(A3+A4-EPU+A5)
    C1=A2*DEFF*EPU
    Z(I)=(B1+SQRT((B1**2)+(4 0*A1*C1)))/(2 0*A1)
    T(I)=A2*(A3+A4-EPU+A5+(DEFF*EPU/Z(I)))
    X1=(5 0*B**2)/(12.0*EPU**2)
    X2=0.5*(1.0-(B**2/EPU**2))
    X3=(1 0-B/(3 0*EPU))
    X4=Z(I)*(X1+X2)/X3
    L=DEFF-Z(I)+X4
    IF (RES(I) LT 0 0) THEN
              ULT(I)=-T(I)*L
    ELSE
              ULT(I)=T(I)*L
    ENDIF
    LIMIT1=0 8*FPU*AS/GAM2
    IF (Z(I) LT DE) THEN
              IF (T(I) LT LIMIT1) THEN
               GO TO 59
```

```
            ENDIF
         ENDIF
C
C   CONCRETE REACHES ULTIMATE STRAIN, PARABOLIC-LINEAR PROFILE
C   IS IN WEB AND FLANGE WITH FUNCTION CHANGEOVER IN THE WEB
C   STEEL ELASTIC
C
      AA=BW*((2 0*A*B)/(3.0*EPU)+A-(A*B/EPU))
      BB=((BR-BW)*A*DE)+(A2*(EPU-A3-A4-A5))
      CC=-(AS*ES*1000.0*DEFF*EPU)
      Z(I)=(-BB+SQRT((BB**2)-(4 0*AA*CC)))/(2.0*AA)
      NUM=BW*(((A*(Z(I)-DE)**2)/2.0)
     &-(1.0*A*(B**2)*(Z(I)**2))/(12.0*EPU**2))
      NUM=NUM+(BR*((A*Z(I)**2/2.0)-(A*(Z(I)-DE)**2)/(2.0)))
      DEN=BW*((2 0*A*B*Z(I))/(3.0*EPU)+(A*Z(I))-(A*DE)-(A*B*Z(I))/(EPU))
      DEN=DEN+(BR*A*DE)
      X4=NUM/DEN
      T(I)=A2*(A3+A4-EPU+A5+(DEFF*EPU/Z(I)))
      L=DEFF-Z(I)+X4
      IF (RES(I).LT.0 0) THEN
                  ULT(I)=-T(I)*L
      ELSE
                  ULT(I)=T(I)*L
      ENDIF
      CHANGE=Z(I)-((B*Z(I))/EPU)
      IF (CHANGE.GT.DE) THEN
                  IF (T(I).LT.LIMIT1) THEN
                    GO TO 59
                  ENDIF
      ENDIF
C
C   CONCRETE REACHES ULTIMATE STRAIN, PARABOLIC-LINEAR PROFILE
C   IS ENTIRELY WITHIN FLANGE, STEEL INELASTIC
C
      ENEW=(0 2*FPU/GAM2)/((0 2*FPU)/(GAM2*ES*1000 0)+0 005)
      G=0 8*FPU/GAM2
      B1=AS*(ENEW*(A3+A4-EPU+A5-G/(ES*1000 0))+G)
      C1=AS*ENEW*DEFF*EPU
      Z(I)=(B1+SQRT((B1**2)+(4 0*A1*C1)))/(2.0*A1)
      T(I)=AS*ENEW*(A3+A4+(DEFF*EPU/Z(I))-EPU+A5-G/(ES*1000 0))+G*AS
      X4=Z(I)*(X1+X2)/X3
      L=DEFF-Z(I)+X4
      IF (RES(I) LT 0 0) THEN
                  ULT(I)=-T(I)*L
      ELSE
                  ULT(I)=T(I)*L
      ENDIF
      LIMIT2=FPU*AS/GAM2
      CHANGE=Z(I)-((B*Z(I))/EPU)
      IF (CHANGE LT DE) THEN
                  IF (T(I) LT LIMIT2) THEN
                    GO TO 59
                  ENDIF
      ENDIF
C
C   CONCRETE REACHES ULTIMATE STRAIN, PARABOLIC-LINEAR PROFILE
C   IS IN WEB AND FLANGE WITH FUNCTION CHANGEOVER IN THE WEB
C   STEEL INELASTIC
C
      AA=BW*((2 0*A*B)/(3 0*EPU)+A-(A*B/EPU))
      BB=((BR-BW)*A*DE)+(AS*ENEW*(A3+A4-EPU+A5-G/(ES*1000 0)))-(G*AS)
      CC=-(AS*ENEW*DEFF*EPU)
      Z(I)=(-BB+SQRT((BB**2)+(4 0*AA*CC)))/(2 0*AA)
      NUM=BW*((A*(Z(I)-DE)**2)/2 0)
     &-((1 0*A*(B**2)*(Z(I)**2))/(12 0*EPU**2))
      NUM=NUM+(BR*((A*Z(I)**2/2.0)-(A*(Z(I)-DE)**2)/(2.0)))
      DEN=BW*((2.0*A*B*Z(I))/(3.0*EPU)+(A*Z(I))-(A*DE)-(A*B*Z(I))/(EPU))
      DEN=DEN+(BR*A*DE)
      X4=NUM/DEN
      T(I)=AS*ENEW*(A3+A4+(DEFF*EPU/Z(I))-EPU+A5-G/(ES*1000.0))+G*AS
      L=DEFF-Z(I)+X4
      IF (RES(I).LT 0.0) THEN
                  ULT(I)=-T(I)*L
      ELSE
                  ULT(I)=T(I)*L
      ENDIF
      CHANGE=Z(I)-((B*Z(I))/EPU)
      IF (CHANGE.GT.DE) THEN
                  IF (T(I).LT.LIMIT2) THEN
                    GO TO 59
                  ENDIF
      ENDIF
C
C   CONCRETE REACHES ULTIMATE STRAIN, PARABOLIC-LINEAR PROFILE
C   IS IN WEB AND FLANGE WITH FUNCTION CHANGEOVER IN THE FLANGE
C   STEEL ELASTIC
C
      AA=(((2.0*A*B)/(3.0*EPU))+A*(1.0-(B/EPU)))*BR
      AA=AA+((BW-BR)*((A*EPU/B)-(A*EPU**2)/(3.0*B**2.0)))
      BB=(BW-BR)*((A*DE*EPU**2)/(B**2)-(2.0*A*DE*EPU/B)
      BB=BB-(A2*(A3+A4-EPU+A5))
      CC=(BW-BR)*(((A*EPU*DE**2)/B)-(A*(DE**2)*EPU**2)/B**2)
      CC=CC-(AS*ES*1000.0*DEFF*EPU)
      DD=(BR-BW)*(A*(DE**3)*EPU**2)/(3 0*B**2)
      ROOT1=0.0
      ROOT2=DEFF
10    ROOT3=(ROOT1+ROOT2)/2.0
      FUNCX1=(AA*ROOT1**3)+(BB*ROOT1**2)+(CC*ROOT1)+DD
      FUNCX2=(AA*ROOT2**3)+(BB*ROOT2**2)+(CC*ROOT2)+DD
      FUNCX3=(AA*ROOT3**3)+(BB*ROOT3**2)+(CC*ROOT3)+DD
      IF (FUNCX3 LT.0 0) THEN
                  ROOT1=ROOT3
      ELSE
                  ROOT2=ROOT3
      ENDIF
      AB=ABS(ROOT1-ROOT2)
      IF (AB GT 0 0001) THEN
                  GO TO 10
      ENDIF
      Z(I)=ROOT3
      NUM=(BW-BR)*(2 0*A*EPU*(Z(I)-DE)**3)/(3.0*Z(I)*B)
      NUM=NUM-((BW-BR)*A*(EPU**2)*((Z(I)-DE)**4)/(4.0*(B**2)*(Z(I)**2)))
      NUM=NUM+BR*(((A*Z(I)**2)/2.0)
     &-((1 0*(12.0*EPU**2))*A*(B**2)*Z(I)**2))
      DEN=(BW-BR)*((A*EPU*(Z(I)-DE)**2)/(Z(I)*B))
      DEN=DEN-((BW-BR)*((A*(EPU**2)*(Z(I)-DE)**3)/(3.0*(B**2)*Z(I)**2)))
      DEN=DEN+(BR*((2 0*A*B*Z(I))/(3 0*EPU)+(A*Z(I)*(1 0-(B)/EPU))))
      X4=NUM/DEN
      T(I)=A2*(A3+A4-EPU+A5+(DEFF*EPU/Z(I)))
      L=DEFF-Z(I)+X4
      IF (RES(I) LT 0 0) THEN
                  ULT(I)=-T(I)*L
      ELSE
                  ULT(I)=T(I)*L
      ENDIF
      CHANGE=Z(I)-((B*Z(I))/EPU)
      IF (CHANGE LT.DE) THEN
                  IF (T(I).LT.LIMIT1) THEN
                    GO TO 59
                  ENDIF
```

```
      ENDIF
C
C     CONCRETE REACHES ULTIMATE STRAIN, PARABOLIC-LINEAR PROFILE
C     IS IN WEB AND FLANGE WITH FUNCTION CHANGEOVER IN THE FLANGE
C     STEEL INELASTIC
C
      AA=(((2.0*A*B)/(3.0*EPU))+A*(1.0-(B/EPU)))*BR
      AA=AA+((BW-BR)*((A*EPU/B)-(A*EPU**2)/(3.0*B**2 0)))
      BB=(BW-BR)*((A*DE*EPU**2)/(B**2)-(2.0*A*DE*EPU)/B)
      BB=BB-(AS*ENEW*(A3+A4-EPU+A5-G/(ES*1000.0)))-G*AS
      CC=(BW-BR)*(((A*EPU*DE**2)/B)-(A*(DE**2)*EPU**2)/B**2)
      CC=CC-(AS*ENEW*DEFF*EPU)
      DD=(BR-BW)*(A*(DE**3)*EPU**2)/(3.0*B**2)
      ROOT1=0.0
      ROOT2=DEFF
   20 ROOT3=(ROOT1+ROOT2)/2.0
      FUNCX1=(AA*ROOT1**3)+(BB*ROOT1**2)+(CC*ROOT1)+DD
      FUNCX2=(AA*ROOT2**3)+(BB*ROOT2**2)+(CC*ROOT2)+DD
      FUNCX3=(AA*ROOT3**3)+(BB*ROOT3**2)+(CC*ROOT3)+DD
      IF (FUNCX3.LT.0.0) THEN
                ROOT1=ROOT3
      ELSE
                ROOT2=ROOT3
      ENDIF
      AB=ABS(ROOT1-ROOT2)
      IF (AB GT 0 0001) THEN
                GO TO 20
      ENDIF
      Z(I)=ROOT3
      NUM=(BW-BR)*(2.0*A*EPU*(Z(I)-DE)**3)/(3.0*Z(I)*B)
      NUM=NUM-((BW-BR)*A*(EPU**2)*((Z(I)-DE)**4)/(4.0*(B**2)*(Z(I)**2)))
      NUM=NUM+BR*(((A*Z(I)**2)/2.0)
     &-((1.0/(12.0*EPU**2)))*A*(B**2)*Z(I)**2))
      DEN=(BW-BR)*((A*EPU*(Z(I)-DE)**2)/(Z(I)*B))
      DEN=DEN-((BW-BR)*((A*(EPU**2)*(Z(I)-DE)**3)/(3.0*(B**2)*Z(I)**2)))
      DEN=DEN+(BR*((2 0*A*B*Z(I))/(3 0*EPU)+(A*Z(I)*(1 0-(B/EPU))))
      X4=NUM/DEN
      T(I)=AS*ENEW*(A3+A4+(DEFF*EPU/Z(I))-EPU+A5-G/(ES*1000 0))+G*AS
      L=DEFF-Z(I)+X4
      IF (RES(I).LT 0 0) THEN
                ULT(I)=-T(I)*L
      ELSE
                ULT(I)=T(I)*L
      ENDIF
      CHANGE=Z(I)-((B*Z(I))/EPU)
      IF (CHANGE LT DE) THEN
                IF (T(I) LT LIMIT2) THEN
                  GO TO 59
                ENDIF
      ENDIF
C
C     STEEL BROKEN, CONCRETE PROFILE PARABOLIC-LINEAR, ALL WITHIN
C     FLANGE
C
      T(I)=LIMIT2
      F1=((LIMIT2-G*AS)/(AS*ENEW)-A3-A4+A5+(G/(ES*1000 0)))
      ES=((B*DEFF)-(3 0*LIMIT2*F1)+(BR*A))/(3 0*(DEFF-(LIMIT2/
     &(BR*A))))
      Z(I)=(DEFF*ES)/(F1+ES)
      EPU=ES
      X1=(3 0*B**2)/(12.0*EPU**2)
      X2=0 5*(1 0-B/(3 0*EPU))
      X3=(1 0-B/(3 0*EPU))
      X4=Z(I)*(X1+X2)/X3
      L=DEFF-Z(I)+X4
      IF (RES(I).LT.0.0) THEN
                ULT(I)=-T(I)*L
      ELSE
                ULT(I)=T(I)*L
      ENDIF
      IF (Z(I).LT.DE) THEN
                GO TO 59
      ENDIF
C
C     STEEL BROKEN, CONCRETE PROFILE PARABOLIC-LINEAR IN WEB AND FLANGE
C     WITH FUNCTION CHANGEOVER IN WEB
C
      T(I)=LIMIT2
      Z(I)=T(I)-(BR*A*DE)
     &-BW*((2.0*A*B*DEFF)/(3 0*F1)-(A*DE)-(A*B*DEFF/F1))
      Z(I)=Z(I)/(BW*((A-((2.0*A*B)/(3.0*F1)))+((A*B)/(F1))))
      E5=(Z(I)*F1)/(DEFF-Z(I))
      NUM=BW*((A*(Z(I)-DE)**2)/(2.0)
     &-(1.0*A*(B**2)*(Z(I)**2))/(12.0*E5**2))
      NUM=NUM+(BR*((A*Z(I)**2/2 0)-(A*(Z(I)-DE)**2)/(2 0)))
      DEN=BW*((2 0*A*B*Z(I))/(3.0*E5)+(A*Z(I))-(A*DE)-(A*B*Z(I))/(E5))
      DEN=DEN+(BR*A*DE)
      X4=NUM/DEN
      L=DEFF-Z(I)+X4
      IF (RES(I) LT.0 0) THEN
                ULT(I)=-T(I)*L
      ELSE
                ULT(I)=T(I)*L
      ENDIF
      CHANGE=Z(I)-((B*Z(I))/E5)
      IF (CHANGE.GT.DE) THEN
                GO TO 59
      ENDIF
C
C     STEEL BROKEN, CONCRETE PROFILE PARABOLIC-LINEAR IN WEB AND FLANGE
C     WITH FUNCTION CHANGEOVER IN FLANGE
C
      T(I)=LIMIT2
      AA=((BR-BW)*(3.0*A*B*F1+A*F1**2))+(BR*((A*B**3)/F1))
      AA=AA+(BR*3.0*A*B**2)
      BB=(BW-BR)*(3 0*A*B*F1*DEFF+6 0*A*B*F1*DE+3.0*A*DE*F1**2)
      BB=BB+BR*((6 0*A*DEFF*B**3)/F1-(6 0*A*DEFF*B**2))
      BB=BB-(BR*((9 0*A*DEFF*B**3)/F1))-3.0*T(I)*B**2
      CC=(BR-BW)*(6 0*A*B*F1*DE*DEFF+3 0*A*B*F1*DE**2)
      CC=CC+(BR-BW)*(3 0*A*F1**2*DE**2)+(6 0*T(I)*DEFF*B**2)
      CC=CC+BR*((3 0*A*B**2*DEFF**2)+(3.0*A*B**3*DEFF**2)/F1)
      DD=(BW-BR)*(3 0*A*B*F1*DEFF*DE**2+A*F1**2*DE**3)
      DD=DD-(3 0*T(I)*B**2*DEFF**2)+(BR*((-1 0*A*B**3*DEFF**3)/F1))
      ROOT1=0 0
      ROOT2=DEFF
   30 ROOT3=(ROOT1+ROOT2)/2.0
      FUNCX1=(AA*ROOT1**3)+(BB*ROOT1**2)+(CC*ROOT1)+DD
      FUNCX2=(AA*ROOT2**3)+(BB*ROOT2**2)+(CC*ROOT2)+DD
      FUNCX3=(AA*ROOT3**3)+(BB*ROOT3**2)+(CC*ROOT3)+DD
      IF (FUNCX3 LT 0 0) THEN
                ROOT1=ROOT3
      ELSE
                ROOT2=ROOT3
      ENDIF
      AB=ABS(ROOT1-ROOT2)
      IF (AB GT 0 0001) THEN
                GO TO 30
      ENDIF
      Z(I)=ROOT3
      EPU=(Z(I)*F1)/(DEFF-Z(I))
```

```
      NUM=(BW-BR)*(2.0*A*EPU*(Z(I)-DE)**3)/(3.0*Z(I)*B)
      NUM=NUM-((BW-BR)*A*(EPU**2)*((Z(I)-DE)**4)/(4.0*(B**2)*(Z(I)**2)))
      NUM=NUM+BR*(((A*Z(I)**2)/2.0)
     &-((1.0/(12.0*EPU**2))*A*(B**2)*Z(I)**2))
      DEN=(BW-BR)*((A*EPU*(Z(I)-DE)**2)/(Z(I)*B))
      DEN=DEN-((BW-BR)*((A*(EPU**2)*(Z(I)-DE)**3)/(3.0*(B**2)*Z(I)**2)))
      DEN=DEN+(BR*((2.0*A*B*Z(I))/(3.0*EPU)+(A*Z(I)*(1.0-(B)/EPU))))
      X4=NUM/DEN
      L=DEFF-Z(I)+X4
      IF (RES(I).LT.0.0) THEN
                ULT(I)=-T(I)*L
      ELSE
                ULT(I)=T(I)*L
      ENDIF
      CHANGE=Z(I)-((B*Z(I))/EPU)
      IF (CHANGE.LT.DE) THEN
                GO TO 59
      ENDIF
C
C     STEEL BROKEN, CONCRETE PROFILE PARABOLIC WITHIN FLANGE
C     AND WEB
C
      T(I)=LIMIT2
      AA=(A*F1**2)*(BW-BR)-(3.0*A*B*F1+A*F1**2)*BR
      BB=(3.0*A*B*F1*DEFF*BR)+(3.0*A*B*F1-3.0*A*F1**2*DE)*(BW-BR)
      CC=(3.0*A*F1)*(F1*DE**2-B*DEFF-B*DE)*(BW-BR)+(6.0*T(I)*DEFF*B**2)
      DD=(3.0*A*B*F1*DEFF*DE-A*F1**2*DE**3)*(BW-BR)
      DD=DD+(3.0*T(I)*B**2*DEFF**2)
      ROOT1=0.0
      ROOT2=DEFF
   40 ROOT3=(ROOT1+ROOT2)/2.0
      FUNCX1=(AA*ROOT1**3)+(BB*ROOT1**2)+(CC*ROOT1)+DD
      FUNCX2=(AA*ROOT2**3)+(BB*ROOT2**2)+(CC*ROOT2)+DD
      FUNCX3=(AA*ROOT3**3)+(BB*ROOT3**2)+(CC*ROOT3)+DD
      IF (FUNCX3.LT.0.0) THEN
                ROOT1=ROOT3
      ELSE
                ROOT2=ROOT3
      ENDIF
      AB=ABS(ROOT1-ROOT2)
      IF (AB.GT.0.0001) THEN
                GO TO 40
      ENDIF
      Z(I)=ROOT3
      EPU=(Z(I)*F1)/(DEFF-Z(I))
      NUM=BW*((8.0*Z(I)*B*A*EPU**(Z(I)-DE)**3)
     &-(3.0*A*EPU**2*(Z(I)-DE)**4))
      NUM=NUM-(8.0*Z(I)**4*B*A*EPU-3.0*A*EPU**2*Z(I)**4)*BR
      NUM=NUM-(3.0*A*EPU**2*(Z(I)-DE)**4
     &-8.0*A*B*Z(I)*EPU*(Z(I)-DE)**3)*BR
      DEN=BW*(A*EPU**2*(Z(I)-DE)**3-3.0*A*B*Z(I)*EPU*(Z(I)-DE)**2)
      DEN=DEN+BR*(Z(I)**3)*(3.0*A*B*EPU-A*EPU**2)
      DEN=DEN-BR*(A*EPU**2*(Z(I)-DE)**3-3.0*A*B*Z(I)*EPU*(Z(I)-DE)**2)
      X4=NUM/DEN
      L=DEFF-Z(I)+X4
      IF (RES(I).LT.0.0) THEN
                ULT(I)=-T(I)*L
      ELSE
                ULT(I)=T(I)*L
      ENDIF
      IF (Z(I).LT.DE) THEN
                GOTO 59
      ENDIF
C
C     STEEL BROKEN, CONCRETE PROFILE PARABOLIC ALL WITHIN FLANGE
C
      T(I)=LIMIT2
      AA=A*DEFF*BR
      BB=-3.0*A*B*DEFF*BR
      CC=3.0*LIMIT2*B*B
      DD=CC*F1
      ROOT1=0.0
      ROOT2=B
   50 ROOT3=(ROOT1+ROOT2)/2.0
      FUNCX1=(AA*ROOT1**3)+(BB*ROOT1**2)+(CC*ROOT1)+DD
      FUNCX2=(AA*ROOT2**3)+(BB*ROOT2**2)+(CC*ROOT2)+DD
      FUNCX3=(AA*ROOT3**3)+(BB*ROOT3**2)+(CC*ROOT3)+DD
      IF (FUNCX3.LT.0.0) THEN
                ROOT1=ROOT3
      ELSE
                ROOT2=ROOT3
      ENDIF
      AB=ABS(ROOT1-ROOT2)
      IF (AB.GT.0.0001) THEN
                GO TO 50
      ENDIF
      Z(I)=(DEFF*ROOT3)/(F1+ROOT3)
      X4=((8.0*B*Z(I))-(3.0*E5*Z(I)))/(4.0*(3.0*B-ROOT3))
      L=DEFF-Z(I)+X4
      EPU=(Z(I)*F1)/(DEFF-Z(I))
      IF (RES(I).LT.0.0) THEN
                ULT(I)=-T(I)*L
      ELSE
                ULT(I)=T(I)*L
      ENDIF
   59 CONTINUE
      RETURN
      END
C     ******************************************************************
      SUBROUTINE MCALC(A,AC,AS,B,EC,E,EPU,ES,GAM2,P,SEC1,ULT,Z,
     &FPU,MN,EPU2,X4,Y,I,T,RES,DF1,DF2,BF1,BF2,BW,DEPTH)
C     ******************************************************************
C     SUBROUTINE MCALC CALCULATES THE SECTION PROPERTIES OF A
C     PRESTRESSED CONCRETE SECTION,XL(I) SUBJECT TO A PARTICULAR
C     MOMENT, RES(I)
C     ******************************************************************
C
      INTEGER I
      DOUBLE PRECISION DEFF,ECN,E(2001),RES(2001),P(2001),ULT(2001)
      DOUBLE PRECISION A,AB,AC,AS,A1,A2,A3,A4,A5,B,B1,BR,C1,EC,ES
      DOUBLE PRECISION ENEW,EPU,EPU2,FPU,G,GAM2,K1,L
      DOUBLE PRECISION LIMIT1,PS,SEC1(2001),X1,X2,X3,X4,MN,Y
      DOUBLE PRECISION T(2001),Z(2001),DF1,DF2,BF1,BF2,BW
      DOUBLE PRECISION AA,BB,CC,DD,DEPTH,DE
      DOUBLE PRECISION ROOT1,ROOT2,ROOT3,FUNCX1,FUNCX2,FUNCX3
      DOUBLE PRECISION NUM,DEN,CHANGE
C
      IF (RES(I).LT.0.0) THEN
                DEFF=(DEPTH-Y)-(E(I)*1000.0)
                ECN=-E(I)
                BR=BF2
                DE=DF2
      ELSE
                DEFF=Y+(E(I)*1000.0)
                ECN=E(I)
                BR=BF1
                DE=DF1
      ENDIF
      LIMIT1=0.8*FPU*AS/GAM2
      A2=AS*ES*1000.0
```

```
      PS=(P(I)*1000.0)/AS
      A3=(PS*AS)/(EC*AC*1000.0)
      A4=(PS*AS*(ECN*1000.0)**2)/(SEC1(I)*EC*1000.0)
      A5=(PS*ES*1000.0)
      IF (EPU2.GT.B) THEN
                GOTO 20
      ELSE
                GOTO 10
      ENDIF
C
C     ***********************************************
C     PARABOLIC CONCRETE COMPRESSION PROFILE SERIES
C     ***********************************************
C
C     PARABOLIC PROFILE IN FLANGE ONLY, STEEL ELASTIC
C
10    K1=((3.0*A*B*EPU2)-(A*EPU2**2))/(3.0*B**2)
      A1=K1*BR
      B1=A2*(A3+A4+EPU2+A5)
      C1=A2*DEFF*EPU2
      Z(I)=(B1+SQRT((B1**2)-(4.0*A1*C1)))/(2.0*A1)
      T(I)=A2*(A3+A4+EPU2+A5-(DEFF*EPU2/Z(I)))
      IF (Z(I).LT.DE) THEN
                IF (T(I).LT.LIMIT1) THEN
                  X4=((3.0*B*Z(I))-(3.0*EPU2*Z(I)))/(4.0*(3.0*B-EPU2))
                  L=DEFF-Z(I)+X4
                  GOTO 333
                ENDIF
      ENDIF
C
C     PARABOLIC PROFILE IN FLANGE AND WEB, STEEL ELASTIC
C
      AA=(K1*BR)+((BW-BR)*((A*EPU2**2)/(3.0*B**2)))
      BB=A2*(EPU2-A5-A4-A3)-(BR-BW)*(A*DE*EPU2**2/(B**2))-A*EPU2/B)
      CC=(BW-BR)*(((A*EPU2**2*DE**2)/(B**2))+((A*EPU2*DE)/(B)))
      CC=CC+(A5*DEFF*EPU2)
      DD=(BR-BW)*((A*EPU2**2*DE**3)/(3.0*B**2))
      ROOT1=0.0
      ROOT2=DEFF
15    ROOT3=(ROOT1+ROOT2)/2.0
      FUNCX1=(AA*ROOT1**3)+(BB*ROOT1**2)+(CC*ROOT1)+DD
      FUNCX2=(AA*ROOT2**3)+(BB*ROOT2**2)+(CC*ROOT2)+DD
      FUNCX3=(AA*ROOT3**3)+(BB*ROOT3**2)+(CC*ROOT3)+DD
      IF (FUNCX3.LT.0.0) THEN
                ROOT1=ROOT3
      ELSE
                ROOT2=ROOT3
      ENDIF
      AB=ABS(ROOT1-ROOT2)
      IF (AB.GT.0.0001) THEN
                GO TO 15
      ENDIF
      Z(I)=ROOT3
      T(I)=A2*(A3+A4+EPU2+A5+(DEFF*EPU2/Z(I)))
      IF (T(I).LT.LIMIT1) THEN
                NUM=BW*((8.0*Z(I)*B*A*EPU2*(Z(I)-DE)**3)
     &-(3.0*A*EPU2**2*(Z(I)-DE)**4))
                NUM=NUM+(8.0*Z(I)**4*B*A*EPU2-3.0*A*EPU2**2*Z(I)**4)*BR
                NUM=NUM+(3.0*A*EPU2**2*(Z(I)-DE)**4
     &-8.0*A*B*Z(I)*EPU2*(Z(I)-DE)**3)*BR
                DEN=BW*(A*EPU2**2*(Z(I)-DE)**3-3.0*A*B*Z(I)*EPU2*(Z(I)-DE)**2)
                DEN=DEN+BR*(Z(I)**3)*(3.0*A*B*EPU2-A*EPU2**2)
                DEN=DEN-BR*(A*EPU2**2*(Z(I)-DE)**3-3.0*A*B*Z(I)*EPU2*(Z(I)-DE)**2)
                X4=NUM/(4.0*DEN)
                L=DEFF-Z(I)+X4
                GOTO 333
      ENDIF
C
C     PARABOLIC PROFILE IN FLANGE AND WEB, STEEL INELASTIC
C
      AA=(K1*BR)+((BW-BR)*((A*EPU2**2)/(3.0*B**2)))
      BB=AS*ENEW*(EPU2+G/(1000.0*ES)-A3-A4-A5)-AS*G
      BB=BB+(BR-BW)*(((A*EPU2**2*DE/B**2)+(A*EPU2/B))
      CC=(BW-BR)*((((A*EPU2**2*DE**2)/(B**2))+((A*EPU2*DE)/(B)))
      CC=CC-(AS*ENEW*DEFF*EPU2)
      DD=(BW-BR)*((A*EPU2**2*DE**3)/(3.0*B**2))
      ROOT1=0.0
      ROOT2=DEFF
16    ROOT3=(ROOT1+ROOT2)/2.0
      FUNCX1=(AA*ROOT1**3)+(BB*ROOT1**2)+(CC*ROOT1)+DD
      FUNCX2=(AA*ROOT2**3)+(BB*ROOT2**2)+(CC*ROOT2)+DD
      FUNCX3=(AA*ROOT3**3)+(BB*ROOT3**2)+(CC*ROOT3)+DD
      IF (FUNCX3.LT.0.0) THEN
                ROOT1=ROOT3
      ELSE
                ROOT2=ROOT3
      ENDIF
      AB=ABS(ROOT1-ROOT2)
      IF (AB.GT.0.0001) THEN
                GO TO 16
      ENDIF
      Z(I)=ROOT3
      T(I)=AS*ENEW*(A3+A4+(DEFF*EPU2/Z(I))-EPU2+A5-G/(1000.0*ES))+G*AS
      NUM=BW*((8.0*Z(I)*B*A*EPU2*(Z(I)-DE)**3)
     &-(3.0*A*EPU2**2*(Z(I)-DE)**4))
      NUM=NUM+(8.0*Z(I)**4*B*A*EPU2-3.0*A*EPU2**2*Z(I)**4)*BR
      NUM=NUM+(3.0*A*EPU2**2*(Z(I)-DE)**4
     &-8.0*A*B*Z(I)*EPU2*(Z(I)-DE)**3)*BR
      DEN=BW*(A*EPU2**2*(Z(I)-DE)**3-3.0*A*B*Z(I)*EPU2*(Z(I)-DE)**2)
      DEN=DEN+BR*(Z(I)**3)*(3.0*A*B*EPU2-A*EPU2**2)
      DEN=DEN-BR*(A*EPU2**2*(Z(I)-DE)**3-3.0*A*B*Z(I)*EPU2*(Z(I)-DE)**2)
      X4=NUM/(4.0*DEN)
      L=DEFF-Z(I)+X4
      GOTO 333
C
C     ***********************************************************
C     PARABOLIC-LINEAR CONCRETE COMPRESSION PROFILE SERIES
C     ***********************************************************
C
C     PARABOLIC-LINEAR PROFILE ALL WITHIN FLANGE, STEEL ELASTIC
C
20    K1=A*(1.0-B/(3.0*EPU2))
      A1=K1*BR
```

```
      B1=A2*(A3+A4*EPU2+A5)
      C1=A2*DEFF*EPU2
      Z(I)=(B1+SQRT((B1**2)+(4.0*A1*C1)))/(2.0*A1)
      T(I)=A2*(A3+A4*EPU2+A5+(DEFF*EPU2/Z(I)))
      IF (Z(I).LT.DE) THEN
                IF(T(I).LT.LIMIT1) THEN
                  X1=(5.0*B**2)/(12.0*EPU2**2)
                  X2=0.5*(1.0-(B**2/EPU2**2))
                  X3=(1.0-B/(3.0*EPU2))
                  X4=Z(I)*(X1+X2)/X3
                  L=DEFF-Z(I)+X4
                  GO TO 333
                ENDIF
      ENDIF
C
C     PARABOLIC-LINEAR PROFILE ALL WITHIN FLANGE, STEEL INELASTIC
C
      ENEW=(0.2*FPU/GAM2)/((0.2*FPU)/(GAM2*1000.0*ES)+0.005)
      G=0.8*FPU/GAM2
      B1=AS*(ENEW*(A3+A4*EPU2+A5-G/(1000.0*ES))+G)
      C1=AS*ENEW*DEFF*EPU2
      Z(I)=(B1+SQRT((B1**2)+(4.0*A1*C1)))/(2.0*A1)
      T(I)=AS*ENEW*(A3+A4+(DEFF*EPU2/Z(I))-EPU2+A5-G/(1000.0*ES))+G*AS
      IF (Z(I).LT.DE) THEN
                IF (T(I).GT.LIMIT1) THEN
                  X1=(5.0*B**2)/(12.0*EPU2**2)
                  X2=0.5*(1.0-(B**2/EPU2**2))
                  X3=(1.0-B/(3.0*EPU2))
                  X4=Z(I)*(X1+X2)/X3
                  L=DEFF-Z(I)+X4
                  GO TO 333
                ENDIF
      ENDIF
C
C     PARABOLIC-LINEAR PROFILE WITHIN WEB AND FLANGE, FUNCTION
C     CHANGEOVER IN WEB, STEEL ELASTIC
C
      AA=BW*((2.0*A*B)/(3.0*EPU2)-A*(A*B/EPU2))
      BB=(BR-BW)*A*DE+(A2*(EPU2-A3-A4-A5))
      CC=(AS*1000.0*ES*DEFF*EPU2)
      Z(I)=(-BB+SQRT((BB**2)+(4.0*AA*CC)))/(2.0*AA)
      NUM=BW*((A*Z(I)-DE)**2)/2.0)
      &-(1.0*A*(B**2)*(Z(I)**2))/(12.0*EPU2**2))
      NUM=NUM+(BR*((A*Z(I)**2/2.0)-(A*DE*Z(I))+(DE**2/2.0)))
      DEN=BW*((2.0*A*B*Z(I))/(3.0*EPU2)
      &+(A*DE)-(A*B*Z(I))/(EPU2))
      DEN=DEN+(BR*A*DE)
      X4=NUM/DEN
      T(I)=A2*(A3+A4+EPU2+A5+(DEFF*EPU2/Z(I)))
      L=DEFF-Z(I)+X4
      CHANGE=Z(I)-((B*Z(I)/EPU2))
      IF (CHANGE GT.DE) THEN
                IF (T(I).LT.LIMIT1) THEN
                  GOTO 333
                ENDIF
      ENDIF
C
C     PARABOLIC-LINEAR PROFILE WITHIN WEB AND FLANGE, FUNCTION
C     CHANGEOVER IN WEB, STEEL INELASTIC
C
      AA=BW*((2.0*A*B)/(3.0*EPU2))-A*(A*B/EPU2))
      BB=(BR-BW)*A*DE+(AS*ENEW*(A3+A4+EPU2+A5-G/(1000.0*ES)))-G*AS
      CC=(AS*ENEW*DEFF*EPU2)
      Z(I)=(-BB+SQRT((BB**2)+(4.0*AA*CC)))/(2.0*AA)
      NUM=BW*((A*Z(I)-DE)**2)/2.0)
      &-(1.0*A*(B**2)*(Z(I)**2))/(12.0*EPU2**2))
      NUM=NUM+(BR*((A*Z(I)**2/2.0)-(A*(Z(I)-DE)**2)/(2.0)))
      DEN=BW*((2.0*A*B*Z(I))/(3.0*EPU2)
      &+(A*Z(I))-(A*DE)-(A*B*Z(I))/(EPU2))
      DEN=DEN+(BR*A*DE)
      X4=NUM/DEN
      T(I)=AS*ENEW*(A3+A4+(DEFF*EPU2/Z(I))-EPU2+A5-G/(1000.0*ES))+G*AS
      L=DEFF-Z(I)+X4
      CHANGE=Z(I)-((B*Z(I)/EPU2))
      IF (CHANGE GT.DE) THEN
                IF (T(I) GT LIMIT1) THEN
                  GOTO 333
                ENDIF
      ENDIF
C
C     PARABOLIC-LINEAR PROFILE WITHIN WEB AND FLANGE, FUNCTION
C     CHANGEOVER IN FLANGE, STEEL ELASTIC
C
      AA=BR*((2.0*A*B)/(3.0*EPU2)+A*(1.0-B/EPU2))
      AA=AA+(BW-BR)*((A*EPU2)/B-(A*EPU2**2)/(3.0*B**2))
      BB=(BW-BR)*((A*DE*EPU2**2)/(B**2)-(2.0*A*DE*EPU2)/B)
      BB=BB-A2*(A3+A4+EPU2+A5)
      CC=(BW-BR)*(((A*EPU2*DE**2)/B)-(A*(DE**2)*EPU2**2)/B**2)
      CC=CC-(AS*1000.0*ES*DEFF*EPU2)
      DD=(BR-BW)*(A*(DE**3)*EPU2**2)/(3.0*B**2)
      ROOT1=0.0
      ROOT2=DEFF
17    ROOT3=(ROOT1+ROOT2)/2.0
      FUNCX1=(AA*ROOT1**3)+(BB*ROOT1**2)+(CC*ROOT1)+DD
      FUNCX2=(AA*ROOT2**3)+(BB*ROOT2**2)+(CC*ROOT2)+DD
      FUNCX3=(AA*ROOT3**3)+(BB*ROOT3**2)+(CC*ROOT3)+DD
      IF (FUNCX3.LT.0.0) THEN
                ROOT1=ROOT3
      ELSE
                ROOT2=ROOT3
      ENDIF
      AB=ABS(ROOT1-ROOT2)
      IF (AB.GT.0.0001) THEN
                GO TO 17
      ENDIF
      Z(I)=ROOT3
      NUM=(BW-BR)*(2.0*A*EPU2*(Z(I)-DE)**3)/(3.0*Z(I)*B)
      NUM=NUM-((BW-BR)*A*(EPU2**2)
      &*((Z(I)-DE)**4)/(4.0*(B**2)*(Z(I)**2)))
      NUM=NUM+BR*(((A*Z(I)**2)/2.0)
      &-((1.0/(12.0*EPU2**2))*A*(B**2)*Z(I)**2))
      DEN=(BW-BR)*((A*EPU2*(Z(I)-DE)**2)/(Z(I)*B))
      DEN=DEN-((BW-BR)*((A*(EPU2**2)
      &*(Z(I)-DE)**3)/(3.0*(B**2)*Z(I)**2)))
      DEN=DEN+(BR*((2.0*A*B*Z(I))/(3.0*EPU2)+(A*Z(I)*(1.0-(B)/EPU2))))
      X4=NUM/DEN
      T(I)=A2*(A3+A4+EPU2+A5+(DEFF*EPU2/Z(I)))
      L=DEFF-Z(I)+X4
      CHANGE=Z(I)-((B*Z(I)/EPU2))
      IF (CHANGE LT.DE) THEN
                IF (T(I) LT LIMIT1) THEN
                  GOTO 333
                ENDIF
      ENDIF
C
C     PARABOLIC-LINEAR PROFILE WITHIN WEB AND FLANGE, FUNCTION
C     CHANGEOVER IN FLANGE, STEEL INELASTIC
C
      AA=(((2.0*A*B)/(3.0*EPU2))+A*(1.0-(B/EPU2)))*BR
      AA=AA+((BW-BR)*((A*EPU2/B)-(A*EPU2**2)/(3.0*B**2.0)))
```

```
      BB=(BW-BR)*((A*DE*EPU2**2)/(B**2)-(2.0*A*DE*EPU2)/B)
      BB=BB-(AS*ENEW*(A3+A4-EPU2+AS-G/(1000.0*ES)))-G*AS
      CC=(BW-BR)*(((A*EPU2*DE**2)/B)-(A*(DE**2)*EPU2**2)/B**2)
      CC=CC-(AS*ENEW*DEFF*EPU2)
      DD=(BR-BW)*(A*(DE**3)*EPU2**2)/(3.0*B**2)
      ROOT1=0.0
      ROOT2=DEFF
   18 ROOT3=(ROOT1+ROOT2)/2.0
      FUNCX1=(AA*ROOT1**3)+(BB*ROOT1**2)+(CC*ROOT1)+DD
      FUNCX2=(AA*ROOT2**3)+(BB*ROOT2**2)+(CC*ROOT2)+DD
      FUNCX3=(AA*ROOT3**3)+(BB*ROOT3**2)+(CC*ROOT3)+DD
      IF (FUNCX3.LT.0.0) THEN
                ROOT1=ROOT3
      ELSE
                ROOT2=ROOT3
      ENDIF
      AB=ABS(ROOT1-ROOT2)
      IF (AB.GT.0.0001) THEN
                GO TO 18
      ENDIF
      Z(I)=ROOT3
      NUM=(BW-BR)*(2.0*A*EPU2*(Z(I)-DE)**3)/(3.0*Z(I)*B)
      NUM=NUM-((BW-BR)*A*(EPU2**2)
     &*((Z(I)-DE)**4)/(4.0*(B**2)*(Z(I)**2)))
      NUM=NUM+BR*(((A*Z(I)**2)/2.0)
     &-((1.0/(12.0*EPU2**2))*A*(B**2)*Z(I)**2))
      DEN=(BW-BR)*((A*EPU2*(Z(I)-DE)**2)/(Z(I)*B))
      DEN=DEN-((BW-BR)*((A*(EPU2**2)
     &*(Z(I)-DE)**3)/(3.0*(B**2)*Z(I)**2)))
      DEN=DEN+(BR*((2.0*A*B*Z(I))/(3.0*EPU2)-(A*Z(I)*(1.0-(B/EPU2)))))
      X4=NUM/DEN
      T(I)=AS*ENEW*(A3+A4+(DEFF*EPU2/Z(I))-EPU2+AS-G/(1000.0*ES))+G*AS
      L=DEFF-Z(I)+X4
      CHANGE=Z(I)-((B*Z(I))/EPU2)
      IF (CHANGE.LT.DE) THEN
                IF (T(I).GT.LIMIT1) THEN
                  GOTO 333
                ENDIF
      ENDIF
  333 MN=T(I)*L
      RETURN
      END
*     ****************************************************
      SUBROUTINE CRACKS1(TEMPP,TEMPN,NODE1,NODE2,LB1,LB2,
     &MCRP,MCRN,COUNTP,COUNTN,SPACE1,SPACE2,H,I1,I2)
*     ****************************************************
*     SUBROUTINE CRACKS CALCULATES ALL NODES WHICH ARE
*     CRACKED
*     ****************************************************
      DOUBLE PRECISION TEMPP,TEMPN,MCRP(2001),MCRN(2001),H
      DOUBLE PRECISION LB1,LB2
      INTEGER COUNTP,COUNTN,NODE1(2001),NODE2(2001),SPACE1,SPACE2
      INTEGER I1,I2,I
*     ****************************************************
*     POSITIVE NODES
*     ****************************************************
      IF (TEMPP.NE.0.0) THEN
      NODE1(I1)=I1
      COUNTP=1
      SPACE1=2*INT((1.5*LB1)/(H*1000.0*2.0))
      I=I1
  140 NODE1(I-SPACE1)=NODE1(I)+SPACE1
      IF (MCRP(NODE1(I)+SPACE1).NE.0.0) THEN
                I=I+SPACE1
                COUNTP=COUNTP+1
                GO TO 140
      ELSE
                NODE1(I+SPACE1)=0.0
                I=I1
  150   NODE1(I-SPACE1)=NODE1(I)-SPACE1
                IF (MCRP(NODE1(I-SPACE1)).NE.0.0) THEN
                  I=I-SPACE1
                  COUNTP=COUNTP+1
                  GO TO 150
                ELSE
                  NODE1(I-SPACE1)=0.0
                ENDIF
      ENDIF
      ENDIF
*     ****************************************************
*     NEGATIVE NODES
*     ****************************************************
      IF (TEMPN.NE.0.0) THEN
      NODE2(I2)=I2
      COUNTN=1
      SPACE2=2*INT((1.5*LB2)/(H*1000.0*2.0))
      I=I2
  394 NODE2(I+SPACE2)=NODE2(I)+SPACE2
      IF (MCRN(NODE2(I+SPACE2)).NE.0.0) THEN
                I=I+SPACE2
                COUNTN=COUNTN+1
                GO TO 394
      ELSE
                NODE2(I+SPACE2)=0.0
                I=I2
        IF (I.NE.1) THEN
  170   NODE2(I-SPACE2)=NODE2(I)-SPACE2
                IF (MCRN(NODE2(I-SPACE2)).NE.0.0) THEN
                  I=I-SPACE2
                  COUNTN=COUNTN+1
                  GO TO 170
                ELSE
                  NODE2(I-SPACE2)=0.0
                ENDIF
        ENDIF
      ENDIF
      ENDIF
      RETURN
      END
*     ****************************************************
      SUBROUTINE CRACKS2(TEMPP,TEMPNA,TEMPNB,NODE1,NODE2A,NODE2B,
     &LB1,LB2A,LB2B,MCRP,MCRNA,MCRNB,COUNTP,COUNTNA,COUNTNB,
     &SPACE1,SPACE2A,SPACE2B,H,I1,I2A,I2B)
*     ****************************************************
*     SUBROUTINE CRACKS CALCULATES ALL NODES WHICH ARE
*     CRACKED
*     ****************************************************
      DOUBLE PRECISION TEMPP,TEMPNA,TEMPNB,H,LB1,LB2A,LB2B
      DOUBLE PRECISION MCRP(2001),MCRNA(2001),MCRNB(2001)
      INTEGER COUNTP,COUNTNA,COUNTNB
      INTEGER NODE1(2001),NODE2A(2001),NODE2B(2001)
      INTEGER SPACE1,SPACE2A,SPACE2B
      INTEGER I1,I2A,I2B,I
*     ****************************************************
*     POSITIVE NODES
*     ****************************************************
      IF (TEMPP.NE.0.0) THEN
      NODE1(I1)=I1
      COUNTP=1
      SPACE1=2*INT((1.5*LB1)/(H*1000.0*2.0))
```

```
      I=I1
140   NODE1(I+SPACE1)=NODE1(I)+SPACE1
      IF (MCRP(NODE1(I+SPACE1)) NE 0 0) THEN
                I=I+SPACE1
                COUNTP=COUNTP+1
                GO TO 140
      ELSE
                NODE1(I+SPACE1)=0 0
                I=I1
150     NODE1(I-SPACE1)=NODE1(I)-SPACE1
                IF (MCRP(NODE1(I-SPACE1)) NE 0 0) THEN
                  I=I-SPACE1
                  COUNTP=COUNTP+1
                  GO TO 150
                ELSE
                  NODE1(I-SPACE1)=0 0
                ENDIF
      ENDIF
      ENDIF
C     ***************************************************
C     NEGATIVE NODES
C     ***************************************************
      IF (TEMPNA NE 0 0) THEN
      NODE2A(I2A)=I2A
      COUNTNA=1
      SPACE2A=2*INT((1 5*LB2A)/(H*1000 0*2 0))
      I=I2A
10    NODE2A(I-SPACE2A)=NODE2A(I)-SPACE2A
      IF (MCRNA(NODE2A(I-SPACE2A)) NE 0 0) THEN
                I=I-SPACE2A
                COUNTNA=COUNTNA+1
                GO TO 10
      ELSE
                NODE2A(I-SPACE2A)=0 0
                I=I2A
       IF (I2A NE 1) THEN
20      NODE2A(I-SPACE2A)=NODE2A(I)-SPACE2A
                IF (MCRNA(NODE2A(I-SPACE2A)) NE 0 0) THEN
                  I=I-SPACE2A
                  COUNTNA=COUNTNA+1
                  GO TO 20
                ELSE
                  NODE2A(I-SPACE2A)=0 0
                ENDIF
       ENDIF
      ENDIF
      ENDIF
      IF (TEMPNB NE 0 0) THEN
      NODE2B(I2B)=I2B
      COUNTNB=1
      SPACE2B=2*INT((1 5*LB2B)/(H*1000 0*2 0))
      I=I2B
30    NODE2B(I-SPACE2B)=NODE2B(I)-SPACE2B
      IF (MCRNB(NODE2B(I-SPACE2B)) NE 0 0) THEN
                I=I-SPACE2B
                COUNTNB=COUNTNB+1
                GO TO 30
      ELSE
                NODE2B(I-SPACE2B)=0 0
                I=I2B
40      NODE2B(I-SPACE2B)=NODE2B(I)-SPACE2B
                IF (MCRNB(NODE2B(I-SPACE2B)) NE 0 0) THEN
                  I=I-SPACE2B
                  COUNTNB=COUNTNB+1
                  GO TO 40
                ELSE
                  NODE2B(I-SPACE2B)=0 0
                ENDIF
      ENDIF
      ENDIF
      RETURN
      END
C     ***************************************************
      SUBROUTINE TFORCEP(N,P,EI,XB,CRACK,NODE1,TEMPP,
     &SPACE1,COUNTP,A,AC,AS,B,EC,E,EPU,ES,GAM2,L,P1,ULT,
     &Z,FPU,Y,RES1,ECR,SEC,M,RES,DF1,DF2,BF1,BF2,BW,DE)
C     ***************************************************
C     SUBROUTINE TFORCE CALCULATES THE TENDON FORCE
C     AS THE BEAM CRACKS,(AND ALSO CHANGES IN EI VALUES)
C     ***************************************************
      DOUBLE PRECISION P(2001),EI(2001),TEMPP,A,AC,AS,B,EC
      DOUBLE PRECISION EPU,ES,GAM2,L,P1(2001),SEC1(2001),ULT(2001)
      DOUBLE PRECISION Z(2001),BR,FPU,MN,EPU2,EPU1,X4,Y,RES1(2001)
      DOUBLE PRECISION SEC(2001),M,RES(2001),E(2001),T(2001),ECR
      DOUBLE PRECISION DF1,DF2,BF1,BF2,BW,DE
      INTEGER N,XB,CRACK(2001),NODE1(2001)
      INTEGER SPACE1,COUNTP,I,V,J,SPACE3,SPACE4
C     ***************************************************
C     CALCULATION OF TENDON FORCE +VE CRACKS
C     ***************************************************
      IF (TEMPP NE 0 0) THEN
      J=1
      I=1
180   IF (I LE (N+1)) THEN
                IF (NODE1(I) NE 0 0) THEN
                  IF (J EQ 1) THEN
      CALL BICHOP(A,AC,AS,B,EC,E,EPU,ES,GAM2,L,P1,ULT,Z,
     &FPU,MN,EPU2,EPU1,X4,Y,I,T,RES1,ECR,SEC,M,EI,P,DF1,DF2,
     &BF1,BF2,BW,DE)
                    SPACE3=SPACE1/1.5
                    THETA=(180 0)/(SPACE3)
                    THETA1=0 0
                    CRACK(XB+J)=I-SPACE3
                    CRACK(XB+J+1)=I
                    DO 190 V=(I-1),(I-SPACE3),-1
                      THETA1=THETA1+THETA
                      P(V)=((P(I)-P(I-SPACE3))/2.0)*
     &  ((COS(THETA1*(3 141593/180 0))+1 0))+P(I-SPACE3)
                      EI(V)=((EI(I)-EI(I-SPACE3))/2.0)*
     &  ((COS(THETA1*(3 141593/180 0))+1 0))+EI(I-SPACE3)
190                 CONTINUE
                    GO TO 220
                  ELSEIF (J LE COUNTP) THEN
      CALL BICHOP(A,AC,AS,B,EC,E,EPU,ES,GAM2,L,P1,ULT,Z,
     &FPU,MN,EPU2,EPU1,X4,Y,I,T,RES1,ECR,SEC,M,EI,P,DF1,DF2,BF1,
     &BF2,BW,DE)
                      SPACE4=(SPACE1/2)
                      THETA=(180 0)/(SPACE4)
                      THETA1=0 0
                      DO 200 V=(I-SPACE1+1),(I-SPACE4),1
                        THETA1=THETA1+THETA
                  SCALE=0 25*(((P(I-SPACE1)+P(I))/2 0)-P(I+SPACE4))
                  SCALE1=0 25*(((EI(I-SPACE1)+EI(I))/2 0)-EI(I+SPACE4))
                        P(V)=((P(I-SPACE1)-P(I+SPACE4)-SCALE)/2 0)*
     &  ((COS(THETA1*(3 141593/180))+1 0))+P(I+SPACE4)+
     &  SCALE
                        EI(V)=((EI(I-SPACE1)-EI(I+SPACE4)-SCALE1)/2.0)*
     &  ((COS(THETA1*(3 141593/180))+1 0))+EI(I+SPACE4)+
     &  SCALE1
200                 CONTINUE
```

```
      THETA=(180.0)/(SPACE4)
      CRACK(XB+2*J-1)=I+SPACE4
      CRACK(XB+2*J)=I
      DO 210 V=(-1.1),(-SPACE4,-1
      THETA1=THETA1+THETA
      P(V)=((P(I)-P(1-SPACE4)*2.0)*
     &    ((COS(THETA1*(3.141593/180.0))+1.0))+P(1-SPACE4)
      E(V)=((E(I)-E(1-SPACE4)*2.0)*
     &    ((COS(THETA1*(3.141593/180.0))+1.0))+E(1-SPACE4)
  210 CONTINUE
      ENDIF
  230 IF (I.EQ.COUNTP) THEN
      CALL BICHOP(A,AC,AS,B,EC,E,EPU,ES,GAM2,LP1,ULT2,
     &EPU,UN,EPU2,EPU1,X4,YLT,RES,ECR,SEC,M,EI,P,DP1,DP2,BF1,
     &BF2,BW,DE)
      THETA1=0.0
      THETA=(180.0)/(SPACE3)
      CRACK(XB+2*J-1)=I+SPACE3
      DO 290 V=(-1.1),(-SPACE3),1
      THETA1=THETA1+THETA
      P(V)=((P(I)-P(1-SPACE3))*2.0)*
     &    ((COS(THETA1*(3.141593/180.0))+1.0))+P(1-SPACE3)
      E(V)=((E(I)-E(1-SPACE3))*2.0)*
     &    ((COS(THETA1*(3.141593/180.0))+1.0))+E(1-SPACE3)
  290 CONTINUE
      ENDIF
      J=J+1
      ENDIF
      I=I+1
      GO TO 240
      ENDIF
      X3=X3-2*COUNTM+1
      SPACE3=SPACE3/5
      THETA=(180.0)/(SPACE3)
```

- **********
- CALCULATION OF TENDON FORCE AT GRADES
- **********

```
      IF (NEW.NE.0) THEN
      I=I
      J=1
  240 IF (I.LE.(N-1)) THEN
      IF (NODE3.NE.0) THEN
      IF (I.EQ.1) THEN
      CALL BICHOP(AC,AS,BC,EC,E,EPU,ES,GAM2,LP1,ULT2,
     &AFPU,UN,EPU2,EPU1,X4,YLT,RES,ECR,SEC,M,EI,P,DP1,DP2,BF1,
     &BF2,BW,DE)
      SPACE4=(SPACE2/2)
      THETA=(180.0)/(SPACE4)
      CRACK(XB+2*J-1)=I-SPACE4
      CRACK(XB+2*J)=I
      DO 260 V=(-1.SPACE2+1),(-SPACE4),1
      THETA1=THETA1+THETA
      P(V)=((P(I)-P(1-SPACE4))*2.0)*
     &    ((COS(THETA1*(3.141593/180.0))+1.0))+P(1-SPACE4)
      E(V)=((E(I)-E(1-SPACE4))*2.0)*
     &    ((COS(THETA1*(3.141593/180.0))+1.0))+E(1-SPACE4)
  260 CONTINUE
      ENDIF
      J=J+1
      ENDIF
      I=I+1
      GO TO 240
      ENDIF
      X3=X3-2*COUNTP+1
      SPACE3=SPACE3/5
      THETA=(180.0)/(SPACE3)
```

- **********
- SUBROUTINE FORCE CALCULATES THE TENDON FORCE
- AS THE BEAM CRACKS/AND ALSO CHANGES IN EI VALUES)
- **********

```
      DOUBLE PRECISION P(200),E(200),ITEMP,ACACABEC
      DOUBLE PRECISION ERR,GAM2,LP1(200),ULT(200),
      DOUBLE PRECISION Z(200),BAFPU,UN,EPU2,EPU1,X4,YLT,RES(200),
      DOUBLE PRECISION SEC(200),UN,ABES(200),LC(200),FC(200),ECR,
      DOUBLE PRECISION DP1,DP2,BF1,BF2,BW,DE
      INTEGER VAR,CRACK(200),NODE(2000)
      INTEGER SPACE,COUNTM,XY,SPACE1,SPACE2,SPACE4
      IF (NEW.NE.0) THEN
      I=1
      J=1
  210 IF (I.LE.(N-1)) THEN
      IF (NODE3.NE.0) THEN
      IF (I.EQ.1) THEN
      CALL BICHOP(AC,AS,BC,EC,E,EPU,ES,GAM2,LP1,ULT2,
     &AFPU,UN,EPU2,EPU1,X4,YLT,RES,ECR,SEC,M,EI,P,DP1,DP2,BF1,
     &BF2,BW,DE)
      SPACE=SPACE1/5
      THETA=(180.0)/(SPACE)
```

- **********
- CALCULATION OF TENDON FORCE AT GRADES
- **********

```
      IF (NEW.NE.0) THEN
      I=I
      J=1
  230 IF (I.LE.(N-1)) THEN
      IF (NODE3.NE.0) THEN
      IF (I.EQ.1) THEN
      CALL BICHOP(AC,AS,BC,EC,E,EPU,ES,GAM2,LP1,ULT2,
     &AFPU,UN,EPU2,EPU1,X4,YLT,RES,ECR,SEC,M,EI,P,DP1,DP2,BF1,
     &BF2,BW,DE)
      SPACE=SPACE1/5
      THETA=(180.0)/(SPACE)
      THETA1=0.0
      CRACK(XB+2*J-1)=I+SPACE4
      CRACK(XB+2*J)=I
      DO 210 V=(-1.1),(-SPACE4,-1
      THETA1=THETA1+THETA
      P(V)=((P(I)-P(1-SPACE4)*2.0)*
     &    ((COS(THETA1*(3.141593/180.0))+1.0))+P(1-SPACE4)
      E(V)=((E(I)-E(1-SPACE4))*2.0)*
     &    ((COS(THETA1*(3.141593/180.0))+1.0))+E(1-SPACE4)
  210 CONTINUE
      ENDIF
      J=J+1
      ENDIF
      I=I+1
      GO TO 240
      ENDIF
      X3=X3-2*COUNTP+1
      SPACE=SPACE1/5
      THETA=(180.0)/(SPACE)
      THETA1=0.0
      CRACK(XB+2*J-1)=I-SPACE3
      CRACK(XB+2*J)=I
      DO 250 V=(-1.1),(-SPACE3),-1
      THETA1=THETA1+THETA
      P(V)=((P(I)-P(1-SPACE3))*2.0)*
     &    ((COS(THETA1*(3.141593/180.0))+1.0))+P(1-SPACE3)
      E(V)=((E(I)-E(1-SPACE3))*2.0)*
     &    ((COS(THETA1*(3.141593/180.0))+1.0))+E(1-SPACE3)
  250 CONTINUE
      ENDIF
      IF (I.EQ.COUNTN) THEN
      CRACK(XB+J)=(-1.SPACE3)
      GO TO 280
      ELSEIF (I.LE.COUNTN) THEN
      CALL BICHOP(AA,AC,AS,B,EC,E,EPU,ES,GAM2,LP1,ULT2,
     &EPU,UN,EPU2,EPU1,X4,YLT,RES,ECR,SEC,M,EI,P,DP1,DP2,BF1,
     &BF2,BW,DE)
      THETA1=0.0
      THETA=(180.0)/(SPACE3)
      CRACK(XB+2*J-1)=I+SPACE3
      DO 290 V=(-1.1),(-SPACE3),1
      THETA1=THETA1+THETA
      P(V)=((P(I)-P(1-SPACE3))*2.0)*
     &    ((COS(THETA1*(3.141593/180.0))+1.0))+P(1-SPACE3)
      E(V)=((E(I)-E(1-SPACE3))*2.0)*
     &    ((COS(THETA1*(3.141593/180.0))+1.0))+E(1-SPACE3)
  290 CONTINUE
      ENDIF
      J=J+1
      ENDIF
      I=I+1
      GO TO 240
      ENDIF
      X3=X3-2*COUNTN+1
```

```
      ENDIF
      RETURN
      END
C     ****************************************************************
      SUBROUTINE BUBBLE(XB,CRACK)
C     ****************************************************************
C     SUROUTINE BUBBLE PERFORMS A BUBBLE SORT FOR CRACKS
C     ****************************************************************
      INTEGER TEMP,CRACK(2001),I,XB
      LOGICAL SORTED
      SORTED=.FALSE.
300   IF(.NOT.SORTED) THEN
            SORTED=.TRUE.
            DO 310 I=1,XB-1
              IF (CRACK(I).GT.CRACK(I+1)) THEN
                TEMP=CRACK(I)
                CRACK(I)=CRACK(I+1)
                CRACK(I+1)=TEMP
                SORTED=.FALSE.
              ENDIF
310   CONTINUE
            GO TO 300
      ENDIF
      RETURN
      END
C     ****************************************************************
      SUBROUTINE INITIAL2(P,NODE1,NODE2,CRACK,XB,N,PF)
C     ****************************************************************
C     SUBROUTINE INIT INITIALISES TENDON FORCE P(I), NODE
C     VALUES AND CRACKED NODES
C     ****************************************************************
      DOUBLE PRECISION P(2001),PF
      INTEGER NODE1(2001),NODE2(2001),CRACK(2001),I,N,XB
      DO 130 I=1,2001,1
            P(I)=PF
            NODE1(I)=0
            NODE2(I)=0
            CRACK(I)=0
130   CONTINUE
      XB=2
      CRACK(1)=1
      CRACK(2)=N+1
      RETURN
      END
C     ****************************************************************
      SUBROUTINE INITIAL3(P,NODE1,NODE2A,NODE2B,CRACK,XB,N,PF)
C     ****************************************************************
C     SUBROUTINE INIT INITIALISES TENDON FORCE P(I), NODE
C     VALUES AND CRACKED NODES
C     ****************************************************************
      DOUBLE PRECISION P(2001),PF
      INTEGER NODE1(2001),NODE2A(2001),CRACK(2001),I,N,XB
      INTEGER NODE2B(2001)
      DO 130 I=1,2001,1
            P(I)=PF
            NODE1(I)=0
            NODE2A(I)=0
            NODE2B(I)=0
            CRACK(I)=0
130   CONTINUE
      XB=2
      CRACK(1)=1
      CRACK(2)=N+1
      RETURN
      END
C     ****************************************************************
      SUBROUTINE SPANSET(A,B,N,L,H,BW,BF1,BF2,DF1,DF2,DE,AC,Y,FCU,
     &ECR,GAM1,XL,ELH,ERH,E1,E,PF,P1,P,DEF,SEC1,EI,EC)
C     ****************************************************************
C     SUBROUTINE SPANSET SETS VARIOUS CRITERIA FOR THE INDIVIDUAL
C     SPANS
C     ****************************************************************
      DOUBLE PRECISION AREA(4),L,H,BF1,BF2,BW,DF1,DF2,DE,CS(4)
      DOUBLE PRECISION TEMP1,AC,Y,SEC2,A,B,FCU,ECR,GAM1,XL(2001)
      DOUBLE PRECISION ELH,ERH,E1,E(2001),PF,P1(2001),P(2001)
      DOUBLE PRECISION DEF(2001),SEC1(2001),EI(2001),EC
      INTEGER N,I
C     ****************************************************************
      N=(L/H+0.5)
      AREA(1)=(BF1*DF1)
      AREA(2)=(DE-DF1-DF2)*BW
      AREA(3)=(BF2*DF2)
      CS(1)=(DF1/2.0)
      CS(2)=DF1+((DE-DF1-DF2)/2.0)
      CS(3)=DE-DF2/2.0
      TEMP1=0.0
      AC=0.0
      DO 11 I=1,3,1
            TEMP1=TEMP1+(AREA(I)*CS(I))
            AC=AC+AREA(I)
11    CONTINUE
      Y=TEMP1/AC
      SEC2=((BF1*DF1**3)+(BF2*DF2**3)+(BW*(DE-DF1-DF2)**3))/12.0
      DO 12 I=1,3,1
            SEC2=SEC2+(AREA(I)*(CS(I)-Y)**2)
12    CONTINUE
      A=0.67*FCU/GAM1
      B=0.00024*SQRT(FCU/GAM1)
      ECR=0.59*SQRT(FCU/GAM1)
      DO 10 I=1,N,1
            XL(I+1)=XL(I)+H
10    CONTINUE
      DO 20 I=1,(N+1),1
            E(I)=(0.004)*((E1*XL(I))/L)*(1-XL(I)/L)
     &  -((ELH/1000.0)-(ELH*XL(I)/(L*1000.0)))
     &  +(ERH*XL(I)/(L*1000.0)))
            DEF(I)=Y+(E(I)*1000.0)
20    CONTINUE
      DO 25 I=1,2001,1
       P1(I)=PF
       P(I)=PF
       SEC1(I)=SEC2
       EI(I)=(EC*SEC1(I))/(10.0**6)
25    CONTINUE
      RETURN
      END
C     ****************************************************************
      SUBROUTINE PRIMARY(AL,LOAD,FD,P,E,N)
C     ****************************************************************
C
C
C     ****************************************************************
      DOUBLE PRECISION AL(2001),LOAD,FD(2007,7),P(2001),E(2001)
      INTEGER N,I
      DO 50 I=1,(N+1),1
            AL(I)=LOAD
            FD(I+3,1)=-(P(I)*E(I))
50    CONTINUE
      RETURN
      END
```

```
C ***********************************************************
      SUBROUTINE INITIAL1(N1,N2,N3,XB1,XB2,XB3,CRACK1,CRACK2,CRACK3,
     &MCRP1,MCRP2,MCRP3,MCRN1,MCRN2A,MCRN2B,MCRN3)
C ***********************************************************
C
C
C ***********************************************************
      INTEGER I,XB1,XB2,XB3,CRACK1(2001),CRACK2(2001),CRACK3(2001)
      INTEGER N1,N2,N3
      DOUBLE PRECISION MCRP1(2001),MCRP2(2001),MCRP3(2001)
      DOUBLE PRECISION MCRN1(2001),MCRN2A(2001),MCRN2B(2001),MCRN3(2001)
      DO 25 I=1,2001,1
            MCRP1(I)=0.0
            MCRP2(I)=0.0
            MCRP3(I)=0.0
            MCRN1(I)=0.0
            MCRN2A(I)=0.0
            MCRN2B(I)=0.0
            MCRN3(I)=0.0
25    CONTINUE
      XB1=2
      XB2=2
      XB3=2
      CRACK1(1)=1
      CRACK2(1)=1
      CRACK3(1)=1
      CRACK1(2)=N1+1
      CRACK2(2)=N2+1
      CRACK3(2)=N3+1
      RETURN
      END
C ***********************************************************
      SUBROUTINE LOADSUM(N,LOAD,AL,C,XB,C1)
C ***********************************************************
      DOUBLE PRECISION LOAD,C(2001),C1(2001),AL(2001)
      INTEGER N,XB,I
      DO 70 I=1,(N+1),1
            AL(I)=LOAD
            C(I)=C(I)+AL(I)
70    CONTINUE
      DO 80 K=1,XB,1
            C1(K)=C1(K)+AL(K)
80    CONTINUE
      RETURN
      END
C ***********************************************************
      SUBROUTINE REVERSE (EI,D,XL,N)
C ***********************************************************
C REVERSES EI AND D VALUES FOR FEMS
C ***********************************************************
      DOUBLE PRECISION EI(2001),D(2001),XL(2001)
      DOUBLE PRECISION TEMP1(2001),TEMP2(2001),TEMP3(2001)
      INTEGER I,N
      DO 13 I=1,(N+1),1
            TEMP1(I)=D(I)
            TEMP2(I)=EI(I)
            TEMP3(I)=XL(I)
10    CONTINUE
      DO 20 I=1,(N+1),1
            D(I)=TEMP1(N+2-I)
            EI(I)=TEMP2(N+2-I)
            XL(I)=TEMP3(N+2-I)
20    CONTINUE
      RETURN
      END
```

```
C ***********************************************************
      SUBROUTINE MDIST(CO1,CO2,CO3,CO4,CO5,CO6,M1,M2,M3,M4,M5,M6,
     &MX1,MX2,MX3,MX4,MX5,MX6,TOTAL)
C ***********************************************************
C PERFORMS MOMENT DISTRIBUTION ON THREE SPAN CONTNUOUS
C BEAMS
C ***********************************************************
      DOUBLE PRECISION CO1,CO2,CO3,CO4,CO5,CO6
      DOUBLE PRECISION M1,M2,M3,M4,M5,M6
      DOUBLE PRECISION MX1,MX2,MX3,MX4,MX5,MX6
      DOUBLE PRECISION DF(6),COF(6)
      DOUBLE PRECISION R(6),CO(6),TOTAL(6),TOTAL1(6)
      INTEGER I
C
      COF(1)=CO1
      COF(2)=0.0
      COF(3)=CO3
      COF(4)=CO4
      COF(5)=0.0
      COF(6)=CO6
      CO(1)=M1
      CO(2)=M2
      CO(3)=M3
      CO(4)=M4
      CO(5)=M5
      CO(6)=M6
      DF(1)=1.0
      DF(2)=((1-CO1*CO2)*MX2)/(((1-CO1*CO2)*MX2)+MX3)
      DF(3)=MX3/(((1-CO1*CO2)*MX2)+MX3)
      DF(4)=MX4/(MX4+((1-CO5*CO6)*MX5))
      DF(5)=((1-CO5*CO6)*MX5)/(MX4+((1-CO5*CO6)*MX5))
      DF(6)=1.0
      DO 10 I=1,6,1
            TOTAL(I)=CO(I)
10    CONTINUE
30    DO 12 I=1,6,1
            TOTAL1(I)=TOTAL(I)
12    CONTINUE
      R(1)=-(DF(1)*CO(1))
      DO 15 I=2,4,2
            R(I)=-DF(I)*(CO(I)+CO(I+1))
            R(I+1)=-DF(I+1)*(CO(I)+CO(I+1))
15    CONTINUE
      R(6)=-(DF(6)*CO(6))
      DO 16 I=1,5,2
            CO(I)=COF(I+1)*R(I+1)
            CO(I+1)=COF(I)*R(I)
16    CONTINUE
      DO 20 I=1,6,1
            TOTAL(I)=TOTAL(I)+R(I)+CO(I)
20    CONTINUE
      I=0
40    I=I+1
      IF (ABS(TOTAL(I)-TOTAL1(I)).GT.0.001) THEN
            GOTO 30
      ELSEIF (I.LT.6) THEN
            GOTO 40
      ENDIF
      RETURN
      END
C ***********************************************************
      SUBROUTINE SM(SM1,SM2,SM3,SM4,TOTAL,E1,E2,P1,P2,N1,N2)
C ***********************************************************
C
C
```

```
C  ********************************************************
      DOUBLE PRECISION P1(2001),P2(2001),E1(2001),E2(2001)
      DOUBLE PRECISION TOTAL(6),SM1,SM2,SM3,SM4
      INTEGER N1,N2
      SM1=TOTAL(1)
      SM2=TOTAL(2)+P1(N1+1)*E1(N1+1)
      SM3=TOTAL(4)+P2(N2+1)*E2(N2+1)
      SM4=TOTAL(6)
      RETURN
      END
C  ********************************************************
      SUBROUTINE ENDS(NO,N,RES,RES1,CR,TEMPP,TEMPN,
     &I1,I2,MCRP,MCRN)
C  ********************************************************
      DOUBLE PRECISION RES(2001),RES1(2001),CR(2001)
      DOUBLE PRECISION MCRP(2001),MCRN(2001),TEMPP,TEMPN
      INTEGER N,I,I1,I2,NO
      DO 500 I=1,(N+1),1
       MCRP(I)=0.0
       MCRN(I)=0.0
  500 CONTINUE
      DO 510 I=1,(N+1),1
              IF (ABS(RES1(I)) GT ABS(CR(I))) THEN
                IF (RES1(I) GT 0.0) THEN
                        MCRP(I)=RES1(I)-(CR(I))
                ENDIF
              ENDIF
              IF (ABS(RES(I)) GT ABS(CR(I))) THEN
                IF (RES(I) LT 0.0) THEN
                        MCRN(I)=RES(I)-(CR(I))
                ENDIF
              ENDIF
  510 CONTINUE
      IF (NO EQ 1) THEN
              TEMPP=MCRP(1)
              TEMPN=MCRN(1)
        I1=1
        I2=1
              DO 520 I=2,(N+1),1
                IF (ABS(TEMPP) LT ABS(MCRP(I))) THEN
                  TEMPP=MCRP(I)
                  I1=I
                ENDIF
                IF (ABS(TEMPN) LT ABS(MCRN(I))) THEN
                  TEMPN=MCRN(I)
                  I2=I
                ENDIF
  520 CONTINUE
      ENDIF
      RETURN
      END
C  ********************************************************
      SUBROUTINE INTRES(RES1,RES)
C  ********************************************************
      DOUBLE PRECISION RES1(2001),RES(2001)
      INTEGER I
      DO 500 I=1,2001
              RES1(I)=RES(I)
  500 CONTINUE
      RETURN
      END
C  ********************************************************
      SUBROUTINE BONDS(BOND,FCU)
C  ********************************************************
      DOUBLE PRECISION BOND,FCU
      BOND=0.28*1.4*SQRT(FCU)/2.0
      RETURN
      END
C  ********************************************************
      SUBROUTINE BONDL(LB,P,AS,BOND,I,PF,STRAND)
C  ********************************************************
      DOUBLE PRECISION LB,P(2001),AS,BOND,PF,STRAND,ASTR
      INTEGER I
      ASTR=AS/STRAND
      LB=((P(I)-PF)*1000.0)/(SQRT(4*3.142*ASTR)*BOND*STRAND)
      RETURN
      END
C  ********************************
      SUBROUTINE RESET(XB,CRACK,N)
C  ********************************
      INTEGER XB,CRACK(2001),I,N,TEMP,CNT,CRACKB(2001)
C
      CNT=0
      TEMP=XB
      DO 10 I=1,TEMP
        IF (CRACK(I) LE 1) THEN
          CNT=CNT+1
        ENDIF
   10 CONTINUE
      DO 20 I=1,2001,1
        CRACKB(I)=CRACK(I)
   20 CONTINUE
      DO 30 I=1,TEMP,1
        CRACK(I)=CRACKB(I+CNT-1)
   30 CONTINUE
      XB=1
      DO 320 I=1,TEMP
              IF (CRACK(I) LT (N+1)) THEN
        IF (CRACK(I) GT 0) THEN
                XB=XB+1
        ENDIF
              ENDIF
  320 CONTINUE
      RETURN
      END
C  ********************************************************
      SUBROUTINE CENTRE(NO,N,RES,RES1,CR,MCRP,MCRN2A,MCRN2B,
     &TEMPP,TEMPNA,TEMPNB,I1,I2A,I2B)
C  ********************************************************
      INTEGER N,I,I1,I2A,I2B,NO
      DOUBLE PRECISION RES(2001),RES1(2001),CR(2001)
      DOUBLE PRECISION MCRP(2001),MCRN2B(2001),MCRN2A(2001)
      DOUBLE PRECISION TEMPP,TEMPNA,TEMPNB
      DO 5 I=1,(N+1),1
        MCRP(I)=0.0
        MCRN2A(I)=0.0
        MCRN2B(I)=0.0
    5 CONTINUE
      DO 10 I=1,(N/2),1
              IF (ABS(RES1(I)) GT ABS(CR(I))) THEN
                IF (RES1(I) GT 0.0) THEN
                        MCRP(I)=RES1(I)-(CR(I))
                ENDIF
              ENDIF
              IF (ABS(RES(I)) GT ABS(CR(I))) THEN
                IF (RES(I) LT 0.0) THEN
                        MCRN2A(I)=RES(I)-(CR(I))
                ENDIF
              ENDIF
   10 CONTINUE
```

```
      DO 20 I=((N/2)+1),(N+1),1
            IF (ABS(RES1(I)) GT ABS(CR(I))) THEN
              IF (RES1(I) GT 0 0) THEN
                        MCRP(I)=RES1(I)-(CR(I))
              ENDIF
            ENDIF
            IF (ABS(RES(I)) GT ABS(CR(I))) THEN
              IF (RES(I) LT 0 0) THEN
                        MCRN2B(I)=RES(I)-(CR(I))
              ENDIF
            ENDIF
20    CONTINUE
      IF (NO EQ 1) THEN
            TEMPP=MCRP(1)
            TEMPNA=MCRN2A(1)
            TEMPNB=MCRN2B(1)
        I1=1
        I2A=1
            DO 30 I=2,(N/2),1
              IF (ABS(TEMPP) LT ABS(MCRP(I))) THEN
                TEMPP=MCRP(I)
                I1=I
              ENDIF
              IF (ABS(TEMPNA) LT ABS(MCRN2A(I))) THEN
                TEMPNA=MCRN2A(I)
                I2A=I
              ENDIF
30      CONTINUE
        I2B=1
            DO 40 I=((N/2)+1),(N+1),1
              IF (ABS(TEMPP) LT ABS(MCRP(I))) THEN
                TEMPP=MCRP(I)
                I1=I
              ENDIF
              IF (ABS(TEMPNB) LT ABS(MCRN2B(I))) THEN
                TEMPNB=MCRN2B(I)
                I2B=I
              ENDIF
40      CONTINUE
      ENDIF
      RETURN
      END
*     ******************************
      SUBROUTINE CHECK(RES,ULT,LN)
*     ******************************
      DOUBLE PRECISION RES(2001),ULT(2001)
      INTEGER LN
      I=1
360   IF (I LE (N+1)) THEN
            IF (ABS(RES(I)*1000000 0) GT ABS(ULT(I))) THEN
              GOTO 370
            ELSE
              I=I+1
              GOTO 360
            ENDIF
      ENDIF
370   RETURN
      END
*     ******************************
      SUBROUTINE MOVEBACK(CRACK,XB)
*     ******************************
      INTEGER CRACK(2001),XB,TEMP(2001)
      DO 10 I=1,2001,1
        TEMP(I)=CRACK(I)
10    CONTINUE
```

```
      RETURN
      END
```

□

Appendix F

Calculations for Shear Reinforcement for Finite Element Model 18

The finite element model of the two-span continuous beam Model 18 require shear reinforcement designed to the following approximate calculations:

The utilmate moments at the centre support and in the spans are calculated from the cracked section analysis programme C.S.A., and have the values -1880 kNm, and 1880kNm respectively. Assuming full redistribution of moments, the ultimate bending moment envelope is shown in figure f1. The ultimate uniformly distributed load can be calculated by the following equation

$$U.D.L. = W \approx \frac{8 \times drape}{L^2} = \frac{8 \times \left(\frac{1880}{2} + 1800\right)}{15^2} = 97.4kN/m \approx 100kN/m \quad (f1)$$

The equation of the bending moment on the left hand span in terms of x is :-

$$M = \frac{WLx}{2} - \frac{Wx^2}{2} - \frac{1880x}{L} \quad (f2)$$

The shear force is calculated as the first differential of equation (f2) :-

$$S = \frac{dM}{dx} = \frac{WL}{2} - Wx - \frac{1880}{L} \quad (f3)$$

Inserting the appropriate values of $W = 100kN/m$ and $L = 15m$, equation (f3) simplifies to :-

$$S = 625 - 100x \quad (f4)$$

The resulting shear force diagram for the whole beam is shown in figure f2. Values of the maximum shear force occur at the supports, where at $x = 0$ the shear force is 625 kN, and at $x = 15$ the shear force is -875 kN, varying linearly between these two values.

Ignoring the contribution from the prestress, the maximum allowable design shear force is calculated from clause 4.3.8.2. as $0.8A_c\sqrt{f_{cu}}$. Hence, this gives a value as :-

$$0.8 \times 400 \times 1000 \times \sqrt{40} = 2024kN \quad (f5)$$

The design ultimate shear resistance must then be calculated for the two conditions where the critical sections are either cracked or uncracked in flexure.

Section uncracked in flexure

The design ultimate shear resistance V_{co} is given by the following equation, outlined in clause 4.3.8.4., equation 54

$$V_{co} = 0.67 b_v h \sqrt{\left(f_{prt}^2 + 0.8 f_{prt} f_{cp}\right)} \qquad \text{(f6)}$$

The design compressive stress at the centroidal axis, f_{cp} is calculated as follows :-

$$f_{cp} = \frac{P}{A_c} = \frac{2000}{400 \times 1000} \times 10^{-3} = 5 kN/mm^2 \qquad \text{(f7)}$$

Table 4.5 from B.S.8110 gives values of $V_{co}/b_v h$ for corresponding values of f_{cp} at various concrete grades, obtained from equation (f6). Hence, for grade 40 concrete, this corresponds to :-

$$\frac{V_{co}}{b_v h} \approx 1.95 \qquad \text{(f8)}$$

Therefore, $$V_{co} \approx 1.95 \times 400 \times 1000 = 780 kN \qquad \text{(f9)}$$

Section Cracked in Flexure

In this case, the design ultimate shear resistance is given by equation 55, outlined in clause 4.3.8.5.

$$V_{cr} = \left(1 - 0.55 \frac{f_{pe}}{f_{pu}}\right) v_c b_v d + M_0 \frac{V}{M} \qquad \text{(f10)}$$

The design concrete shear stress v_c is obtained from table 3.9, B.S.8110, having calculated the percentage of steel present in the section :-

$$\frac{100 A_s}{bd} = \frac{100 \times 1700}{400 \times 800} = 0.531 \qquad \text{(f11)}$$

Using the value calculated in equation (f11), from table 3.9, the design concrete shear stress is calculated as :-

$$v_c \approx 0.5\,N/mm^2 \qquad \text{(f12)}$$

To calculate the moment M_0 necessary to produce zero tension in the extreme tension fibre, the prestress is :-

$$f_{pt} = \frac{P}{A} + \frac{Pey}{I} = \left(\frac{2000}{400\times1000} + \frac{2000\times300\times500}{3.33\times10^{10}}\right)\times10^3 = 14.01\,N/mm^2 \qquad \text{(f13)}$$

Therefore,

$$M_0 = 0.8 f_{pt}\frac{I}{y} = 0.8\times14.01\times\frac{3.33\times10^{10}}{500} = 746\,kNm \qquad \text{(f14)}$$

Equation (d10) then gives a value of V_{cr} as :-

$$V_{cr} = (1-0.55\times0.69)\times0.5\times400\times800\times10^{-3} + \left(746\times\frac{875}{1880}\right) = 446.7\,kN \qquad \text{(f15)}$$

This complies with the stipulation that V_{cr} must be greater than $0.1bd\sqrt{f_{cu}} = 202$. The lesser of V_{co} and V_{cr} is taken as the design ultimate shear resistance, in this case :-

$$V_c = 446.7\,kN \qquad \text{(f16)}$$

<u>Provision of shear reinforcement</u>

Clause 4.3.8.8 states that where the shear exceeds $V_c + 0.4b_v d$, shear links must be provided according to equation 57 :-

$$\frac{A_{sv}}{s_v} = \frac{V - V_c}{0.87 f_{yv} d} \qquad \text{(f17)}$$

Hence,
$$\frac{A_{sv}}{s_v} = \frac{(875-446.7)\times10^3}{(0.87\times460\times800)} = 1.338$$

Therefore, per metre length of the beam, the area of shear reinforcement to be provided is :

1388 mm^2

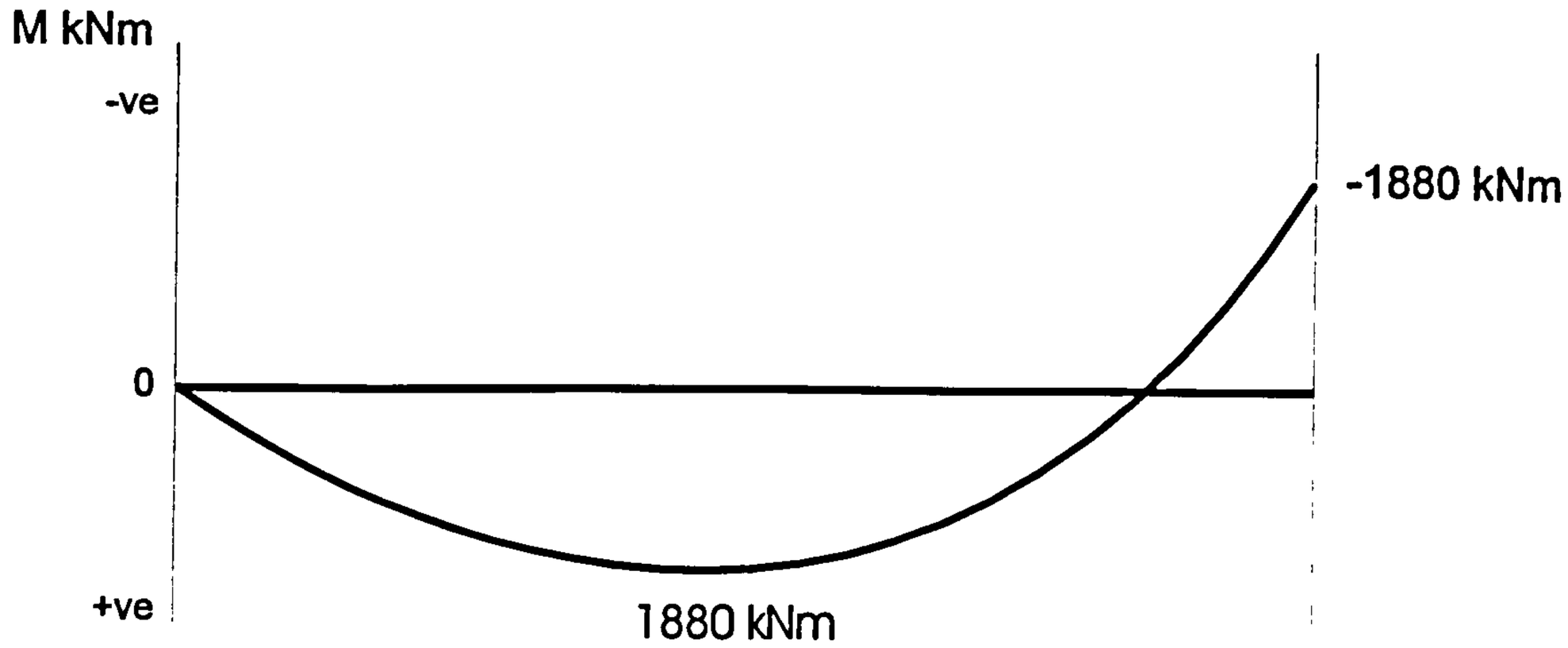

Figure F1. Ultimate Bending Moment Envelope for L.H. Span

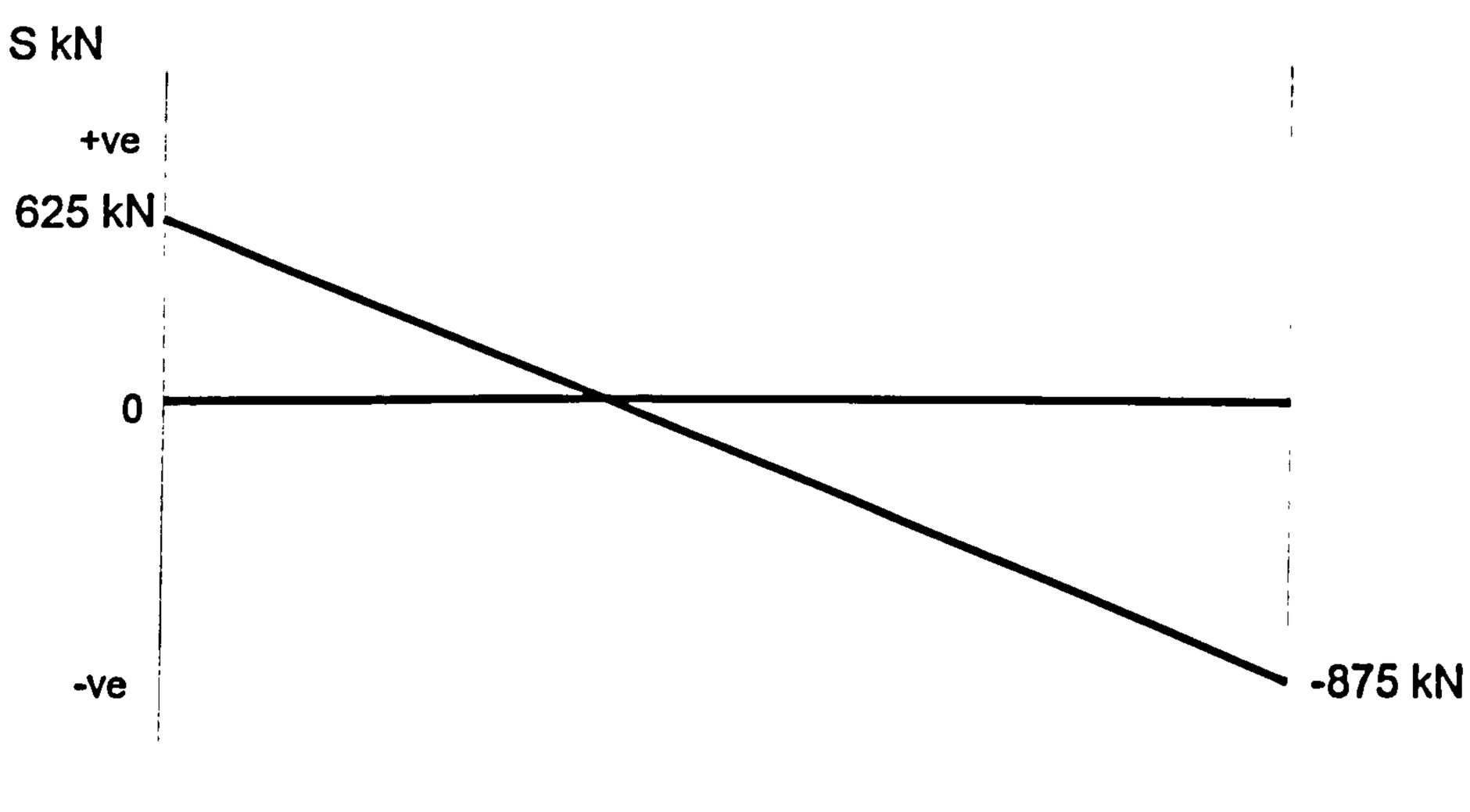

Figure F2. Shear Force Envelope corresponding to Ultimate Bending Moment